Analysis of the function and regulation of the centrosomal protein NEDD1 during cell division and development

A thesis submitted for the

degree of Doctor of Philosophy

Jantina Manning

B.Biotech. (Hons.)

Enrolled through the Department of Medicine, Faculty of Health Sciences, University of Adelaide

Research conducted in the Department of Haematology, Institute of Medical and Veterinary Science, Adelaide

July 2009

Table of Contents

Amendments

Abstract

- Line 5: "neural precursor cell expressed, developmentally down-regulated gene 1" should follow Nedd1

Abbreviations

- The following abbreviations should be included: SCL, stern cell leukemia; Plk, polo-like kinase; γ-TuRC, γ-tubulin ring complex; MOPS, 3-{N-morpholino] propanesulfonic acid; FA, formamide; TMR, tetramethyl-rhodamine

Chapter 1

- p11, line 7: "was" should be deleted
- p15, line 13: results should read "can result"
- p16, line 12: beidl should read "biedl"

Chapter 2

- Throughout: manufacturers' should read manufacturer's
- p28, line 15: "at 260 nm" should be added after (OD)
- p30, line 18: "KOAc" should read "potassium acetate", KCL should read "KCl"
- p34, line 11: $\Delta\Delta C_T$ method is C_t value for any sample normalised to GAPDH minus the C_t value for the calibrator also normalised to GAPDH
- p41, line 1: "laminar flow" should be deleted
- p47, line 19: "mAmps" should read "mAMPs"
- p53, line 5: "dioxygen" should read "digoxigenin"
- p80, line 1 and 2: "Fig. 7C-E" and "Fig. 7C" should read "Fig. 4.7C-E" and "Fig. 4.7C"

Chapter 4

- p88, line 6/7: should read " This chapter has confirmed that NEDD1 can be regulated by its phosphorylation state."

Chapter 5

- p93, line 9: "sufficient" should read "required"
- p96, line 21: "flag-conjugated" should read "flag antibody-conjugated"
- p104, line 25: "Fig. 5.10" should read "Fig. 5.11"
- p105, line 25: "caused" should read "may cause"

Chapter 6

- Figure 6.7D: the final lane (1-676) should also be labelled "no immunoprecipitation"
- p118, line 13: "other in" should read "in other"
- p118, line 23: "(human neuronal protein C)" should be inserted after HuC

Chapter 7

- p130, line 25: "the primary" should read "one"

References

- Zhang 2009 reference should include "122, 2240-2251"

Abstract

The centrosome is the major microtubule organising centre of cells and serves as a centralised location for controlling many cellular processes. A critical component of the centrosome is the γ-tubulin ring complex (γ-TuRC) which is required for the nucleation of microtubules, correct formation of the mitotic spindle and hence progression of the cell cycle. NEDD1 (mouse: Nedd1), was recently discovered as a centrosomal protein which functions primarily in targeting the γ-TuRC to the centrosome and spindle.

Given the fundamental role of the centrosome in mitosis and other processes, it is no surprise that this organelle is essential during mouse development. To examine the precise role of the centrosome during development, this study analysed the expression and localisation of Nedd1 during mouse embryogenesis. This revealed a dynamic localisation of Nedd1 and the centrosome during development, and provides further evidence for their critical role in development.

To investigate the regulation of NEDD1, its expression during the cell cycle was analysed. It was found that phosphorylation is the primary method of NEDD1 regulation. Additionally, it was observed that Nedd1 levels decreased upon the entry of mouse embryonic fibroblasts into cell culture-induced senescence (an irreversible state of cell cycle arrest). This correlated with a loss of centrosomal integrity. Ablation of Nedd1 in healthy cells caused premature senescence and centrosome abnormalities, suggesting that Nedd1 and the centrosome may contribute to this senescence.

NEDD1 is also important in the recruitment of the γ-TuRC to the centrosome, which is essential for correct centrosome biogenesis and function. This study identified a 62 amino acid region of NEDD1 that interacts with γ-tubulin and can abrogate its function. Key

residues important for this interaction were also revealed. Additional interacting proteins of NEDD1 were also identified, and the chaperone TCP-1α was characterised in more detail and shown to regulate NEDD1.

Given the currently known functions of NEDD1, it was expected to be important in development. Zebrafish were chosen as a model to study this because of their many advantages for developmental studies. A zebrafish homologue of NEDD1 was identified that displayed a similar localisation and function to mammalian NEDD1. Depletion of this protein caused lethality or phenotypic abnormalities which were most obvious in the central nervous system, depending on the extent of knockdown. This demonstrates that NEDD1 is critical for development, particularly in the nervous system.

The results presented in this thesis contribute to the understanding of the function and regulation of NEDD1, and thus also the centrosome, and highlights the importance of this protein during development. Additionally, this study forms the foundation for further work on centrosomes, using NEDD1 as a marker for centrosomal dynamics and function.

Declaration

This work contains no material which has been accepted for the award of any other degree or diploma in any university or other tertiary institution to Jantina Manning and, to the best of my knowledge and belief, contains no material previously published or written by another person, except where due reference has been made in the text.

I give consent to this copy of my thesis when deposited in the University Library, being made available for loan and photocopying, subject to the provisions of the Copyright Act 1968. The author acknowledges that copyright of published works contained within this thesis (as listed below*) resides with the copyright holder of those works.

I also give permission for the digital version of my thesis to be made available on the web, via the University's digital research repository, the Library catalogue, the Australasian Digital Theses Program (ADTP) and also through web search engines, unless permission has been granted by the University to restrict access for a period of time.

* **Manning, J.**, Colussi, P., Koblar, S., and Kumar S. (2008). Nedd1 expression as a marker of dynamic centrosomal localization during mouse embryonic development. *Histochem Cell Biol, 129*(6),751-64.

Jantina Manning

Publications

The following publications have resulted from work performed by the candidate during the period of this candidature:

Manning, J., Colussi, P., Koblar, S., and Kumar S. (2008). Nedd1 expression as a marker of dynamic centrosomal localization during mouse embryonic development. *Histochem Cell Biol, 129*(6), 751-64.

Manning, J. and Kumar, S. (2007). NEDD1: function in microtubule nucleation, spindle assembly and beyond. *Int J Biochem Cell Biol, 39*(1), 7-11.

Ekberg, J., Schuetz, F., Boase, NA., Conroy, SJ., **Manning, J.**, Kumar, S., Poronnik, P., Adams, DJ. (2007). Regulation of the voltage-gated K(+) channels KCNQ2/3 and KCNQ3/5 by ubiquitination. Novel role for Nedd4-2. *J Biol Chem*, *282*(16),12135-42.

Acknowledgments

I must begin by thanking my supervisor, Professor Sharad Kumar for giving me the opportunity to conduct my research under his supervision, and for helping me to develop my scientific skills. Thanks also to my co-supervisor, Dr. Dimitrios Cakouros, for his support, encouragement and humour. I must also thank the University of Adelaide for providing me with an Australian Postgraduate Award and a Reginald Walker Faculty of Health Sciences Scholarship, as well as the Royal Adelaide Hospital Research Committee for awarding me a DAWES scholarship.

I thank Sonia Shalini in the laboratory for helping with the experiments in chapter 5, Martin Lewis (University of Adelaide) for conducting the zebrafish injections, and Simon Koblar (University of Adelaide) for his guidance with all the neural work. I am grateful to J.L. Salisbury (Mayo Clinic, MN, USA) for the gift of the centrin antibody, B. Edde (CNRS, Montpellier, France) for the GT335 antibody, and R. Morimoto (Northwestern University, IL, USA) for the HSP70 antibody. Thanks especially to Donna for her continual interest in my project, hours of proof-reading and even more hours of chatting in our office. Thanks also to Tash, Kathryn, Loretta, Natalie, Hazel, Lien, and other members of the Molecular Regulation Laboratory and the Lymphatic Development Laboratory, for friendship, support and encouragement during my time in the laboratory.

Finally I thank my family and my four-legged friend, for their continual support and encouragement. Thanks especially to my husband John, for his love and understanding during the good times and frustrating times of my research. I've finally made it!

Abbreviations

γTuRC	γ-tubulin ring complex
aa	amino acid
AP	alkaline phosphatase
BCIP	5-bromo-4-chloro-indolyl-phosphatase
bp	base pair
BSA	bovine serum albumin
C	carboxyl
Cdk	cyclin-dependent kinase
cDNA	complementary deoxyribonucleic acid
CNS	central nervous system
DAB	3, 3’ diaminobenzidine
DEPC	diethyl pyrocarbonate
DIG	digoxigenin
DMF	dimethylformamide
DNA	deoxyribonucleic acid
DOC	deoxycholate
DRG	dorsal root ganglia
DTT	1,4-dithiothreitol
E	embryonic day
E. coli	*Escherichia coli*
ECL	enhanced chemiluminescence
EDTA	ethylenediaminetetra-acetic acid
FBS	fetal bovine serum
FL	full length
g	gravity
GENSAT	gene expression nervous system atlas
GFP	green fluorescent protein
GRP	glucose-related protein
GST	glutathione-S-transferase
h	hour(s)
HAUS	human augmin complex
HEPES	N-2-hydroxyethylpiperazine-N'-2-ethanesulfonic acid
His	histidine

hpf	hours post fertilisation
HRP	horse radish peroxidase
HSP	heat shock protein
IB	immunoblot
INL	inner neuroblastic layer
IP	immunoprecipitation
IPTG	isopropyl-β-D-thiogalactopyranoside
JUP	junction plakoglobin
kb	kilobase
kDa	kiloDalton
L	leucine
LB	Luria-Bertani
LV	lens vesicle
MBT	midblastula transition
MEF	mouse embryonic fibroblast
min	minute(s)
MO	morpholino
MOPS	3-(n-morpholino) propanesulfonic acid
MQ	milli-Q
mRNA	messenger ribonucleic acid
MS	mass spectrometry
MTOC	microtubule organising centre
NBT	nitroblue tetrazolium
NCBI	National Center for Biotechnology Information
NEDD1/Nedd1	*neural precursor cell expressed, developmentally down-regulated gene 1*
Ni-NTA	nickel-nitrilotriacetic acid
NP-40	nonidet P40
OD	optical density
ONL	outer neuroblastic layer
ORF	open reading frame
p	passage
PAGE	polyacrylamide gel electrophoresis
PBS	phosphate buffered saline
PCM	pericentriolar matrix
PCR	polymerase chain reaction
PEG	polyethylene glycol
PFA	paraformaldehyde

pH3	phosphorylated histone H3
PI	propidium iodide
PLB	protein loading buffer
PVDF	polyvinylidene difluoride
Q	glutamate
qPCR	quantitative polymerase chain reaction
RNA	ribonucleic acid
RNAse	ribonuclease
RS	replicative senescence
RT	room temperature
SA-β-gal	senescence associated β-galactosidase
SDS	sodium dodecyl sulfate
sec	second(s)
SEM	standard error of the mean
siRNA	small interfering RNA
SSC	sodium chloride-sodium citrate
TAE	tris-acetate-EDTA
TCP-1	t-complex protein 1
TEMED	tetramethylethylenediamine
WT	wild type
X-gal	5-bromo-4-chloro-3-indolyl-β-D-galactosidase

1. Introduction

1.1. The centrosome

The centrosome was first described in the early 1900s by Theodor Boveri (Boveri, 1901). It was observed as a small focus of dense material within a cell that anchored the ends of thin cytoplasmic or spindle fibres. It is now known that this dense structure is the centrosome, which serves as the primary microtubule organising centre (MTOC) of animal cells. Centrosomes exist in yeast as the spindle pole body (Knop *et al*., 1999) and in plants as nucleating centres (Chan *et al*., 2003). The core component of the mammalian centrosome consists of two centrioles, which are symmetrical barrel-shaped structures made up of nine sets of triplet microtubules, linked by interconnecting fibres. The two centrioles lie at right angles to each other in close proximity at one end and are identical except that the older (maternal) centriole has additional appendages at the distal end (Fig. 1.1) (Doxsey, 2001). Surrounding the centrioles is a cloud of proteinaceous matrix called the pericentriolar material (PCM). This matrix is a network of fibres and protein aggregates and is the site of microtubule nucleation of the centrosome (Sluder, 2005). Over 500 proteins have been localised to the centrosome (Andersen *et al*., 2003) and this list is continuing to grow.

1.2. Centrosome function

The main function of the centrosome is as the primary MTOC of the cell. Microtubules are filamentous polymers in all eukaryotic cells and their organisation involves the initiation and growth of microtubules (microtubule nucleation) mediated by the core centrosomal protein γ-tubulin and its complex proteins (γ-tubulin ring complex, γTuRC) (Raynaud-Messina and Merdes, 2007). This organisation is important for many processes during animal development, such as the construction of a bipolar mitotic spindle during cell division, which is critical for the correct replication of a cell to form two daughter cells. Microtubule organisation is also important for other processes during the rest of the cell cycle such as establishing and maintaining cell polarity and shape, and transporting proteins, vesicles and organelles within the cell (Doxsey, 2001, Doxsey *et al*., 2005, Schatten, 2008). Many centrosomal proteins also localise to the basal body, which is identical to the centriole, and

Fig. 1.1 Centrosome structure

The centrosome is composed of a pair of centrioles located at right angles to each other. The two centrioles are linked by interconnecting fibres, and the maternal centriole contains additional appendages. Both centrioles are surrounded by a cloud of pericentriolar material (PCM) that nucleates microtubules. (Adapted from Doxsey *et al*., 2001).

forms the base of cilia and flagella (Dawe *et al*., 2007). These tail-like microtubule projections play important sensory and motility functions, and their organisation is also mediated by centrosomal proteins (Kellogg *et al*., 1994). Hence the centrosome (and the proteins required for its regulation and function) is important for many aspects of cell growth and proliferation.

The essential role of centrosomes in cell division and development has been questioned by multiple studies in recent years. In *Drosophila*, null mutants of the centrosomal protein centrosomin (cnn) still develop into adults although they display abnormalities such as a lack of astral microtubules emanating from spindle poles and male sterility (Megraw *et al*., 2001). Additionally, flies harbouring a mutation in *DSas-4*, which leads to a failure of centriole and centrosome replication, also live to adulthood, although they require a maternal contribution of this protein for embryogenesis to proceed (Basto *et al*., 2006, Stevens *et al*., 2007). Hence, centrosomes in *Drosophila* appear to be required for embryogenesis, but are not necessary for later development in this species. In mammals, whilst the mitotic spindle can be formed in the absence of a complete centrosome, the downstream consequences of centrosomal disruption, such as the inhibition of cell cycle progression, are eventually toxic to the cell (Hinchcliffe *et al*., 2001, Khodjakov and Rieder, 2001). As such, the centrosome appears to be critical for development in mice. Indeed, null mutants of the core centrosomal protein γ-tubulin die at the blastocyst stage (Yuba-Kubo *et al*., 2005). Additionally, null mutants of the centrosome associated polo-like kinase Sak, arrest at embryonic day (E)7.5 with defects in mitosis and increased apoptotic cell death (Hudson *et al*., 2001). The reason these species respond differently to a lack of functional centrosomes is not well understood, but has been postulated to involve mammals possessing more complicated checkpoints and stringent responses to abnormal centrosomes (Badano and Katsanis, 2006).

1.3. The cell cycle

One of the best characterised functions of the centrosome is its role in the cell division cycle. The cell cycle can be divided into four fundamental phases; S phase (DNA synthesis), M phase (mitosis), and two gap phases G1 and G2 (Fig. 1.2A) (Nigg, 2001, Afonso *et al*., 2007). During S phase, replication of DNA takes place, while during M phase the replicated chromosomes segregate and cell division (cytokinesis) occurs resulting in two identical daughter cells. The gap phases separate M and S phase and allow for requirements such as cell growth and protein synthesis to occur. The centrosome plays important roles during all stages of the cell cycle (Doxsey *et al*., 2005). Following cytokinesis, in G1, a normal cell inherits one centrosome consisting of two centrioles. During interphase (the period between two mitotic divisions), the centrosome nucleates cytoplasmic microtubules to organise them in astral arrays from the centrosome to function as a scaffold for other proteins. This microtubule nucleation is also important for determining cell polarity and cell motility (Sluder, 2005). The centrioles separate towards the end of G1 and duplication begins as pro-centrioles form on the proximal end of each centriole during S phase (Fig. 1.2A). This is coincident with the phosphorylation of many centrosome substrates (Lacey *et al*., 1999, Afonso *et al*., 2007). Both daughter centrosomes become mature by the completion of G2. Subsequently, in mitosis is where the centrosome plays its most established role. This is to mediate the assembly and organisation of the mitotic spindle in order to determine spindle polarity and the plane of cell cleavage essential for correct chromosome segregation (Barr *et al*., 2004).

Mitosis consists of six main stages; prophase, prometaphase, metaphase, anaphase, telophase and cytokinesis (Fig. 1.2B) (Pines and Rieder, 2001). During prophase, chromatin in the nucleus begins to condense and the two centrosomes move to opposite poles of the cell. In prometaphase, the nuclear envelope is broken down and proteins attach to the centromeres, forming the kinetochores which anchor spindle microtubules. These microtubules extend from the centrioles and form spindle fibres during metaphase, along which the paired chromosomes are aligned. The paired chromosomes are separated

Fig.1.2 The centrosome cycle

(**A**) A cell inherits a pair of centrioles (one centrosome) after cell division which separate towards the end of G1 phase. Pro-centrioles form on the proximal end of each original centriole during S phase, and elongation is completed by the end of G2 phase. The two pairs of centrioles move to opposite poles of the cell and anchor the spindle microtubules during mitosis. Chromosomes are aligned on the spindle during this phase. Gap phase 1 (G1), Synthesis phase (S), Gap phase 2 (G2), Mitosis (M). (Adapted from Afonso *et al*., 2007).

(**B**) Throughout the six stages of mitosis the centrosome functions to nucleate and organise microtubules. Prophase indicates the entry into mitosis, and the spindle is assembled during prometaphase. The chromosomes are pulled apart during anaphase and after new membranes form around the two new cells in telophase, the spindle fibres disperse. Each daughter cell inherits a single centrosome which is duplicated during interphase. (Adapted from Barr *et al*., 2004).

A

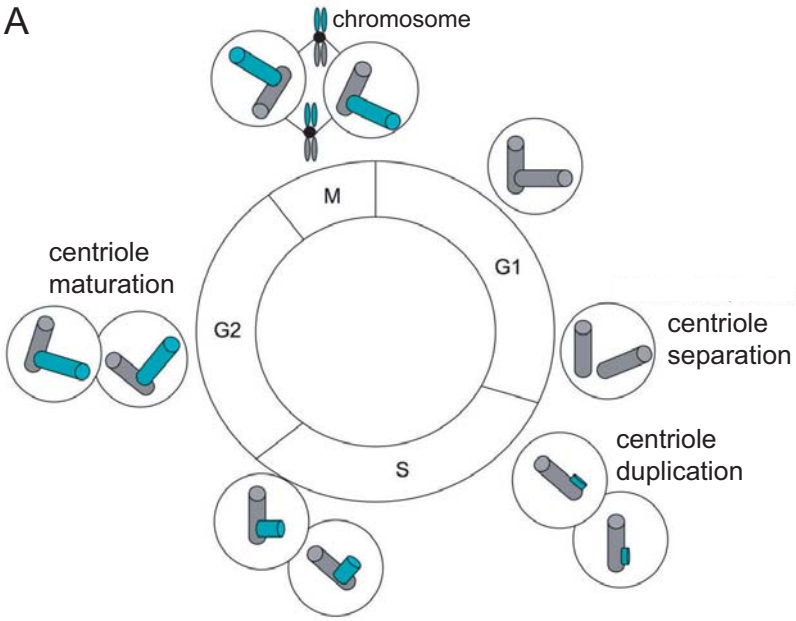

B

NOTE:
This figure is included in the print copy of the thesis held in the University of Adelaide Library.

towards each centrosome during anaphase to move to opposite sides of the cell. During telophase, membranes form around the two new cells and the spindle fibres disperse. This is followed by cytokinesis when the contractile ring around the cell pinches it into two daughter cells.

The process of mitosis is regulated through two primary post-translational mechanisms, protein phosphorylation and protein degradation. The most prominent proteins involved in this regulation are the cyclin-dependent kinases (Cdks) and their regulatory subunits the cyclins, together with several other protein kinases (Nigg, 2001). Malfunctions of these regulatory proteins and other proteins involved in mitosis can lead to centrosome and spindle defects, a loss of cell cycle control, and therefore cell abnormalities and death.

1.3.1. The centrosome and cell cycle regulation

The centrosome contains hundreds of proteins that have roles in numerous different cellular processes (Andersen *et al*., 2003). Of these proteins, many are involved in the regulation of cell cycle progression. Since the centrosome is duplicated at the G1-S transition, it is not surprising that it is important in the regulation of this process (Hoffmann, 2004). The centrosome also plays a role in the G2-M transition, which is primarily controlled by cyclin B1 activation (Kramer *et al*., 2004, De Boer *et al*., 2008). Cyclin B1 is present in the cytoplasm before prophase. Active Cdk1-cyclin B1 is recruited to the centrosome during prophase following a loss of its inhibitor, Checkpoint kinase 1 (Chk1) from the centrosome, which allows the progression of mitosis (Jackman *et al*., 2003, Kramer *et al*., 2004). The centrosome associated kinases Aurora A and Polo-like kinase 1 (Plk1) have also been linked to mitotic progression (Hirota *et al*., 2003, Sumara *et al*., 2004). Hence, the centrosomal localisation of such proteins contributes to maintaining the proper timing of the stages of cell division, including progression into mitosis.

1.3.1.1. A lack of functional centrosomes leads to cell cycle arrest

The importance of the centrosome in cell cycle regulation has been highlighted by studies which have removed core centrosomal components by methods such as laser ablation or

microdissection. These studies reveal that cells without centrosomes can form acentrosomal MTOCs with functional mitotic spindles, but many fail to cleave into two daughter cells (Khodjakov and Rieder, 2001, Khodjakov *et al*., 2002). Regardless of cleavage fate, none of the cells initiate DNA replication, and all enter G1 arrest. The depletion of individual centrosomal proteins can also induce a G1 arrest, with defects in centrosome structure, organisation, duplication and cilia formation (Gromley *et al*., 2003, Keryer *et al*., 2003, Mikule *et al*., 2007). These cells display an increase in the level of the checkpoint control protein p53 at the centrosome, due to its phosphorylation and stabilisation as a response to cellular stress. Consequently, the levels of the p53 transcriptional target, the Cdk-inhibitor p21, are also increased and this causes the G1 arrest by blocking downstream activators of the cell cycle (Srsen *et al*., 2006, Mikule *et al*., 2007). Therefore, it appears that the loss of centrosomal proteins constitutes a form of stress that activates p53. Additionally, a role for centrosomal proteins in G2-M arrest has been suggested, as the depletion of pericentrin, which normally anchors the γTuRC to the centrosome, also causes G2-M arrest by mis-localising the γTuRC away from the spindle. This causes spindle defects and an activated a checkpoint response (Zimmerman *et al*., 2004).

1.3.1.2. Extra centrosomes can promote tumourigenesis

In contrast, cells containing extra centrosomes tend to bypass cell cycle checkpoints, although they often display defects in mitosis (Wong and Stearns, 2003, Uetake and Sluder, 2004). Normally, centrosome number is maintained by tight control of the centrosome duplication cycle. However, many tumours display increased centrosome numbers (centrosome amplification) which generally results in multipolar mitoses and aneuploidy (chromosome loss or gain) (D'Assoro *et al*., 2002). Additionally, induced centrosome amplification has recently been shown to drive tumourigenesis in flies (Basto *et al*., 2008). In theory, centrosome amplification should be deleterious with high levels of aneuploidy causing cell death, but many cell lines and tumours overcome this problem by clustering multiple centrosomes together to form a bipolar spindle (Gergely and Basto, 2008). Hence

cells have devised a mechanism to cope with extra centrosomes, and this does not seem to cause cell cycle arrest, but rather can promote excessive cell proliferation and tumourigenesis.

Therefore, the centrosome is important for controlling many aspects of the cell cycle, primarily by providing a scaffold for cell cycle regulators and their activity. Given that the identification of proteins with centrosomal localisation is rapidly growing, it is probable that the centrosome will be found to be important in additional processes regulating cell cycle progression.

1.4. Senescence

Cellular senescence was first described in 1961 when it was discovered that human cells derived from embryonic tissues can only divide a finite number of times in culture (Hayflick and Moorhead, 1961). Senescent cells enter a state of irreversible growth arrest in the G1 to S phase transition of the cell cycle (Sherwood *et al*., 1988), and unlike cells in other phases of cell cycle arrest, can remain metabolically active for long periods of time (Goldstein, 1990). As well as proliferation arrest, senescent cells display additional phenotypes. Some cells become resistant to apoptotic death and most show morphological and metabolic changes including cellular enlargement, increased lysosome biogenesis and atypical senescent-associated β-galactosidase activity (SA-β-gal) (Fig. 1.3A) (Dimri *et al*., 1995). Evidence indicates that this process in human cells, known as replicative senescence (RS), is a result of shortening of telomeres, which are DNA repeats capped at the end of linear chromosomes (Harley *et al*., 1990). Telomerase normally functions to maintain telomere length and therefore prevents its otherwise progressive shortening. In the absence of telomerase, as in aging cells, each round of DNA replication leaves up to 200 base pairs (bp) of unreplicated 3' telomeric DNA. This eventually causes cells to stop dividing and undergo RS (Harley *et al*., 1990, Levy *et al*., 1992). Senescence can also be triggered by other events such as DNA damage, cell culture or oxidative stress, cytotoxic

A

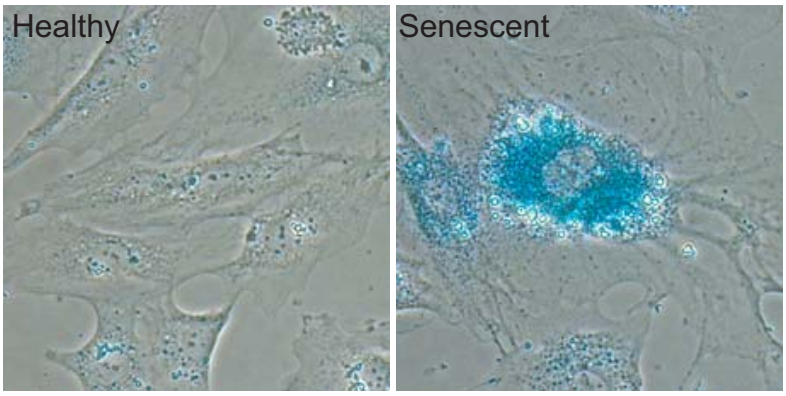

B

NOTE:
This figure is included in the print copy of the thesis held in the University of Adelaide Library.

Fig. 1.3 Cellular senescence and causes

(**A**) Senescent cells display senescence-associated β-galactosidase (SA-β-gal) activity (blue) and show morphological changes such as cellular enlargement.

(**B**) Senescence can be triggered by many different stimuli. (Adapted from Collado *et al*., 2006).

drugs, over-expression of certain tumour suppressor genes such as p53, or as a protective cellular response to strong mitogenic signalling by oncogenes such as Ras, Raf1 and MEK (Fig. 1.3B) (Atadja *et al*., 1995, Serrano *et al*., 1997, Lin *et al*., 1998, Zhu *et al*., 1998, Ben-Porath and Weinberg, 2005). This mechanism is termed premature senescence. Importantly, the inactivation of p53 by means such as oncogenic activation, can result in cells that are resistant to senescence (Shay *et al*., 1991). Hence, senescence is implicated as a tumour suppressive mechanism, and there is much evidence demonstrating that escape from senescence is associated with malignant transformation (Ponten, 1976, Campisi, 2001).

1.4.1. Regulation of senescence

The main effectors of senescence are p53, its transcriptional target p21, and the retinoblastoma protein Rb (Ben-Porath and Weinberg, 2005). The co-ordination and regulation of these proteins is a complex process, which is often initiated upstream of p53. In a healthy cycling cell, the levels of p53 are kept low, partly by the E3 ubiquitin ligase, Mdm2 which targets p53 for degradation (Fig. 1.4A) (Kulju and Lehman, 1995). Therefore, there is little p53 protein to bind to the promoter of p21 and activate its transcription. Because p21 is a Cdk inhibitor, when its levels are low, the Cdk4/6-cyclin D1 and Cdk2-cyclin E complexes are maintained in an active state (Stein *et al*., 1999). This results in the phosphorylation of Rb, which dissociates it from its interaction with the E2F transcription factors (Narita *et al*., 2003). Hence, the E2F factors are released and able to activate the transcription of many genes involved in cell cycle progression.

When senescence is induced there is an increase in the levels of p53 protein which can be caused by a variety of factors (Fig. 1.4B). The level of the cell cycle inhibitor $p19^{ARF}$ can be activated, which binds to and sequesters Mdm2 away from p53 (Lowe and Sherr, 2003). Hence p53 is not targeted for degradation. Additionally, p53 can be activated by phosphorylation from checkpoint proteins such as ATM/ATR and Chk1/2 (Shiloh, 2001). The resultant increase in active p53 can cause senescence independently of Rb. It also

Fig 1.4 Pathways of senescence activation

(**A**) In a healthy cycling cell, the level of p53 is kept low, partly by Mdm2. As a result, the level of p21 is low and the Cdk4/6-cyclin D1 and Cdk2-cyclinE complexes are active. The resultant phosphorylation of Rb dissociates it from its interaction with the E2F transcription factors and the transcription of many genes involved in cell cycle progression is activated. In this pathway, the levels of cell cycle inhibitors are all low (grey circles).

(**B**) The induction of senescence can be caused by an increase in p53 independently of Rb, or as a result of Rb hypo-phosphorylation. The increase in p53 levels occurs by a variety of factors, including the activation of $p19^{ARF}$ which sequesters Mdm2 away from p53. Additionally, p53 can be phosphorylated by ATM/ATR and Chk1/2, leading to an increase in p21 which inactivates the Cdk-Cyclin complexes. As a result, Rb remains hypo-phosphorylated and bound to E2F factors to inhibit their transcription of cell cycle targets. p16 can also be up-regulated which contributes to the inactivation of Cdk2-cyclin E complexes.

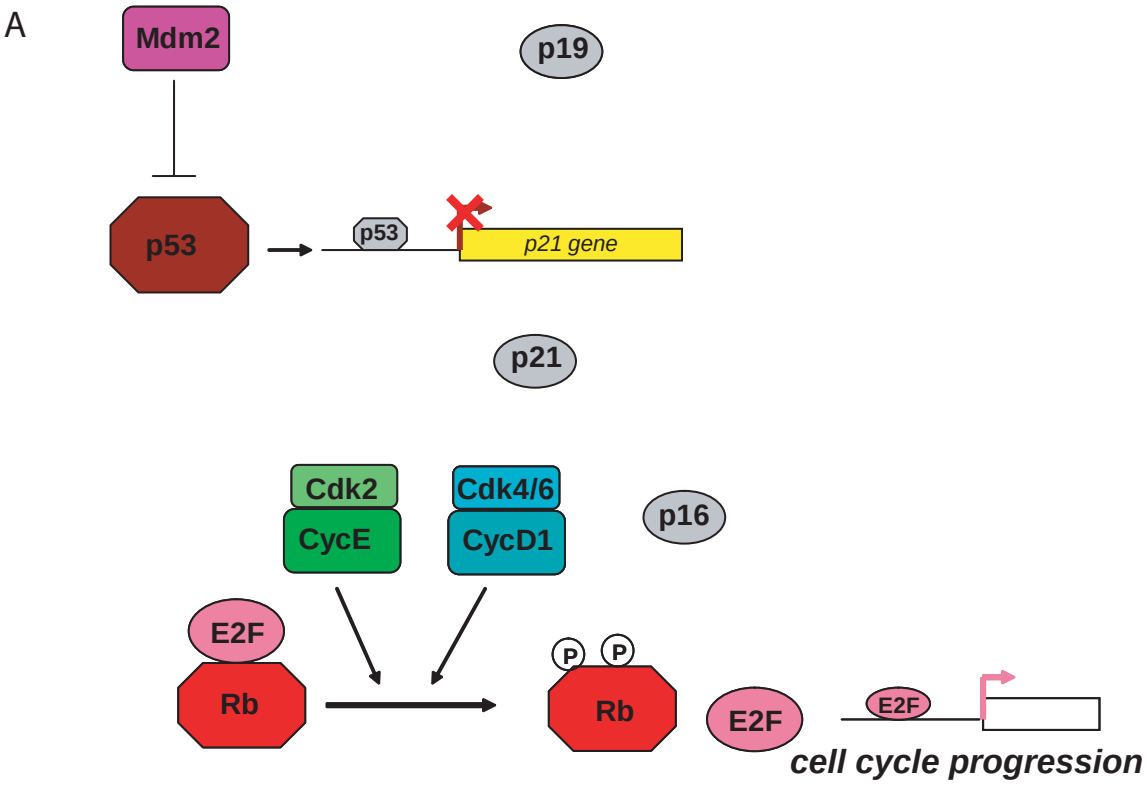
A
Mdm2
p19
p53
p53
p21 gene
p21
Cdk2
CycE
Cdk4/6
CycD1
p16
E2F
Rb
P
P
Rb
E2F
E2F
cell cycle progression

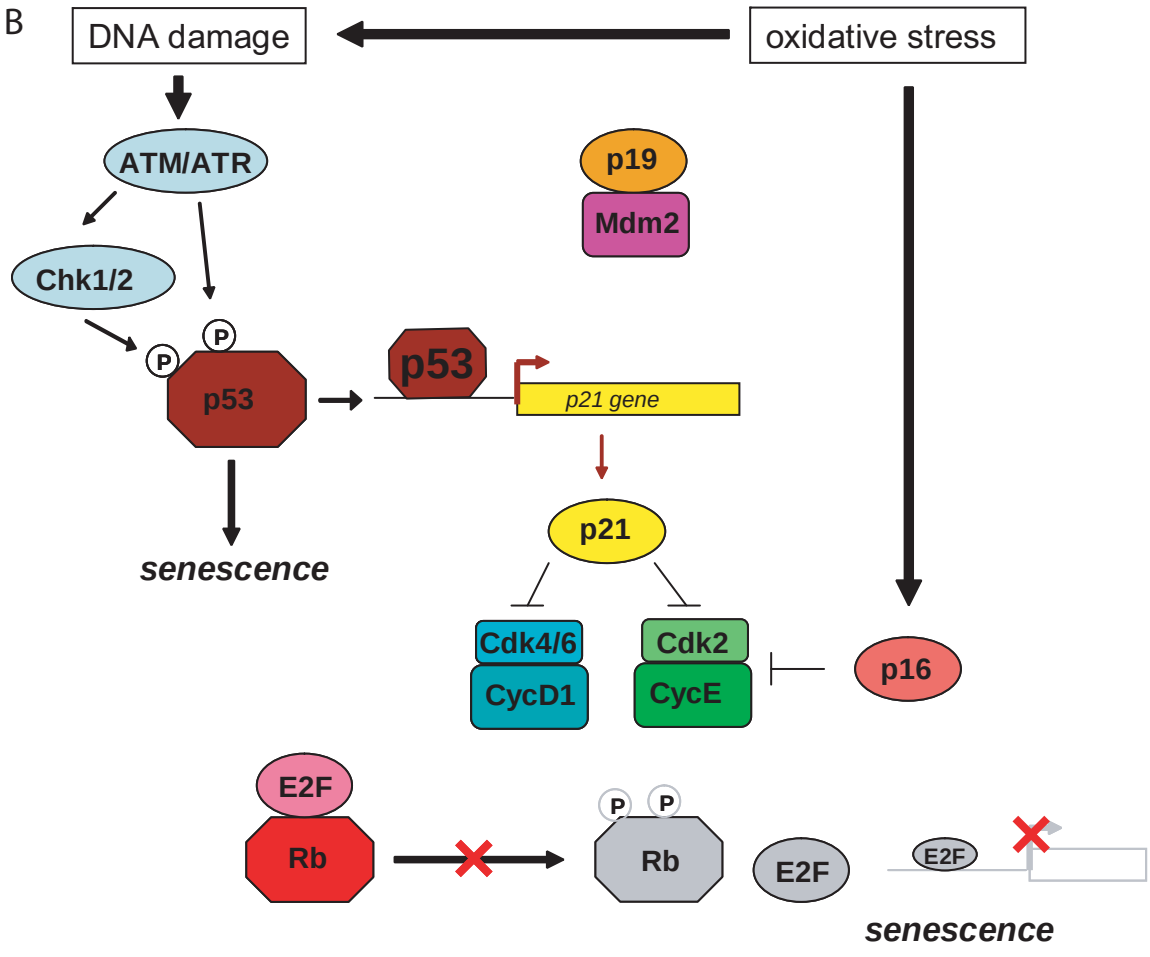
B
DNA damage
oxidative stress
ATM/ATR
p19
Mdm2
Chk1/2
P
P
p53
p53
p21 gene
senescence
p21
Cdk4/6
CycD1
Cdk2
CycE
p16
E2F
Rb
P
P
Rb
E2F
E2F
senescence

results in an increase in its transcriptional target p21 which can then inactivate Cdk-cyclin complexes such that they can no longer phosphorylate Rb (Narita *et al*., 2003). In its hypo-phosphorylated form, Rb remains bound to E2F factors and inhibits their transcription of cell cycle targets, resulting in senescence. Additionally, the Cdk-inhibitor p16 can be up-regulated in senescence, which also contributes to the inactivation of Cdk2-cyclin E complexes (Ben-Porath and Weinberg, 2005). The level of involvement of the various proteins discussed appears to depend on the initial trigger of senescence. Of interest to this study, senescence induced by oxidative stress can be mediated through the DNA damage pathway, involving ATM/ATR activation, or through reactive oxygen species activating p16 and therefore inactivating Rb (Fig. 1.4B) (Ben-Porath and Weinberg, 2005).

Mouse embryonic fibroblasts (MEFs) are often used as a model to study senescence, despite the differences between human and rodent cells. MEFs spontaneously overcome RS to become immortalised, whereas human cells rarely do (Todaro and Green, 1963). Additionally, senescence in MEFs relies predominantly on the $p19^{ARF}$/p53 pathway, whereas human fibroblasts rely on both p53 and Rb (Campisi, 2001). Finally, MEFs senesce after fewer population doublings than human fibroblasts even though they have longer telomeres and constitutively express telomerase (Wright and Shay, 2000). It has been determined that MEFs senesce as a result of oxidative stress in culture which causes extensive DNA damage and resembles hydrogen peroxide induced senescence in human cells (Parrinello *et al*., 2003). The centrosome has been linked to DNA damage responses, in particular the G2/M checkpoint which arrests cells in the presence of damaged DNA. This is thought to be because it provides a central location for the docking of many proteins important in this checkpoint (Sibon, 2003, Wang *et al*., 2009). However, the role of the centrosome in senescence is less well understood.

1.4.2. Centrosomes and senescence

As discussed in section 1.3.1.1, perturbation of centrosomes can lead to a G1 arrest, often as a consequence of a stress-induced checkpoint. However some cells do not arrest

immediately, and enter S phase after a delay. These cells are predisposed to undergo premature senescence (Srsen and Merdes, 2006). Indeed, depletion of the centrosomal proteins pericentriolar material 1 (PCM1) and pericentrin have been shown to result in a reduced number of cells entering S phase (Srsen *et al*., 2006). Additionally, the overall levels of p53 and p21 are up-regulated, and the level of phosphorylated Rb is reduced. PCM1 depleted cultures display a ten-fold increase of SA-β-gal staining. Hence, it has been proposed that these cells displayed a stress-driven response to centrosome defects which causes the cells to enter senescence. The idea of the centrosome as a centre for stress-related signalling seems plausible considering its central location in the microtubule network and its ability to provide a scaffold for molecules involved in the cell cycle and its regulation.

Despite numerous studies showing that centrosome abnormalities can lead to senescence, there is very little known about the role that the centrosome plays in cases of senescence caused by other means, such as oncogene-induced senescence or cell culture-induced senescence in primary cells. However, a study in primary human mammary epithelial cells (HMECs), which normally proliferate for 5-20 population doublings before undergoing senescence, showed that small subpopulations (vHMECs) have the ability to keep proliferating, bypassing senescence (McDermott *et al*., 2006). Interestingly, about 30% of these vHMECs accumulate supernumerary centrosomes due to a loss of p16, correlating with an increase in genomic instability. This indicates that centrosomal integrity may be important for controlling cell growth. Given the importance of senescence in protecting cells with damaged DNA or other defects from proliferation, and as a tumour suppressive mechanism, studying the role of the centrosome and how it contributes to senescence is highly valuable.

1.5. Centrosomes during mammalian development

Aside from its role in the cell cycle and proliferation, the centrosome is involved in a range of other cellular processes including establishing and maintaining cell polarity, positioning

organelles within the cell and directing intracellular traffic. Centrioles also provide the base structure for the growth of cilia and flagella which play important motility and sensory functions (Sloboda and Rosenbaum, 2007). Given its role in these diverse processes, it is no surprise that the centrosome is important during development. Indeed, centrioles and centrosomes appear to be essential during development in mice, as knockouts of the centrosomal proteins, γ-tubulin and Sak are embryonically lethal (see 1.2) (Hudson *et al*., 2001, Yuba-Kubo *et al*., 2005). Due to the early lethality of these mice, it was has not been possible to study the role of these centrosomal proteins in aspects of later development. However, by various other means the centrosome has been shown to be important in development, particularly in the formation and function of the nervous system and in cell and tissue polarisation (Salas *et al*., 1997, Chang *et al*., 2006, Higginbotham and Gleeson, 2007).

1.5.1. Central nervous system development

Formation of the vertebrate nervous system is a complex process that is tightly regulated during development, and requires correct centrosomal function. In the developing mammalian neocortex of the central nervous system (CNS), similar to in other regions of the brain, neurons are generated from neural progenitor cells that reside in the proliferative ventricular zone (VZ) lining the ventricle of the neural tube (Donovan and Dyer, 2005). This VZ is composed of a layer of mitotically active neuroepithelial cells that eventually give rise to all cell types in the mature brain (Bayer and Altman, 1991). After mitosis, daughter cells then migrate towards the cortical surface. These progenitor cells can undergo two types of cell division, partly determined by the position of the centrosome (Higginbotham and Gleeson, 2007). Initially, most divisions are symmetric, generating two identical daughter cells that adopt a progenitor fate. As cortical development proceeds these cells then begin to undergo asymmetric division which produces two distinct daughter cells – one of which remains as a progenitor cell, the other specifying to a neuron. Towards the end of corticogenesis, progenitors can give rise to two neural daughter cells. The cell fate specification seems to be the result of cell cleavage plane orientation (Chenn *et al*., 1998).

This is regulated in part by the centrosomally localised heterotrimeric guanine-nucleotide binding proteins (G proteins) which are involved in signalling by exchanging guanosine molecules in biochemical reactions (Roychowdhury and Rasenick, 2008). It has been shown that the β and γ subunits of these proteins orientate the mitotic spindle perpendicular to the ventricular surface in the developing neocortex (Sanada and Tsai, 2005). Disrupting these proteins causes a shift of the mitotic spindle axis and results in the overproduction of neurons. Therefore, the G protein β and γ subunits are required for asymmetric cell fate choices of progenitors. Given that these proteins localise to the centrosome, it is likely that other centrosomal proteins may also be important in this process.

After proliferation and differentiation, post-mitotic neurons migrate to their specific locations in the CNS and are critical for the development of this system (Hatten, 2002). Cell migration is by leading edge extension, nuclear translocation into the leading edge and then retraction of the trailing process. The centrosome appears to be involved in all of these processes (Badano *et al*., 2005). Additionally, asymmetric centrosome-mediated dynamics in the early post-mitotic stage instruct neural polarity, as centrosomes cluster with the Golgi apparatus and endosomes to dictate the polarity of the first neuritic projection (de Anda *et al*., 2005). Hence, the centrosome contributes to neural proliferation, differentiation, migration and polarity.

1.5.2. Retinal development

Another well characterised region of the CNS is the retina. The vertebrate retina is a light sensitive tissue lining the inner surface of the eye, made up of many cell types that can be grouped into seven major classes produced in an evolutionary order (Donovan and Dyer, 2005). These seven classes can all arise from a single retinal progenitor cell, however there may be some retinal progenitor cells that have a bias for differentiating into a particular cell type (Cepko *et al*., 1996). Proliferation of retinal cells must therefore be strictly regulated such that there is a correct ratio of cell types. Indeed, uncoupling proliferation from cell fate specification can lead to many retinal diseases (Donovan and Dyer, 2005).

Structural details of the development of the mouse eye (including the retina) have been well described, but the localisation and role of the centrosome during the prenatal stages has not been investigated. In the developing chick retinal pigment epithelium, the centrosomal protein γ-tubulin has been shown to localise under the apical membrane from early in development, but the importance of this has not been assessed (Rizzolo and Joshi, 1993). However, strong evidence for the importance of the centrosome in the retina has come from a study that found that an in-frame deletion in the centrosomal protein CEP290 leads to early-onset retinal degeneration (Chang *et al*., 2006). The intracellular trafficking along microtubules, which is normally regulated by CEP290, is perturbed in mice with this deletion and this causes the mis-localisation of ciliary and phototransduction proteins. This results in photoreceptor degeneration in the retina. Hence, the centrosome links microtubule organisation and ciliary function in the retina, and plays a direct role in the disease state of retinal degeneration. Characterising the localisation of the centrosome and its constituents in the prenatal eye is therefore important in order to understand the role of this organelle in development and disease.

1.5.3. Polarisation

The centrosome is also thought to be important in the establishment and maintenance of polarity. Polarisation is a process used to specifically traffic proteins and organise cells into tissues and organs (Salas *et al*., 1997). Polarised epithelia line cavities and ducts in a variety of tissues and organs, creating physical barriers that separate adjacent biological compartments (Meads and Schroer, 1995). In these cells, the plasma membrane is composed of distinct apical and basolateral domains that face the lumenal and serosal environments respectively. An intact microtubule cytoskeleton and the apical distribution of centrioles and MTOCs are important in controlling this organisation (Meads and Schroer, 1995, Salas *et al*., 1997), implicating the centrosome in this process. Despite these implications, the role of the centrosome in polarisation has not been well studied. Given the

importance of polarisation in development and disease, it is crucial to understand the contribution of the centrosome to this process.

1.6. Centrosome function in disease

1.6.1. Centrosomes and cancer

Given its key functions in many aspects of development, it is not surprising that abnormal centrosome function is implicated in many diseases. Importantly, the incorrect function or localisation of centrosomal proteins can result in abnormal centrosome numbers. Consequently, because of the role of the centrosome in organising a bipolar spindle in order to segregate chromosomes into two daughter cells, abnormal centrosome numbers can result in multipolar spindles, cell division into multiple cells and therefore uncontrolled growth (Fukasawa, 2005). In support of this, centrosome amplification is a frequent event in almost all types of solid tumours and leads to aneuploidy and genomically unstable cells (Nigg, 2002, Sluder and Nordberg, 2004, Fukasawa, 2005).

The abnormalities in centrosome numbers that are commonly seen in cancer cells can arise from several mechanisms, including excessive rounds of centrosome duplication. This centrosome amplification often occurs following the loss of tumour suppressor genes, such as p53, as demonstrated in p53 deficient mice (Fukasawa *et al*., 1996). Normally, in response to DNA stress, p53 is up-regulated which in turn transactivates p21 to block the initiation of centrosome duplication. In cells lacking p53, p21 is not activated and centrosomes are allowed to duplicate excessively. Interestingly, in humans the loss of p53 is not sufficient for centrosome duplication, and also requires the over-expression of cyclin E due to more stringent checkpoint controls (Bunz *et al*., 2002). Other factors have also been shown to contribute to centrosome amplification, such as the inhibition of proteins involved in the DNA repair pathway (Bertrand *et al*., 2003). Regardless of the cause, excess centrosomes within a cell is an irreversible problem because there is no checkpoint for aborting mitosis in response to extra spindle poles (Sluder and Nordberg, 2004). Given that

the result of centrosome amplification is often uncontrolled cell growth and cancer promotion, this is inevitably deleterious to the organism.

1.6.2. Other centrosome related diseases

In addition to the role of the centrosome in cancer, it is also involved in various other cellular processes that are not necessarily associated with cell division (Badano *et al*., 2005). The ubiquitin-proteasome degradation pathway, neuronal migration, and microtubule transport are some of the processes targeted in these non-cell cycle, centrosome-related diseases.

1.6.2.1. Ubiquitin dependent proteasomal degradation

Although they are found throughout the cytosol, proteasomes (proteolytic complexes that degrade proteins) are concentrated at the centrosome and interact with γ-tubulin (Gordon, 2002). Mis-localisation of the proteasome away from the centrosome impairs the ubiquitin-proteasome pathway (Gordon, 2002). Dysfunction of the proteasome is evident in a number of neurodegenerative diseases, including Parkinson disease. This disease results from mutations in Parkin, an E3 ubiquitin ligase that can localise to the centrosome by binding to γ-tubulin, and targets proteins for degradation (Zhao *et al*., 2003). Hence, the centrosome may play a role in diseases characterised by the accumulation of proteins normally targeted for degradation via the ubiquitin-proteasome pathway.

1.6.2.2. Neuronal migration

Neural migration is crucial to the development of the mammalian CNS. The centrosome has been implicated in many aspects of neural migration, and it appears to be involved in several diseases resulting from defects in this migration (Badano *et al*., 2005). An example is lissencephaly, a disease which results in human brain malformations because of neural migration defects caused by mutations in the lissencephaly 1 gene (LIS1) (Hirotsune *et al*., 1998). The LIS1 protein localises to the centrosome and binds to centrosomal proteins and the microtubule-dependent motor protein dynein to regulate motor transport along the microtubules (Faulkner *et al*., 2000, Wynshaw-Boris and Gambello, 2001). LIS1 also facilitates the transport of newly synthesised microtubules from the centrosome to the

periphery of the cell to enable cell movement (Feng *et al*., 2000, Badano *et al*., 2005). The connection of LIS1 with the centrosome demonstrates the involvement of this organelle in diseases where microtubule transportation and neural migration are defective, such as lissencephaly.

1.6.2.3. Basal body and ciliary disease

The basal body is formed from a centriole and is a short cylindrical structure of microtubules that project cilia (microtubular hair-like structures) out from the cell to detect extracellular signals. Functionally, a number of centrosomal proteins localise to these structures at different phases of the cell cycle (Badano *et al*., 2005). The centrosome orchestrates and regulates cargo trafficking to maintain structural and functional ciliary integrity, since no protein synthesis occurs inside cilia. Defects in this process have been linked to a number of diseases, including Bardet-beidl syndrome (BBS) – a pleiotropic disorder that results in retinal degeneration, obesity, learning difficulties and malformations (Ansley *et al*., 2003). Hence, the centrosome also plays a role in ciliary disease. Given the rapidly growing identification of centrosomal proteins it is likely that the role of this organelle in different diseases will continue to grow, making it important for further study.

1.7. Zebrafish development

Given the early lethality of mouse knockout models of the centrosomal proteins γ-tubulin and Sak (Hudson *et al*., 2001, Yuba-Kubo *et al*., 2005), it has been difficult to study the role of the centrosome and its constituents during later stages of development in this species. Of importance to this project given the link of centrosomes to the cell cycle and cell division, zebrafish (*Danio rerio*) provide the opportunity to study early cell divisions and tissue specific cellular proliferation. This species is an ideal model for developmental studies due to the rapid growth and large numbers of translucent embryos. There is also a relatively simple approach to depleting genes of interest to varying degrees in these embryos, in order to assess their function in development. Additionally, identification of the genes that are important for cell division in eukaryotes has revealed that many of these genes are

highly evolutionarily conserved in zebrafish (Shepard *et al*., 2004). Hence zebrafish provide an excellent model system to study the role of centrosomal proteins during development.

1.7.1. The zebrafish cell cycle

In zebrafish, the first seven cell divisions are synchronous and cycle directly between the synthesis phase and mitosis. The midblastula transition (MBT) occurs during the tenth cell division (about 3 hours post fertilisation; hpf). From this stage on, cells also proceed through intermediary G phases, lose synchrony, have activated checkpoints and display cellular motility (Kane and Kimmel, 1993). As in other organisms, regulation of the cell cycle is critical in zebrafish development as shown by a large scale N-ethyl-N-nitrosourea (ENU) mutagenesis screen which identified a number of mutants in cell cycle genes (Kane *et al*., 1996). These early arrest mutants display phenotypes including mitotic arrest and abnormal nuclei, revealing their importance in development. Further support for the importance of cell cycle regulation in zebrafish comes from the mutant *cassiopeia* line that has a loss-of-function of the SCL-interrupting locus (*SIL*) gene, which is involved in cell cycle regulation and mitotic spindle organisation. These mutants are embryonically lethal, but before death display increased numbers of mitotic cells and have disorganised spindles often lacking one or both centrosomes (Pfaff *et al*., 2007). Hence the disruption of cell cycle regulatory genes in zebrafish causes cell cycle defects, including centrosomal abnormalities, similar to what has been observed in mammals.

1.7.2. Zebrafish neural development

An understanding of the development of the zebrafish nervous system is also pivotal to this study. As in mammals, zebrafish neural cells undergo fate decisions, control proliferation and differentiation, sense and interpret positional signals, establish polarity, regulate motility and adherence, and form axonal connections throughout the brain (Kimmel, 1993). Therefore the behaviour of neural cells is very dynamic, and must be orchestrated in a proper spatial and temporal manner. Zebrafish neurulation is initiated early in embryogenesis, and a solid neural tube becomes evident around the 6-10 somite stage (Kimmel, 1993). The neural lumen becomes visible around the 17 somite stage

(approximately 17 hpf), after which time the anterior neural tube dilates in three specific locations to form the future forebrain, midbrain and hindbrain ventricles (Lowery and Sive, 2005). Since zebrafish continue to grow throughout life, neurogenesis is thought to extend into adulthood (Woo and Fraser, 1995). Unlike in other vertebrates, dividing cells in zebrafish neurulation frequently contribute progeny to both sides of the neural tube (Papan and Campos-Ortega, 1999). This bilateral distribution is permitted by the perpendicular orientation of mitoses (Geldmacher-Voss *et al*., 2003). Outside of this specific feature, zebrafish neurulation is comparable to that of other vertebrates, and hence this species provides an ideal model to study the role of centrosomal proteins in this process.

1.7.3. Centrosomes during zebrafish development

Surprisingly, there have been limited studies on the centrosome during zebrafish embryogenesis and neural development. However, it has been shown that the core centrosomal protein γ-tubulin has a dynamic distribution during early zebrafish development, with a marked localisation to the primordial blastodisc (site of embryo development) upon maturation, suggesting that it may be important for development (Liu and Lessman, 2008). Functionally, depletion of the centrosomal protein Cep290 from zebrafish has been found to cause defects in the nervous and renal systems, and in the retina, due to its role in cilia (Sayer *et al*., 2006). More recently, the depletion of two novel centrosomal proteins, Cep70 and Cep131, was shown to result in zebrafish that still possessed centrosomes but had shortened and dysfunctional cilia (Wilkinson *et al*., 2009). The phenotype of these embryos resembles those of mutants for intraflagellar transport proteins (IFTs), with altered kidney and ear development and randomised left-right asymmetry, again due to defects in cilia. Hence, centrosomal proteins appear critical for normal ciliary development and function in zebrafish. Thus far, the role of centrosomes in other processes in zebrafish development have not been analysed. However, this species provides an excellent model to study centrosome function, and to further characterise zebrafish homologues of mammalian centrosomal proteins.

1.8. Nedd1

1.8.1. Nedd1 discovery

The *neural precursor cell expressed, developmentally down-regulated gene 1* (mouse: *Nedd1,* human: *NEDD1)* was originally discovered in a screen to identify genes highly expressed in early mammalian CNS development (Kumar *et al*., 1992). *Nedd1* was one of a set of ten genes identified from a mouse neural precursor cell derived library that had high levels of mRNA expression in the early embryonic brain (day 10) and was down-regulated during development. Of particular interest to this study, Nedd1 was originally detected as a 660 amino acid (aa) protein with a low level of expression in all tissues and cell lines analysed (Kumar *et al*., 1994). Over-expression of Nedd1 using viral vectors caused growth suppression, hence it was postulated that *Nedd1* may be a growth suppressor gene. At this time, the human cDNA (*NEDD1*) was also cloned and mapped to chromosome 12q22 by fluorescence *in situ* hybridisation (Takai *et al*., 1995). More than fifteen years after its discovery, a function of NEDD1 was elucidated. Initial observations in our laboratory, as well as two other laboratories have identified NEDD1 as a centrosomal protein that is critical for correct mitotic progression (Haren *et al*., 2006, Luders *et al*., 2006, Manning and Kumar, 2007). The centrosomal localisation of NEDD1 is consistent with an earlier report that found NEDD1 as a part of the human centrosome proteome (Andersen *et al*., 2003).

1.8.2. NEDD1 structure and homologues

A Clustal W2 analysis of NEDD1 sequences reveals that this protein is highly conserved in mammals (humans, chimpanzee, mouse and chicken shown) and among vertebrates as diverse as frogs and fish (Fig. 1.5A). There are also distantly related homologues in plants and invertebrates (sea urchin and fly shown). Indeed, the *Drosophila* homologue (Dgp71WD), the *Xenopus* homologue (XNEDD1), and the *Arabidopsis* homologue (NEDD1) have been characterised and have been shown to function similarly to mammalian NEDD1 (see 1.8.3 and 1.8.7) (Gunawardane *et al*., 2003, Verollet *et al*., 2006, Liu and Wiese, 2008, Zeng *et al*., 2009). Additionally, orthologues of this protein have been identified in earlier land plants such as mosses and lycophytes, suggesting that this protein is highly

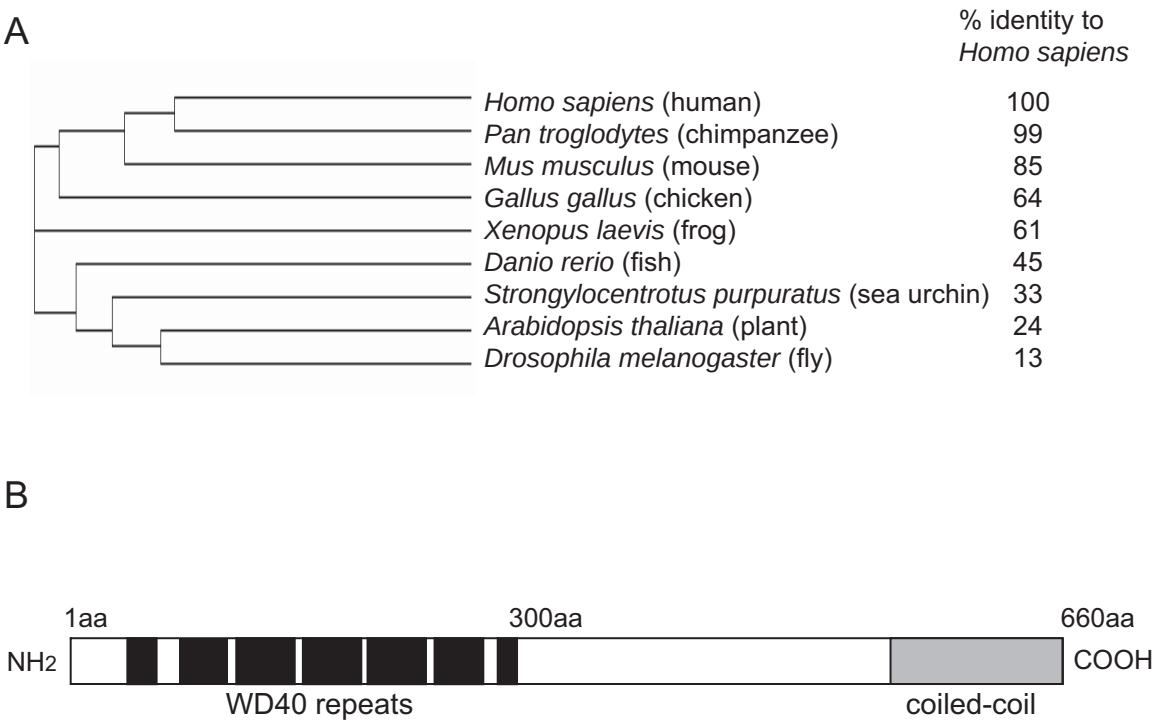

Fig. 1.5 Evolutionary conservation and structure of NEDD1

(**A**) NEDD1 protein sequences from different species identified by a BLAST search or published sequences, were aligned and sorted into a cladogram tree using Clustal W2 (see 2.2). The branches are of equal length, showing common ancestry but not evolutionary distance. The percentage of protein sequence identity to *Homo sapiens* NEDD1 was calculated in Clustal W2.

(**B**) A motif search of *Homo sapiens* NEDD1 was conducted using Scansite Motif Scan (see 2.2). NEDD1 contains seven WD40 repeats in the N-terminal half of the protein and a coiled-coil region in the 100 amino acids at the C-terminus.

evolutionarily conserved and evolved in ancient times (Zeng *et al*., 2009). The highest homology between various NEDD1 proteins lies in the WD40 domain containing N-terminal halves of the proteins, and in the C-terminal 100 amino acids which appear to encode a coiled-coil structure which is important for protein interactions (Fig. 1.5B and data not shown). WD40 domains are protein-protein interaction motifs found in a wide variety of eukaryotic proteins (Smith *et al*., 1999). These WD repeats form a propeller-like structure with several blades, each composed of a four-stranded anti-parallel β-sheet. This structure provides a platform for the binding of other proteins. Thus many WD40 proteins provide a scaffold for the recruitment of large protein complexes, and this is also likely to be the case for NEDD1.

1.8.3. Characterisation of the γTuRC

As NEDD1 is a centrosomal protein, it is important to recognise what is known about this organelle. Much of the current understanding of the centrosome and its functions has come from the study of one of its major constituents, γ-tubulin. γ-tubulin is an abundant protein found in MTOCs in components such as the centrosome, spindle poles, and in large protein complexes in the cytosol (Wiese and Zheng, 1999). Its primary function is microtubule nucleation, which is important in many cellular processes, including the formation of the mitotic spindle. A detailed characterisation of γ-tubulin has been conducted in *Drosophila melanogaster* (Verollet *et al*., 2006), and two main γ-tubulin complexes were identified in this species. The γ-tubulin small complex (γTuSC) is composed of two γ-tubulin molecules and two associated grip motif containing proteins Dgrip84 and Dgrip91. The other main γ-tubulin containing complex is the γ-tubulin ring complex (γTuRC). This is composed of the γTuSC, the Dgrips75, 128, 163, and a WD40 repeat region protein, Dgp71WD. Deletion of each of the individual Dgrip proteins of the γTuRC results in flies that are viable but have similar phenotypes including impaired assembly of the γTuRC, which leads to moderate mitotic defects (Verollet *et al*., 2006). Additionally, the females are sterile due to a failure to undergo normal oogenesis. Cells depleted of these components accumulate in prometaphase and most have over-condensed chromosomes. Depletion of Dgp71WD from

cells appears to have no affect on assembly of the γTuRC or the localisation of γ-tubulin at the centrosome. This protein does however bind directly to γ-tubulin and its depletion impairs the localisation of γ-tubulin along spindle microtubules and also disrupts mitosis, with an accumulation of cells in prometaphase as seen for depletion of the Dgrip proteins (Gunawardane *et al*., 2003). Dgp71WD mutant flies live to adulthood but have a shorter lifespan and the females are sterile (Verollet *et al*., 2006). From these studies it appears that Dgp71WD is dispensable for the assembly and recruitment of the γTuRC to the centrosome but is required for the function of this complex.

Mammals also possess a γTuRC, comprising of γ-tubulin and GCPs (γ-tubulin complex proteins) (Gunawardane *et al*., 2003). Previously, GCPs 2-6 had been identified in mammalian cells, and have been shown to function with γ-tubulin to nucleate microtubules (Murphy *et al*., 2001). Shortly after the onset of this study, NEDD1 (also named GCP-WD) was identified as part of the γTuRC, and as the mammalian homologue of Dgp71WD due to its similar structure, function and 21% overall identity (Haren *et al*., 2006, Luders *et al*., 2006).

1.8.4. Characterisation of mammalian NEDD1 function

Support for NEDD1 being part of the γTuRC comes from its ability to bind to components of the γTuRC. It has been shown that the 89 amino acids at the C-terminus of NEDD1 are required and sufficient for its interaction with the γTuRC (Luders *et al*., 2006). In contrast to Dgp71WD in *Drosophila*, the depletion of NEDD1 in mammalian cells causes an almost complete loss of γ-tubulin from the centrosome, whereas other centrosomal proteins are unaffected (Haren *et al*., 2006, Luders *et al*., 2006). NEDD1 depletion also causes a loss of γ-tubulin from the mitotic spindle. This indicates that mammalian NEDD1 mediates the localisation of the γTuRC to the centrosome and mitotic spindle. Consequently, similar to γ-tubulin depletion, the downstream consequences of NEDD1 depletion are dispersion of the MTOC, impaired centrosomal and chromatin nucleation of microtubules, mitotic chaos and cell cycle arrest (Haren *et al*., 2006, Luders *et al*., 2006). Since NEDD1 does not affect the

cytoplasmic localisation of γ-tubulin, cytoplasmic nucleation is not affected by the loss of NEDD1 (Luders *et al*., 2006). Additionally, it has been demonstrated that the phase of cell cycle arrest caused by NEDD1 depletion depends on the p53 status of the cells, as p53-positive cells arrest in G1 whereas p53-negative cells arrest in mitosis due to a lack of a functional G1/S checkpoint (Tillement *et al*., 2009). It also appears that NEDD1 is necessary for daughter centriole assembly during duplication or for centriole maturation, since one study showed that depletion leads to only one centriole at each pole (Haren *et al*., 2006). In combination, these results show that NEDD1 is a protein of critical importance in cell division and proliferation.

Interesting, not all of the detectable NEDD1 protein co-sediments with γ-tubulin in a sucrose gradient, the rest is found in low molecular weight fractions not associated with γ-tubulin (Luders *et al*., 2006). Currently, it is not known if this pool of NEDD1 has a separate function that is independent of γ-tubulin, or if it somehow becomes activated to bind to γ-tubulin at a later time. Investigating this pool of NEDD1 may reveal additional functions of this protein.

1.8.5. NEDD1 regulation

Since NEDD1 plays a critical role in the cell cycle, especially in mitosis, the activity and localisation of this protein must be strictly controlled in order for the cell cycle to progress normally. A common method of regulating proteins is by phosphorylation. Analysis of the sequence of NEDD1 reveals that it contains many possible phosphorylation sites. Previously, it was discovered that mammalian NEDD1 is phosphorylated during mitosis at a Cdk1 consensus site at serine 411 (referred to as S418 by Luders *et al*. due to an alternative start site) (Luders *et al*., 2006). A mutant S411A NEDD1 localises to the centrosome but not the spindle and displaces γ-tubulin from the spindle, indicating that phosphorylation at this site is important for the function of NEDD1 in mitosis. Recently, it has been shown that there are many additional sites of NEDD1 phosphorylation (Haren *et al*., 2009, Zhang *et al*., 2009). One study identified that Nedd1 is phosphorylated in mitosis by Cdk1 at T550, and this primes the protein for further phosphorylation by Plk1 at four

sites: T382, S397, S426 and S637 (Zhang *et al*., 2009). These post-translational modifications are required for the interaction of NEDD1 with Plk1, and have also been suggested to promote the interaction of NEDD1 with γ-tubulin and the resultant targeting of γ-tubulin to the centrosome (Fig. 1.6). However, although Plk1 is required for the localisation of NEDD1 and γ-tubulin to the centrosome, it was shown to not directly control these events and was suggested to involve the regulation of intermediate centrosomal proteins (Zhang *et al*., 2009). These intermediate proteins are likely to include Cep192, pericentrin and Cep215/Cdk5Rap2, as their centrosomal localisation has recently been shown to be disturbed in Plk1 depleted cells (Haren *et al*., 2009).

Indeed, these proteins as well as others are required for the correct localisation of NEDD1 and/or γ-tubulin (Fig. 1.6). Cdk5Rap2 and Cep72, although not studied in relation to NEDD1, are important for the targeting of γ-tubulin to the centrosome (Fong *et al*., 2008, Oshimori *et al*., 2009). Cep192 which is a major regulator of PCM recruitment, centrosome maturation and centriole duplication, is dependent on pericentrin for its centrosomal localisation during mitosis, and this is also required for the localisation of NEDD1 and γ-tubulin to the centrosome (Gomez-Ferreria *et al*., 2007, Zhu *et al*., 2008a). Additionally, the spindle associated protein FAM29A interacts with NEDD1 and is required for its localisation, as well as that of γ-tubulin, to the mitotic spindle (Zhu *et al*., 2008b). The interaction and regulation of NEDD1 by these upstream proteins is important for its correct function in recruiting the γTuRC to sites of microtubule nucleation, and hence promoting cell growth and division. NEDD1 has also been detected in a complex with the transcriptional co-activator p300 (Jung *et al*., 2005). This complex also contained proteins involved in DNA damage repair, and nuclear hormone receptor co-activators. The interaction of NEDD1 with p300 has not been confirmed, but this may suggest another role or method of regulation of NEDD1 that has yet to be discovered. The continued investigation into centrosomal dynamics and mitotic progression will unquestionably reveal additional proteins important in the regulation of NEDD1.

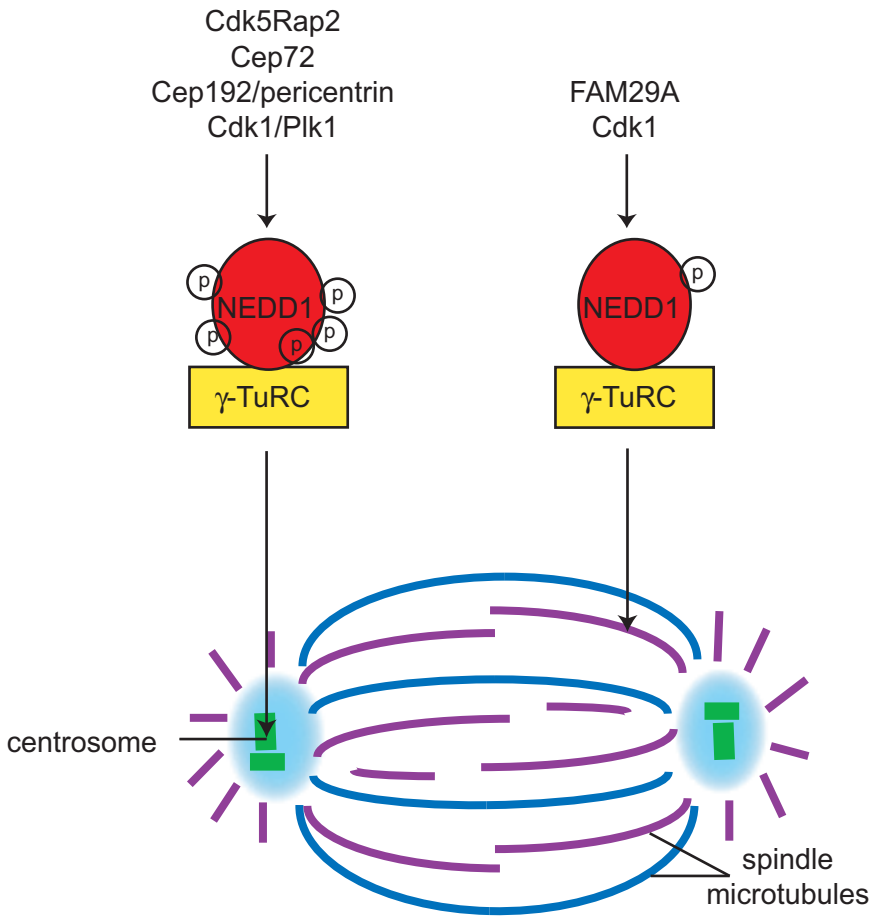

Fig. 1.6 Recruitment of the NEDD1/γ-TuRC to the centrosome and mitotic spindle

The NEDD1/γ-TuRC is targeted to the centrosome by several proteins including Cdk5Rap2, Cep72, Cep192 and pericentrin, and phosphorylation at multiple sites by Cdk1 and Plk1. The interaction of NEDD1 with FAM29A promotes the targeting of this complex to the mitotic spindle, as does the phosphorylation of NEDD1 at the consensus Cdk1 site at S411.

Additionally, *Nedd1* has recently been shown to be regulated at the mRNA level by the RNA binding protein Sam68, which is known to play a role in several aspects of RNA metabolism such as alternative splicing (Chawla *et al*., 2009) and nuclear export (Li *et al*., 2002). Male Sam68 knockout mice are infertile due to the aberrant differentiation of spermatids into spermatozoa (Paronetto *et al*., 2009). A number of testicular transcripts in these mice are down-regulated, most often of genes involved in the cell cycle or cell death, including *Nedd1*. Hence, it appears that Sam68 is required for the transcription of *Nedd1* mRNAs during male germ cell differentiation. Whether transcriptional control of Nedd1 is also important later in development, or in progression of the cell cycle, is currently unknown.

1.8.6. Nedd1 functional differences in various species

As described in sections 1.8.3 and 1.8.4, mammalian NEDD1 and the *Drosophila* homologue Dgp71WD appear to function slightly differently. Whilst the depletion of mammalian NEDD1 results in dramatically reduced amounts of γ-tubulin at the centrosome and spindle, Dgp71WD depletion does not affect γ-tubulin at the centrosome, but is important for its spindle localisation. There may be a number of explanations for this difference. Perhaps most plausible is that there may have been incomplete ablation of protein in the depletion of Dgp71WD from *Drosophila* cells, leaving enough endogenous Dgp71WD to recruit γ-tubulin effectively to the centrosome. However, there may be actual functional differences between the two species, possibly due to the fact that the C-terminal region of human NEDD1 that binds to γ-tubulin is highly conserved in many species, but only shares 12% identity with *Drosophila* Dgp71WD. A recent study explored the functional differences of NEDD1 further, using *Xenopus* egg extracts as a model system (Liu and Wiese, 2008). In this system, *Xenopus* NEDD1 (XNEDD1) depletion does not reduce the levels of γ-tubulin at the centrosome, similar to the *Drosophila* homologue, and the majority of XNEDD1 exists in a complex that does not contain γ-tubulin. The main effect of XNEDD1 depletion is a reduction in γ-tubulin localising to microtubules. From this study it was concluded that XNEDD1 is not required for the assembly, maintenance or recruitment of the

γTuRC to the centrosome, but rather is required for microtubule organisation. Whilst NEDD1 does play a role in microtubule organisation in mammalian cells, it is also important for the centrosomal localisation of γ-tubulin (Haren *et al*., 2006, Luders *et al*., 2006). Whether this is a true reflection of distinct functions of NEDD1 in different species, or merely a result of different experimental systems is currently unknown.

Recently, a *NEDD1* homologue in flowering plants (*Arabidopsis thaliana*) was identified (Zeng *et al*., 2009). This gene was shown to be essential in this species, as no homozygous *NEDD1* mutant offspring could be recovered from a T-DNA insertion mutant. Normally, plants undergo asymmetrical cell division to create a small generative cell and a large vegetative cell (Lee *et al*., 2007). Plants containing mutant non-functional *NEDD1* display compromised asymmetric division, resulting in the absence of generative cells and failed gametogenesis. Additionally, there is a collapse in microtubule organisation in the phragmoplast. This is a structure that forms during late cytokinesis and serves as a scaffold for cell plate assembly and subsequent formation of a new cell wall separating the two daughter cells (Otegui *et al*., 2005). This is similar to what is observed in cells lacking γ-tubulin (Pastuglia *et al*., 2006), and results in a failure of cytokinesis and pollen grains lacking sperm cells (Zeng *et al*., 2009). Therefore, NEDD1 in plants is required for the function of γ-tubulin in organising microtubules. As this species does not contain centrosomes, the effect of the non-functional NEDD1 mutant on γ-tubulin localisation to this organelle could not be analysed. However, plants display microtubule nucleation at other MTOCs, and it would be interesting to analyse whether γ-tubulin localisation to these sites is affected in this *Arabidopsis* NEDD1 mutant.

It is also interesting that some plants appear to contain multiple NEDD1 homologues (Zeng *et al*., 2009). The lycophyte *Selaginella moellendorffii* and the moss *Physcomitrella patens* contain two and four NEDD1 homologues respectively. As NEDD1 in these species has not been investigated, the function of these different NEDD1 family members is currently unknown. However, it is possible that they regulate the γTuRC differently, and if so, this may

support the functional differences of NEDD1 in the species discussed in this chapter. Regardless of the observed differences between species, which could be resolved with further analysis, all studies have shown that NEDD1 is important for microtubule organisation and the correct progression through mitosis, and hence is a crucial protein in cell growth and division.

1.9. Summary and project aims

At the beginning of this study, NEDD1 was a protein of unknown function. Observations from our laboratory and others have now shown that NEDD1 is a centrosomal protein, which functions primarily as a recruitment factor for the γTuRC, to enable microtubule nucleation and organisation. This microtubule organisation is critical for mitosis to proceed correctly and hence for cell proliferation, and presumably organism development. However, as a still relatively novel protein, there is not much known about the role of NEDD1 during development, and its function in processes other than microtubule organisation. Additionally, there are some unexplained variations in the function of NEDD1 in different species. Thus the primary aims of this research were to:

1. Evaluate the localisation and expression of Nedd1 during mammalian development.
2. Evaluate the regulation of Nedd1 during the cell cycle and its contribution to senescence.
3. Further evaluate the interaction of NEDD1 with γ-tubulin and other potential binding partners.
4. Evaluate the importance and physiological roles of NEDD1 during development using zebrafish as a model system.

2. Materials and Methods

2.1. Materials

All chemical reagents were of analytical grade (or the highest grade obtainable) and purchased from Sigma unless stated otherwise.

2.2. *In silico* analysis

Alignments and phylogenetic trees were conducted using Clustal W2 (http://www.ebi.ac.uk/Tools/clustalw2/index.html) (Larkin *et al*., 2007). Protein tertiary structure was assessed using Predict Protein (www.predictprotein.org) (Rost *et al*., 2004), and the helical wheel identified using Mobyle@Pasteur (http://mobyle.pasteur.fr/cgi-bin/portal.py?form=pepwheel) (Rice *et al*., 2000). Protein motif searches were conducted with Scansite Motif Scan (http://scansite.mit.edu/motifscan_seq.phtml) (Obenauer *et al*., 2003). Intron/exon boundaries were retrieved from ensembl (http://www.emsembl.org).

2.3. DNA manipulation

2.3.1. DNA quantification

DNA concentration was measured using a NanoDrop1000 spectrophotometer (Thermo Scientific), assuming that an optical density (OD) of 1.0 correlates to 50 μg/ml of DNA.

2.3.2. Restriction endonuclease digestion

DNA was digested using appropriate restriction endonucleases (New England Biolabs) at 5 units of enzyme/μg DNA in a total volume of 10 μl containing 1x digestion buffer (New England Biolabs), 0.1 mg/ml bovine serum albumin (BSA) and MQ H_2O for 1h at 37ºC. Reactions were stopped by the addition of 10x DNA loading dye (0.25% bromophenol blue, 0.25% xylene cyanol, 30% glycerol) to a final concentration of 1x, followed by gel electrophoresis.

2.3.3. Electrophoresis of DNA

DNA was analysed by electrophoresis in 0.7 – 2% agarose gels in TAE buffer (Tris-Ac-EDTA: 40 mM Tris-acetate, 1 mM EDTA pH 8.0), depending on the expected DNA fragment size. Prior to electrophoresis, DNA loading buffer to a final concentration of 1x was added to samples, then loaded onto gels immersed in TAE buffer. Electrophoresis was performed at 100 volts. DNA was stained with ethidium bromide solution (2 μg/ml) and visualised under ultraviolet light on a transilluminator at 254 nm (BTS-20.M, UVItec).

2.3.4. Purification of DNA from solution or agarose

To purify DNA in solution, the UltraClean™ PCR Clean-up Kit was used (Mo Bio Laboratories), according to the manufacturers' instructions. To purify DNA from agarose, the UltraClean™ GelSpin DNA Purification Kit was used (Mo Bio Laboratories), according to the manufacturers' instructions.

2.3.5. Phenol/chloroform DNA purification

To purify DNA to be used for RNA synthesis, the DNA solution was made up to 100 μl in sterile MQ H_2O, 100 μl phenol/chloroform (1:1) added to the tube and vortexed thoroughly for 15 sec. The aqueous and solvent layers were separated by centrifugation at 16000*x*g for 10 min. The upper aqueous phase was transferred to a new tube and precipitated with 2 volumes of ethanol, 0.1 volumes of 3 M NaAc pH 4.6, 1 μl glycogen (Roche) and incubated for 30 min at -70 ºC. DNA was pelleted by centrifugation at 16000*x*g for 10 min and the pellet washed in 70% ethanol. The pellet was air dried and resuspended in 20-50 μl sterile MQ H_2O.

2.3.6. Dephosphorylation of vector DNA and ligation with inserts

After restriction endonuclease digestion of vector DNA, 1 μl of calf alkaline phosphatase (Roche) was added directly to the digestion reaction and incubated for a further 30 min at 37ºC. DNA fragments to be ligated were placed in a mix (total volume 10 μl) containing 1 unit of T4 DNA ligase (New England Biolabs) and 1x ligation buffer (New England Biolabs) then incubated overnight at 4°C.

2.3.7. pGEM-T-Easy cloning

Cloning into the pGEM-T-Easy vector (Promega) was conducted according to the manufacturers' instructions. Prior to ligation, PCR was conducted using the Expand High Fidelity PCR System (Roche) in order to generate 3' A overhangs according to the manufacturers' instructions.

2.3.8. Gateway Cloning

TOPO cloning into the entry vector was conducted using the pENTR-SD/D-TOPO Cloning Kit (Invitrogen), according to the manufacturers' instructions. Transfer into the destination vector was conducted using Gateway LR Clonase II enzyme mix (Invitrogen), according to the manufacturers' instructions.

2.3.9. Preparation and transformation of chemically competent Escherichia coli

5 ml of Ψ broth (20 g/L Bacto-tryptone [BD Biosciences], 5 g/L Bacto-yeast extract [BD Biosciences], 5 g/L $MgSO_4$, adjusted to pH 7.6 with KOH) was inoculated with a single *Escherichia coli* (*E. coli*) colony (*DH5*α or *TOP10* strains) and grown overnight at 37°C with shaking. This was subcultured into 100 ml of Ψ broth and grown for 90 min at 37°C with shaking. The culture was then chilled on ice for 15 min and the cells harvested by centrifugation at 5000*x*g for 15 min at 4°C. The medium was aspirated and the cells resuspended in 40 ml of ice-cold TfbI (30 mM KOAc, 100 mM KCL, 10 mM $CaCl_2.2H_20$, 50 mM $MnCl_2.4H_20$, 15% glycerol, adjusted to pH 5.8 with 0.2 M CH_3COOH and filter sterilised), on ice for 5 min. Cells were pelleted at 5000*x*g, resuspended in 4 ml of ice-cold TfbII (10 mM MOPS, 75 mM $CaCl_2.2H_20$, 10 mM KCL, 15% glycerol, adjusted to pH 6.5 with 0.5 M KOH and filter sterilised). Cells were incubated on ice for 15 min and then transferred as 50 μl aliquots into pre-chilled 1.5 ml microfuge tubes on dry ice. Aliquots were stored at -70°C.

For transformation, chemically competent *E. coli* cells were thawed on ice for 5 min. 5 μl of ligation mix was added to cells and incubated on ice for 30 min. Cells were heat shocked for

80 sec at 42°C and cooled on ice for 2 min. 200 μl of Luria-Bertani broth (LB, 1% [w/v] bacto-tryptone, 0.5% yeast extract, 1% NaCl, pH 7.0) was added and the culture incubated at 37°C with shaking. 100 μl of the cell suspension was plated onto L-agar plates (LB + 15 g/L Bacto-agar [BD Biosciences]) supplemented with the appropriate antibiotics for vector encoded resistance (100 μg/ml ampicillin, 25 μg/ml kanamycin, or 34 μg/ml chloramphenicol) and incubated overnight at 37°C. For vectors encoding genes for blue/white selection, 4 μl of 1 M isopropylthio-β-thiogalactosidase (IPTG) (Progen) and 40 μl of 20 mg/ml 5-bromo-4-chloro-3-indolyl-β-D-galactosidase (X-gal) (Progen) were spread onto plates prior to plating the transformants.

2.3.10. Plasmid purification

DNA for restriction digestion and sequencing was prepared using mini-prep columns (Mo Bio Laboratories) according to manufacturers' instructions, using 1.5 ml of overnight culture. High quality plasmid DNA was prepared using midi-prep columns (Qiagen), according to manufacturers' instructions, using 100 ml of overnight culture.

2.4. DNA amplification and sequencing

2.4.1. Primer design

All primers were purchased from Geneworks. Oligonucleotides were received as dried pellets and were resuspended at 100 ng/μl in sterile MQ H_2O. Restriction enzyme sites are shown in bold, the start or end of the gene specific product underlined, and the mutated codons are in italics. All primers are given in the 5' to 3' direction.

p21 mRNA expression (qPCR):

1. QPCRmp21f	AGTGTGCCGTTGTCTCTTCG
2. QPCRmp21r	ACACCAGAGTGCAAGACAGC
3. GAPDHf	AGACAGCCGCATCTTCTTGT
4. GAPDHr	GAATTTGCCGTGAGTGGAGT

Generating myc-tagged NEDD1 constructs:

5. hmNd1BglII	AAACCTCAG
6. hND1XhoI	CG**CTCGAG**TCAAAAGTGGGCCCG
7. hND1572BglI	TATGGCCGACAGCATTGG
8. hND1571XhoI	CCG**CTCGAG**TCATATTTTTTCTGAGAG

Generating His- and GST-tagged NEDD1/γ-tubulin constructs:

9. gTubNdeIf	**CATATG**CCGAGGGAAATCATC
10. gTubBglIIr	**ATCT**TCACTGCTCCTGGG
11. hNd1572SalIf	**GTCGAC**GCCGACAGCATTGG
12. hNd1NotIr	G**GCGGCCGC**TCAAAAGTGGGCCCG

Generating GFP-tagged NEDD1 constructs (TOPO Gateway cloning):

13. hNd1TOPOf	CACCATGCAGGAAAACCTC
14. hNd1TOPO572f	CACCATGGCCGACAGCATTGG
15. hNd1TOPO635f	CACCATGAGATACTCAGTGAATG
16. hNd1TOPO586f	CACCATGTCCATTCAAATTCG
17. hNd1TOPO599f	CACCATGACGTTGGATGACTT
18. hNd1TOPO611f	CACCATGATTGTTAATTTGC
19. hNd1TOPO625f	CACCATGCAACTGAATGAAATGC
20. hNd1634Xho1r	CCG**CTCGAG**TCATTCCAGCAAAGAATGC
21. hNd1571Xho1r	CCG**CTCGAG**TCATATTTTTTCTGAGAG

Mutagenesis of NEDD1:

22. hNd1L642Qf	CTCAGTGAATGAAGGT*CAA*GTGGCTGAAATTGAAAG
23. hNd1L642Qr	CTTTCAATTTCAGCCAC*TTG*ACCTTCATTCACTGAG
24. hNd1L649Qf	GTGGCTGAAATTGAAAGA*CAA*CGAGAAGAAAAC
25. hNd1L649Qr	GTTTTCTTCTCG*TTG*TCTTTCAATTTCAGCCAC
26. hNd1L656Qf	GAAGAAAACAAAAGA*CAA*CGGGCCCACTTTTG
27. hNd1L656Qr	CAAAAGTGGGCCCG*TTG*TCTTTTGTTTTCTTC

Generating V5-tagged junction plakoglobin:

28. PlakoTOPOERIf	CACCC**GAATTC**GGGAGGTGATGAACCTG
29. PlakoXhoIr	CG**CTCGAG**CTAGGCCAGCATGTG

Cloning zNEDD1 from cDNA for antibody production and *in situs*:

30. zNEDD1SalIf	GCGC**GTCGAC**CGAGGACGTCACACGG
31. zNEDD1FLSalIf	GCGC**GTCGAC**GAGCCCAGCGGCGTG

32. zNEDD1SalIf ATGGC**GTCGAC**CATGGAGGACGTCAC

33. zNEDD1422r CCGCTAGTGGAGCC

Creating myc-tagged zNEDD1 constructs:

34. zNEDD1NotIr AATT**GCGGCCGC**CTAATAGTTGGCTCG

35. zNEDD1598SalIfmyc GC**GTCGAC**CGCTCCACTCACTTC

36. zNEDD1615SalIfmyc GC**GTCGAC**CGCACTGGAGGACTTC

37. zNEDD1614NotIr CC**GCGGCCGC**CTACTCATGAATCATGTTAC

38. zNEDD1597NotIr CC**GCGGCCGC**CTAAGACTCCACTGCTGC

39. zNEDD1588SalIfmyc GC**GTCGAC**CGCTGCTGCTCCAGCC

40. zNEDD1444SalIfmyc GC**GTCGAC**CGACATTTTCTCCCCT

Sequencing (in addition to previous primers described):

41. zNEDDD1seq698r CAGACGATCTTCTTGTCC

42. zNEDDD1seq1274f GGGAAGCAGAAGGACAGC

43. zNEDDD1seq551f GTGGATCTGTGGCCCTTTGG

44. JUPseq679f GGCATCCCTGCTCTGGTC

45. JUPseq1247r CCAACCTGACATGCAACAAC

46. pCMV-f CTCAAACCTGTTTGGTGTTG

47. pCMV-r GATCCGGTACTAGAGGAACTGAAAAAC

48. pGEX5' GGGCTGGCAAGCCACGTTTGGTG

49. pGEX3' CCGGGAGCTGCATGTGTCAGAGG

50. T7 TAATACGACTCACTATAGGG

51. SP6 CATTTAGGTGACACTATAG

2.4.2. Polymerase Chain Reaction (PCR)

Pfu polymerase (Stratagene) was used in all cloning reactions due to its high proof reading activity. DNA was synthesised using 100 ng plasmid DNA template, or 5 μl cDNA product, 2.5 units *Pfu* polymerase, 100 ng forward and reverse primers, 0.2 mM dNTPs in 1x *Pfu* PCR buffer (Stratagene) in a total volume of 50 μl sterile MQ H_2O. Reactions were performed on a Mastercycler (Eppendorf), with the following conditions: 2 min at 95°C, followed by 30 cycles of 95°C for 30 sec, 58°C for 30 sec and 72°C for 1 min/kb, followed by a final 10 min extension at 72°C. All reactions were held at 15°C.

2.4.3. cDNA synthesis

2 μg of total RNA was used to synthesise cDNA using the High-Capacity cDNA Reverse Transcription Kit (Applied Biosystems) according to the manufacturers' instructions.

2.4.4. qPCR

Samples for qPCR (quantitative PCR) were prepared from cDNA using the RT² SYBR Green qPCR Master Mix (SA Biosciences) according to the manufacturers' instructions. Samples were run on a Rotor Gene 6000 machine (Corbett Research) with the following conditions: 2 min at 50°C, 15 min at 95°C, followed by 40 cycles of 95°C for 15 sec, 60°C for 25 sec and 72°C for 10 min, followed by a 3 min extension at 72°C. Melt curve was achieved by a ramp from 72°C to 99°C with 5 sec for each step. Reactions were performed in triplicate and the mRNA expression levels normalised against the internal control gene *GAPDH* using the $\Delta\Delta C_T$ method. Data was analysed using the Rotor-Gene 6000 Series Software (Corbett Research). This experiment was performed by Dimitrios Cakouros.

2.4.5. Site-directed mutagenesis

Mutation of 1-3 DNA bases was conducted using the Quikchange Site-Directed Mutagenesis Kit (Stratagene) according to the manufacturers' instructions. 5 μl of the reaction was checked on a 1% agarose gel and transformed into *DH5α* chemically competent *E. coli* cells. Plasmid DNA was extracted by mini-prep (2.3.10) and sequenced (2.4.6) to confirm the presence of the desired mutations.

2.4.6. DNA sequencing

The sequence of all DNA constructs was verified using the BigDye Terminator v3.1 Cycle Sequencing Kit (Applied Biosystems). DNA from the sequencing reactions (10 μl) contained 1μl BigDye Terminator v3.1, 1 μl supplied BigDye buffer (10x), 100 ng sequencing primer and 200 ng template DNA. The sequencing reaction (1 min activation at 96ºC, 25 cycles of 10 sec at 96ºC, 5 sec of 50ºC and 4 min at 60ºC) was precipitated with 40 μl 75% isopropanol for 15 min at room temperature (RT) and centrifuged for 20 min at 16000*x*g. The precipitated DNA was then washed with 125 μl 75% isopropanol and centrifuged again

at 16000*x*g for 5 min. The supernatant was discarded and the pellet air-dried. DNA sequencing products were analysed using an ABI Prism 3730 DNA Analyser by the Molecular Pathology Division (IMVS, Adelaide).

2.5. DNA constructs

2.5.1. Purchased vectors

pCMV-Myc (Clontech)
pcDNA3.1/nV5-DEST (Invitrogen)
pcDNA3.1 (+) (Invitrogen)
pBlueScript KS- (Stratagene)
pcDNA-DEST53 (Invitrogen)
pET-15b (Novagen)
pGEX-4T-3 (Amersham Biosciences)
pGEX-2T-2 (Amersham Biosciences)
pENTR-SD/D-TOPO (Invitrogen)
pGEM-T-Easy (Promega)
pCMV6-XL5-junction plakoglobin (human cDNA TrueClone for junction plakoglobin, transcript variant 1, OriGene)

2.5.2. Mammalian expression constructs

pCMV-Myc-NEDD1 (1-660 aa) primers 5, 6
pCMV-Myc-NEDD1 (1-571 aa) primers 5, 8
pCMV-Myc-NEDD1 (572-660 aa) primers 6, 7

Full length (FL: 1-660 aa) or various regions of NEDD1 were PCR amplified and cloned into *Bgl*II/*Xho*I of pCMV-Myc to create various NEDD1 constructs fused to an N-terminal myc-tag. These constructs were used for immunoprecipitations.

pcDNA3.1/nV5-DEST-junction plakoglobin primers 28, 29

Junction plakoglobin was PCR amplified from pCMV6-XL5-junction plakoglobin and cloned into the entry vector pENTR-SD/D-TOPO and then the destination vector pcDNA3.1/nV5-DEST using the Gateway system (Invitrogen) to create an N-terminal V5-tagged construct. This construct was used for immunoprecipitations.

pcDNA-DEST53-NEDD1 (1-660 aa) primers 6, 13
pcDNA-DEST53-NEDD1 (1-571 aa) primers 8, 13
pcDNA-DEST53-NEDD1 (572-660 aa) primers 6, 14
pcDNA-DEST53-NEDD1 (572-634 aa) primers 14, 20
pcDNA-DEST53-NEDD1 (635-660 aa) primers 6, 15
pcDNA-DEST53-NEDD1 (625-660 aa) primers 6, 19
pcDNA-DEST53-NEDD1 (611-660 aa) primers 6, 18
pcDNA-DEST53-NEDD1 (586-600 aa) primers 6, 16
pcDNA-DEST53-NEDD1 (599-600 aa) primers 6, 17

FL (1-660 aa) or various regions of NEDD1 were PCR amplified from pCMV-Myc-NEDD1 (1-660 aa) and cloned into the entry vector pENTR-SD/D-TOPO and then the destination vector pcDNA-DEST53 using the Gateway system to create different regions of NEDD1 fused to an N-terminal GFP-tag. These constructs were used for immunoprecipitations and localisation studies.

pCMV-Myc-NEDD1 (L642Q) primers 22, 23
pCMV-Myc-NEDD1 (L649Q) primers 24, 25
pCMV-Myc-NEDD1 (L656Q) primers 26, 27

Wild type (WT) pCMV-Myc-NEDD1 was used as a template to create various mutant NEDD1 constructs fused to an N-terminal myc-tag. These constructs were used for immunoprecipitations.

pCMV-Myc-NEDD1 (L642Q/L649Q) primers 24, 25
pCMV-Myc-NEDD1 (L642Q/L656Q) primers 26, 27

pCMV-Myc-NEDD1 (L642Q) was used as a template to create various double mutant NEDD1 constructs fused to an N-terminal myc-tag. These constructs were used for immunoprecipitations.

pCMV-Myc-NEDD1 (L642Q/L649Q/L656Q) primers 26, 27

pCMV-Myc-NEDD1 (L642Q/L649Q) was used as a template to create a triple mutant NEDD1 construct fused to an N-terminal myc-tag. This construct was used for immunoprecipitations.

pcDNA-DEST53-NEDD1 (572-660 aa) (L642Q) primers 22, 23

pcDNA-DEST53-NEDD1 (572-660 aa) was used as a template to create a mutant NEDD1 construct fused to an N-terminal GFP-tag. This construct was used for localisation studies.

pcDNA-DEST53-NEDD1 (572-660 aa) (L642Q/L649Q) primers 24, 25

pcDNA-DEST53-NEDD1 (572-660 aa) (L642Q) was used as a template to create a double mutant NEDD1 construct fused to an N-terminal GFP-tag. This construct was an intermediate in cloning the triple mutant construct.

pcDNA-DEST53-NEDD1 (572-660 aa) (L642Q/L649Q/L656Q) primers 26, 27

pcDNA-DEST53-NEDD1 (572-660 aa) (L642Q/L649Q) was used as a template to create a triple mutant NEDD1 construct fused to an N-terminal GFP-tag. This construct was used for localisation studies.

pCXN2-NEDD1

This construct, of NEDD1 fused to a C-terminal flag-tag in the pCXN2 vector, was created by Paul Colussi. This construct was used for immunoprecipitation before the silver stain gel.

pcDNA3.1-zNEDD1

pBlueScript KS-zNEDD1 Promoter + open reading frame (ORF) was used to digest out zNEDD1 at *Kpn*I/*Not*I and insert into *Kpn*I/*Not*I of pcDNA3.1 This construct was used for testing the zNEDD1 antibody, immunoprecipitations and localisation studies.

pCMV-Myc-zNEDD1 (1-676 aa)	primers 30, 34
pCMV-Myc-zNEDD1 (1-598 aa)	primers 30, 38
pCMV-Myc-zNEDD1 (1-614 aa)	primers 30, 37
pCMV-Myc-zNEDD1 (598-676 aa)	primers 34, 35
pCMV-Myc-zNEDD1 (614-676 aa)	primers 34, 36
pCMV-Myc-zNEDD1 (588-676 aa)	primers 34, 39
pCMV-Myc-zNEDD1 (444-676 aa)	primers 34, 40

pBlueScript KS-zNEDD1 ORF was used as a template to PCR amplify FL (1-676 aa) or various regions of zNEDD1 and clone into *Sal*I/*Not*I of pCMV-Myc to create N-terminal myc-tagged constructs. These constructs were used for immunoprecipitations.

2.5.3. Bacterial expression constructs

pET-15b-γ-tubulin primers 9, 10

γ-tubulin was PCR amplified from HEK293T cDNA and cloned into *Nde*I/*Bgl*II of pET-15b to create an N-terminal histidine (His)-tag. This construct was used to assess direct interactions.

pGEX-4T-3-NEDD1 (572-660 aa) primers 11, 12

NEDD1 (572-660 aa) was PCR amplified from pCMV-Myc-NEDD1 (1-660 aa) and cloned into *Sal*I/*Not*I of pGEX-4T-3 to create an N-terminal GST-tag. This construct was used to assess direct interactions.

pGEX-4T-3-NEDD1 (572-660 aa) (L642Q) primers 22, 23
pGEX-4T-3-NEDD1 (572-660 aa) (L642Q/L649Q) primers 24, 25
pGEX-4T-3-NEDD1 (572-660 aa) (L642Q/L656Q) primers 26, 27
pGEX-4T-3-NEDD1 (572-660 aa) (L642Q/L649Q/L656Q) primers 26, 27

pGEX-4T-3-NEDD1 (572-660 aa) was used as a template to create various mutant NEDD1 (572-660 aa) constructs fused to an N-terminal GST-tag. These constructs were used to assess direct interactions.

pGEX-2T-2-zNEDD1 (425-676 aa)

pBlueScript KS-zNEDD1 ORF was used to digest out zNEDD1 at *Xho*I/*Not*I and insert into *Sal*I/*Not*I of pGEX-2T-2. This construct was used to produce the GST-zNEDD1 antigen injected into rabbits to generate the zNEDD1 antibody.

2.5.4. Cloning/transcription constructs

pBlueScript KS-zNEDD1 ORF (1-676 aa) primers 30, 34

zNEDD1 ORF was PCR amplified from cDNA made from 24 hpf WT zebrafish embryos and cloned into *Sal*I/*Not*I of pBlueScript KS-. This construct was used as a template for generating the antigen for antibody production.

pBlueScript KS-zNEDD1 Promoter + ORF primers 31, 34

zNEDD1 promoter region + ORF was PCR amplified from cDNA made from 24 hpf WT zebrafish embryos and cloned into *Sal*I/*Not*I of pBlueScript KS-. This construct was used as a template for making the pcDNA3.1-zNEDD1 mammalian expression construct and to generate capped mRNA for zebrafish injections.

pGEM-T-Easy-zNEDD1 (1-422 aa) primers 32, 33

pBlueScript KS-zNEDD1 Promoter + ORF was used as a template to PCR amplify zNEDD1 (1-422 aa) and clone it into pGEM-T-Easy. This construct was used as a template for *in situ* probes.

2.6. RNA analysis

2.6.1. Preparation of diethylpyrocarbonate treated H_2O

1 ml of diethylpyrocarbonate (DEPC) was added to 1 L MQ H_2O, mixed and left overnight at 37ºC. The solution was then autoclaved and cooled to RT before use.

2.6.2. Total RNA preparation

For RNA extraction from cells, cells were scraped off the tissue culture flasks, counted (see 2.7.1), pelleted at 4000*x*g in a microcentrifuge and resuspended in 1 ml TRIzol reagent (Invitrogen) per 5-10x10^6 cells. For RNA extraction from zebrafish, 50 embryos were anesthetised in tricaine (see 2.10.2), snap frozen in liquid nitrogen and lysed in 500 μl TRIzol. TRIzol RNA preparation was conducted according to the manufacturers' instructions (Invitrogen).

2.6.3. RNA gel electrophoresis

5 μl of RNA samples were mixed with formaldehyde running buffer (4 μl formaldehyde, 10 μl formamide, 2.5 μl 10x MOPS solution [1x: 20 mM MOPS, pH 7.0, 1mM EDTA pH 8.0, 8mM NaAc], 1 μl ethidium bromide [400 μg/ml]) and denatured for 10 min at 65 ºC. Samples were chilled on ice and 2 μl RNA loading dye added (50% glycerol, 1mM EDTA pH 8.0, 0.25% bromophenol blue, 0.25% xylene cyanol). 5 μl 0.5-10 kb RNA ladder (Invitrogen) was also treated as above. Samples were loaded onto a 1.5% agarose gel containing 1x MOPS and 2.2 M formaldehyde in DEPC-treated H_2O, and electrophoresed dry (with buffer just below the level of the gel) in 1x MOPS buffer. Gels were electrophoresed at 80 volts for 2 h. The gel was washed several times in sterile MQ H_2O prior to scanning with a FluorImager 595 (Molecular Dynamics) with a 610 nm filter.

2.6.4. RNA quantification

RNA concentration was measured using a NanoDrop1000 spectrophotometer (Thermo Scientific), assuming that an optical density (OD) of 1.0 correlates to 40 μg/ml of RNA.

2.7. Tissue culture and cellular analysis

2.7.1. Cell lines and culture

Mouse embryonic fibroblasts (MEFs) were isolated from E14.5 C57Bl/6 embryos by Lien Ho (Ho *et al*., 2009). MEFs, mouse spontaneously immortalised fibroblasts (NIH-3T3s), mouse neuroblastoma cells (N18) and human cervical cancer cells (HeLa) were cultured in Dulbecco's Modified Eagle's Medium (GIBCO) supplemented with 10% fetal bovine serum (FBS, GIBCO), 50 units/ml penicillin, 0.05 mg/ml streptomycin at 37^{o}C in 5% CO_2. Human immortalised T lymphocyte cells (Jurkat) and human embryonic kidney cells (HEK293T) were cultured in RPMI-1640 (GIBCO) with the same supplements. Other cells lines used for protein extraction were retrieved from liquid nitrogen and not cultured. These included human leukemic cell lines (K562 and CEM), human breast cancer cell lines (MCF7, T47D, MDA-468 and MDA-231), and mouse embryonic carcinoma cell lines (P19 and PCC4). Cell

culture was carried out in Class II biohazard laminar flow hoods (Gelman Sciences) and cells were maintained in log phase. Cell density was calculated using a haemocytometer and viability determined by trypan blue (0.8% w/v in phosphate buffered saline [PBS], pH 7.4) dye exclusion. To passage cells, medium was aspirated, cells rinsed in PBS and detached by incubation in trypsin (0.054% w/v trypsin [Difco] in Hank's balanced salt solution [GIBCO]). Following treatment with trypsin for several min, cells were removed to a tube in complete medium and spun down in a centrifuge for 5 min at 400*x*g. The cell pellet was resuspended in complete medium and the cells seeded into fresh dishes or flasks.

2.7.2. Calculation of doubling time

Population doubling time was calculated using the formula: $\ln 2/(\ln[A/A_0])/t$ where A = cell number at t = 0, A_0 = initial cell number, t = time (hours since last passage).

2.7.3. Cryopreservation and thawing of cells

Cells in log phase were harvested, pelleted by centrifugation at 400*x*g for 5 min and resuspended in complete medium at $5x10^6$ cells/ml. 500 μl of cryoprotectant (30% FBS/20% dimethyl sulphoxide, 50% media) was added to a 500 μl aliquot of cells in cryopreservation tubes (Nunc). Cells were frozen by controlled rate freezing and stored in liquid nitrogen tanks. Cells were thawed rapidly in a 37°C water bath and then resuspended in 10 ml warm media. Cells were centrifuged at 400*x*g, washed again in media before being seeded into tissue culture flasks.

2.7.4. Transient transfections of DNA

24 h prior to transfection, cells were seeded in 6-well plates at $2x10^5$ cells per well for MEFs, $5x10^5$ cells per well for NIH-3T3s or $8x10^5$ cells per well for HEK293Ts and HeLas. For cell staining, cells were seeded into glass coverslips which were sterilised by flaming with ethanol. For transfection, 10 μl Lipofectamine 2000 reagent (Invitrogen), and 4 μg DNA (in separate microfuge tubes) were each diluted in 250 μl OptiMem serum-free media (JRH) and incubated for 5 min at RT. For transfection of two DNA constructs, 2 μg of each

construct was used. The Lipofectamine 2000 and DNA complexes were pooled and incubated for a further 20 min, then added to the cells and incubated for 18-24 h.

2.7.5. Transient transfections of siRNA

siRNA constructs were designed to target the following sequences (5'-3'direction):

mNedd1 siRNA #1: GAGACATTGTGAATCTGCAAGTGGA (Invitrogen)

mNedd1 siRNA #2: CCGGCACATCAAGTACTCATTGTTT (Invitrogen)

hNEDD1: GGGCAAAAGCAGACATGTG (Qiagen)

hTCP-1α: GGGAGAAGTCAAATGGAGAGT (Qiagen)

Negative Universal Control (Medium GC) (Invitrogen)

For Nedd1/NEDD1: One day prior to transfection, cells were seeded in 6-well plates at $2x10^5$ cells per well for MEFs or $8x10^5$ cells per well for HeLas. For siRNA transfection, 5 μl Lipofectamine 2000 reagent (Invitrogen), and 6 μl of each mouse Nedd1 siRNA pooled, or 12 μl of the human NEDD1 siRNA were each diluted in 250 μl OptiMem serum-free media (JRH) and incubated at RT for 5 min. The Lipofectamine 2000 and siRNA complexes were pooled and incubated for a further 20 min, then added to the cells and incubated for 72 h. A second siRNA transfection was conducted 72 h after the first transfection, and left for a further 48 h.

For TCP-1α: HeLa cells were seeded and transfected with 3 μl of TCP-1α siRNA as for NEDD1 siRNA transfection. After 30 h, 2 mM thymidine was added to the cells for 16 h to synchronise the cells in S phase, and cells were then released into fresh media for 8 h. A second thymidine block was added for 16 h, together with a second siRNA transfection. After 48 h, the cells were released into fresh media containing 40 ng/ml nocodazole for 8 h, to synchronise cells in mitosis before harvesting.

2.7.6. Cell culture synchronisation (Jurkat cells)

$1x10^6$ Jurkat cells were seeded in wells of a 6-well dish with 100 ng/ml of nocodazole added to the media. After 16 h, cells were washed 3x with PBS and fresh media added. Cells were

collected at various time points after release from the block by centrifugation at 10000*x*g for 5 min. For immunoblotting, the pellet was frozen at -20°C until further processing. For flow cytometry, the pellet was processed immediately.

2.7.7. Flow cytometry

Pelleted cells were resuspended in 1 ml stain solution (3% w/v PEG 6000, 500 μg/ml PI, 180 units/ml RNAse, 0.1% triton-X, 4 mM $Na_3C_6H_5O_7$ pH 7.8, adjusted to pH 7.2) for 30 min at 37°C, then 1 ml salt solution added (3% w/v PEG 6000, 500 μg/ml PI, 0.1% triton-X, 0.4 M NaCl, pH 7.2) and incubated overnight in the dark at 4°C. Samples were analysed on an EPICS XL-MCL flow cytometer (Beckman Coulter).

2.7.8. β-galactosidase assay

Cells were plated onto glass coverslips 24 h prior to staining. Cells were fixed and stained using the Senescence β-galactosidase Staining Kit (Cell Signaling), according to the manufacturers' instructions. Cells were incubated for 24-48 h at 37°C prior to being imaged on a CKX41 microscope (Olympus), and photographed with a DP20 camera (Olympus).

2.7.9. Cell staining (immunofluorescence)

Cells were plated onto glass coverslips 24 h prior to staining. Cells were fixed in 100% methanol for 5 min at -20°C, washed in PBS and incubated in blocking solution (1% FBS/PBS) for 30 min. Primary antibodies in blocking solution were added for 2 h at RT (see 2.8.13 for antibody details and dilutions). Cells were then washed 3x in PBS and secondary antibodies (1:1000 rabbit Alexa Fluor 488 and/or 1:1000 mouse Alexa Fluor 568, Molecular Probes) were added in blocking solution for 1 h at RT. Cells were washed again 3x in PBS and stained with Hoechst 33342 (Molecular Probes) for 1 min. Cells were mounted in Prolong Gold Antifade reagent (Molecular Probes). Images were obtained using a confocal microscope (Radiance 2100, BioRad Laboratories) equipped with two lasers, an Argon ion 488 nm (14 mW) and a Green HeNe 543 nm (1.5 mW), and a UV lamp. Images were processed using Adobe Photoshop CS2 Version 9.0.

2.8. Protein analysis

2.8.1. GST protein expression and purification

Colonies of *E. coli* BL21 Star (DE3) One shot chemically competent cells (Invitrogen) transformed with the appropriate glutathione S-transferase (GST)-expression plasmids were used to inoculate overnight cultures. The following morning, cultures were subcultured 1:30 into 500 ml of LB containing ampicillin (100 μg/ml) and chloramphenicol (34 μg/ml) and grown for 2 h at 37°C in a shaking incubator. Protein expression was induced by the addition of 1 mM IPTG for 2 h. Cells were pelleted by centrifugation at 8000*x*g for 15 min at 4°C and the bacterial pellets resuspended in PBS. Cells were lysed by the addition of 1 mg/ml lysozyme, frozen, then thawed and sonicated (2x 30 sec bursts on ice). Cells were clarified by centrifugation at 16000*x*g for 30 min at 4°C, and 1 mM DTT added.

For GST purification, 750 μl glutathione sepharose beads (GE healthcare) were washed with 10 bed volumes of PBS and centrifuged at 400*x*g for 2 min at RT. Protein lysates were added to the beads and incubated overnight at 4°C with gentle rotation. The next day, the beads were pelleted by centrifugation at 400*x*g for 2 min at 4°C, the supernatant removed and the beads mixed with 7.5 ml PBS and loaded onto a column. The beads were washed in the column with 3x 7.5 ml cold PBS and eluted 3x with cold glutathione elution buffer (10 mM reduced glutathione, 50 mM Tris-HCl pH 8.0). The resultant pooled eluate was dialysed into PBS in dialysis tubing (Biorad) overnight at 4°C, with one change of PBS after 2 h. If required, the purified protein was concentrated in YM-30 centricon columns (Millipore) according to the manufacturers' instructions.

2.8.2. His protein expression and purification

Protein expression of His-tagged γ-tubulin was conducted as for GST proteins in 2.8.1. To denature the protein in order to increase solubility for purification, the pellet was lysed in lysis buffer B (100 mM NaH_2PO_4, 10 mM Tris-HCL, 8 M urea, adjusted to pH 8.0) for 2 h at RT with gentle vortexing. The debris was pelleted by centrifugation at 10000xg for 20 min,

supernatant added to 300 μl of 50% slurry of Ni-NTA (Invitrogen) for 3 h at RT with shaking and then loaded onto a column. The column was washed twice with wash buffer C (100 mM NaH_2PO_4, 10 mM Tris-HCL, 8 M urea, adjusted to pH 6.3) and eluted with 0.5 ml buffer D (100 mM NaH_2PO_4, 10 mM Tris-HCL, 8 M urea, adjusted to pH 5.9) followed by 0.5 ml buffer E (100 mM NaH_2PO_4, 10 mM Tris-HCL, 8 M urea, adjusted to pH 4.5). The eluates were pooled and checked on a coomassie gel, and then refolded by dialysis in refolding buffer with a graded series of urea buffer for 24 h each (0.05 M Tris pH 8.0, 0.005% triton x-100, 2 mM GSH, Urea [6M, 4M, 2M, 1M, 0]).

2.8.3. Protein extraction

For immunoprecipitation: About $1x10^6$ cells were lysed in 200 μl lysis buffer (20 mM Tris pH 7.5, 150 mM NaCl, 10% glycerol, 1% triton-X 100, 2 mM EDTA and protease inhibitor cocktail solution [Roche]). Cells were incubated on a rotor for at least 30 min at 4°C before being centrifuged at 16000*x*g for 5 min. The lysate supernatant was transferred to a new tube.

For direct immunoblotting: cells were lysed in RIPA buffer (150 mM NaCl, 1% NP-40, 0.5% DOC, 0.1% SDS, 50 mM Tris pH 7.4, 5 mM EDTA and protease inhibitor cocktail solution [Roche]). Cells were frozen and then thawed 3x in liquid nitrogen with vortexing and pipetting between each freeze, before being centrifuged at 16000*x*g for 5 min. The lysate supernatant was transferred to a new tube.

2.8.4. Protein concentration quantification

Protein concentration was calculated using the BioRad Protein Assay (Biorad). A standard curve was established by preparing serial dilutions of BSA in the range of 0.05-1.0 mg/ml. The dye reagent concentrate was mixed with H_2O (1:4), and 200 μl was added to each 10 μl sample, at a 1:10 dilution in H_2O. The colour change was measured as optical density at 540 nm using an EL808 Ultra Microplate reader (Bio-tek Instruments, Inc.) using the supplied program KC4 3.3 Rev 10.

2.8.5. Co-immunoprecipitation

Cell lysates were pre-cleared with 20 μl Protein G agarose beads (GE Healthcare) prepared to a slurry of 50% in lysis buffer (see 2.8.3), incubated with gentle rocking for 2 h at 4°C. The solutions were then centrifuged at 16000*x*g, the lysate removed from the beads and transferred to a new tube with 40 μl fresh beads and 1 μl primary antibody, and incubated with gentle rocking overnight at 4°C. The mix was then centrifuged for 1 min at 16000*x*g at 4°C and the pellet was washed 3x with 700 μl of lysis buffer and once in PBS, keeping the samples on ice during the washes. The pellet was resuspended in 50 μl of 2x Protein Loading Buffer (PLB, 100 mM Tris-HCl pH 6.8, 200 mM DTT, 4% SDS, 0.2% bromophenol blue, 20% glycerol). Prior to analysis by immunoblotting the sample was heated for 5 min at 100°C, then loaded on a sodium dodecyl sulfate polyacrylamide gel electrophoresis (SDS-PAGE) gel.

For immunoprecipitation with the flag-conjugated beads used in the silver stain gel, 20 μl of ANTI-FLAG M2 Affinity Gel (Sigma) was used according to the manufacturers' instructions. Elution was achieved using the 3X FLAG Peptide (Sigma) in a 50 μl volume, according to the manufacturers' instructions. Prior to analysis by immunoblotting 10 μl of 4x PLB was added to the sample and heated for 5 min at 100°C, then loaded on an SDS-PAGE gel.

2.8.6. Direct interactions

20 μl of glutathione sepharose beads were washed twice in NTEN buffer (20 mM Tris pH 7.4, 0.1 mM EDTA, 100 mM NaCl, 0.5% NP-40), with centrifugation at 1000*x*g for 2 min. 2.5 μg of purified proteins were added with or without 50 μg HEK293T cell lysate that was pre-cleared with 20 μl of glutathione sepharose beads for 1 h at 4°C. The reactions were left overnight at 4°C, and then washed 4x with NTEN buffer. Bound proteins were eluted with 30 μl of 2x PLB and boiled for 5 min. 15 μl of samples were loaded into each lane of an acrylamide gel. These experiments were performed by Sonia Shalini.

2.8.7. SDS-Page and protein transfer

Resolving polyacrylamide gels of varying percentage were prepared with the following reagents: 10-15% polyacrylamide solution (Biorad), 37.5 mM Tris pH 8.8, 0.1% SDS, 0.1% ammonium persulfate, 0.05% TEMED (GIBCO). The resolving gels were cast with Hoefer plates and spacers, and overlayed with a 5% stacking gel (5% polyacrylamide, 0.125 M Tris-HCL pH 6.8, 0.1% SDS, 0.1% ammonium persulfate, 0.1% TEMED into which a comb of 10 wells was inserted. The assembled gel was placed in a Hoefer minigel tank (Amersham Biosciences) and submerged in protein electrophoresis buffer (25 mM Tris pH 8.3, 250 mM glycine, 0.1% SDS). Samples were prepared for electrophoresis by boiling in an equal volume of 2x PLB. 5 μl Kaleidoscope marker (Biorad) and prepared samples were loaded into the wells of the protein gel and run through the stacking gel at 20 mAMPs, and through the resolving gel at 30 mAMPs. When the dye front reached the bottom of the gel, separated proteins were transferred to a polyvinylidine difluoride (PVDF) membrane using a Hoefer semi-dry transfer apparatus (Amersham Biosciences). The transfer apparatus was assembled as follows: two sheets of whatman filter paper pre-soaked in protein transfer buffer (49 mM Tris, 39 mM glycine, 0.0375% SDS, 20% methanol, pH 8.3) were placed on the cathode (+) of the apparatus. A same-sized piece of PVDF in transfer buffer was placed on top of the whatman followed by the gel and another two pieces of whatman. Proteins were transferred to the membrane for 90 min at 130 mAmps.

2.8.8. Immunoblotting

PVDF membranes were blocked in 5% skim milk powder in PBST (0.1% Tween20/PBS) for 1-2 h and incubated with primary antibodies overnight at 4˚C (see 2.8.13 for antibody details and dilutions). After washing in PBST, the membranes were incubated with rabbit secondary ECL IgG Horseradish Peroxidase (HRP) linked whole antibody (GE Healthcare) to detect NEDD1 or IgG Affinity Isolated Alkaline Phosphatase (AP) Conjugated antibody (Chemicon) to detect all other proteins, for 2 h at RT. Detection of bound HRP antibody was achieved using ECL Plus (GE Healthcare) and developed on X-ray film (Fujix). Detection of

bound AP was achieved using ECF substrate (GE Healthcare,) and developed using a Typhoon 9410 (Molecular Dynamics) and ImageQuant software (GE Healthcare).

2.8.9. Coomassie staining

SDS-Page gels were washed once in H_2O and stained with 0.25% w/v Coomassie Brilliant Blue R-250 (Biorad) in MQ H_2O overnight. Gels were then soaked in destain solution (40% methanol, 10% acetic acid in MQ H_2O) for 1-2 h.

2.8.10. Silver stain

SDS-PAGE gels were washed 2x in 10% ethanol for 5 min each, then washed 3x in MQ H_2O for 3 min each. They were then stained with 0.1% $AgNO_3$ for 30 min, washed in MQ H_2O for 10 sec, then immersed in developing solution (3% Na_2CO_3, 0.02% CH_2O) for 10 min. The reaction was stopped by adding 1% CH_3COOH for 10 min. Gels were then washed 3x in MQ H_2O and immersed in Farmer's Reducer (30 mM $C_6FeK_3N_6$, 100 mM $Na_2S_2O_3.5H_20$) until the silver stain disappeared, then rinsed with MQ H_2O until the yellow disappeared. The steps were repeated a second time and the gel photographed by the Adelaide Proteomics Facility.

2.8.11. Proteomics

The following proteomic analysis was conducted by the Adelaide Proteomics Facility:
Bands were excised from the gel, chopped into 1 mm^3 pieces and destained using 15 mM potassium ferricyanide and 50 mM sodium thiosulphate, reduced and alkylated with iodoacetamide, then digested with 100 ng of trypsin per sample. The resulting tryptic peptides were extracted from the gel pieces with 50% acetonitrile containing 1% formic acid followed by 100% acetonitrile. The volumes of the final samples were reduced from approximately 120 mL to ~1 mL by vacuum centrifugation. The peptides were then diluted to ~6 mL in 0.1% FA and transferred to an autosampler vial or MS/MS analysis using the liquid chromatographyelectrospray ionisation ion-trap mass spectrometer. 3 μl of each sample was chromatographed using an Agilent Protein ID Chip column assembly (40 nL trap column with 0·075 x 43 mm C-18 analytical column) housed in an Agilent HPLC-Chip

Cube Interface connected to an a HCT ultra 3D-Ion-Trap mass spectrometer (Bruker Daltonik GmbH). The column was equilibrated with 3% acetonitrile / 0·1% formic acid at 0·5 mL/min and the samples eluted with an acetonitrile gradient (3%-30% in 30 min). Ionizable species (300 < m/z < 1,200) were trapped and one or two of the most intense ions eluting at the time were fragmented by collision-induced dissociation. MS and MS/MS spectra were subjected to peak detection using DataAnalysis (Version 2.4, Bruker Daltonik GmbH). The combined MS and MS/MS mass lists were exported in Mascot generic format and submitted to the in-house Mascot database-searching engine.

2.8.12. Antibody purification

A Nedd1 antibody to detect mouse and human NEDD1 was designed and made by Paul Colussi against the C-terminal 361 amino acids of mouse Nedd1 (Manning *et al*., 2008). This was affinity purified before use with Nedd1 antigen expressed and purified as in 2.8.1. To do this, 0.3 g of cyanogen bromide-activated sepharose was washed 3x in 10 ml 1 mM HCl, centrifuging at 400*x*g for 1 min each wash. The sepharose was then washed 2x in coupling buffer (0.1M Na_2CO_3, 0.5 M NaCl pH 8.5) at RT, and 3 mg of purified antigen diluted in 5 ml of coupling buffer and added to the sepharose overnight at 4˚C. The sepharose was then washed in coupling buffer and 10 ml of ethanolamine buffer (1 M C_2H_7NO, 0.5 M NaCl pH 8.0) added for 2 h at RT on a rotor. The sepharose was washed in wash buffer (0.1M $NaCH_3COO$, 0.5 M NaCl, adjusted to pH 4.0) and then 3x in coupling buffer, and 2x in PBS before being stored at 4˚C as a 50% slurry in PBS + 0.1% NaN_3.

A GST-sepharose column was prepared as above using GST as the antigen. Anti-GST antibodies from the serum were removed by washing GST-sepharose 2x in sodium phosphate buffer (0.1 M Na_2HPO_4 adjusted to pH 8.2 with NaH_2PO_4), adding filtered serum diluted 1:1 in sodium phosphate buffer and rotating for 1 h at 4˚C. The sepharose was centrifuged and the supernatant transferred to the antigen-sepharose column washed 2x in sodium phosphate buffer. Samples were rotated overnight at 4˚C, then washed with 20 bed volumes of sodium phosphate buffer until the OD of the eluate measured 0, using a

BioPhotometer at 600nm (Eppendorf). Samples were eluted with 500 μl 0.1 M glycine into 100 μl Tris-HCl pH 8.6 until the OD was less than 0.1. Fractions were combined and dialysed against PBS + 0.02% NaN_3.

2.8.13. Other antibodies

Primary antibodies used for immunoblotting and immunocytochemistry or immunohistochemistry are below. Secondary antibodies as detailed in the text, were all used at a dilution of 1:1000 (see 2.7.9, 2.8.8 and 2.10.13).

Antibody	**Host species**	**Clone and supplier**	**Immun-blot dilution**	**Immuno-staining dilution**
Acetylated α-tubulin	mouse	6-11B6-11B-1, Sigma	N/A	1:500
α-tubulin	mouse	236-10501, Molecular Probes	N/A	1:1000
β-actin	mouse	AC-15, Sigma	1:5000	N/A
Centrin	mouse	20H5,Gift from J.L. Salisbury, Mayo Clinic, MN, USA	N/A	1:500
Cyclin B1	mouse	Ab-3, NeoMarkers	1:500	N/A
GFP	mouse	7.1 and 13.1 mixed, Roche	1:1000	N/A
GFP	rabbit	Ab290, Abcam	N/A (1 μl used for IP)	1:1000
GT335	mouse	Gift from B. Edde, CNRS, Montpellier, France	N/A	1:500
γ-tubulin	mouse	GTU-88, Sigma	1:5000	1:500
HSP70	mouse	3a3, gift from R. Morimoto Laboratory, Northwestern University, IL, USA	1:5000	N/A
HuC	mouse	16A11, Molecular Probes	N/A	1:1000
Myc	mouse	9E10, Roche	1:1000	N/A
Myc	goat	Ab9132, Abcam	N/A (1 μl used for IP)	N/A
N-cadherin	mouse	GC-4, Sigma	N/A	1:100
Nedd1 pre-immune serum	rabbit	Made by Paul Colussi (Manning *et al*., 2008)	1:5000	1:1000
Nedd1 purified serum	rabbit	See 2.8.12	1:500	1:50
P16	rabbit	M-156, Santa Cruz	1:500	N/A
P19	rabbit	Ab80, Abcam	1:1000	N/A

Antibody	Host species	Clone and supplier	Immun-blot dilution	Immuno-staining dilution
P21	mouse	F5, Santa Cruz	1:500	N/A
Phalloidin-Alexa Fluor 594	mouse	A12381, Molecular Probes	N/A	1:20
pH3	rabbit	D2C8, Cell Signaling	N/A	1:100
TCP-1α	rat	CTA-191, Stressgen	1:1000	N/A
zNEDD1 serum	rabbit	See 2.10.5	1:1000	N/A
zNEDD1 pre-immune serum	rabbit	See 2.10.5	1:1000	N/A
zNEDD1 purified serum	rabbit	See 2.10.5 and 2.8.12	1:1000	1:200

2.9. Mouse manipulation

2.9.1. Animals and sectioning

C57Bl/6 embryos were scavenger embryos, under ethics approval of other projects in the laboratory. Embryos at appropriate stages were dissected and fixed in 4% paraformaldehyde(PFA)/PBS overnight at 4˚C. Embryos were then washed in PBS, cryoprotected in 30% sucrose/PBS overnight at 4˚C before being frozen in TissueTek OCT compound (Sakura Finetek). Frozen embryos were then cryosectioned in 10 µm saggital or coronal sections onto glass slides using a cryostat (Leica CM1950).

2.9.2. Immunohistochemistry on paraffin sections (colour)

Sections were processed using the Elite Rabbit IgG Vectastain ABC kit (Vector Laboratories) according to the manufacturers' instructions for staining paraffin sections with the following modifications: α-NEDD1 primary antibody was incubated overnight (see 2.8.13 for antibody details and dilution), biotinylated antibody was incubated for 3 h. Colour staining was achieved using DAB peroxidase substrate kit (Vector Laboratories), according to the manufacturers' instructions. Images were acquired using a BX51 microscope

(Olympus) with UPlanApo objectives, fitted with a DP70 camera (Olympus) and processed with Olysia Bioreport software (Olympus).

2.9.3. Immunohistochemistry on frozen sections (fluorescence)

Sections were fixed with 100% methanol for 5 min at -20˚C, then washed in TBST (100 mM Tris HCl, 150 mM NaCl pH 7.5, 0.05% Tween20). Sections were then incubated in blocking buffer (60% maleate buffer [100 mM maleic acid, 150 mM NaCl, pH 7.4], 20% goat serum, 2% Blocking Reagent [Roche]) for 3 h at RT, and primary antibody added overnight in blocking buffer (see 2.8.13 for antibody details and dilutions). After 3x 5 min washes in TBST, sections were incubated with secondary antibodies (1:1000 rabbit Alexa Fluor 488 and 1:1000 mouse Alexa Fluor 568, Molecular Probes) diluted in blocking buffer for 3 h at RT, or with directly conjugated primary antibody (Phalloidin-Alexa Fluor 594). Sections were stained with Hoechst 33342 (Molecular Probes) for 1 min and mounted in Prolong Gold Antifade reagent (Molecular Probes). Images were obtained using a confocal microscope as in 2.7.9.

2.10. Zebrafish manipulation

Ethics approval for zebrafish use and manipulation was granted by the Animal Ethics Committee, The University of Adelaide, for the duration of this study.

2.10.1. Zebrafish maintenance and staging

Zebrafish were maintained in the Adelaide Zebrafish Facility (Molecular Life Sciences Building, Adelaide University, Australia) at 28.5˚C under standard conditions as described (Westerfield, 1995). Collected embryos were maintained in embryo medium (13.72 mM NaCl, 0.54 mM KCl, 0.025 mM Na_2HPO_4, 0.044 mM K_2HPO_4, 1 mM $CaCl_2$, 1 mM $MgSO_4$, 0.035% [w/v] $NaHCO_3$). Developmental stages were determined by using both hours post fertilisation (hpf) and morphological features (Kimmel *et al*., 1995).

2.10.2. Zebrafish embryo anesthetisation and fixation

Prior to manipulation, zebrafish embryos were anesthetised in 200 μg/ml tricaine. Embryos were dechorionated manually and fixed in 4% PFA/PBS overnight at 4˚C.

2.10.3. Generation of RNA probes

Anti-sense and sense digoxygen (DIG) labelled riboprobes were generated from a pGEM-T-Easy plasmid containing amino acids 1-422 of zebrafish NEDD1. The plasmid was linearised at the 5' or 3' end of the clone using *Hinc*II or *Not*I enzymes respectively and phenol/chloroform purified (see 2.3.5). RNA was transcribed *in vitro*, incorporating DIG-11-UTP by T7 or T3 RNA polymerase for the sense and anti-sense probes respectively, using the DIG RNA labelling kit (Boehringer Mannheim) according to the manufacturers' instructions. 5 μl of probe was checked on an RNA agarose gel (see 2.6.3). To determine labelling efficiency, 1 μl of probe, 1/10, 1/100 and 1/1000 dilutions were spotted onto nitrocellulose wet with 20x SSC (3 M NaCl, 0.3 M $Na_3C_3H_5O(CO_2)_3$, adjusted to pH 7) and then dried. The RNA was ultraviolet cross-linked to the filter, washed in 20x SSC and blocked in 5% skim milk in TBST (see 2.9.3) for 30 min at RT. The filter was incubated with 1:5000 dilution of anti-DIG-AP (Boehringer Mannheim) for 30 min, washed twice with TBST, rinsed in AP buffer (100 mM NaCl, 50 mM $MgCl_2$, 100 mM Tris HCl pH 9.5, 0.1% Tween20), then the AP detected by incubating in a solution of (per 1 ml) 3.5 μl BCIP (50 mg/ml in dimethylformamide [DMF], Roche) and 4.8 μl NBT solution (100 mg/ml in 70% DMF, Roche) in darkness.

2.10.4. In situ mRNA analysis

For embryos older than 24 hpf, embryo medium was replaced at 10 hpf with 0.0045% phenylthiourea in embryo medium to prevent pigmentation. Embryos were fixed at the appropriate stages in 4% PFA/PBS overnight at 4˚C, and then washed in PBST (see 2.8.8). Chorions were removed with forceps, and embryos placed in methanol at -20˚C for between 2 h and 1 week. Embryos were rehydrated through 5 min washes in 75%, 50%, 25% in PBST, and then washed 4x in 100% PBST. Embryos 24 hpf and older were digested with

10 μg/ml proteinase K for 10 min, before being refixed in 4% PFA/PBS for 20 min, and washed 4x with PBST. The embryos were then pre-hybridised in hybridisation buffer (50% deionised formamide, 5x SSC, 2% Blocking Reagent [Roche], 0.1% Tween20, 0.5% CHAPS, 50 μg/ml yeast RNA, 50 μg/ml heparin, 5mM EDTA), for 2 h at 70˚C. 400 ng of the RNA DIG probe was then added to the embryos in 400 μl fresh hybridisation buffer and incubated at 70°C overnight. The next day, embryos were rinsed 3x in hybridisation buffer, washed 2x 15 min in hybridisation buffer, 1x 30 min in 50% hybridisation buffer/50% 2x SSCT, 2x 30 min in 50% formamide/2x SSCT, 1x 15 min in 2x SSCT, 2x 30 min in 0.2x SSCT, all at 70˚C. The embryos were blocked in PBST + 1% BSA for 1 h at RT, then incubated with 1:2000 dilution anti-DIG-AP overnight at 4˚C, followed by 5x 30 min washes in PBST. Embryos were then rinsed in AP buffer (see 2.10.3), and the AP detected as in 2.10.3. Embryos were then rinsed several times in PBST, fixed in 4% PFA/PBS for 20 min and dehydrated in 5 min washes of 25%, 50%, 75% methanol in PBST. There were then 2x 5 min washes in 100% methanol, before the embryos were sunk in 2:1 benzyl benzoate:benzyl alcohol mix. Embryos were then rehydrated in 5 min washes of 75%, 50%, 25% methanol in PBST, before 2x 10 min washes in PBST and cleared in 80% glycerol/PBST overnight before being mounted onto slides. A Zeiss Axiophot microscope was used with DIC (Nomarski differential interference contrast) optics (Zeiss). Images were captured using a HC1000 digital 3CCD colour camera (Fujix) and compiled using Adobe Photoshop 6.0 software.

2.10.5. Zebrafish antibody production

To create a zebrafish NEDD1 antibody, the C-terminal 252 amino acids of zebrafish NEDD1 was fused to GST (pGEX-2T-2-zNEDD1) and expressed and purified as in 2.8.1. Two rabbits were injected with 4 doses of antigen at 0.5 mg/dose each 3 weeks apart (IMVS, Gilles Plains). A test bleed was taken after the third dose, and the bleed out taken one week after the final dose. The bleed out serum was affinity purified against the recombinant protein as in 2.8.1. Purified antibody was dialysed against PBS and stored at -20˚C in 50% glycerol/0.02% NaN_3/PBS.

2.10.6. Protein extraction from zebrafish

To extract protein from zebrafish, embryos were anesthetised and dechorionated (see 2.10.2), before the yolks were removed manually with forceps and needles. The embryos were then vortexed in Ringers solution (55 mM NaCl, 1.8 mM KCl, 1.25 mM $NaHCO_3$) for 5 min to dissolve the remaining yolk, before being centrifuged at 4000*x*g for 5 min and the supernatant removed. Cells were then lysed in RIPA buffer as in 2.8.3 and subjected to immunoblotting as in 2.8.8.

2.10.7. Image Quant protein quantification

The intensity of protein bands was quantitated and normalised to γ-tubulin bands using ImageQuant (Molecular Dynamics).

2.10.8. MO design and resuspension

Morpholino oligos (MOs) were designed and synthesised by GeneTools (and resuspended in nuclease free MQ H_2O to give a stock solution of 2 mM. Anti-sense MO sequences are given in the 5'-3' direction.

zNEDD1 MO1: ACGTCCTCCATCCCAGCAGCCTTGT
(+11 to -14 with respect to the start of the zNEDD1 ORF, initiation codon underlined)

zNEDD1 MO2: AAGTGTAGACAATGTAAATGATATG
(-27 to -51 with respect to the start of the zNEDD1 ORF)

mcMO1: ACcTCCTCgATgCCAcCAcCCTTGT
Mismatch control MO representing zNEDD1MO1 with 5 base alterations (lower case)

Control MO: AAGTGTAGACAATGTAAATGATATG
Standard negative control MO with no known target in zebrafish

p53 MO: GCGCCATTGCTTTGCAAGAATTG
Standard p53 MO designed by GeneTools

2.10.9. MO injection

Prior to microinjection, MO stock samples were diluted to the required concentration in MQ H_2O. For all experiments involving microinjection, MOs were injected into the cytoplasm at the 1 cell stage of zebrafish embryos using an MPPI-2 Pressure Injector (Applied Scientific Instrumentation Inc.). Injections were performed by Martin Lewis or Simon Wells (Adelaide

University). Injected embryos were maintained at 28.5˚C in embryo media (see 2.10.1) and analysed 24 h after injection except where stated otherwise.

2.10.10. Generating capped mRNA for rescue

5 μg of zNEDD1 in pBlueScript KS-zNEDD1 Promoter + ORF was linearised with the *Sac*II restriction enzyme and phenol/chloroform purified (see 2.3.5). 600 ng of linear DNA was used to make capped mRNA with the G(5')ppp(5')G Cap Analog (Ambion) using the MEGAscript T7 kit (Ambion), according to the manufacturers' instructions, except that a cap analog:GTP ratio of 4:1 was used. Capped mRNA was stored in aliquots at -70˚C.

2.10.11. Light microscopy

24 h after injection, embryos were anesthetised, mounted onto a glass slide and photographed at 4x and 10x on a BX51 microscope (Olympus) with UPlanApo objectives, fitted with a DP70 camera (Olympus) and processed with Olysia Bioreport software (Olympus).

2.10.12. Detection of apoptosis in whole-mount embryos (TUNEL)

Zebrafish embryos were fixed overnight in 4% PFA/PBS and dehydrated in 5 min washes of 25%, 50%, 75% methanol in PBST, followed by 2x 10 min washes in PBST, incubation in 100% acetone for 10 min at –20ºC, and 3x 5 min rinses in PBST. Embryos were permeabilised by incubation in fresh 0.1% $Na_3C_3H_5O(CO_2)_3$ in PBST for 15 min, followed by 3x 5 min rinses in PBST. Embryos were assayed by TUNEL using the *In Situ* Cell Death Detection Kit, TMR Red (Roche) according to the manufacturers' instructions. Embryos were mounted onto a slide under a coverslip supported by two pieces of double sided tape. Coverslips were sealed to the glass using clear nail varnish. Images were acquired on a BX51 microscope (Olympus) with UPlanApo objectives, with a 488 nm and 568 nm filter, fitted with a DP70 camera (Olympus) and processed with Olysia Bioreport software (Olympus).

2.10.13. Whole mount immunohistochemistry (pH3 and acetylated α-tubulin)

Embryos were fixed and permeabilised in 100% methanol overnight at -20°C and rehydrated in 5 min washes of 75%, 50%, 25% methanol in PBST, before 2x 10 min washes in PBST. Embryos were then incubated in blocking solution (0.1% BSA, 10% goat serum in PBST) for at least 1 h. The blocking solution was removed and primary antibody added (α-phosphorylated histone H3 [pH3] or acetylated α-tubulin [see 2.8.13 for antibody details and dilutions]) in fresh blocking solution. Embryos were incubated with gentle rocking overnight at 4°C. Embryos were then washed extensively in 1x PBST (several changes over 2 h) before being incubated with secondary antibody (1:1000 rabbit or mouse Alexa Fluor 488, Molecular Probes) in fresh blocking solution for at least 2 h at RT with gentle rocking. Embryos were then washed 3x in PBST for 1 h each, cleared overnight in PBST/80% glycerol and mounted as in 2.10.12. Embryos stained with α-pH3 were viewed and photographed as in 2.10.12. Embryos stained with α-acetylated tubulin were viewed and photographed on a confocal microscope as in 2.7.9.

2.10.14. Whole mount immunohistochemistry (HuC)

Embryos were fixed in 4%PFA/PBS overnight followed by several washes in PBST. Embryos were then incubated on a rotor with 0.5% H_2O_2 and 0.5% goat serum for 30 min at RT, washed in PBST for 10 min, and then blocked and stained with α-HuC using the Elite mouse IgG Vectastain ABC Kit (Vector Laboratories), according to the manufacturers' instructions (see 2.8.13 for antibody details and dilution). For development of colour the DAB substrate kit for peroxidise was used (Vector Laboratories) according to the manufacturers' instructions. Embryos were then washed 3x in PBST for 10 min each, then cleared, mounted as in 2.10.4 and photographed as in 2.10.11.

2.10.15. OCT sectioning and immunohistochemistry

For sectioning, embryos were fixed in 100% methanol overnight at –20ºC, rehydrated in 5 min washes of 75%, 50%, 25% methanol in PBST, before 2x 10 min washes in PBST. Embryos were then sunk in 30% sucrose/PBST for at least 3 h, before being embedded into

TissueTek OCT compound (Sakura Finetek), and frozen on dry ice. Frozen embryos were then cryosectioned in 10 µm sections onto glass slides using a cryostat (Leica CM1950). Sections were stained and analysed as in 2.9.3, using α-zNEDD1 and α-γ-tubulin antibodies (see 2.8.13 for antibody details and dilutions).

2.11. Statistical Analysis

To determine significance, a two-tailed t-Test (Two-Sample Assuming Equal Variances) was conducted using Microsoft Excel. A p value of <0.05 was considered statistically significant.

3. Expression of Nedd1 during mouse embryonic development

3.1. Introduction

Given the role of the centrosome in many diverse processes, it is no surprise that this organelle is important during development. Indeed, centrosomes are essential during mouse embryogenesis, as knockouts of the core centrosomal protein γ-tubulin, are embryonic lethal at the blastocyst stage (Yuba-Kubo *et al*., 2005). Despite the importance of the centrosome during this process, the expression and localisation of centrosomal proteins during mouse embryonic development has not been well characterised. Two particular aspects of development were the focus of this study; the establishment of the nervous system, and the polarisation of tissues.

Establishment and growth of the CNS are examples of where the centrosome plays important roles in embryogenesis. The nervous system is highly complex and is tightly regulated during development as neural progenitor cells proliferate, exit the cell cycle and differentiate into specific cell types (Donovan and Dyer, 2005). The centrosome contributes to all of these processes (de Anda *et al*., 2005, Higginbotham and Gleeson, 2007). Given that Nedd1 has been identified as a centrosomal protein in our laboratory and others (Haren *et al*., 2006, Luders *et al*., 2006, Manning and Kumar, 2007), and was initially discovered as a protein with a high level of expression in neural precursor cells (Kumar *et al*., 1992), it was suspected that it may also play a role in the development of the nervous system. Support for this is provided by the GENSAT (Gene Expression Nervous System Atlas) database made available by the National Center for Biotechnology Information (NCBI). This database contains thirteen images of mouse embryos and adults labelled for *Nedd1* mRNA expression. These images reveal that *Nedd1* is expressed in many cell types in the mouse embryo, but is concentrated in the brain and retina, which are major components of the CNS. Taken together, this information suggests a possible function of Nedd1 in the development of the CNS.

The centrosome is also important in the polarisation of cells and tissues, a process used to traffic proteins and organise cells into tissues and organs, that is most obvious in neurons and epithelial cells (Salas *et al*., 1997). Many factors are important in controlling this process, including an intact microtubule cytoskeleton and the apical distribution of MTOCs (Meads and Schroer, 1995, Salas *et al*., 1997), again implicating the centrosome and Nedd1 in this developmental process.

Therefore, the aim of this chapter was to analyse the expression and localisation of Nedd1, as a marker for centrosome dynamics, during mouse embryonic development, in particular during establishment of the neural system and in polarisation (Manning *et al*., 2008). This would provide an insight into the importance of Nedd1 and the centrosome in these developmental processes.

3.2. The Nedd1 antibody is a reliable marker for cell and embryo immunostaining

To examine the localisation and expression of Nedd1 during development, an antibody targeted against the C-terminal half of mouse Nedd1 protein was utilised. The purified serum recognised a band by immunoblotting at the expected mass of approximately 73 kDa in human cell lines (HEK293T embryonic kidney cells and MCF7 breast adenocarcinoma cells shown) and mouse cell lines (mouse embryonic fibroblasts [MEFs], N18 neuroblastoma cells and P19 embryonic carcinoma cells shown) (Fig. 3.1A). This band was present at similar levels in all cell lines tested. Some cell lines appeared to have additional bands at higher molecular masses, but the nature of these protein species has not been investigated, and are possibly non-specific. Pre-immune serum from the same rabbit did not recognise the 73 kDa band, indicating that it is specific for Nedd1 protein. In addition to immunoblotting, this antibody was also used as a marker for Nedd1 in cell staining. The localisation of Nedd1 in centrosomes has been demonstrated, as NEDD1 has previously been shown to co-localise in cell culture with the centrosomal protein, γ-tubulin (Haren *et al*., 2006, Luders *et al*., 2006). In this study Nedd1 was also observed in centrosomal-like dots

Fig. 3.1 The Nedd1 antibody specifically recognises Nedd1 in cultured cells

(**A**) Human (HEK293T and MCF7) and mouse (MEF, N18 and P19) cell lysates were probed with purified α-Nedd1 serum, or pre-immune serum from the same rabbit. Nedd1 serum reveals a prominent band at approximately 73 kDa on immunoblot in all cell lines, and this is not detected with pre-immune serum.

(**B**) MEF or HEK293T cells were stained with Nedd1 (green), and Hoechst 33342 (blue) to mark the nucleus. Nedd1 displays faint cytoplasmic staining and distinct centrosome-like dots that are not present when staining with pre-immune serum.

(**C**) MEFs were stained with Nedd1 (green), α-tubulin (red, microtubules) and Hoechst 33342 (blue). Nedd1 is present on the spindle poles and microtubules.

Scale bars represent 40 μm.

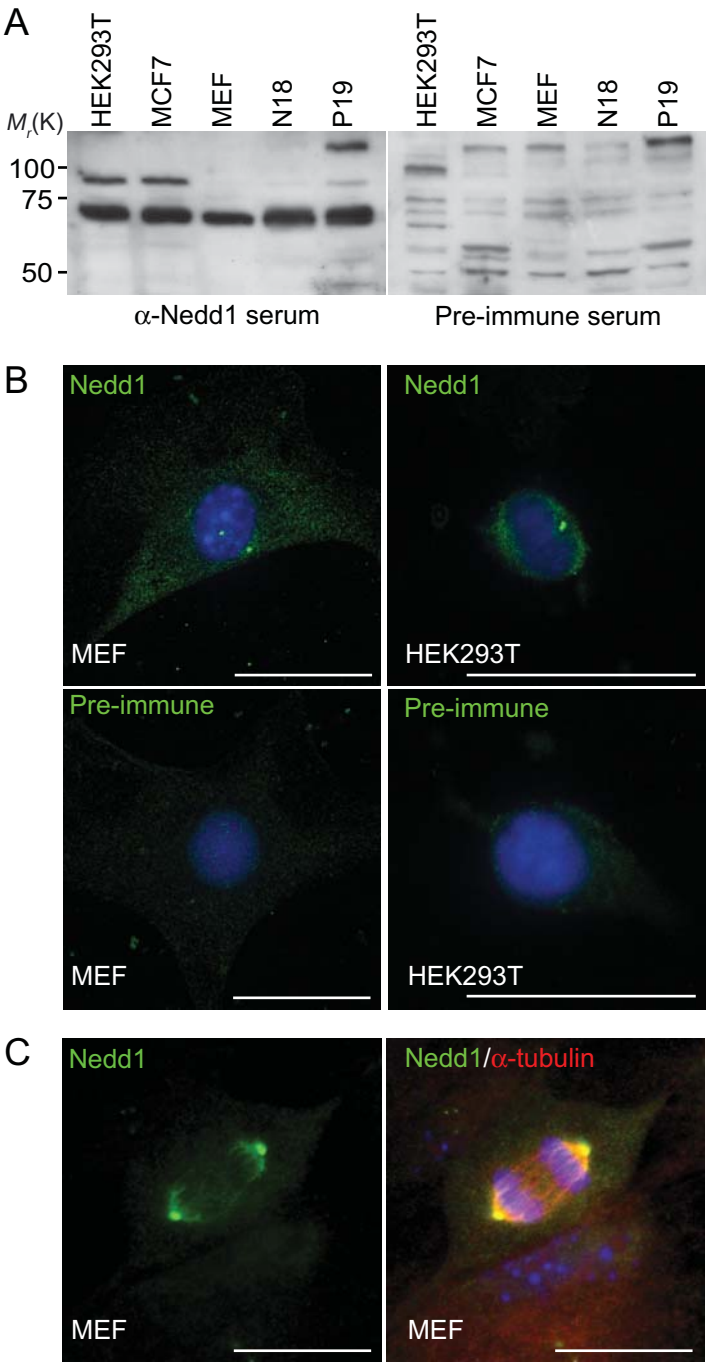
A
HEK293T
MCF7
MEF
N18
P19
HEK293T
MCF7
MEF
N18
P19
M_r(K)
100
75
50
α-Nedd1 serum
Pre-immune serum
B
Nedd1
MEF
Nedd1
HEK293T
Pre-immune
MEF
Pre-immune
HEK293T
C
Nedd1
MEF
Nedd1/α-tubulin
MEF

in interphase cells of mouse and human origin such as MEFs and HEK293Ts (Fig. 3.1B). This staining was not seen with pre-immune serum. Nedd1 was also detected at the spindle poles, and along the spindle microtubules of mitotic cells, co-localising with the microtubule marker α-tubulin (Fig. 3.1C). Hence, this antibody is a reliable marker for Nedd1 in cultured cells.

Nedd1 could also be detected with this antibody in mouse embryo sections, using colour and fluorescent staining. Colour staining revealed that Nedd1 expression was greatest in regions of high proliferation, such as in the cochlea of mouse embryos at embryonic day (E)14.5 (Fig. 3.2A). This staining pattern showed Nedd1 as a predominantly cytosolic protein in the apical region of polarised cells, but did not provide enough resolution to detect Nedd1 in centrosomal-like structures. However, this could be seen using a fluorescent secondary antibody to reveal Nedd1 expression. These stainings showed that Nedd1 in polarised regions was indeed present in centrosome-like dots in cells, as well as in the immediately surrounding cytoplasm (Fig. 3.2B). Pre-immune serum did not show any definite staining, indicating the antibody was specifically detecting Nedd1. Therefore, this Nedd1 antibody marks the centrosome in cells and embryos, and is suitable for both immunocytochemistry/immunohistochemistry and immunoblotting.

3.3. Nedd1 co-localises with centriole and basal body markers

To verify the specificity and precise localisation of Nedd1 in the centrosome, its co-localisation with centrosomal components was examined. γ-tubulin is known to localise at the periphery of the organised pericentriolar material, and within the proximal end of the centriolar barrel (Fuller *et al*., 1995). The co-localisation of Nedd1 with γ-tubulin in cell lines was confirmed, as shown in primary MEFs (Fig. 3.3A). In this study, Nedd1 was also shown to co-localise with centrin (Fig. 3.3B) which is present in centrioles and the pericentriolar lattice (Salisbury *et al*., 2002), and GT335 (Fig. 3.3C) which recognises post-translationally modified glutamylated α- and β-tubulin, specifically in the centrioles of non-neuronal cells

Fig. 3.2 The Nedd1 antibody specifically recognises Nedd1 in tissues

(**A**) Sections of a paraffin embedded E14.5 mouse embryo were stained with purified α-Nedd1 serum, or pre-immune serum. Nedd1 is present in all cells but concentrated in areas such as the apical region of polarised cells of the cochlea. The box is enlarged in the adjacent image. No staining is evident with pre-immune serum.

(**B**) Frozen cryosections of an E14.5 embryo were stained with purified α-Nedd1 serum or pre-immune serum (green), and Hoechst 33342 to mark the nucleus (blue). Nedd1 is present in centrosome-like dots in all cells but concentrated in areas such as the apical region of polarised cells of the cochlea. No specific staining is evident with pre-immune serum. The box is enlarged in the adjacent image.

Scale bars represent 40 μm.

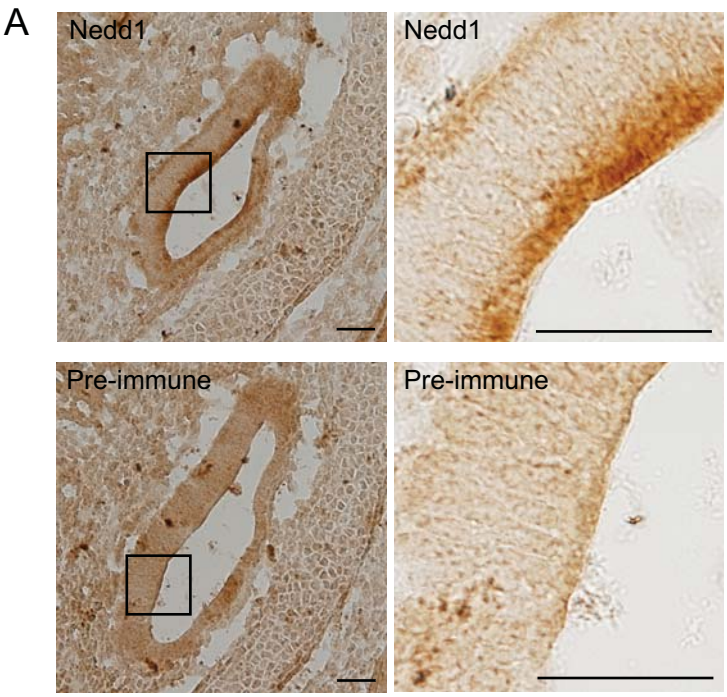
A
Nedd1
Nedd1
Pre-immune
Pre-immune
B
Nedd1
Nedd1
Pre-immune
Pre-immune

Fig. 3.3 Nedd1 co-localises with centrosomal markers

MEFs were stained with Nedd1 (green), centrosome markers (red), and Hoechst 33342 to mark the nucleus (blue) (**A**-**D**). Cryosections of an E14.5 embryo were stained with Nedd1 (green), acetylated α-tubulin (red) and Hoechst 33342 (blue) (**E**). The centrosomes are enlarged in the inset.

(**A**) Nedd1 co-localises with the pericentriolar and centrosomal marker, γ-tubulin.

(**B**, **C**) Nedd1 co-localises with the centriolar markers centrin and GT335.

(**D**, **E**) Nedd1 co-localises in the centrosome with acetylated α-tubulin, but not along the ciliated microtubules, in MEFs (**D**) and in the duodenum of the mouse embryo (**E**).

Scale bars represent 40 μm.

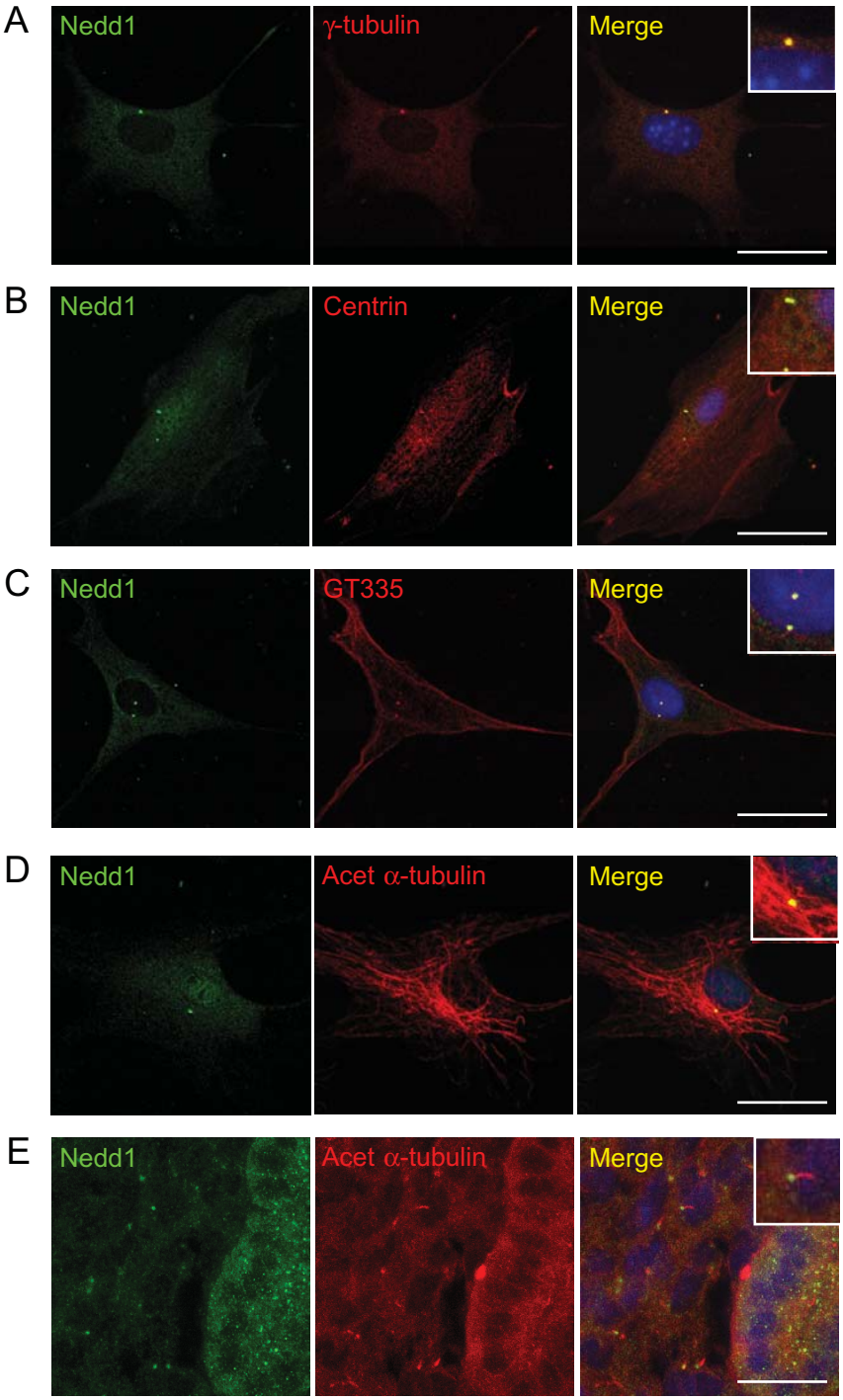
A
Nedd1
γ-tubulin
Merge
B
Nedd1
Centrin
Merge
C
Nedd1
GT335
Merge
D
Nedd1
Acet α-tubulin
Merge
E
Nedd1
Acet α-tubulin
Merge

(Bobinnec *et al*., 1998). The co-localisation of Nedd1 with these markers supports that Nedd1 is present in centrioles.

Additionally, the expression of Nedd1 in centrioles suggested that it may also localise to the basal bodies at the base of cilia, which are centriolar derived structures (see 1.2). In MEFs, the mother centriole of the centrosome serves as the basal body and nucleates cilia development (Hartman *et al*., 2009). In these cultured cells, acetylated α-tubulin decorates many microtubules, some of which appear to be primary cilia and as such this protein can be used as a marker for cilia (Piperno *et al*., 1987). Therefore, the co-localisation of Nedd1 with acetylated α-tubulin was examined in MEFs. Nedd1 was seen partially co-localised with this marker in the centriole/basal body, but did not extend along the microtubule fibres (Fig. 3.3D). The localisation of Nedd1 in basal bodies of primary cilium was more obvious in a section of the mouse embryo duodenum where Nedd1 could be seen in the basal body at the base of acetylated α-tubulin positive cilia (Fig. 3.3E). These results demonstrate that Nedd1 is a marker of centrioles in the centrosome and basal body.

3.4. Expression of Nedd1 in the mouse embryonic nervous system

As Nedd1 was originally identified as a protein with high expression in neural progenitor cells, its expression during neural development was characterised, as a marker for the centrosome. In the developing mouse embryo, the neural tube is the rudiment of the CNS, which comprises the brain, brainstem and spinal cord (Gilbert, 2000). In mice, the hollow cavity of the neural tube is formed by about E10 (Schoenwolf and Desmond, 1984). At E11.5, Nedd1 was present in all cells but concentrated in apically localised centrosomal-like structures of cells at the ventricular zone of the neural tube (Fig. 3.4A). These are highly proliferating neuroepithelial cells as can be seen by the staining of N-cadherin, which is expressed apically at adherins junctions in neuroepithelial cells of the early neural tube (see 1.5.1) (Akitaya and Bronner-Fraser, 1992, Aaku-Saraste *et al*., 1996, Nakagawa and Takeichi, 1998). Indeed, Nedd1 appeared to have a similar localisation in all the ventricular

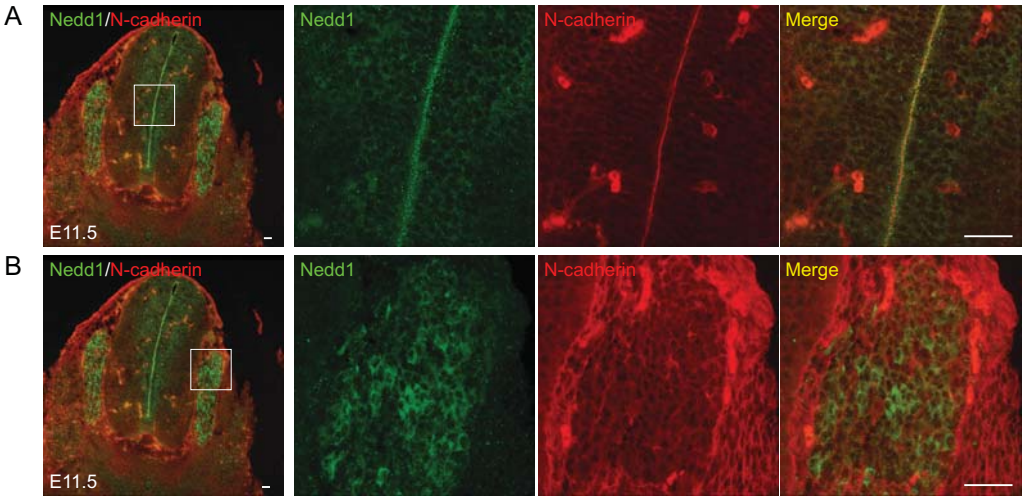

Fig. 3.4 Expression of Nedd1 in the mouse nervous system at E11.5

Coronal cryosections of E11.5 embryos were stained with Nedd1 (green) and N-cadherin (red). The box is enlarged in the adjacent image.

(**A**) Nedd1 is present in a centrosomal-like dot in all cells but shows strongest expression at the adherins junctions (N-cadherin) of the ventricular zone cells of the neural tube.

(**B**) There is strong expression of Nedd1 in the centrosome and in the cytoplasm of some cells of the dorsal root ganglia (DRG).

Scale bars represent 40 μm.

regions of the embryo, although they are not clearly defined at this stage (E11.5, data not shown). Hence Nedd1, as part of the centrosome, is most highly expressed in cells of the CNS that are actively proliferating.

From E9.5, neuroepithelial cells at the dorsal midline of the neural tube give rise to the neural crest. Neural crest cells are a migratory stem cell population that can be divided into four main populations; cranial, cardiac, vagal and trunk (Gilbert, 2000). Each of these cell populations migrate along specific pathways to contribute to distinct cell and tissue types (Trainor, 2005). Trunk neural crest cells give rise to populations such as melanocytes, glia and neurons of the dorsal root ganglia (DRG) and the autonomic nervous system (Kasemeier-Kulesa *et al*., 2005). Interestingly, at E11.5, Nedd1 showed high expression in some cells of the DRG, identified by the surrounding N-cadherin staining (Fig. 3.4B). This expression appeared to be cytoplasmic, in addition to the usual centrosomal localisation seen in other cell types. The function of this cytoplasmic pool of Nedd1 in DRG neurons is currently unknown.

By E14.5, the apical expression of Nedd1 and N-cadherin in the neural tube was reduced, as compared to E11.5 (Fig 3.5A). This correlates with an increase in differentiation and a reduction in the proliferation rate of these cells at this later stage of development (Kaufman, 1992). Nedd1 staining was still observed in the centrosomal structures and cytoplasm of cells in the DRG, although it also appeared to be reduced compared to E11.5 (Fig. 3.5B). There was again high expression of Nedd1 in all ventricular zones at E14.5 as expected because these cells are still highly proliferative (ventricular zone of fourth ventricle shown, Fig. 3.5C) (Kaufman, 1992).

3.5. Nedd1 co-localises with γ-tubulin in ventricular zones, but not in the DRG

In order to clarify whether this Nedd1 staining was indicative of general centrosomal protein localisation in the developing nervous system, embryo sections were also co-stained for γ-

Fig. 3.5 Expression of Nedd1 in the mouse nervous system at E14.5

Coronal cryosections of E14.5 embryos were stained with Nedd1 (green) and N-cadherin (red). The box is enlarged in the adjacent image.

(**A**) Expression of Nedd1 and N-cadherin is reduced in the neural tube when compared to E11.5.

(**B**) Nedd1 expression is reduced but remains centrosomal and cytoplasmic in the DRG.

(**C**) At E14.5, Nedd1 displays intense staining in centrosomes of proliferating cells in the fourth ventricle.

Scale bars represent 40 μm.

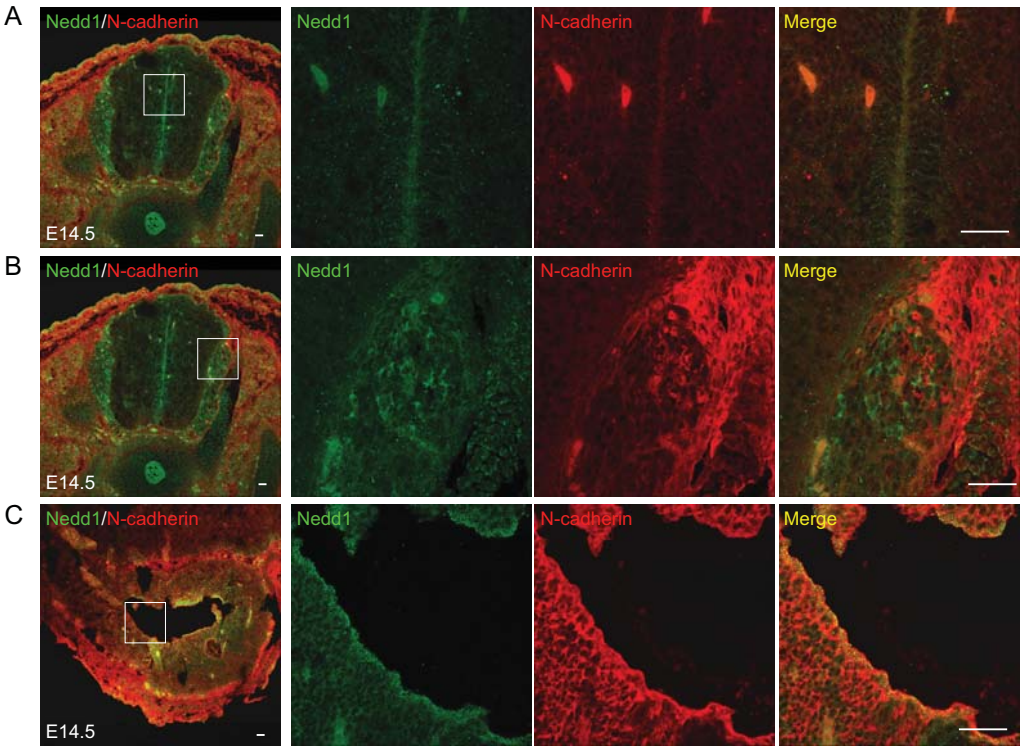
A
Nedd1/N-cadherin
Nedd1
N-cadherin
Merge
E14.5
B
Nedd1/N-cadherin
Nedd1
N-cadherin
Merge
E14.5
C
Nedd1/N-cadherin
Nedd1
N-cadherin
Merge
E14.5

tubulin. In ventricular zones, such as in the neural tube at E11.5, there was perfect co-localisation of Nedd1 with γ-tubulin, confirming that Nedd1 is localised in the centrosomes of these cells (Fig. 3.6A and B). However, the strong cytoplasmic expression of Nedd1 seen in the DRG was not observed for γ-tubulin. Rather, γ-tubulin in these cells was detected as a centrosomal spot, or as weak diffuse cytoplasmic staining (Fig. 3.6A and C). This observation is an example of a possible γ-tubulin and centrosome-independent function of Nedd1.

3.6. Expression of Nedd1 in the mouse embryonic eye

As an outgrowth of the brain, the retina is one of the best characterised regions of the CNS. Images provided by the NCBI in the GENSAT database show that mouse embryos and adults express high levels of *Nedd1* mRNA in the retina (see 3.1). Therefore, in addition to analysing the expression of Nedd1 in the developing mouse brain, its expression and localisation was also characterised in the developing eye.

Ocular development in the mouse begins at around E8 when a slightly flattened area of neural ectoderm in the central part of the prospective forebrain region forms as the optic placode (Kaufman, 1992, Foster *et al*., 2003). Shortly after this, a thickening of the surface ectoderm forms the lens placode (Chow and Lang, 2001). Nedd1 staining was first analysed in E11.5 embryos, since changes in the lens become apparent around this time as the lens placode is converted into the lens vesicle (LV), which appears as a spherical cavity (Fig. 3.7A). The localisation of the centrosome in the eye at this stage has not been described. By about E11.5, polarity is established as the cells of the posterior wall of the lens vesicle become elongated and their nuclei tend to be located in the basal region of these cells. At this stage, Nedd1 staining was observed at the apical edge of anterior and posterior lens vesicle cells (Fig. 3.7A, represented diagrammatically in C). There was complete co-localisation with the centrosomal marker γ-tubulin, indicating that this staining represents Nedd1 in the centrosomes of these cells. Also by E11.5, the optic vesicle of the forebrain

Fig. 3.6 Nedd1 co-localises with γ-tubulin in ventricular zones, but not in the DRG of the mouse nervous system

Coronal cryosections of E11.5 embryos were stained with Nedd1 (green) and γ-tubulin (red). The box is enlarged in the adjacent image. Examples of enlarged cells from the corresponding image are shown in the insets.

(**A**) At low magnification (10x), Nedd1can be seen to co-localise with γ-tubulin in the neural tube, but not in the DRG.

(**B**) At higher magnification (40x), Nedd1 can be seen to completely co-localise with γ-tubulin in the centrosomes of ventricular zone cells of the neural tube.

(**C**) In the DRG, the intense cytoplasmic expression of Nedd1 is not shown by γ-tubulin.

Scale bars represent 40 μm.

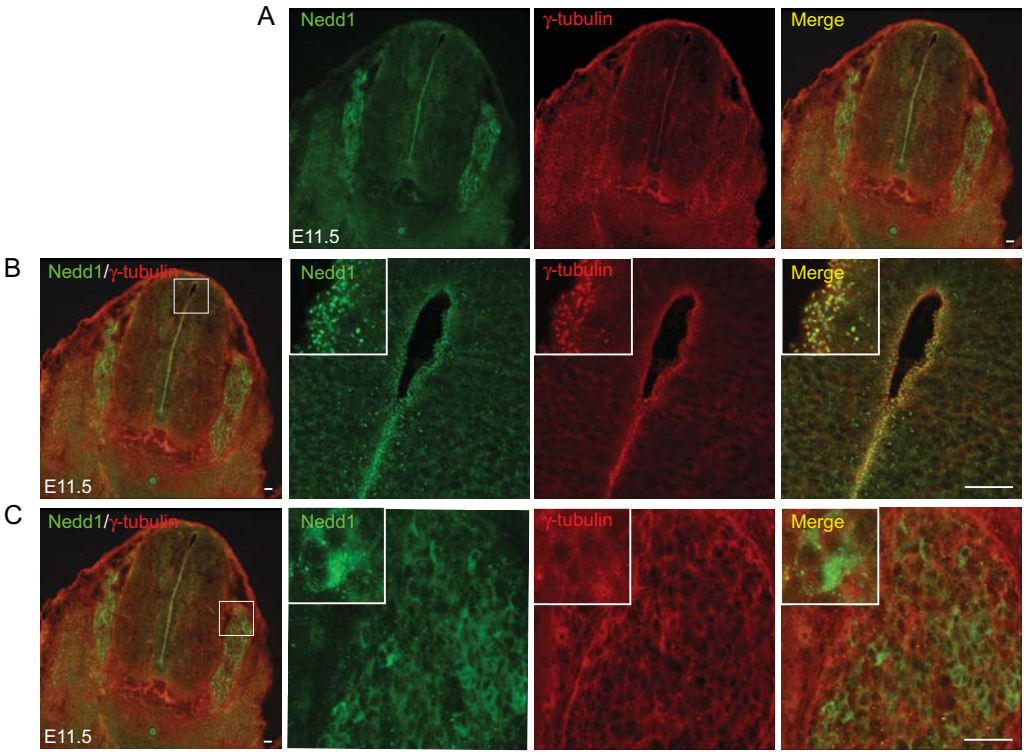
A
Nedd1
γ-tubulin
Merge
E11.5
B
Nedd1/γ-tubulin
Nedd1
γ-tubulin
Merge
E11.5
C
Nedd1/γ-tubulin
Nedd1
γ-tubulin
Merge
E11.5

Fig. 3.7 Expression of Nedd1 in the mouse eye at E11.5

Saggital cryosections of E11.5 embryos were stained with Nedd1 (green), γ-tubulin (red) and Hoechst 33342 to mark the nucleus (blue) (**A**-**B**)**.** LV (Lens Vesicle). The box is enlarged in the adjacent image.

(**A**) Nedd1 co-localises with γ-tubulin in centrosomes in the apical region of polarised epithelial cells in the lens.

(**B**) Nedd1 co-localises with γ-tubulin at the apical surface of polarised cells in the invaginated neural ectoderm of the retina.

(**C**) Schematic representing Nedd1/centrosome localisation in the E11.5 eye. A (Anterior wall of lens vesicle), P (Posterior wall of lens vesicle), INE (Invaginated Neural Ectoderm), PE (Pigment Epithelium). Nedd1 localises in centrosomes at the apical edge of cells of anterior and posterior cells of the lens, and at the apical surface of invaginated neural ectoderm retinal cells.

Scale bars represent 40 μm.

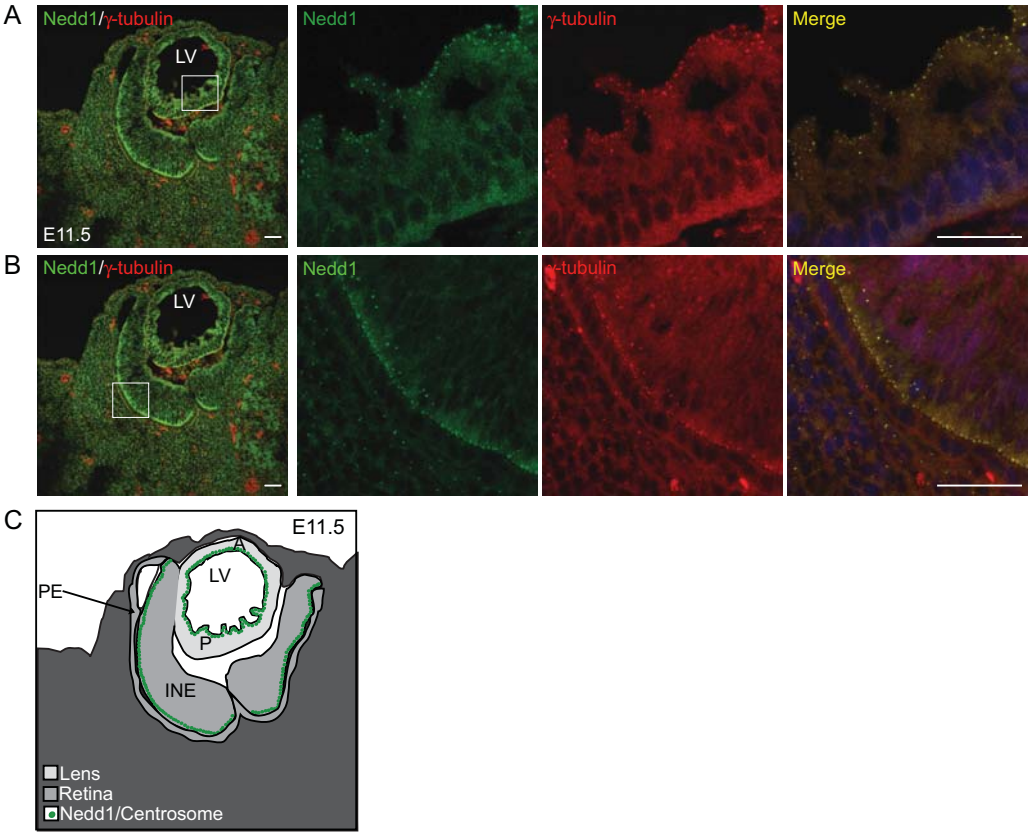
A
Nedd1/γ-tubulin
LV
E11.5
Nedd1
γ-tubulin
Merge
B
Nedd1/γ-tubulin
LV
Nedd1
γ-tubulin
Merge
C
E11.5
PE
LV
P
INE
Lens
Retina
Nedd1/Centrosome

has invaginated to form the neural ectoderm of the optic cup. The invaginated neural ectoderm (INE) becomes the future neural retina and undergoes intense proliferation. In contrast, the outer layer of the neural ectoderm which becomes the future pigment epithelium (PE) of the retina, remains relatively inactive (Pei and Rhodin, 1970). Nedd1 was found in a polarised pattern at the apical (ventricular) surface of the actively proliferating invaginated neural ectoderm of the retina, again co-localising with γ-tubulin in centrosomes (Fig. 3.7B and C).

As development progresses, the lens is organised into an anterior monolayer of lens epithelial cells and a posteriorly positioned terminally differentiated lens fibre cell mass (Chow and Lang, 2001). The lens fibre cells increase in length until by E13, the lumen of the lens vesicle has virtually completely disappeared. New lens fibres are added from the cells at the equatorial region of the lens, so that the lens can increase in volume. At E14.5, Nedd1 was seen in polarised lens epithelial cells at the boundary of the lens fibre cells, co-localising with γ-tubulin (Fig. 3.8A and represented diagrammatically in C). At this stage, the neural retina begins to differentiate to form two cell layers; an inner and an outer neuroblastic layer (INL, ONL) (Pei and Rhodin, 1970). Nedd1 localisation in the retina was seen in a polarised fashion at the apical surface of the ONL (Fig. 3.8B and 3.8C). Therefore Nedd1 has highest expression in centrosomes of highly proliferating cells in the developing eye. The polarised localisation of Nedd1, and therefore the centrosome, is summarised in a schematic model of an E11.5 and E14.5 eye (Fig. 3.7C and 3.8C respectively).

3.7. Nedd1 localises in basal bodies of cilia in the mouse embryonic eye

As described earlier (see 3.3), Nedd1 localised to the centriolar basal body structures at the base of cilia in cells. These structures are also apparent in the embryonic eye. In several cell types, a single non-motile cilium is generated from a basal body during cell differentiation (Horst *et al*., 1990). The basal body of this cilium has been shown to contain γ-tubulin, which is responsible for the nucleation of microtubules (Muresan *et al*., 1993). In

Fig. 3.8 Expression of Nedd1 in the mouse eye at E14.5

Saggital cryosections of E14.5 embryos were stained with Nedd1 (green), γ-tubulin (red) and Hoechst 33342 to mark the nucleus (blue) (**A**-**B**). The box is enlarged in the adjacent image.

(**A**) At E14.5, there is apical polarised expression of Nedd1 in the lens epithelial cells, co-localising with γ-tubulin.

(**B**) In the retina, this Nedd1 expression is again in a polarised pattern in the ventricular region of cells of the outer neuroblastic layer (ONL). INL (Inner Neuroblastic Layer).

(**C**) The schematic represents Nedd1/centrosome expression in the E14.5 eye. C (Cornea), LE (Lens Epithelium), LF (Lens Fibres). Nedd1 localises in centrosomes at the apical edge of lens epithelial cells and at the ventricular surface of ONL cells of the retina.

Scale bars represent 40 μm.

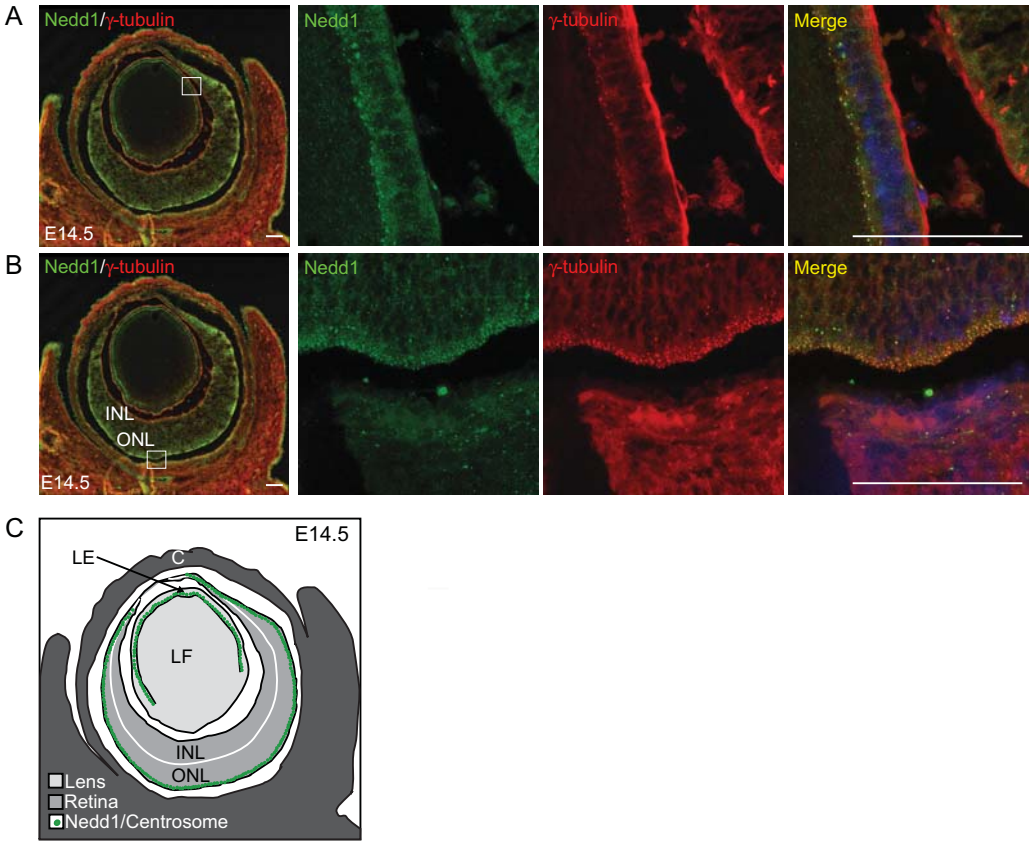
A
Nedd1/γ-tubulin
Nedd1
γ-tubulin
Merge
E14.5
B
Nedd1/γ-tubulin
Nedd1
γ-tubulin
Merge
INL
ONL
E14.5
C
E14.5
LE
C
LF
INL
ONL
Lens
Retina
Nedd1/Centrosome

this study, the primary cilium was observed in the apical region in cells of both the lens and retina of the developing mouse eye (E11.5 shown), as marked by acetylated α-tubulin staining of cilia (Fig. 3.9A and B respectively). Although not detected in the cilia microtubules, Nedd1 was present in the supporting basal bodies of these cilia, confirming its consistent localisation in these structures.

3.8. Nedd1 displays a polarised localisation during mouse embryonic development

Given that Nedd1, as a centrosomal marker, was expressed in a polarised fashion in the lens and the retina of the mouse embryonic eye, it was next aimed to see whether this localisation was consistent in other polarised tissues and organs. It has been previously shown by electron microscopy that centrosomes align along the apical surface of some polarised cells (Tucker *et al*., 1992). To further investigate the localisation of centrosomes in polarised epithelial cells, the expression of Nedd1 was analysed in embryos at E15.5. The lung, gut and cochlea epithelia were selected because they are all known to be polarised at this stage. During lung development, the first indication of the detailed architecture of the future lung becomes obvious at E14.5-15, with the formation of terminal bronchioles that are now seen dispersed throughout the lungs (Kaufman, 1992). In this study, cross sections through the bronchioles with cell boundaries marked by actin (stained with phallodin) showed the polarisation of cells within this tubular structure (Fig. 3.10A). Nedd1 localised to the very apical edge of these polarised cells. A similar tube of epithelial cells resides in the duodenum. Again, Nedd1 localised to the apical edge of cells in this organ (Fig. 3.10B). It appears that in this region, sectioning results in multiple cells being present on the border of the tube, as evidenced by phallodin staining of actin. This results in many centrosomes being present in this region because of multiple cell layers, but there were never more than two centrosomes per cell observed.

In the auditory system of the mouse embryo resides the cochlea, a hollow chamber of bone which also displays obvious polarity (Bermingham-McDonogh *et al*., 2006). The cochlea

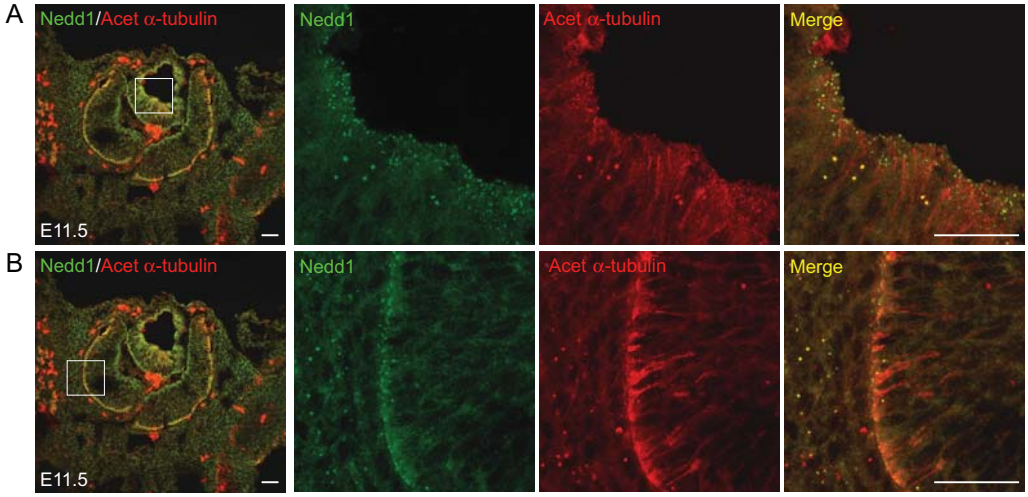

Fig. 3.9 Nedd1 localises at the base of cilia *in vivo*

Saggital cryosections of E11.5 embryos were stained with Nedd1 (green) and acetylated α-tubulin (red). The box is enlarged in the adjacent image.

(**A**) Nedd1 co-localises at the base of acetylated α-tubulin positive cilia, but not along the cilia microtubules in the apical region of the lens (**B**) and retina.

Scale bars represent 40 μm.

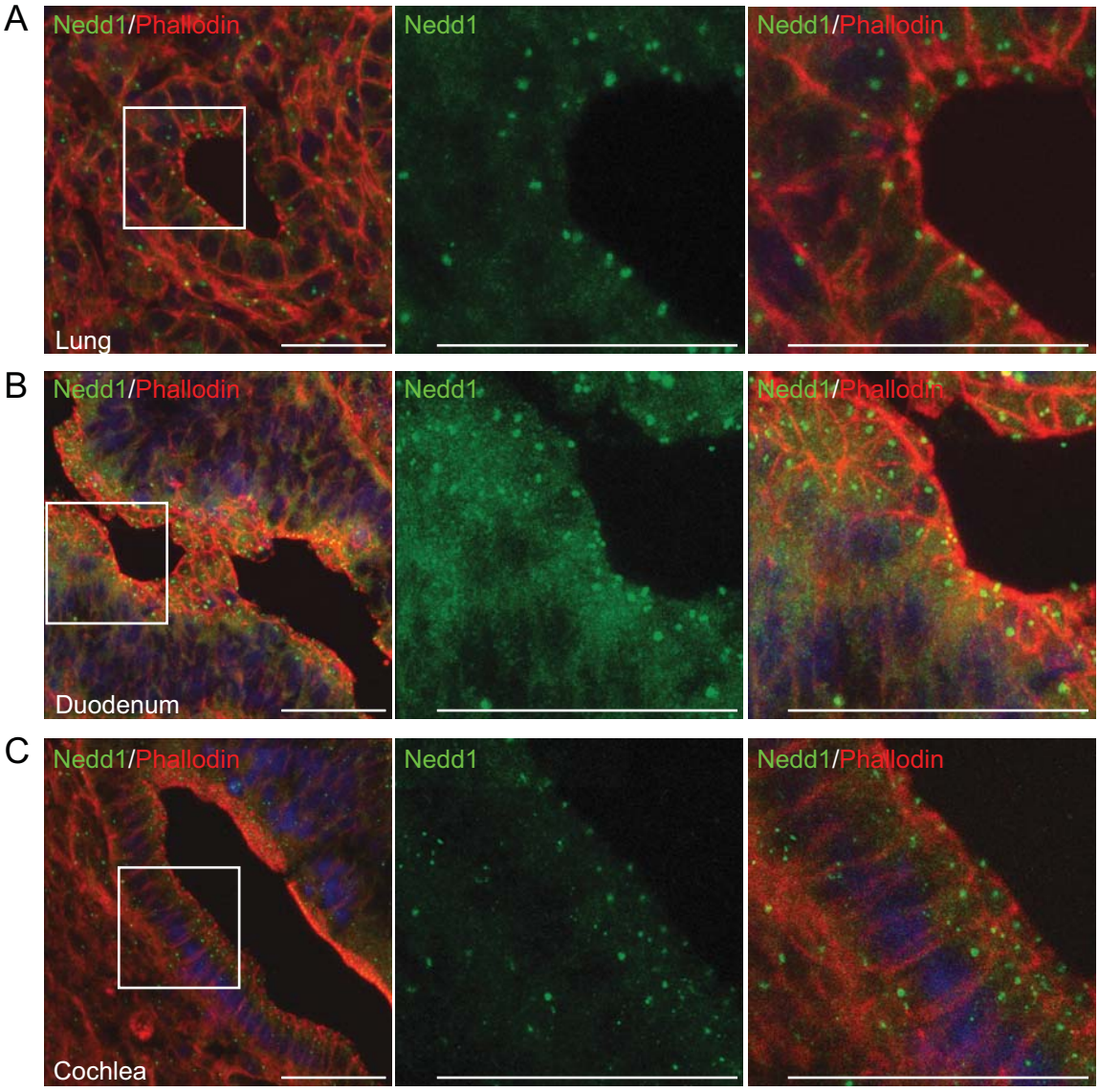

Fig. 3.10 Nedd1 displays a polarised expression in the mouse embryo

Saggital cryosections of E15.5 embryos were stained with Nedd1 (green), phallodin (red), and Hoechst 33342 to mark the nucleus (blue). The box is enlarged in the adjacent image.

(**A**) Nedd1 displays an apical localisation in cells of the lung, (**B**) duodenum and (**C**) cochlea. The actin cell boundaries are marked with phallodin.

Scale bars represent 40 µm.

duct develops from the otocyst beginning at around E11 in mice (McKenzie *et al*., 2004). At E13, the entire epithelium of the cochlea is composed of a homogenous population of epithelial cells. By E16, developing inner hair cells in the basal region of the duct are arranged in a well-ordered row. Indeed, in sections of the cochlea at E15.5, phallodin staining defines a chamber of cells with obvious polarity. Nedd1 was again seen localised at the apical surface in these well-ordered cells (Fig. 3.10C), as in the lung and duodenum described earlier. Therefore, in all the polarised cell types studied, Nedd1 marks the centrosome, localised at the apical surface of the cells.

3.9. Discussion

The centrosome is a well studied organelle, particularly during the cell cycle, but there have been limited studies characterising its role in development. However, it is known that the core centrosomal protein γ-tubulin is crucial for embryogenesis, as these gene deficient mouse embryos die at the blastocyst stage due to mitotic disarray and arrest (Yuba-Kubo *et al*., 2005). To gain further understanding of the centrosome during development, this study has described a highly specific and reliable antibody to Nedd1 (Fig. 3.1 and 3.2), a protein originally identified in our laboratory in a screen for genes potentially involved in embryonic development of the CNS (Kumar *et al*., 1992, Kumar *et al*., 1994). The localisation of Nedd1 with γ-tubulin has been confirmed, and extended to a co-localisation with other centriolar markers (Fig. 3.3). Additionally, this study has shown that Nedd1 is present in the centriolar basal body structures at the base of non-motile cilia, partially co-localising with acetylated α-tubulin (Fig. 3.9). This single, non-motile primary cilium is present in most vertebrate cells and functions in many processes including signalling and the cell cycle (Pan and Snell, 2007, Sloboda and Rosenbaum, 2007). Given its localisation, it is plausible that Nedd1 may contribute to the function of cilia. These data highlight the reliability of Nedd1 as a marker for the centrosome and basal body during development.

Since *Nedd1* was originally identified as a gene that displayed high expression in neural precursor cells, this protein was utilised as a marker for the centrosome during development of the nervous system in mouse embryogenesis. In the mammalian CNS, the ventricular zone and the subventricular zone are highly proliferative regions that generate the majority of neurons (Brazel *et al*., 2003). In the neuroepithelium of the neural tube in embryonic ferrets, the centrosome has been previously shown to asymmetrically localise near the lumen of the ventricular zone, together with adherins junctions proteins such as N-cadherin and β-catenin (Chenn *et al*., 1998). This study has demonstrated that consistent with this, Nedd1 also has high expression in the ventricular zone of the neural tube at E11.5 in the mouse, concentrated at the apical cell surface as shown by N-cadherin staining (Fig. 3.4). This expression is reduced as the embryo develops and the rate of proliferation decreases (Fig. 3.4 and 3.5) (Kaufman, 1992). The Nedd1 expression observed was indeed representative of centrosomes, shown by the co-localisation with γ-tubulin (Fig. 3.6). Hence Nedd1, as part of the centrosome, is likely to be important in the proliferation of cells in the CNS during development.

Aside from its role in proliferation, the centrosome also plays important roles in differentiation by controlling the orientation of the mitotic spindle and therefore the cleavage plane of cells (Higginbotham and Gleeson, 2007). Changes in the cleavage plane can result in the differential distribution of asymmetrically localised proteins, such as those associated with adherins junctions, to produce daughter cells with different fates (Chenn *et al*., 1998). Interestingly, the centrosome can be targeted to adherins junctions, possibly by the interaction of the centrosomal protein dynein with β-catenin (Ligon *et al*., 2001). Additionally, other centrosomally localised proteins such as subunits of the G proteins, have been shown to be required for the correct orientation of the mitotic spindle and therefore cleavage plane and cell fate (Sanada and Tsai, 2005). Hence, centrosomal proteins such as Nedd1, are likely to be important in functions other than proliferation during neurogenesis, contributing to neural cell fate specification through their association with adherins junctions and controlling the orientation of the spindle.

As well as in the neural tube, high Nedd1 expression was also observed in the developing DRG (Fig. 3.4 and 3.5). The cells of the DRG arise from neural crest cells that migrate from the neural tube and undergo a distinct developmental programme (Koblar *et al*., 2000). In neural migration, the centrosome is initially located ahead of the nucleus in the direction of migration (Gregory *et al*., 1988). A leading process then extends forward, the centrosome moves into this leading process, and the nucleus then translocates towards the centrosome (Bellion *et al*., 2005). The centrosome appears to be critical for these processes to occur normally (Higginbotham and Gleeson, 2007). Hence Nedd1, as part of the centrosome, may be important for the migration of neural crest cells to the DRG. Interestingly, in addition to its centrosomal localisation, a large proportion of Nedd1 in some DRG neurons was localised to the cytoplasm (Fig. 3.6). This diffuse cytoplasmic localisation was not observed for γ-tubulin, and is the first example of differential localisation of these two primarily centrosomal proteins. The role of this cytoplasmic Nedd1 is currently unknown, but could contribute to the high neural expression of Nedd1 that was described when this protein was first identified. This discovery leads to many questions and requires further study to determine the role of this pool of Nedd1 in the CNS.

The eye is a highly specialised extension of the nervous system (Chow and Lang, 2001). Structural details of the development of the mouse eye have been well described, but the localisation and role of the centrosome during prenatal stages has not been investigated. The vertebrate lens consists of only one cell type present in different stages of differentiation (Dahm *et al*., 2007). In undifferentiated cells of the adult bovine anterior lens epithelium, there is a single centrosome, located adjacent to the nucleus (Dahm *et al*., 2007). At later stages, before the onset of elongation, the centrosome relocates to the apical ends of epithelial cells and then disappears. The centrosome appears again in lens fibre cells at the epithelial-fibre cell interface. From the results in this chapter, similar observations of Nedd1, and therefore centrosome localisation, were made in the developing mouse lens at E11.5 and E14.5 (Fig. 3.7 and 3.8). This suggests that the centrosome may

be important in the early development of the mouse lens. The functional significance of the disappearance and relocation of the centrosome is not yet known, but Nedd1 has now been identified as another marker to begin investigating this. Similarly, not much is known about the centrosome in the developing mouse retina. In the adult zebrafish retina, centrosomes are located at the ventricular surface of the retinal neuroepithelium (Malicki, 1999, Zolessi *et al*., 2006). This also appears to be the case in the developing mouse prenatal retina as Nedd1 displays a polarised localisation at the apical surface of the invaginated neural ectoderm at E11.5 and the outer neuroblastic layer of cells at E14.5 (Fig. 3.7 and 3.8). Differentiation of the retina into the final seven major classes of cell types does not occur until later in development, so it is not clear what happens to Nedd1 and the centrosome in these cell types. However, it has been shown that the centrosome plays a crucial role in maintaining photoreceptor cells in the adult retina, as a study found that an in-frame deletion in the centrosomal protein CEP290 leads to early-onset retinal degeneration (Chang *et al*., 2006). Hence, the centrosome and its constituents, such as Nedd1, are likely to also be important in later stages of development involving additional cell types.

Given that Nedd1 displayed an apical localisation in polarised cells of the eye, this study also aimed to investigate this localisation in other polarised cell types. In most cells, microtubules radiate from a typically centrally located centrosome, surrounded by a sphere of pericentriolar material. In several epithelial cell types, such as in the liver, kidney, intestine and cochlea, the centrosome ceases to act as the conventional MTOC upon polarisation (Srsen and Merdes, 2006). Instead, centrosomal proteins are localised along the apical region of the cell, or in a ribbon-like zone along the plasma membrane such as in adult mouse cochlea cells (Tucker *et al*., 1992). The results reported in this chapter support the previous data on the localisation of the centrosome in these cell types, and provide a description of the expression and localisation of a centrosomal protein in different polarised regions of the developing mouse embryo. Nedd1 protein was found in centrosomes at the apical surface of epithelial cells in the lung, duodenum and the cochlea (Fig. 3.10). In these cells, microtubules run in parallel arrays, with the minus ends at the apical surface, and the

plus ends at the basal surface. These microtubules are not associated with the centrosome (Meads and Schroer, 1995). Although the organisation of the microtubule network has been suggested to result from nucleation at non-centrosomal sites (Meads and Schroer, 1995), a number of systems provide evidence for the release of microtubules from the centrosome after nucleation has occurred (Keating *et al*., 1997). Hence, centrosome disruption could lead to the disorganisation of microtubules in epithelial cells, and a loss of polarity. The consequences of this would be dramatic, as polarity is critical for many factors such as providing a barrier between internal and external environments, membrane transport and the distribution of cell fate determinants (Meads and Schroer, 1995). Therefore, it is important to understand the localisation and expression of centrosomal proteins in the developing embryo, as this study has demonstrated with Nedd1, so that their contribution to polarity can be assessed further.

The centrosome continues to be revealed as an organelle that displays multiple functions, and has been implicated in numerous cell cycle and non-cell cycle related processes. It is therefore obvious that this organelle must play important roles during development, but this has not been well explored to date. This study has provided an important characterisation of the centrosome, and one of its constituents Nedd1, during the processes of neural development and polarisation in mouse embryogenesis. This should provide a basis for further study into its role in development.

4. Nedd1, as a component of the centrosome, is important in the cell cycle and senescence

4.1. Introduction

The function of the centrosome during the cell cycle has been well studied, and it is known to play many different roles in this process (Doxsey *et al*., 2005). Given the centrosomal localisation of NEDD1, it is therefore likely that this protein also plays an important role during the cell cycle. Indeed, it has been previously shown that the depletion of NEDD1 in mammalian cells results in a loss of microtubule nucleation which leads to spindle defects and mitotic chaos (Haren *et al*., 2006, Luders *et al*., 2006). Hence the function and regulation of this protein is critical for normal progression through the cell cycle. In regards to its regulation, it has thus far been demonstrated that *Nedd1* is regulated transcriptionally by the Sam68 RNA binding protein during male germ cell differentiation in mice (Paronetto *et al*., 2009). Additionally, at the protein level NEDD1 can be phosphorylated on multiple residues and this is required for the localisation of NEDD1 to the centrosome, and to spindle fibres during mitosis (Luders *et al*., 2006, Haren *et al*., 2009, Zhang *et al*., 2009). Phosphorylation is a common method of regulation of cell cycle proteins, as is protein degradation (Nigg, 2001). Whether NEDD1 is also controlled by protein degradation or other methods of regulation during the cell cycle remains unknown.

The cell cycle can be arrested in response to many different types of stress. Certain stimuli and conditions lead to an irreversible state of this cell cycle arrest, called senescence. Cells in senescence remain metabolically active, but display metabolic and morphological changes (Dimri *et al*., 1995). This process can occur as a protective mechanism to inhibit cell proliferation after DNA damage, oxidative stress, oncogenic activation and many other stimuli. Mechanistically, senescence normally involves the activation of the tumour suppressor proteins p53 and Rb, and their signalling partners including the Cdk inhibitors p16, p19 and p21 (Ben-Porath and Weinberg, 2005).

Recent evidence has suggested that centrosome abnormalities are one of the factors that can trigger senescence, in addition to causing arrest in different phases of the cell cycle by

activating various checkpoints. In particular, ablation of the centrosome or its components forces cells to enter cell cycle arrest and can predispose them to senescence (Srsen *et al*., 2006, Mikule *et al*., 2007). Hence, centrosomal integrity is important in maintaining actively proliferating cells. The role that the centrosome plays in senescence caused by other factors, such as oncogenes or oxidative stress is unknown.

Therefore the aims of this chapter were two-fold. Firstly, to extend the cell cycle analysis of NEDD1 to determine if this protein is regulated by methods in addition to phosphorylation. Secondly, to assess the role of Nedd1 in senescence in order to provide a greater understanding of the involvement of this protein, and the centrosome, in this form of cellular arrest. Mouse embryonic fibroblasts were employed for this analysis as they are commonly used as a model of senescence (Sherr and DePinho, 2000, Parrinello *et al*., 2003).

4.2. NEDD1 is expressed in all cell types with variable expression

Since NEDD1 is a centrosomal protein, it was expected to be present in all cell types, as centrosomes are required for mammalian cell growth and division (Badano and Katsanis, 2006). To confirm this, a range of human and mouse cell lines were lysed and assessed for protein levels. The human cells included transformed embryonic kidney cells (HEK293T), cervical cancer cells (HeLa), leukemic cell lines (Jurkat, CEM and K562) and cell lines derived from breast tumours (MCF7, T47D, MDA-468 and MDA-231). As expected, NEDD1 was detected in all cell types analysed, although levels of expression varied between the cell lines (Fig. 4.1A). Additionally, the protein often appeared as a doublet on immunoblot presumably representing the previously reported phosphorylated and non-phosphorylated forms of NEDD1 (see 4.3) (Luders *et al*., 2006). The mouse cells included neurally-derived cancer cell lines (N18 and PCC4), transformed fibroblasts (NIH-3T3) and primary mouse embryonic fibroblasts (MEFs). Nedd1 was again detected in all cell types with varied expression (Fig. 4.1B). Interestingly, the level of Nedd1 protein also varied within the same

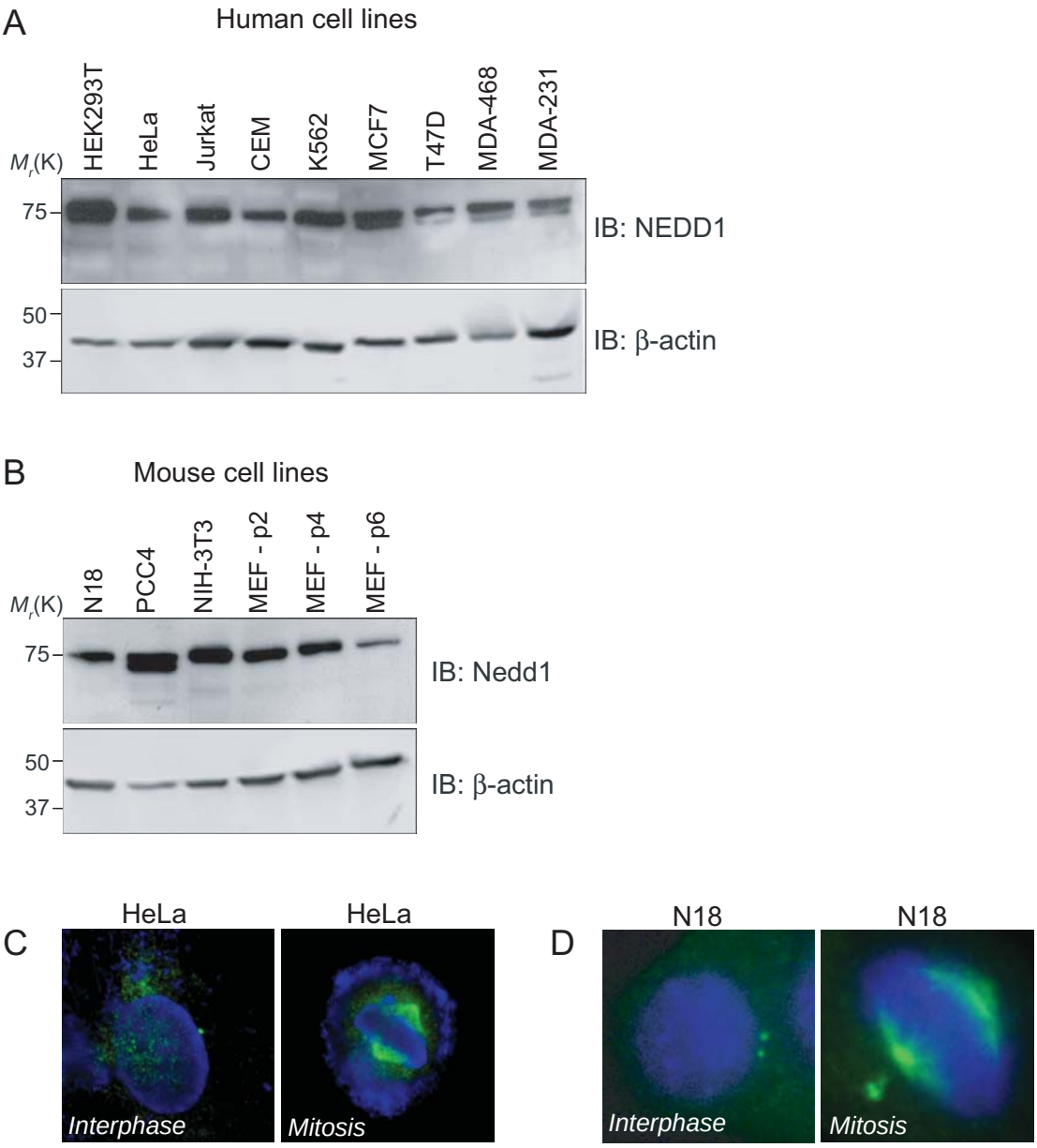

Fig. 4.1 NEDD1 is expressed in all cell types with variable expression

Various cell lines were lysed and assessed for NEDD1 protein levels. 50 µg of protein is loaded in each lane (**A**-**B**).

(**A**) NEDD1/Nedd1 is present in all human and (**B**) mouse cell lines at various levels, and the expression decreases with passage number (p) in primary cells (MEFs). β-actin serves as a loading control.

(**C**) Human HeLa cells and (**D**) mouse N18 cells were stained with NEDD1 antibody (green) and Hoechst 33342 to mark the nucleus (blue). In interphase, NEDD1/Nedd1 can be seen as a single or double centrosomal dot, and in mitosis it is enriched in the centrosomes and also localises along the spindle microtubules.

cell type, depending on the passage number, or age of the cells. This was most evident in primary cells, as late passage MEFs (passage 6) exhibited much lower Nedd1 expression.

To further confirm and analyse the protein levels of NEDD1 in mammalian cells, the NEDD1 antibody was also used to immunostain and localise this protein within cells. As previously observed (Fig. 3.1), two types of localisation of NEDD1 were seen, in both human (HeLa) and mouse (N18) cell lines (Fig. 4.1C and D respectively). In interphase cells, NEDD1 was detected in centrosomes (one or two depending on the stage of the cell cycle) and a small amount in the cytoplasm. In mitotic cells, there was an increase in the amount of NEDD1 present in centrosomes, and this protein was also detected on the spindle microtubules. This localisation was consistent in all cell lines tested (data not shown), and suggests that NEDD1 is expressed in all cell types.

4.3. NEDD1 is highest at mitosis and phosphorylated

As noted previously, NEDD1 appeared as a doublet on immunoblot in some cell types (Fig. 4.1). The higher molecular mass band was suspected to signify a phosphorylated form of the protein. Indeed, shortly after commencement of this project, a phosphorylated form of NEDD1 was identified (Haren *et al*., 2006, Luders *et al*., 2006), and this has recently been confirmed (Zhang *et al*., 2009). This phosphorylated form of NEDD1 becomes apparent during mitosis (Luders *et al*., 2006, Haren *et al*., 2009, Zhang *et al*., 2009). In order to determine if controlling the phosphorylation state is the main method of NEDD1 regulation, or if protein levels are regulated by other mechanisms during the cell cycle, cells were synchronised and total NEDD1 protein levels assessed. The Jurkat leukemic cell line was used for this study since these cells grow in suspension making them more amenable for flow cytometry studies, and NEDD1 is expressed at a high level in these cells (Fig. 4.1A). Cells were synchronised in mitosis using nocodazole and released from the block for a number of hours. Cell cycle phase was determined by measuring DNA content by flow cytometry. The majority of cells were synchronised in mitosis one hour after release from

the nocodazole treatment, as seen by the shift in DNA content from 2N to 4N (Fig. 4.2A). Additionally, cyclin B1 protein expression is known to be highest during late G2 phase and mitosis (Miyazaki and Arai, 2007), and this correlated to 0-1 hours after release from the nocodazole block (Fig. 4.2B). The higher molecular mass phosphorylated form of NEDD1 was present during mitosis, and was de-phosphorylated or degraded as the cells exited mitosis. It was also observed in this experiment that the total levels of NEDD1 remained fairly constant during the cell cycle. Therefore it is apparent that the primary regulation of NEDD1 which distinguishes between an interphase and mitotic form of the protein, appears to be by phosphorylation and not by a change in total protein levels.

4.4. Nedd1 expression decreases in MEFs as they enter senescence

From the analysis of protein levels in various cell types at different passages, it was observed that the level of Nedd1 expression in primary MEFs decreased with the passage number (age) of the cells (Fig. 4.1). To confirm this observation and further investigate if Nedd1 levels reflect cellular age, MEFs were used as a model system for cells that grow for a finite number of divisions in cell culture before entering senescence. Over multiple experiments and different batches of cells, MEFs isolated from E14.5 embryos survived and proliferated until passage 5-6, after which time their population doubling time was dramatically increased (example shown in Fig. 4.3A). The population doubling time of these cells at passage 6 was approximately 320 hours as opposed to cells from passage 1 doubling every 28 hours. After passage 6, the cells eventually recovered and the doubling time decreased again (data not shown). This is likely to be due to a population of cells escaping senescence and proliferating again as a result of spontaneous immortalisation that is characteristic of MEFs in culture (Todaro and Green, 1963). However, this study only analysed cells until the majority of the population first entered senescence (passage 6). To confirm that these cells were indeed entering senescence, a β-galactosidase assay was performed to stain cells that express senescence-associated β-galactosidase (SA-β-gal) activity (Dimri *et al*., 1995). Correlating with the doubling time, it was evident that the

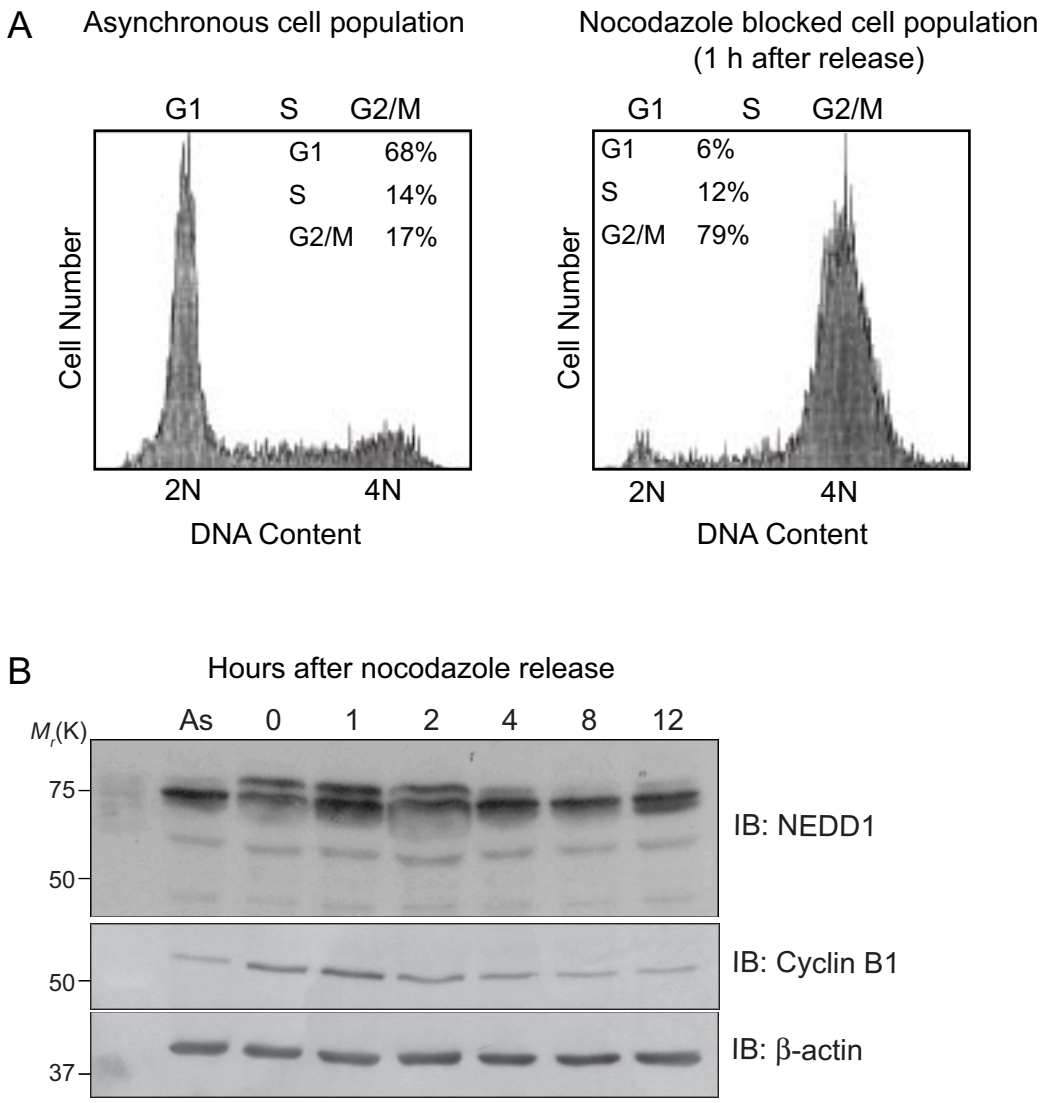

Fig. 4.2 NEDD1 is highest at mitosis and phosphorylated

Jurkat cells were synchronised in mitosis with nocodazole.

(**A**) Asynchronous cells, or nocodazole synchronised cells 1 h after release from the block were analysed for DNA content by flow cytometry. 79% of the synchronised cells display a shift to a G2/M peak, compared to 17% in asynchronous cells, indicating that the majority of cells are blocked in G2 or M phase.

(**B**) Asynchronous cells (As) or synchronised cells at various time points after release were lysed and immunoblotted for NEDD1 and cyclin B1. A higher molecular mass band, presumably corresponding to phosphorylated NEDD1 is present when the cells are in mitosis (indicated by DNA content and higher cyclin B1 levels) about 0-1 h after release from the block. β-actin serves as a loading control.

Fig. 4.3 MEFs enter senescence after six passages

MEFs were harvested from an E14.5 embryo and continually cultured until senescence.

(**A**) At each passage, cells were counted and doubling time calculated (see 2.7.2). By the sixth passage, the doubling time has greatly increased.

(**B**) At each passage, the cells were analysed for SA-β-gal, which stains senescent cells blue. By passage 6, a high proportion of cells are blue, indicating that senescence has been activated.

Scale bars represent 40 μm.

A

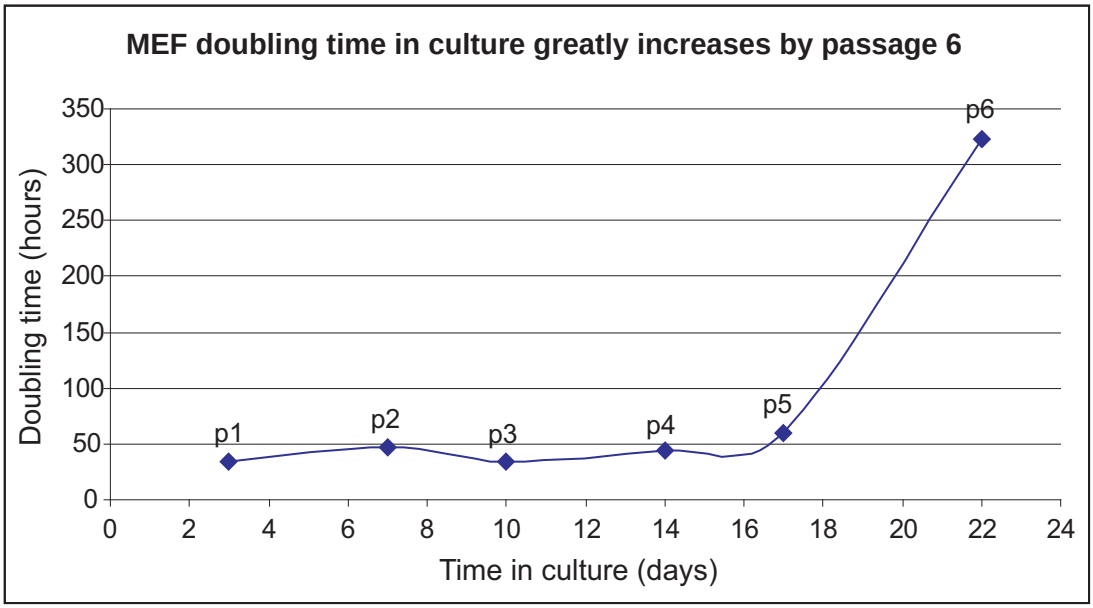
MEF doubling time in culture greatly increases by passage 6
Doubling time (hours)
350
300
250
200
150
100
50
0
p1
p2
p3
p4
p5
p6
0
2
4
6
8
10
12
14
16
18
20
22
24
Time in culture (days)

B

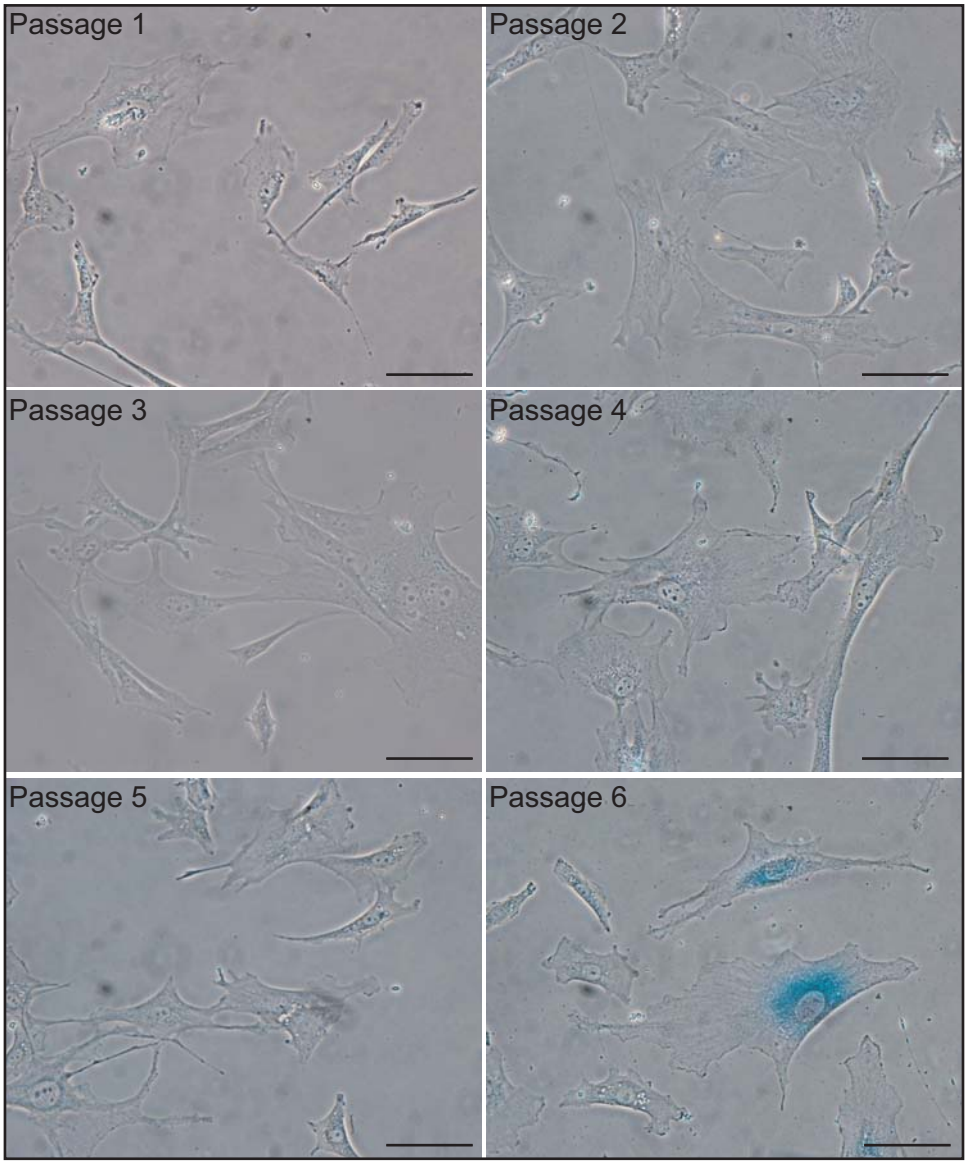
Passage 1
Passage 2
Passage 3
Passage 4
Passage 5
Passage 6

majority of cells were senescent at passage 6 (Fig. 4.3B). However, there were still some cells that did not appear senescent at this passage, and had likely become immortalised, which explains the continued growth of these cells for additional passages.

In order to determine the protein levels of Nedd1 in these MEFs, cell lysates at each passage were analysed by immunoblotting. As expected given the previous preliminary data, Nedd1 protein was detected in early passage MEFs but was dramatically reduced and barely detectable in MEFs at passage 6 which were primarily senescent (Fig. 4.4A, top panel). Interestingly, γ-tubulin levels remained unchanged over the 6 passages, suggesting that the reduction of Nedd1 was not a general consequence of reduced centrosomal proteins, but specific to Nedd1 (Fig. 4.4A, second panel). Senescence can result from varied stimuli and trigger the activation of proteins in different pathways as discussed in the introduction (see 1.4). In order to confirm the induction of senescence in these MEFs, protein levels of p16, p19 and p21, which are known to be involved in senescence were analysed. Expression of all of these proteins was increased from about passage 3, and stayed high as the cells entered senescence (passage 6) (Fig. 4.4A. bottom 3 panels). In addition, the level of *p21* mRNA transcript was analysed in some of the passages using quantitative real-time PCR (qPCR). This correlated well with the protein expression, as *p21* mRNA was increased at passage 4 and again at passage 6 (Fig. 4.4B). Hence, Nedd1 levels in these MEFs decreased as the cells entered senescence, shown by increased SA-β-gal activity and an up-regulation of the senescent markers p16, p19 and p21.

4.5. Cells with abnormal centrosome numbers increase in senescent MEFs

Given that Nedd1 protein levels decreased as the MEFs were passaged, it was next assessed if there were also changes in centrosome structure or integrity in these cells. To test this, cells from an early healthy passage (passage 1) and a late senescent passage (passage 6) were stained for centrosomal proteins. At passage 1, almost all cells presented the expected centrosomal staining. Using both Nedd1 and γ-tubulin as markers, cells had a

Fig. 4.4 Nedd1 expression decreases as MEFs enter senescence

MEFs were lysed and assessed for various proteins and *p21* mRNA expression at each passage until senescence.

(**A**) 50 μg of total protein was loaded onto multiple gels for immunoblotting with different antibodies. Nedd1 is expressed in passages 1-5, but is barely detectable at passage 6 when the cells enter senescence as shown by an increase in protein expression of typical markers of senescence p16, p19 and p21. γ-tubulin levels remain constant.

(**B**) *p21* mRNA expression was quantitated by qPCR at passages 1, 4 and 6, and shows an increase in expression as the cells are passaged. Error bars show standard error of the mean (SEM), where n = 3 replicates. This experiment was conducted by Dimitrios Cakouros in the laboratory.

A

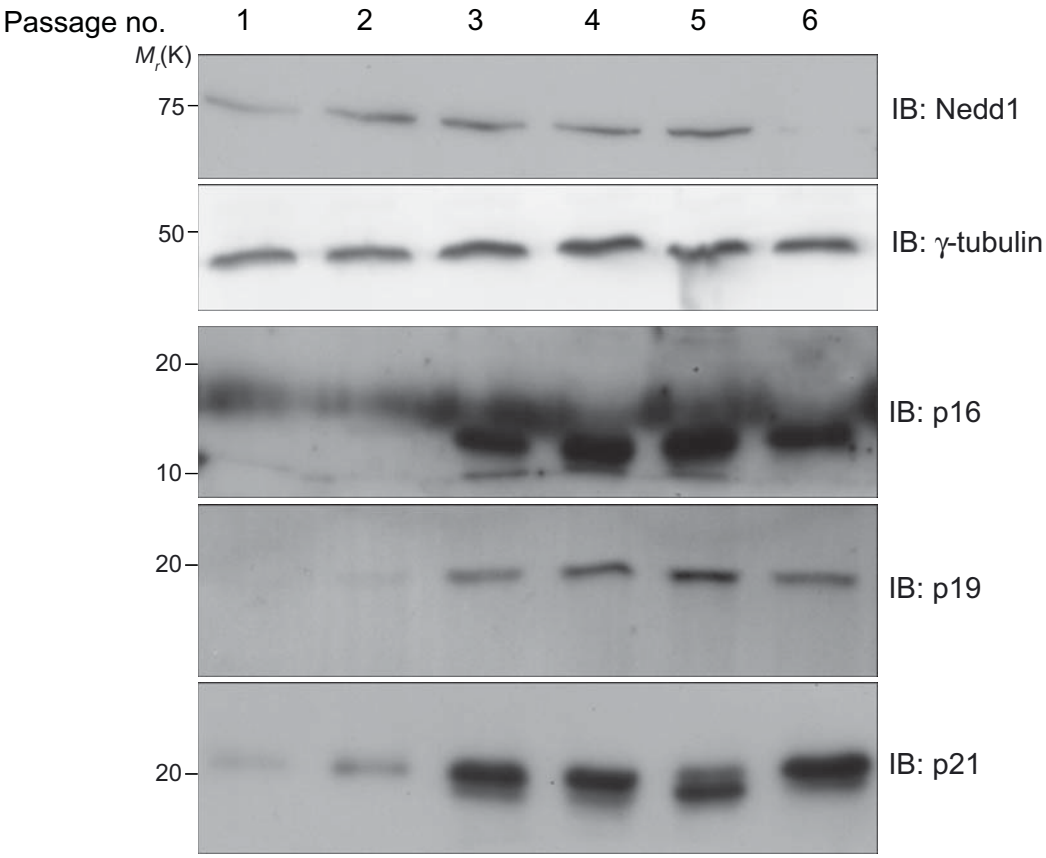
Passage no.
1
2
3
4
5
6
M_r(K)
75
50
20
10
20
20
IB: Nedd1
IB: γ-tubulin
IB: p16
IB: p19
IB: p21

B

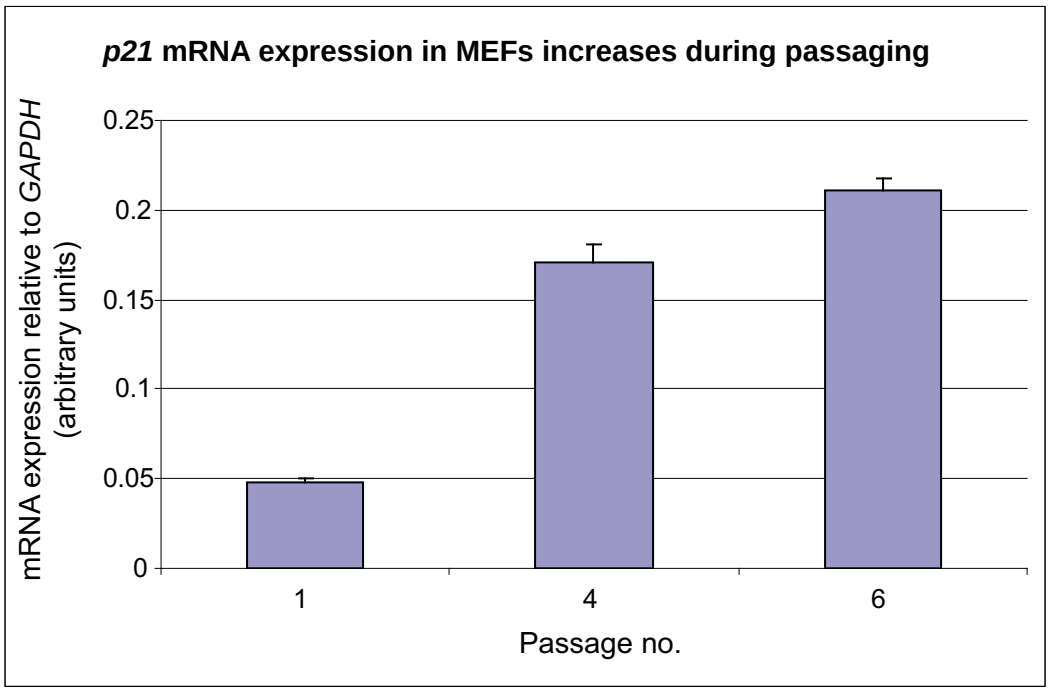
p21 mRNA expression in MEFs increases during passaging
mRNA expression relative to GAPDH (arbitrary units)
0.25
0.2
0.15
0.1
0.05
0
1
4
6
Passage no.

single or double centrosomal dot (Fig. 4.5A and B). Nedd1 and γ-tubulin always perfectly co-localised in these cells. Even though total Nedd1 levels were barely detectable by immunoblot at passage 6, the Nedd1 antibody was still able to detect Nedd1 in the centrosomes of these cells at a similar intensity to passage 1 MEFs. However, at this passage it was apparent that numerous cells displayed abnormal centrosomes (Fig. 4.5C-E). In most cases, there were an increased number of centrosomal dots. Often these dots appeared smaller in size than the centrosomes at passage 1, and were sometimes distributed throughout the cell (Fig. 4.5C and D) and sometimes clustered together (Fig. 4.5E). As in early passage cells, Nedd1 and γ-tubulin always perfectly co-localised.

Upon quantification of the centrosomal dots in cells from passage 1 to passage 6, it was observed that there was a gradual increase in the number of cells with greater than 2 centrosomes from passage 1 (1%) to passage 5 (6%), and then a greater increase at passage 6 (16%) (Fig. 4.6A). This correlates with the time that the majority of these cells become senescent (Fig. 4.3). In the cells with greater than 2 centrosomes, the actual number of centrosomes usually ranged from 3-5, however there were also a proportion of cells that displayed 6 or more centrosomes (Fig. 4.6B). Although it was not technically possible to co-stain cells for centrosomal markers and the senescent marker SA-β-gal, it appeared that the abnormal centrosomes were occurring in morphologically flatter and larger cells, indicating that they were senescent.

4.6. The centrosomes in senescent MEFs appear to become fragmented

It was then assessed if the increase in supernumerary centrosomes was due to the fragmentation or over-duplication of centrosomes. To address this question, cells at passage 1 and passage 6 were co-stained with Nedd1 and the centriolar marker, GT335. At this resolution it was often impossible to detect two centrioles within each centrosome, however at passage 1, all Nedd1 and GT335 dots appeared normal with 1-2 centrosomal structures per cell (Fig. 4.7A and B). At passage 6, there were many cells with greater than

Fig. 4.5 Cells with abnormal centrosome numbers increase in senescent MEFs

MEFs were stained for Nedd1 (green), γ-tubulin (red) and Hoechst 33342 to mark the nucleus (blue), at each passage until senescence.

(**A**-**B**) At passage 1 (p1), most cells display normal numbers of centrosomes with either one (**A**) or 2 (**B**) centrosomes co-staining with Nedd1 and γ-tubulin.

(**C**-**E**) By passage 6 (p6), many cells display >2 centrosomal structures either distributed throughout the cell (**C**-**D**) or in close proximity to each other (**E**). The centrosomes are enlarged in the insets in (**E**).

Scale bars represent 20 μm.

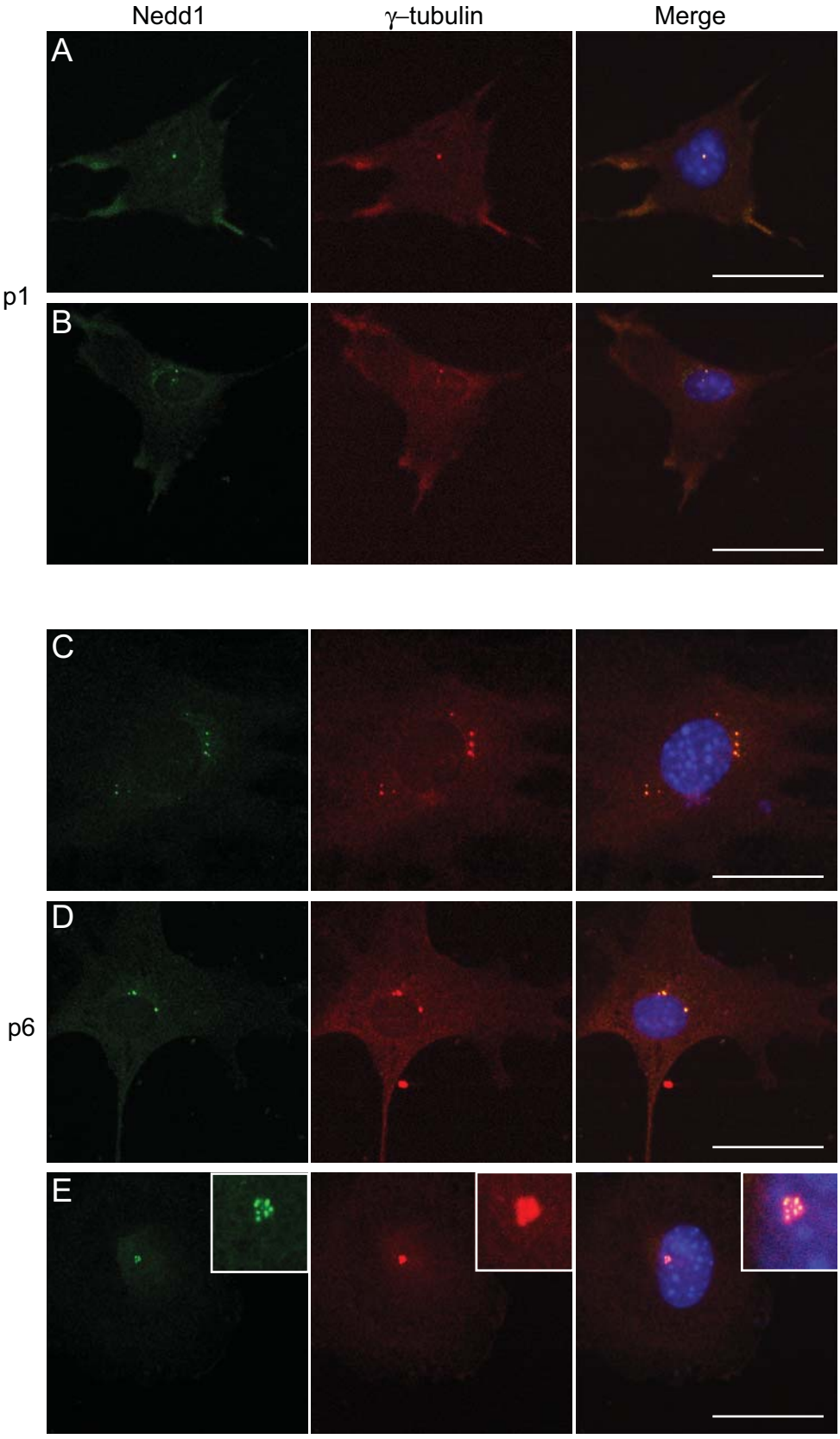
Nedd1
γ–tubulin
Merge
A
B
p1
C
D
p6
E

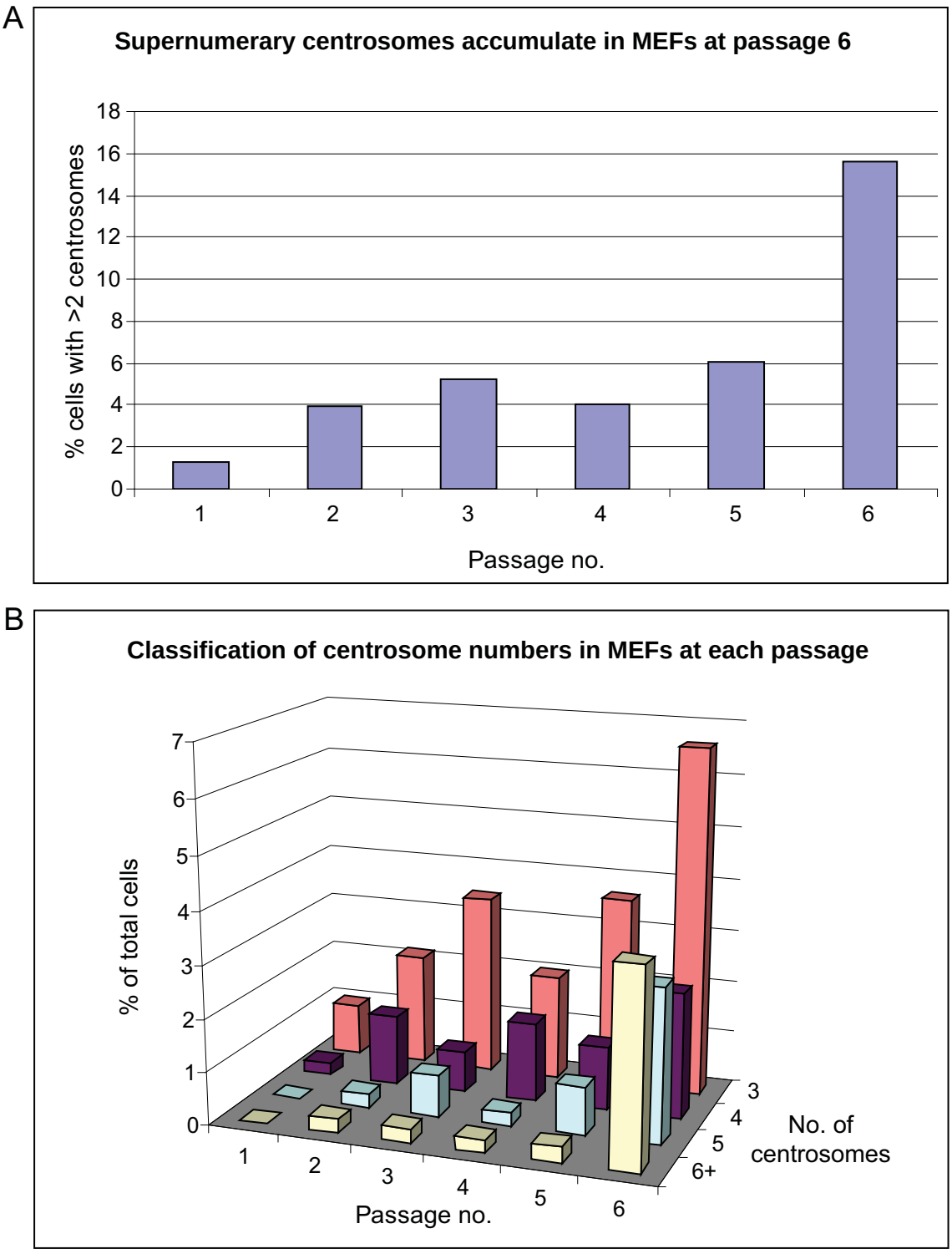

Fig. 4.6 Quantification of abnormal centrosomes in senescent MEFs

The numbers of centrosomes in cells from passage 1 and 6 (examples shown in Fig. 4.5) were counted. At least 300 cells were counted for each passage.

(**A**) The percentage of cells with >2 centrosomes rises sharply between passages 5 and 6.

(**B**) Of the cells displaying >2 centrosomes, most have 3 centrosomes, but some have 4 or more.

Fig. 4.7 Cells at passage 6 contain fragmented centrosomes

Cells were stained for Nedd1 (green), GT335 (red) and Hoechst 33342 to mark the nucleus (blue), at passage 1 and 6.

(**A**-**B**) At passage 1 (p1), most cells display normal numbers of centrosomal structures with either 1 (**A**) or 2 (**B**) pairs of centrioles co-staining with Nedd1 and GT335. Each pair of centrioles normally appears as a single dot at this resolution.

(**C**-**E**) By passage 6 (p6), some cells displaying >2 centrosomal structures have complete co-localisation of Nedd1 and GT335 in all centriole-like dots (**C**-**D**), and other cells have some Nedd1 positive but GT335 negative dots (arrows, **E**). The dots are often smaller in centrosomal structures at p6. The centrosomes are enlarged in the insets in (**C**).

Scale bars represent 20 μm.

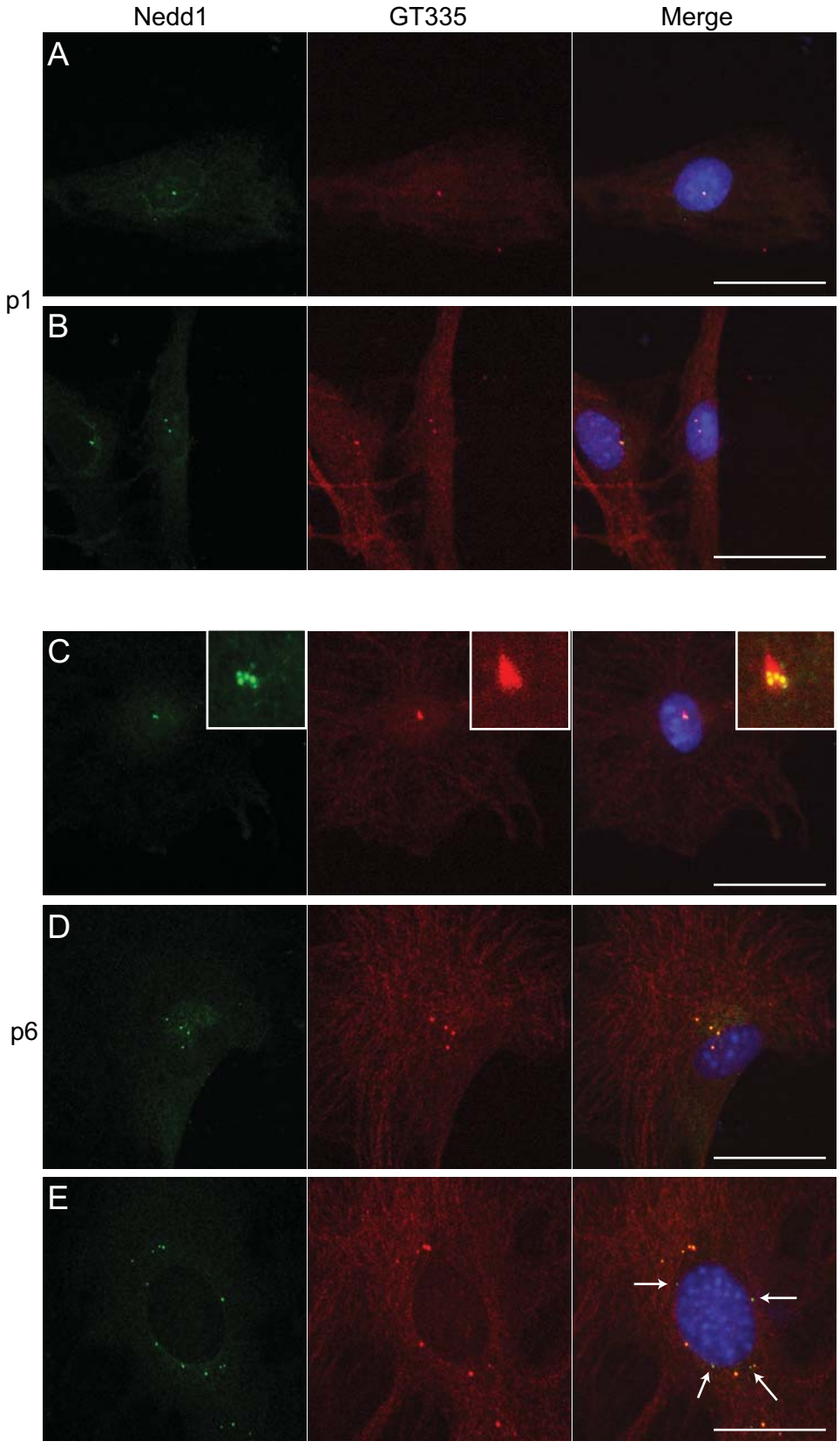
Nedd1
GT335
Merge
A
p1
B
C
D
p6
E

2 centrosomal structures, and they often appeared smaller in size (Fig. 7C-E). Additionally, although in most cells there was co-staining of Nedd1 and GT335 in all dots (Fig. 7C and D), there were some cells that contained dots only positive for Nedd1 and not GT335 (arrows, Fig. 4.7E). This indicates that these dots may have been fragments of centrosome material, and did not contain an intact centriole. The possibility of centrosome over-duplication was not explored in this study and may still be occurring. However, due to the smaller size and lack of complete localisation of the centriole marker within all dots, centrosome fragmentation was predicted to be the primary mechanism for the supernumerary centrosomes.

4.7. A reduction of Nedd1 can cause premature entry into senescence

From these experiments, it was unknown whether the reduction in Nedd1 levels and centrosome abnormalities was a reflection of cells entering senescence, or if these changes somehow contributed to the fate of the cells entering senescence. To investigate this, Nedd1 levels were depleted in MEFs at an early passage (passage 1). No change was observed in Nedd1 or γ-tubulin levels in control scrambled siRNA treated cells over the course of the experiment (Fig. 4.8A-C). After a double transfection of Nedd1 siRNA over 5 days in culture, Nedd1 levels were drastically reduced (Fig. 4.8D). After removal of the siRNA at day 5, the cells gradually re-gained Nedd1 expression 8 days and 11 days after the initial siRNA transfection (Fig. 4.8E, F).

To investigate if this reduction in Nedd1 could cause premature entry of the early passage MEFs into senescence, cells depleted of Nedd1 were assessed for SA-β-gal activity various days after Nedd1 knockdown. Cells treated with control scrambled siRNA showed no increase in senescent cells (<5% SA-β-gal stained cells at each day) (Fig. 4.9A). However, cells depleted of Nedd1 showed an increase in senescent cells 8 and 11 days after the initial Nedd1 siRNA transfection (12% and 22% SA-β-gal stained cells respectively). This was significant at day 8 ($p = 0.01$), and approaching significance at day 11 ($p = 0.05$) (Fig.

Fig. 4.8 Nedd1 expression can be reduced in MEFs using siRNA

Passage 1 MEFs were transfected with a control scrambled siRNA or Nedd1 siRNA twice for 48h and 72h each, and then stained for Nedd1 (green) and γ-tubulin (red) on day 5 when the siRNA was removed and again on day 8 and day 11.

(**A**-**C**) At all days in the control scrambled siRNA there is no reduction of Nedd1 or γ-tubulin protein.

(**D**) After 5 days of Nedd1 siRNA treatment, the levels of Nedd1 and γ-tubulin are dramatically reduced at the centrosome.

(**E**-**F**) The levels of these proteins gradually increases 8 days after the initial transfection (3 days after siRNA removal) and again 11 days after the initial transfection (3 days after siRNA removal).

Scale bars represent 40 μm.

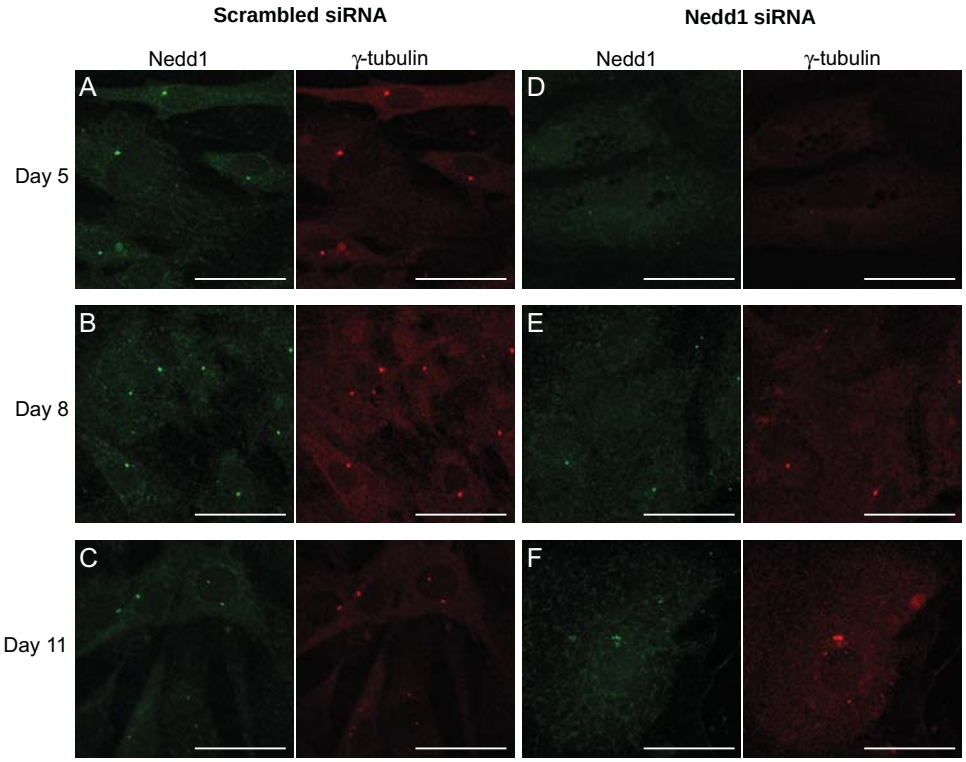
Scrambled siRNA
Nedd1 siRNA
Nedd1
γ-tubulin
Nedd1
γ-tubulin
A
D
Day 5
B
E
Day 8
C
F
Day 11

Fig. 4.9 Nedd1 depletion causes premature entry of MEFs into senescence

An aliquot of cells treated with scrambled or Nedd1 siRNA as in Fig. 4.8 were stained for the senescence marker SA-β-gal at day 5 when the siRNA was removed and again at day 8 and day 11.

(**A**) Cells treated with a scrambled siRNA maintain low levels of positive SA-β-gal staining on day 5, 8 and 11. Cells treated with Nedd1 siRNA have relatively low levels of SA-β-gal staining after 5 days of Nedd1 depletion, but blue cells become more abundant 8 days after initial depletion, and again after 11 days.

(**B**) The number of SA-β-gal expressing cells was counted. At day 8 there is a significant increase the amount of senescent cells in the Nedd1 siRNA treated cells compared with control cells at day 8. At day 11, this is approaching significance (due to the wide variation in response of MEF cells). There is also a significant increase in the number of senescent cells between days 5 and 11 of the Nedd1 siRNA treated group. Approximately 300 cells were counted for each group. Error bars show SEM, where n = 3 independent experiments. p values are calculated using a one-tailed students t-test (see 2.11).

Scale bars represent 40 μm.

A

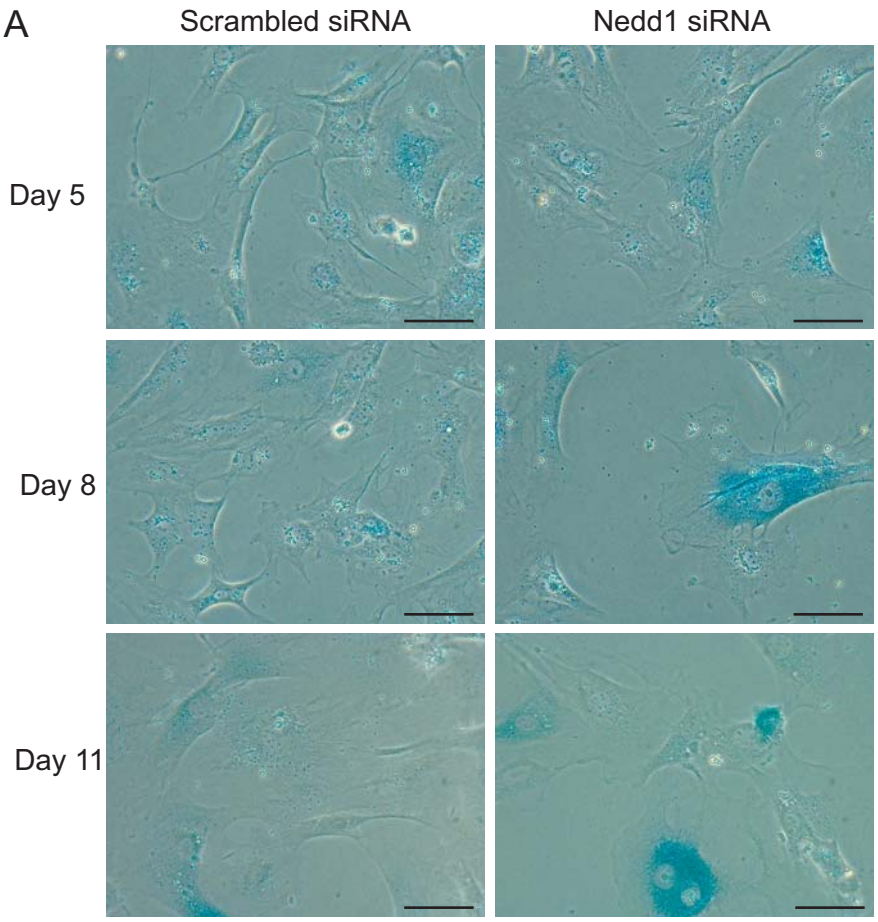
Scrambled siRNA
Nedd1 siRNA
Day 5
Day 8
Day 11

B

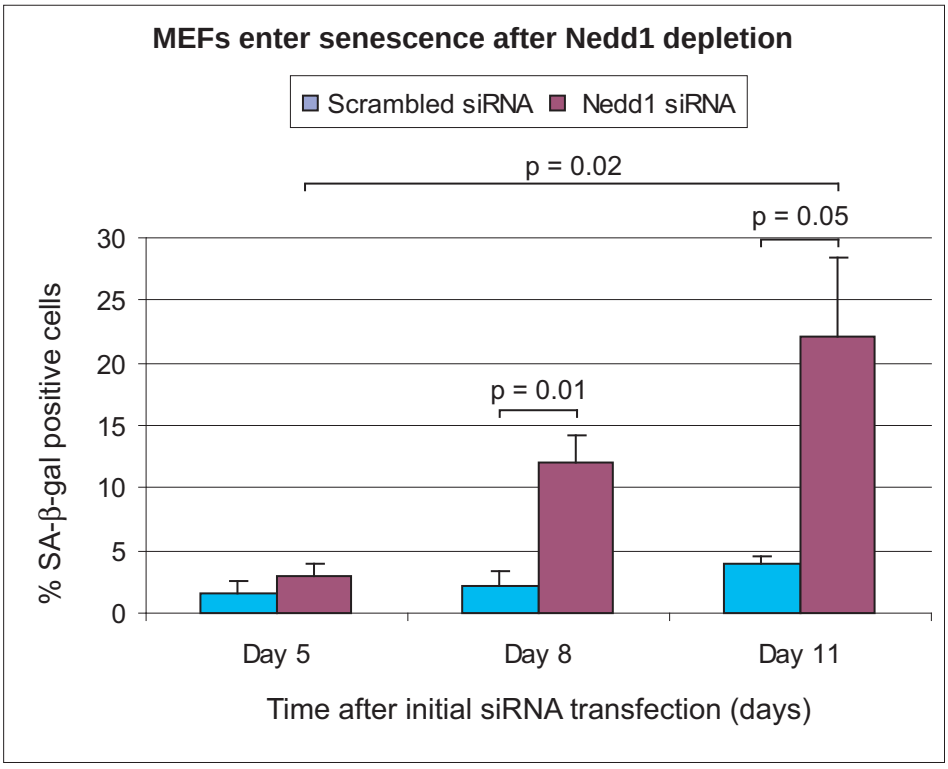
MEFs enter senescence after Nedd1 depletion
Scrambled siRNA
Nedd1 siRNA
p = 0.02
p = 0.05
p = 0.01
% SA-β-gal positive cells
30
25
20
15
10
5
0
Day 5
Day 8
Day 11
Time after initial siRNA transfection (days)

4.9B). Additionally, there was a significant increase in senescence between days 5 and 11 in the Nedd1 siRNA treated group ($p = 0.02$), indicating that the number of cells in senescence increased over time, even when Nedd1 was becoming re-expressed in the cells.

4.8. A reduction of Nedd1 can cause centrosome abnormalities

Given that the senescence occurring in late passage MEFs was also accompanied by an increase in supernumerary centrosomes (Fig. 4.6), it was next assessed whether the depletion of Nedd1 from early passage MEFs could also induce centrosome abnormalities. Depletion of Nedd1 reduces the levels of γ-tubulin at the centrosome (Fig. 4.8), but not the centriole marker GT335, hence GT335 was used for staining in these cells. Indeed, whilst almost all cells in the control scrambled siRNA treated cells had 1-2 centriole pairs (Fig. 4.10A-C, each pair only visible as one centrosomal dot), after 5 days of Nedd1 depletion there were many cells that showed greater than 2 centrosomal structures (Fig. 4.10D). This was increased at both 8 and 11 days after initial Nedd1 depletion (Fig. 4.10E-G). The GT335 positive dots were sometimes smaller in Nedd1 depleted cells, suggesting that they may be centrosomal fragments. When these centrosomal dots were quantitated, the number of cells with greater than 2 centrosomal structures in the Nedd1 depleted cells was increased to 28% at day 5, 38% at day 8 and 45% at day 11. This was significant at all time points when compared to control treated cells which had approximately 10% of cells with greater than 2 centrosomal structures at all days ($p = <0.05$) (Fig. 4.10G). Again, there was also a significant increase in the accumulation of centrosomal structures between days 5 and 11 in the Nedd1 siRNA treated group ($p = 0.01$), indicating that the centrosome abnormalities increased over time, even when Nedd1 was becoming re-expressed in the cells.

Fig. 4.10 Nedd1 depletion causes abnormal centrosomes

An aliquot of cells treated with control or Nedd1 siRNA as in Fig. 4.8 were then stained for Nedd1 (green) and GT335 (red) at day 5 when the siRNA was removed and again at day 8 and day 11.

(**A**-**C**) At all time points in the control scrambled siRNA, Nedd1 and GT335 staining show normal centrioles (1-2 pairs per cell).

(**D**) 5 days after the first Nedd1 siRNA transfection, the level of Nedd1 is dramatically reduced at the centrosome, and GT335 staining reveals some cells have >2 centrosomal structures.

(**E**-**F**) At 8 and 11 days after Nedd1 siRNA transfection, there are more cells with >2 centrosomal structures even though Nedd1 is becoming re-expressed.

(**G**) The number of centrosomal structures in control scrambled siRNA treated and Nedd1 siRNA treated cells was quantitated. At days 5, 8 and 11 there is a significant increase in the number of cells containing >2 centrosomal structures in the Nedd1 siRNA treated cells compared with control cells. Additionally, there is a significant increase in the number of cells with >2 centrosomes between day 5 and day 11 in the Nedd1 siRNA treated cells. About 300 cells were counted for each group. Error bars show SEM, where n = 3 independent experiments. p values are calculated using a one-tailed students t-test (see 2.11).

Scale bars represent 40 μm.

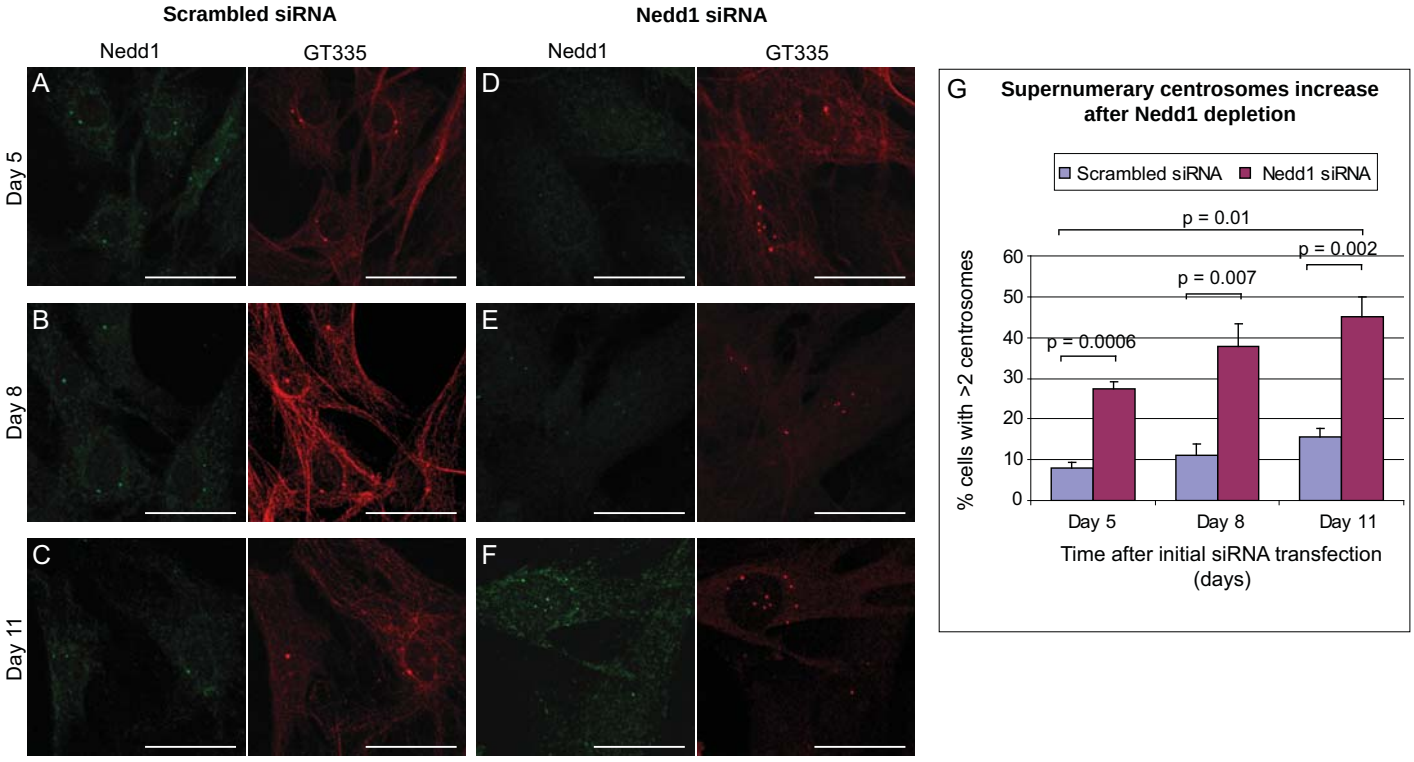
Scrambled siRNA
Nedd1 siRNA
Nedd1
GT335
Nedd1
GT335
A
B
C
D
E
F
Day 5
Day 8
Day 11
G
Supernumerary centrosomes increase after Nedd1 depletion
Scrambled siRNA
Nedd1 siRNA
p = 0.01
p = 0.002
p = 0.007
p = 0.0006
% cells with >2 centrosomes
0
10
20
30
40
50
60
Day 5
Day 8
Day 11
Time after initial siRNA transfection (days)

4.9. Discussion

Many stages of the cell cycle are controlled by centrosome function and dynamics (Doxsey *et al*., 2005). As such it was predicted that NEDD1, as a core component of the centrosome, may play a role in the cell cycle. Indeed, the results presented in this chapter provide evidence for the regulation of NEDD1 in this process, and also in senescence. Numerous signals are required for cell cycle progression, including the regulation of many components of the centrosome (Lange, 2002). In particular, phosphorylation and degradation are key events that regulate proteins which form part of the centrosome (Doxsey *et al*., 2005). Previous studies on NEDD1 have identified phosphorylation as an important method of regulation of this protein (Luders *et al*., 2006, Haren *et al*., 2009, Zhang *et al*., 2009). Phosphorylation of at least one site (S411) during mitosis has been shown to be essential for the recruitment of γ-tubulin to the mitotic spindle and therefore correct spindle formation. Other sites of phosphorylation contribute to the centrosomal localisation of NEDD1 and γ-tubulin (Zhang *et al*., 2009). This study aimed to determine if there are other methods of NEDD1 regulation that contribute to cell cycle progression. NEDD1 was shown to be present in all cell lines analysed and displayed a consistent localisation to the centrosomes and mitotic spindle, with a small amount in the cytoplasm (Fig. 4.1). Hence it is likely to play a similar role in all cell types. In some cells, NEDD1 was present as a doublet on immunoblot, and the higher molecular mass band has been attributed to the phosphorylated form of the protein that occurs during mitosis (Zhang *et al*., 2009). Presumably, the samples which displayed this band had a higher proportion of cells in mitosis at the time of harvesting. Indeed, upon analysis of NEDD1 protein in synchronised cells, it was observed that NEDD1 was phosphorylated in mitosis, as previously reported (Fig. 4.2). The total amount of NEDD1 protein remained similar as the cells progressed through the cell cycle, the only difference being the presence of the higher molecular mass phosphorylated band during mitosis.

The phosphorylation of many centrosome proteins, often promoted by the accumulation of active Cdk1 at the centrosome, signals mitotic entry (Pines, 1995). Recently, it has been

confirmed that NEDD1 is phosphorylated by Cdk1, which then allows subsequent phosphorylation by Plk1 (Haren *et al*., 2009, Zhang *et al*., 2009). The fact that NEDD1 depletion can act synergistically with a Plk1 inhibitor to cause cell cycle arrest (Tillement *et al*., 2009), highlights the importance of the role of Plk1 in phosphorylating and activating NEDD1 mitotic function. It has been suggested that the centrosome acts as a regulatory site to organise the phosphorylation of proteins upon mitotic entry (Fabbro *et al*., 2005). Hence, it is probable that the most important feature of NEDD1 is its centrosomal localisation which allows its phosphorylation and therefore the progression of the cell cycle through mitosis.

It has also been demonstrated that the inhibition of proteasome activity, which is normally responsible for protein degradation, causes an accumulation of several proteins including NEDD1 and γ-tubulin at the pericentriolar material (Zhao *et al*., 2003, Didier *et al*., 2008). This impairs centrosome-dependent microtubule nucleation and suggests that the turnover of centrosomal proteins by proteasomal degradation is important for proper centrosomal function. However, the results in study have shown that the total protein levels of NEDD1 do not appear to be altered in the cell cycle of cultured cells. Hence, NEDD1 appears to be regulated primarily by phosphorylation during the cell cycle. Further investigation would be required to determine if there is a contribution of protein degradation to NEDD1 regulation in the cell cycle.

While these studies on the regulation of NEDD1 were being conducted, it was observed that the total level of Nedd1 protein was decreased in primary MEFs that had been passaged until they entered senescence (Fig. 4.1). Given the importance of this protein in cell cycle progression, it was hypothesised that Nedd1 may also play a role in senescence. The centrosome has been heavily implicated in senescence in recent years, however the majority of studies have focused on the induced disruption of centrosomal proteins causing this arrest (Srsen *et al*., 2006, Srsen and Merdes, 2006, Mikule *et al*., 2007). The involvement of the centrosome in cases of senescence induced by other stimuli, such as DNA damage, oxidative stress and oncogenic activation remains less clear. MEFs at a late

passage are a model system of oxidative stress induced senescence, as standard culture conditions include atmospheric (20%) oxygen which causes DNA damage and senescence (Parrinello *et al*., 2003). Given the reduction of Nedd1 protein levels in late passage MEFs, this was identified as a good system to study whether a decrease in this centrosomal protein was linked to senescence.

The results presented in this chapter describe the culture of MEFs in atmospheric oxygen, which grow for five passages before experiencing a greatly increased population doubling time and entry of the majority of cells into senescence (Fig. 4.3). Upon analysis of the proteins levels at each passage of these cells, it was found that Nedd1 remained constant for the first five passages, and then was greatly reduced as the cells entered senescence at passage six (Fig. 4.4). This correlated with an increase in p16, p19 and p21, which are typical markers of senescence as previously observed in MEFs (see 1.4) (Parrinello *et al*., 2003). A suitable p53 antibody could not be accessed for this study, however the increase in p21 levels also suggest an activation of p53 in this induction of senescence (Ben-Porath and Weinberg, 2005). Interestingly, the level of γ-tubulin did not change as these cells entered senescence (Fig. 4.4). Hence, it appears that the reduction in Nedd1 at the time of senescence does not correlate with a reduction of all centrosomal proteins. Therefore Nedd1 appears to be regulated differently than other centrosomal proteins, and may have an additional function outside of its currently known role in the centrosome.

The obvious question from this work was whether the reduction of Nedd1 in these late passage MEFs contributes to the induction of senescence, or is merely a downstream response of the cells to senescence. To address this question, Nedd1 was depleted from early passage MEFs for a number of days before being allowed to re-express (Fig. 4.8). It was predicted that if a medium reduction in Nedd1 levels could be maintained for a number of days, such that cells did not immediately enter cell cycle arrest, a population of senescent cells might be identified. Indeed, 8 days after initial Nedd1 depletion, an increase in the proportion of senescent cells was observed (Fig. 4.9). This was further increased 11 days

after depletion, even though Nedd1 levels had been restored at this time. Hence, the depletion of Nedd1 for a sustained period of time is able to induce senescence. NEDD1 depletion in transformed cancerous cell lines has previously been observed to induce cell cycle arrest in the G1 and M phases of the cell cycle (Tillement *et al*., 2009). Whilst it was not analysed in the study, there may have been a proportion of cells that also arrested in similar phases of the cell cycle in this system. However, it is likely that MEFs respond differently to Nedd1 depletion since they are a primary untransformed cell line, and this may explain the induction of senescence as opposed to G1 or M phase arrest in these cells. Indeed, the disruption of other centrosomal proteins does not always result in senescence, however this has been observed for the depletion of PCM1 and pericentrin from primary human fibroblasts (Srsen *et al*., 2006). The fact that Nedd1 levels are reduced in late passage MEF senescence occurring due to oxidative stress, and that Nedd1 depletion can cause early passage MEFs to enter premature senescence suggests a possible additional and specific role for Nedd1 in oxidative stress-induced senescence. To decipher a mechanism for this requires further investigation.

Closer analysis of senescent MEFs revealed the presence of centrosome abnormalities. Despite the decreased levels of total Nedd1 protein on immunoblot at this passage, Nedd1 was still detectable in centrosomes at similar levels to early passage cells. This indicates that the reduction of Nedd1 seen at passage 6 does not correlate to a specific depletion of centrosomal Nedd1, rather it is total levels of the protein that are affected. It was apparent that while the cells were growing at a normal rate they had 1-2 centrosomes, as expected. However at passage 6, when the majority of cells had entered senescence, many cells also displayed abnormal supernumerary centrosomes, observed by both Nedd1 and γ-tubulin staining (Fig. 4.5 and 4.6). Although the percentage of cells with supernumerary centrosomes was still relatively low (16% at passage 6), this is likely to represent a much larger pool of the senescent population, for two reasons. Firstly, not all of the cells at passage 6 were positive for SA-β-gal activity. Hence, a pool of the population had not yet entered senescence. Secondly, abnormal centrosomes can be toxic to cells (Fukasawa,

2007), and so some of the cells with abnormal centrosome probably died before analysis. This result correlates well with a study in human Chang liver cells, which identified that 20% of cells exposed to low doses of hydrogen peroxide, which causes an increase in reactive oxygen species, accumulated supernumerary centrosomes compared with 5-7% in controls (Chae *et al*., 2005).

It has been suggested that NEDD1 is important in centriole assembly and duplication (Haren *et al*., 2006). As such, it was expected that the reduction in total Nedd1 levels in passage 6 MEFs may have resulted in centrosome abnormalities due to a reduction in the number of centrosomes, rather than the supernumerary centrosomes observed in this study. Additionally, centrosome amplification is commonly linked to tumourigenesis (see 1.3.1.2) (Fukasawa, 2005), and as such would not be expected in senescence cells. To explain the results observed, it was hypothesised that the abnormal centrosomes in senescent MEFs may have been fragmented or incorrectly assembled, rather than over-amplified. To distinguish between centrosome fragmentation and over-duplication, observing centrosomal structures in detail by electron microscopy is the best technique. However, after unsuccessful attempts at this technique, it was not possible in the scope of this project. Another method of determining centrosome fragmentation has been to observe the size of centrosomal structures (Date *et al*., 2006). To employ this technique, cells were stained with the centriolar marker GT335. In cells from passage 6 displaying a high proportion of senescence, the centrosomal-like dots were often much smaller than in early passage cells (Fig. 4.5 and 4.7). Additionally, not all of the Nedd1 positive dots co-stained for GT335, suggesting that they contained some centriolar material that did not include the centriole component glutamylated tubulin which is stained by GT335 (Fig. 4.7). Hence, it appears that senescent MEFs accumulate fragmented rather than over-duplicated centrosomes. Future work would be required to confirm this observation, especially by electron microscopy. However, it is at least clear that senescent MEFs display abnormal centrosomes.

It was possible that the supernumerary centrosomes in these senescent MEFs may have been occurring independently of the reduction in total Nedd1 levels, instead caused by other unknown factors. In order to analyse this, Nedd1 was again depleted from early passage MEFs and centrosome integrity evaluated. Since a depletion of Nedd1 also results in a loss of γ-tubulin from the centrosome, GT335 was used as a centriole marker to observe centrosomal structures in these cells. At each time point starting at 5 days after initial Nedd1 depletion, there was a significant increase in the number of cells containing supernumerary centrosomes compared to control treated cells (Fig. 4.10). This was again hypothesised to be fragmented centrosomes since they were often small in size, although this still remains to be proven. Therefore it is likely that the fragmented centrosomes observed in senescent MEFs was due to the reduction in Nedd1 levels. Given that the centrosome abnormalities in Nedd1 depleted cells increased 5 days after siRNA treatment, but the senescent cells did not appear until day 8, it appears that centrosome fragmentation is an early event in this process, and this then leads to the induction of senescence.

Further evidence for Nedd1 depletion causing centrosome fragmentation has been shown by others, as the short-term depletion of NEDD1 in a transformed cell line (HeLa) causes greater than two pericentrin positive dots in about 10% of cells (Luders *et al*., 2006). This observation aligns well with a recent study on components of the human augmin complex (HAUS) which localise to the centrosome and mitotic spindle (Lawo *et al*., 2009). Depletion of components of the HAUS complex causes disorganised bipolar and multipolar spindles and fragmented centrosomes (Lawo *et al*., 2009). Importantly, FAM29A, one of these complex proteins, has been shown to interact with NEDD1 in a cell cycle dependent manner, and recruit NEDD1 and therefore also γ-tubulin to the centrosome and mitotic spindle (Zhu *et al*., 2008b). In the absence of HAUS components, the levels of NEDD1 and γ-tubulin at the centrosome are reduced, and there is a mis-localisation of motor proteins away from the spindle (Lawo *et al*., 2009). The centrosomes cannot sustain the resultant counterbalancing forces at the spindle pole and this leads to their fragmentation. The results in this chapter show that as MEFs come to the end of their replicative life span, the levels of

Nedd1 are down-regulated, possibly as a result of oxidative stress, however the mechanism for this remains unknown. Although Nedd1 is still present at the centrosome in these cells, it is tempting to speculate that its function is compromised. This may then contribute to counterbalancing forces at the centrosome as with HAUS depletion which leads to centrosome fragmentation and then senescence.

This chapter has provided more insight into the regulation of NEDD1 by showing that this protein is primarily controlled through its phosphorylation status. Additionally, a role for this protein in senescence has been revealed. As senescence has been implicated as a protective mechanism against unlimited proliferation, and to evade tumourigenesis, this is critically important in the function of this protein. The requirement for a functional centrosome has previously been shown to be essential in the correct proceeding of the cell cycle. This chapter provides evidence that the dysfunction or down-regulation of the centrosomal protein Nedd1 can induce centrosomal abnormalities and senescence. Further work is required to determine the mechanism by which Nedd1 depletion exerts these effects.

5. NEDD1 interacts with γ-tubulin and other proteins

5.1. Introduction

The primary function of NEDD1 that has been identified thus far is its interaction with the γTuRC and its subsequent recruitment of this complex to the centrosome. The γTuRC can then function to nucleate centrosomal microtubules in interphase and spindle microtubules in mitosis. This microtubule nucleation is crucial in the establishment of a bipolar spindle and hence the correct division of a cell into two daughter cells with an exact set of chromosomes. One study has identified the C-terminal half of NEDD1 (340 aa) as the region responsible for interacting with the γTuRC (Haren *et al*., 2006). This interaction has been confirmed and extended to the C-terminal 89 amino acids in another study (Luders *et al*., 2006). Additionally, this interaction has been suggested to be aided by the phosphorylation of certain resides within NEDD1 by the mitotic kinases Cdk1 and Plk1 (Zhang *et al*., 2009). Identification of the precise region of NEDD1 that interacts with the γTuRC would provide a greater understanding of this interaction, and may facilitate the identification of other interacting partners of the γTuRC that contain a similar sequence.

Thus far, it is apparent that NEDD1 interacts with the γTuRC as a complex. However, it is unknown whether NEDD1 interacts directly with γ-tubulin, or if it interacts via an adaptor protein, such as one of the other proteins in the complex. Deciphering this would allow a greater understanding of the role of NEDD1 in γTuRC recruitment and function. There have been several other centrosomal proteins proposed to recruit the γTuRC to the centrosome, that are known or potential binding partners of NEDD1 (Gomez-Ferreria *et al*., 2007, Fong *et al*., 2008, Zhu *et al*., 2008a, Zhu *et al*., 2008b, Oshimori *et al*., 2009, Uehara *et al*., 2009). The discovery of other centrosomal interacting partners of NEDD1 would provide further information about the function and regulation of NEDD1. Additionally, there may be other non-centrosomal interactors of NEDD1. In support for this, there is a proportion of NEDD1 in a lower molecular weight complex that does not associate with γ-tubulin (Luders *et al*., 2006). Identifying interacting partners of NEDD1 in this complex may reveal γ-tubulin independent functions of NEDD1.

The aims of this chapter were two-fold. Firstly, to further analyse the NEDD1/γTuRC interaction in order to determine whether this is a direct interaction and to identify the region and residues important for the interaction. Secondly, to determine other binding partners of NEDD1 in order to elucidate more about the function and regulation of this protein.

5.2. NEDD1 interacts with γ-tubulin through amino acids 572-660

Previous studies have reported that NEDD1 interacts with the core centrosomal protein, γ-tubulin (Haren *et al*., 2006, Luders *et al*., 2006). Before extending this analysis further, this interaction was first confirmed with endogenous proteins in mammalian cells. Either NEDD1, γ-tubulin (as a positive control), or HSP70 (an unrelated antibody as a negative control) were immunoprecipitated and assessed for any interacting γ-tubulin. As expected γ-tubulin was detected in the lysates before immunoprecipitation, but due to the low endogenous levels of NEDD1, only a very faint band was observed for this protein in the inputs (Fig. 5.1A). When NEDD1 was immunoprecipitated, γ-tubulin was also detected. This confirms that γ-tubulin does indeed interact with NEDD1. The immunoprecipitation of γ-tubulin did not result in any interacting NEDD1 visible on western blot (Fig. 5.1A), but this could be due to the low levels of endogenous NEDD1, or the inability of the NEDD1 antibody to access NEDD1 protein when bound to γ-tubulin.

Both of the previously mentioned studies on NEDD1 identified the C-terminal half of the protein as being responsible for the interaction with γ-tubulin, and this was further narrowed down to amino acids 572-660 of NEDD1 (labelled as 579-667 in Luders *et al*.) (Haren *et al*., 2006, Luders *et al*., 2006). This interaction was confirmed using endogenous γ-tubulin and myc-tagged transfected NEDD1 constructs (Fig. 5.1B). γ-tubulin was seen to immunoprecipitate with full length NEDD1 (1-660 aa) and a construct expressing 572-660 aa, but not 1-571 aa (Fig. 5.1C). Hence it was confirmed that NEDD1 interacts with γ-tubulin through amino acids 572–660.

Fig. 5.1 NEDD1 interacts with γ-tubulin through amino acids 572-660

(**A**) The interaction of endogenous NEDD1 and γ-tubulin was assessed in HEK293T cells. Due to its low level of expression, NEDD1 is barely visible in the input lysates prior to immunoprecipitation (1:20 lysates loaded), however γ-tubulin is present (first lane). Both NEDD1 and γ-tubulin are detected in lysates immunoprecipitated with the NEDD1 antibody, indicating an interaction (second lane). In the reciprocal experiment, NEDD1 is not detected when γ-tubulin is immunoprecipitated (third lane). The additional bands are IgG, detectable because an antibody raised in the same species was used for both the immunoprecipitation and the immunoblotting. In negative controls, γ-tubulin and NEDD1 are not detected when an unrelated antibody (HSP70) was used for the immunoprecipitation or no antibody was added (fourth and fifth lanes, respectively).

(**B**) Full length NEDD1 (1-660 aa), or two truncation constructs (1-571 aa and 572-660 aa) were fused to a myc tag at their N-terminus. These constructs were used in (C).

(**C**) The interaction of full length and truncated forms of myc-tagged NEDD1 with endogenous γ-tubulin was assessed in HEK293T cells. Expression is confirmed for all constructs in the inputs (1:20 lysates loaded). γ-tubulin is immunoprecipitated with full length (1-660 aa) NEDD1, and 572-660 aa NEDD1 but not 1-571 aa, using a myc antibody. There are some degradation products or background bands when full length and 1-571 aa NEDD1 are transfected. When no antibody is added in the negative controls, no γ-tubulin is immunoprecipitated.

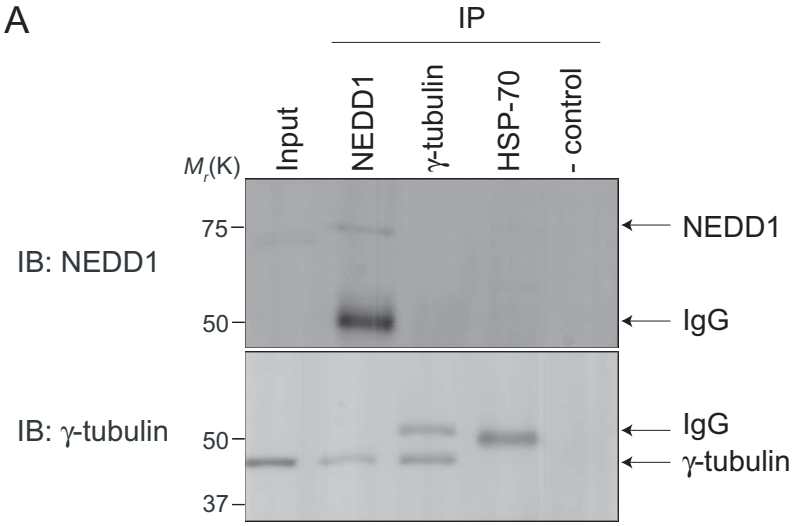
A
IP
Input
NEDD1
γ-tubulin
HSP-70
- control
M_r(K)
75
50
IB: NEDD1
NEDD1
IgG
IB: γ-tubulin
50
37
IgG
γ-tubulin


B
1 aa
572 aa
660 aa
myc-
1-660
myc-
1-571
myc-
572-660

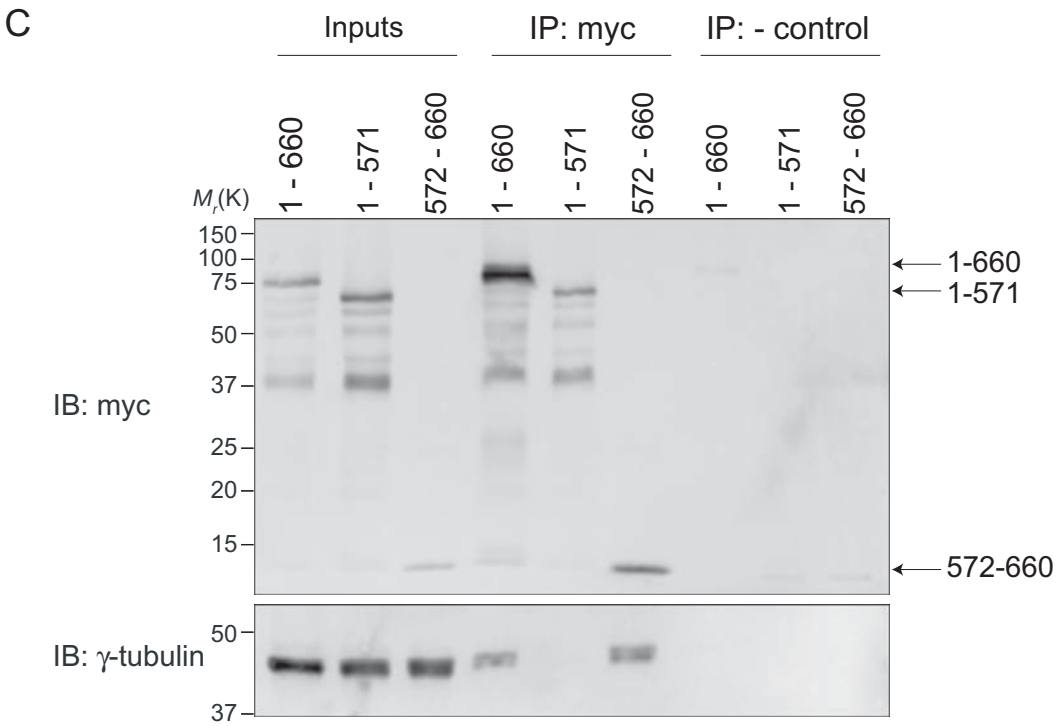
C
Inputs
IP: myc
IP: - control
1 - 660
1 - 571
572 - 660
1 - 660
1 - 571
572 - 660
1 - 660
1 - 571
572 - 660
M_r(K)
150
100
75
50
37
25
20
15
IB: myc
1-660
1-571
572-660
IB: γ-tubulin
50
37

5.3. NEDD1 interacts with γ-tubulin directly

It was next assessed whether the interaction between NEDD1 and γ-tubulin occurs directly, or requires some intermediate proteins. To do this, an *in vitro* system was employed, where either a GST-tagged short form of NEDD1 (572-660 aa) or His-tagged γ-tubulin was expressed in *E. coli* and purified, as well as GST alone. The purified proteins were added together to glutathione sepharose beads either with or without a mammalian cell lysate that would contain any additional binding partners. All proteins were expressed well. It was observed that γ-tubulin was bound to NEDD1 in the presence or absence of HEK293T cell lysate (Fig. 5.2). This indicates that NEDD1 (572-660 aa) can bind to γ-tubulin directly.

5.4. A helical region in amino acids 599-660 of NEDD1 interacts with γ-tubulin

Sections 5.2 and 5.3 confirmed the region of interaction between NEDD1 and γ-tubulin as amino acids 572-660 of NEDD1. This region contains a helical structure that spans amino acids 550 to 660 of full length NEDD1, whereas the rest of the protein is mainly composed of β-sheets (Fig. 5.3A). Upon further analysis of this helical structure, it is apparent that it is composed of three smaller helical regions, with the last helix containing the most amino acids with a high probability of representing a helix (639-660) (Fig. 5.3B). Hence, it was predicted that the interaction between NEDD1 and γ-tubulin may be mediated by the helical structure of NEDD1.

Based on the helical structure of this protein, shorter constructs of NEDD1 fused to an N-terminal GFP-tag were generated in order to narrow down the 572-660 aa region of NEDD1 thus far shown to be required for binding to γ-tubulin (Fig. 5.4A). Given that there was a break in the helical structure of NEDD1 at approximately 635 aa, and a tight helix from 639-660 aa (Fig. 5.3B) it was predicted that the helix within either 635-660 aa or 572-634 aa may be sufficient for binding to γ-tubulin. All of the GFP-NEDD1 constructs were detected in

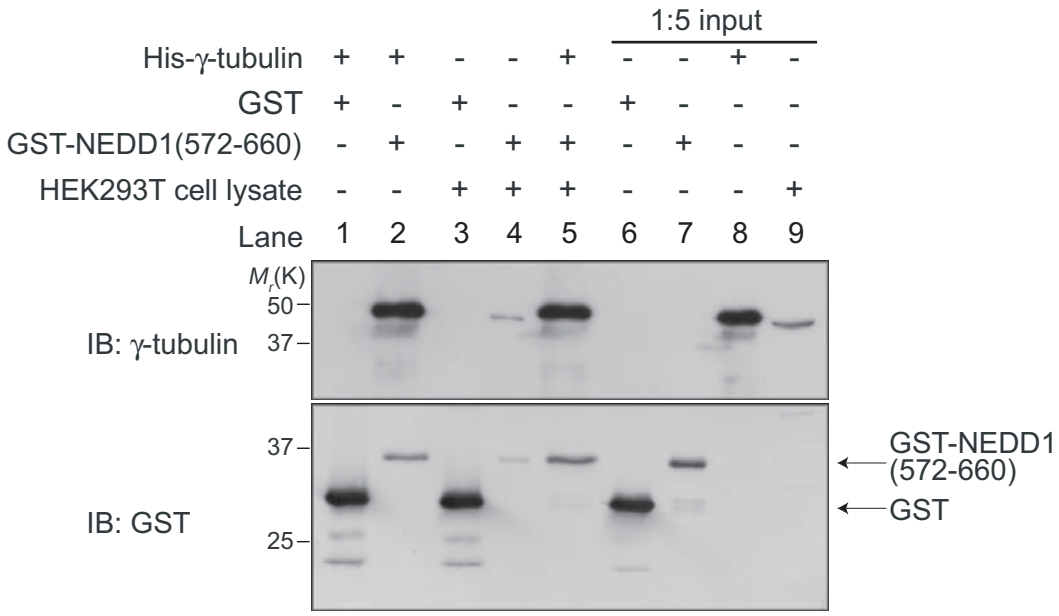

Fig. 5.2 NEDD1 interacts with γ-tubulin directly

The interaction of NEDD1 (572-660 aa) and γ-tubulin was assessed *in vitro*. Glutathione sepharose beads coated with recombinant GST or GST-NEDD1 (572-660 aa) were incubated with His-γ-tubulin, with or without the addition of HEK293T cell lysate. All tagged proteins are expressed well, as seen in the inputs (lanes 6-8), and endogenous γ-tubulin is also expressed in the HEK293T lysate (lane 9). After incubation with the beads and washing away of unbound proteins, γ-tubulin is not bound to GST alone (lane 1), but is bound to GST-NEDD1 both in the absence and presence of lysate (lanes 2 and 5 respectively). Endogenous γ-tubulin in the lysate does not to bind to GST alone (lane 3), but does bind to GST-NEDD1 (lane 4). This experiment was conducted in the laboratory by Sonia Shalini.

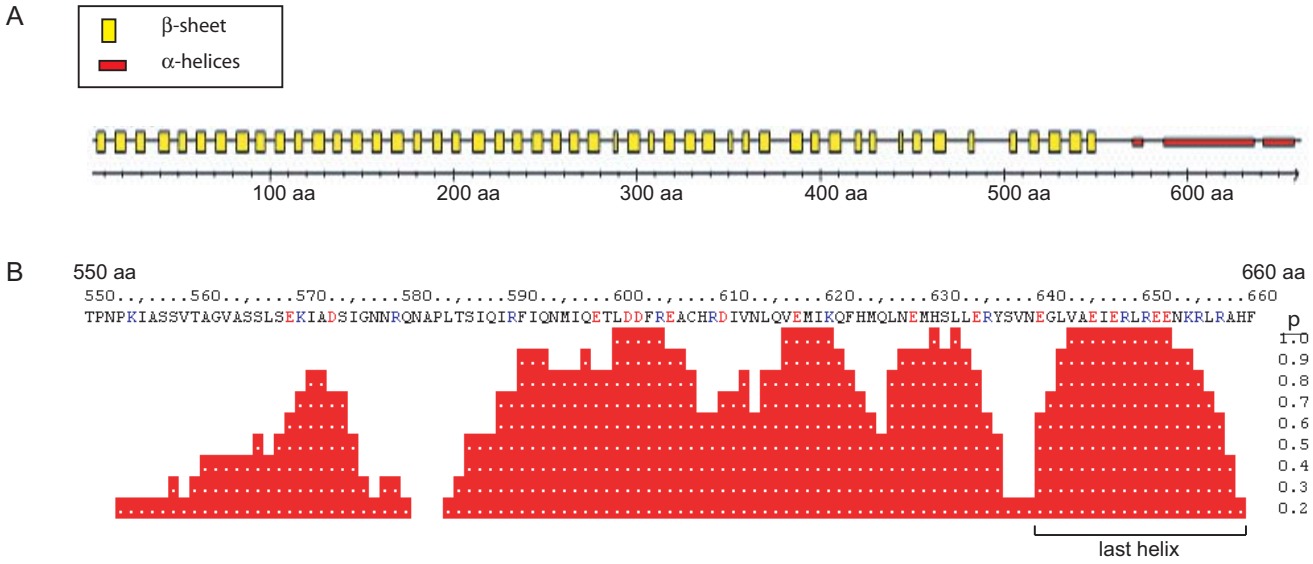

Fig. 5.3 NEDD1 interacts with γ-tubulin through a helical region

The PredictProtein engine (see 2.2) was used to assess the tertiary structure of human NEDD1.

(**A**) The majority of NEDD1 protein is composed of β-sheets, spanning amino acids 1-550. However, the region of NEDD1 between amino acids 550-660 consists mainly of helical structures.

(**B**) Closer observation of the helical structure of amino acids 550-660 reveals that this region is predicted to encode three helical structures, with the last helix containing the most residues with a high probabilty (p) as being part of a helix.

Fig. 5.4 NEDD1 interacts with γ-tubulin through amino acids 599-660

(**A**) Multiple truncated regions of NEDD1 were fused to GFP at their N-terminus. The region from 1-571 aa is not to scale.

(**B**) The interaction of NEDD1 and γ-tubulin was assessed with endogenous γ-tubulin and GFP-tagged truncated NEDD1 constructs in HEK293T cells. The expression of γ-tubulin and all NEDD1 constructs is confirmed in the inputs, although some constructs have poor expression (Inputs, 1:20 lysates loaded). All GFP-NEDD1 constructs are able to be immunoprecipitated with a GFP antibody (IP: GFP). γ-tubulin is able to be immunoprecipitated with full length (1-660 aa), 572-660 aa, 586-660 aa and 599-660 aa NEDD1 only. The upper bands in the γ-tubulin immunoblot are IgG. When no antibody is added in the negative controls, no γ-tubulin is immunoprecipitated (IP: - control).

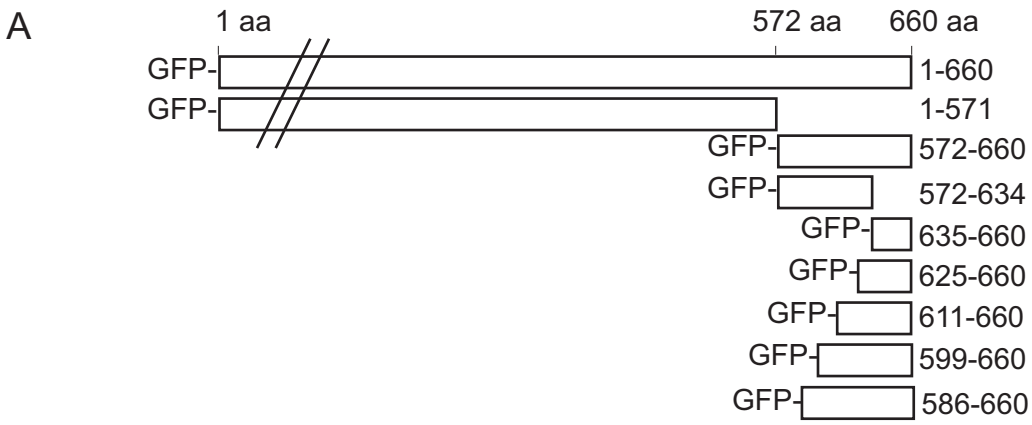
A
1 aa
572 aa
660 aa
GFP-
1-660
GFP-
1-571
GFP-
572-660
GFP-
572-634
GFP-
635-660
GFP-
625-660
GFP-
611-660
GFP-
599-660
GFP-
586-660

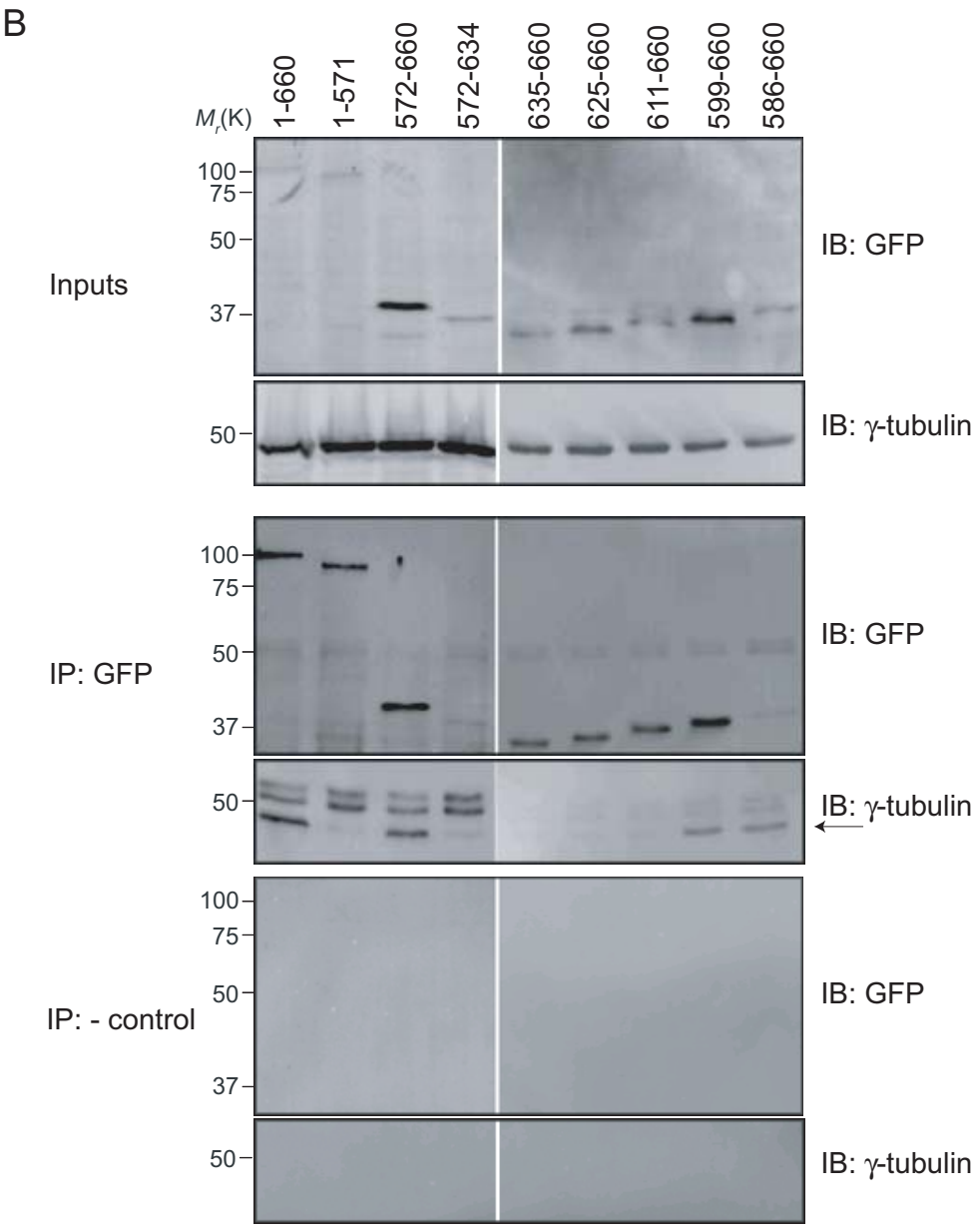
B
1-660
1-571
572-660
572-634
635-660
625-660
611-660
599-660
586-660
M_r(K)
100
75
50
37
Inputs
IB: GFP
50
IB: γ-tubulin
IP: GFP
IB: GFP
IB: γ-tubulin
IP: - control
IB: GFP
IB: γ-tubulin

Fig. 5.5 Amino acids 599-660 of NEDD1 can sequester γ-tubulin away from the centrosome

Mammalian NIH-3T3 cells were transfected with various truncated NEDD1 constructs fused to GFP at their N-terminus and stained for GFP (green, to detect NEDD1) and γ-tubulin (red). The box on the right is an enlargement of the γ-tubulin stained centrosomes in the transfected cells. Each image contains representative transfected and non-transfected cells. Full length GFP-NEDD1 (1-660 aa) localises to the centrosome and does not alter γ-tubulin levels at the centrosome. No other constructs are detected at the centrosome. GFP-NEDD1 (572-660 aa) sequesters γ-tubulin away from the centrosome, whereas GFP-NEDD1 (1-571 aa) has no affect on γ-tubulin at the centrosome. GFP-NEDD1 (599-660 aa) is able to reduce γ-tubulin levels at the centrosome but not as much as 572-660 aa. All other constructs which are not able to bind to γ-tubulin have no effect (611-660 aa shown as an example).

Scale bars represent 10 μm.

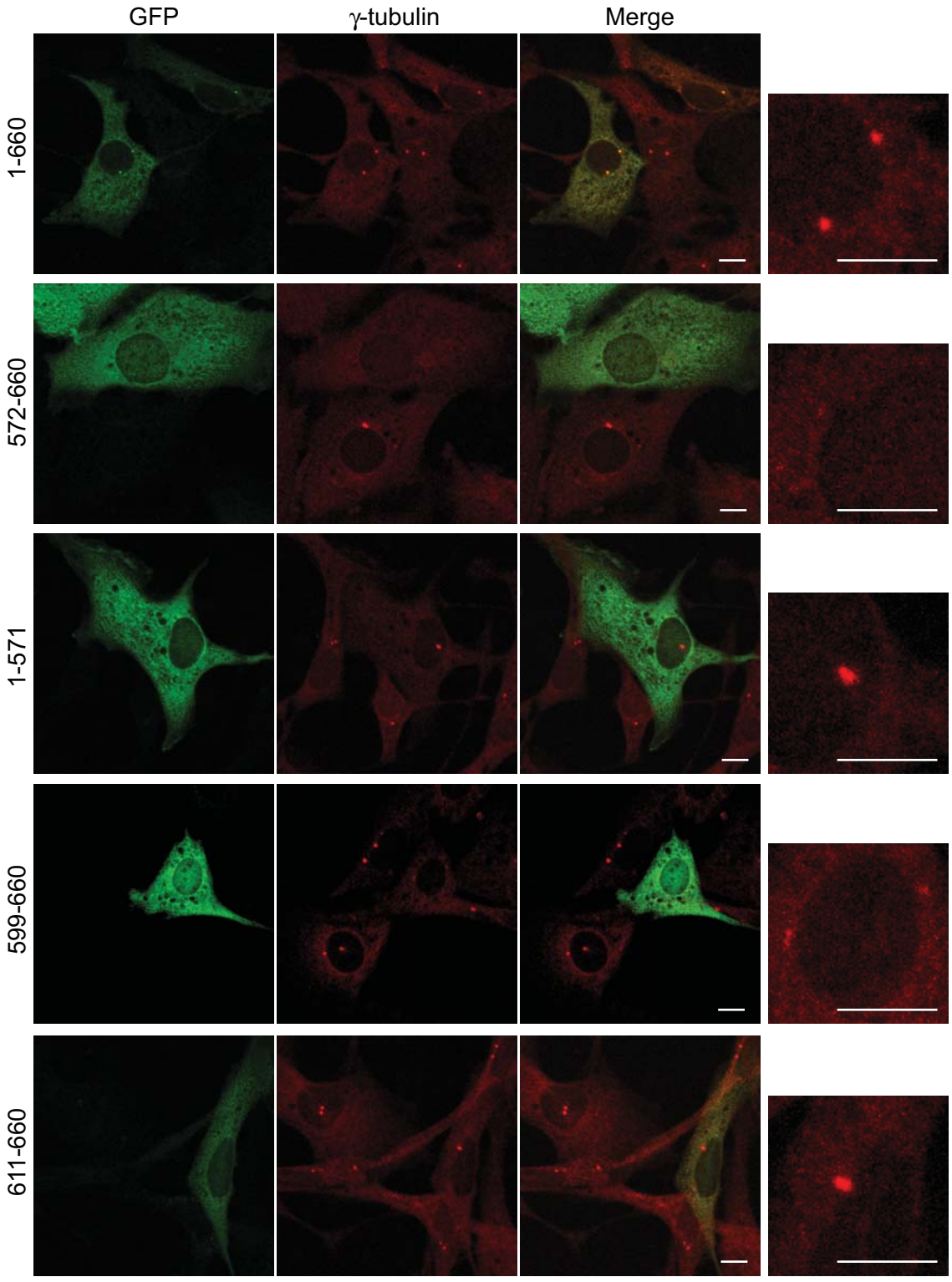
GFP
γ-tubulin
Merge
1-660
572-660
1-571
599-660
611-660

cell lysates, although some had poor expression (Fig. 5.4B, inputs). However, all of the constructs were able to be immunoprecipitated with a GFP antibody (Fig. 5.4B, IP:GFP). As in previous experiments, when immunoprecipitated with a GFP antibody, full length NEDD1 (1-660 aa) and the 572-600 aa construct were able to co-immunoprecipitate γ-tubulin, and the 1-571 aa construct was not (Fig. 5.4B, IP:GFP). However, neither the region 572-634 aa or 635-660 aa was able to co-immunoprecipitate γ-tubulin suggesting that these regions alone are not sufficient for binding. Subsequently, additional constructs were made to search for the minimal region required for the interaction and the 599-660 aa region was found to be sufficient to immunoprecipitate γ-tubulin. Hence, the interaction of NEDD1 and γ-tubulin requires amino acids 599-660 of NEDD1.

5.5. NEDD1 amino acids 599-660 sequesters γ-tubulin away from the centrosome

Previously, it has been demonstrated that the C-terminal half of NEDD1 is sufficient to bind to γ-tubulin but does not localise to the centrosome. Over-expression of this construct causes a loss of γ-tubulin from the centrosome by sequestering it into the cytoplasm, acting as a dominant-negative form of the protein (Luders *et al*., 2006). Given that the previous results of this study identified amino acids 599-660 of NEDD1 as sufficient for the γ-tubulin interaction, it was tested whether this small construct could also sequester γ-tubulin away from the centrosome. As expected, moderate over-expression of GFP-tagged full length NEDD1 (1-660 aa) localised to the centrosome and did not have any effect on the amount of γ-tubulin at the centrosome when compared to untransfected cells (Fig. 5.5). Expression of GFP-NEDD1 (572-660 aa) which is known to bind γ-tubulin but not localise to the centrosome, resulted in a dramatic reduction of γ-tubulin levels at the centrosome. In contrast, expression of GFP-NEDD1 (1-571 aa) which has been suggested to localise to the centrosome (Luders *et al*., 2006), but does not bind to γ-tubulin, did not alter the levels of γ-tubulin. This construct did not appear to localise to the centrosome in this study. Importantly, GFP-NEDD1 (599-660 aa), which was the minimal region found to interact with

γ-tubulin, also resulted in a reduction of γ-tubulin levels at the centrosome, although this was not as dramatic as for GFP-NEDD1 (572-660 aa). None of the constructs that did not co-immunoprecipitate γ-tubulin in Fig 5.4 caused a change in γ-tubulin levels at the centrosome (611-660 aa shown as an example). Hence, amino acids 599-660 of NEDD1 are sufficient and necessary to bind to γ-tubulin and sequester it away from the centrosome, acting as a dominant-negative NEDD1.

5.6. Mutations in the helical region of NEDD1 cause a loss of affinity for γ-tubulin

Previous results demonstrated that the interaction of NEDD1 and γ-tubulin occurs through the helical region of NEDD1. Therefore, a helical wheel prediction of the last helix of NEDD1 (635-660 aa) was next conducted in order to find the precise residues that may important for this helical structure and its interaction with γ-tubulin (Fig. 5.6A). This helix was chosen since it has the highest probability of representing a helix within the region of NEDD1 shown to bind γ-tubulin (Fig. 5.3B). The residues in this wheel can be divided into three classes: aliphatic (non-polar and hydrophobic), hydrophilic, and positively charged. Various patterns of these residues in the wheel can promote helix formation. In this helical structure, residues determined as being potentially important for the interaction are V638, L642, L649 and L656 (analysed by Christopher Bagley, Adelaide Proteomics Facility). These residues reside in a hydrophobic 'stripe' along the helical axis which can often engage in hydrophobic interactions with a partner protein. Upon analysis of the identified residues in an alignment of NEDD1 proteins across different species, L642 was the only residue conserved in all species analysed (Fig. 5.6B). Therefore an L642Q mutation was generated by converting the hydrophobic leucine (L) residue to a bulky hydrophilic glutamine (Q) residue, in order to test if disruption of the helical structure of NEDD1 would affect its interaction with γ-tubulin. Additional single mutants, L649Q and L656Q, double mutants including L642Q, and a triple mutant of all three sites combined were also generated, as these extra sites are conserved in all species analysed except *Drosophila* (Fig. 5.6B).

Fig. 5.6 Mutations within the helical structure of NEDD1 cause a loss of affinity for γ-tubulin

(**A**) The sequence encoding the final helix of NEDD1 (635-660 aa) was analysed in the Mobyle Pepwheel program (see 2.2) for the residues which lie on the helical turns of NEDD1. Aliphatic, hydrophobic and positively charged residues are colour coded as shown in the legend. Aliphatic residues in a hydrophobic stripe predicted to be important for binding are also shown.

(**B**) Protein sequences of NEDD1 (635-660 aa) in multiple species were aligned using Clustal W2 (see 2.2). Boxes show the leucine residues at positions L642, L649 and L656 that were selected for mutational analysis. From this alignment, L642 was predicted as being the most important residue for binding to γ-tubulin since it was conserved in all species analysed including the more distant *Drosophila* homologue of NEDD1 (asterisks indicate conserved residues).

(**C**) The selected mutations were introduced into a myc-tagged full length NEDD1 construct, and transfected into HEK293T cells. The expression of all NEDD1 constructs and γ-tubulin is confirmed in the inputs (1:20 lysates loaded). All myc-NEDD1 constructs are able to be immunoprecipitated with a myc antibody. As shown previously, γ-tubulin is immunoprecipitated with wild type (WT) full length NEDD1 but not with NEDD1 (1-571 aa). There is a loss of γ-tubulin immunoprecipitated with the L642Q mutant NEDD1, but this is not seen for the single NEDD1 mutants of L649Q or L656Q. Double mutants including L642Q also reduce the immunoprecipitation of γ-tubulin, as does the L642Q/L649Q/L656Q triple mutant, but these constructs appear to have no greater effect than the single L642Q mutant. The upper band in the γ-tubulin immunoblot is IgG.

A

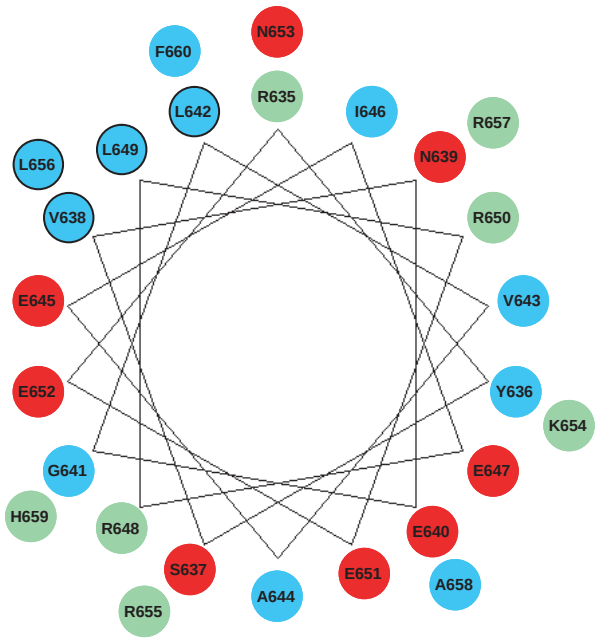
N653
F660
R635
L642
I646
R657
N639
L649
L656
R650
V638
V643
E645
Y636
E652
K654
E647
G641
H659
R648
E640
S637
E651
A658
A644
R655

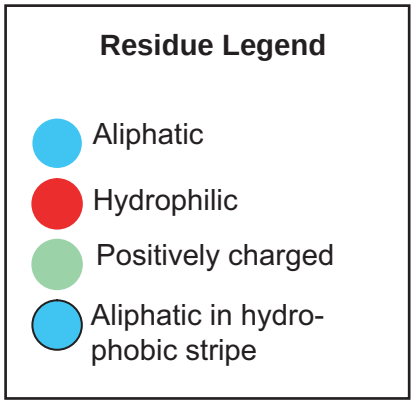
Residue Legend
Aliphatic
Hydrophilic
Positively charged
Aliphatic in hydro-
phobic stripe

B

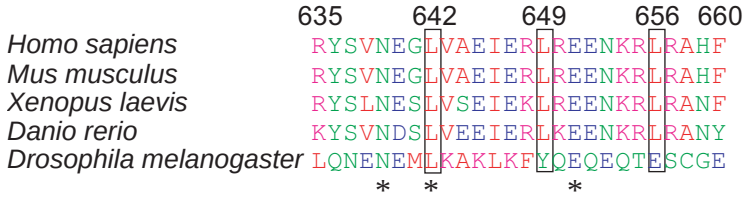
635
642
649
656
660
Homo sapiens RYSVNEGLVAEIERLREENKRLRAHF
Mus musculus RYSVNEGLVAEIERLREENKRLRAHF
Xenopus laevis RYSLNESLVSEIEKLREENKRLRANF
Danio rerio KYSVNDSLVEEIERLKEENKRLRANY
Drosophila melanogaster LQNENEMLKAKLKFYQEQEQTESCGE
* * *

C

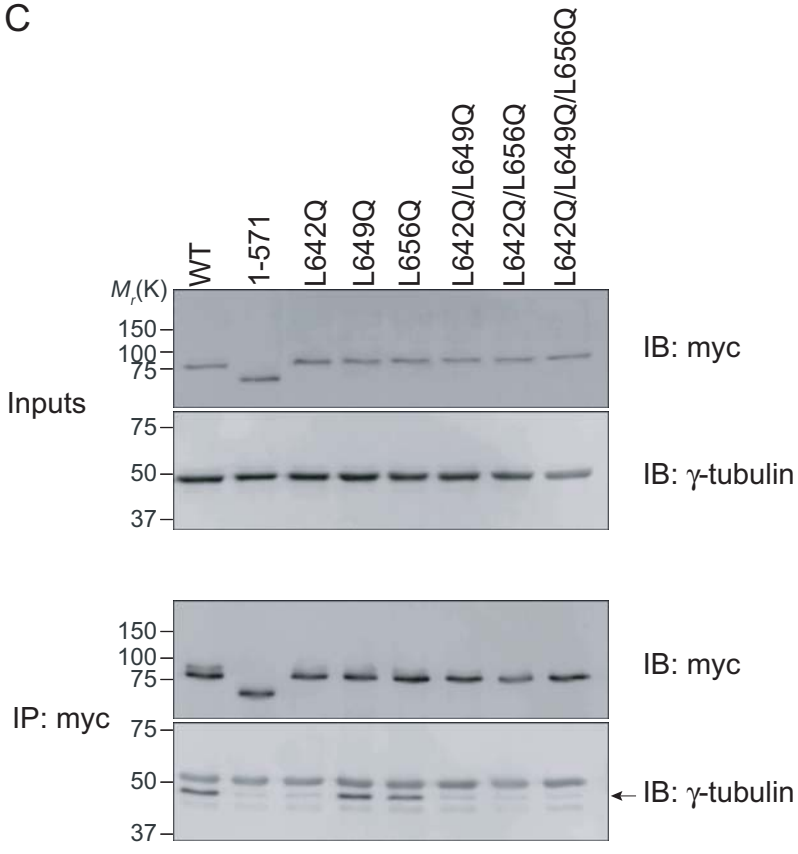
WT
1-571
L642Q
L649Q
L656Q
L642Q/L649Q
L642Q/L656Q
L642Q/L649Q/L656Q
M_r(K)
150
100
75
Inputs
IB: myc
75
50
37
IB: γ-tubulin
150
100
75
IP: myc
IB: myc
75
50
37
IB: γ-tubulin

These constructs were then utilised to determine if the generated mutations affect the binding of NEDD1 to γ-tubulin. As expected from previous results, a myc-tagged full length (1-660 aa) wild type NEDD1 was able to immunoprecipitate γ-tubulin, but a construct containing only amino acids 1-571 aa of NEDD1 was not (Fig. 5.6C). Importantly, the NEDD1 L642Q mutant also resulted in a dramatic loss of γ-tubulin binding. The other single mutations, L649Q and L656Q appeared to have no effect. As expected, double and triple mutants containing the L642Q mutation also reduced the binding of γ-tubulin. This did not appear to have a greater effect than L642Q alone, although this was difficult to conclude as the levels of γ-tubulin were already low when this single mutant was immunoprecipitated.

In order to confirm the above results and to provide additional evidence as to whether these mutants retain some binding to γ-tubulin, the L642Q, L649Q and L656Q mutations were generated in a GST-tagged NEDD1 (572-660 aa) construct as single, double and triple mutants and incubated with His-tagged γ-tubulin and glutathione sepharose beads. All proteins expressed well (Fig. 5.7). As expected, His-tagged γ-tubulin was able to bind to wild type GST-NEDD1 (572-660 aa). There was still some γ-tubulin bound to the L642Q mutant, but this was reduced when compared to wild type protein (Fig. 5.7). The double mutants also reduced the amount of bound γ-tubulin, and interestingly the triple mutant had an even greater reduction in γ-tubulin binding. This suggests that certain amino acids within the last C-terminal helix of NEDD1, especially L642, are important in binding to γ-tubulin.

5.7. Mutations in the helical region of NEDD1 affect γ-tubulin localisation

Given that mutations in NEDD1 had now been identified that resulted in a reduced binding of NEDD1 to γ-tubulin, it was assessed whether these mutated proteins could also modulate the localisation of γ-tubulin. In order to test this, mutations were generated in a GFP-tagged NEDD1 (572-660 aa) construct. As seen previously, this short form of wild type GFP-NEDD1 did not localise to the centrosome, and caused a dramatic reduction of γ-tubulin at

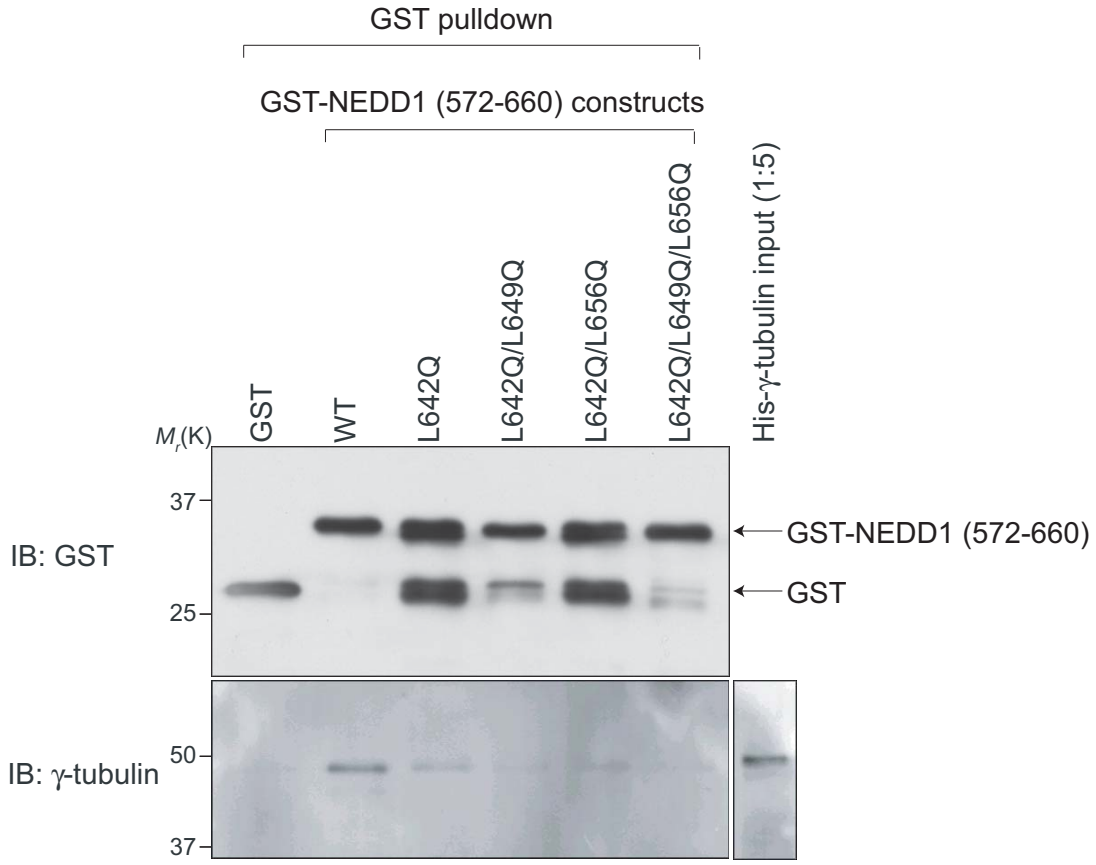

Fig. 5.7 Mutations of NEDD1 within the helical structure cause a loss of affinity for γ-tubulin *in vitro*

The interaction of wild type or mutant NEDD1 (572-660 aa) with γ-tubulin was assessed *in vitro*. Glutathione sepharose beads coated with recombinant GST or GST-NEDD1 (572-660 aa) mutants were incubated with His-γ-tubulin. All GST-tagged proteins are expressed well and bind to the beads, and His-γ-tubulin is also expressed in the inputs. After incubation with the beads and washing away unbound proteins, γ-tubulin is not bound to GST alone, but is bound to wild type (WT) GST-NEDD1. There is a reduction of binding of γ-tubulin to the single mutant L642Q NEDD1, and also to the double mutants. The triple mutant has an even greater reduction in binding of γ-tubulin. There are some degradation products present in the GST-NEDD1 mutant contructs that appear to represent cleaved GST. This experiment was conducted by Sonia Shalini in the laboratory.

the centrosome by binding to this protein and pulling it into the cytoplasm (Fig. 5.8A). The single L642Q mutation had varied effects on γ-tubulin at the centrosome, depending on the cell. In some cells, the L642Q construct appeared to behave almost identically to wild type, causing a dramatic loss of γ-tubulin from the centrosome (Fig. 5.8B). However, in the majority of cells there was either only a small reduction in the levels of γ-tubulin at the centrosome (Fig. 5.8C), or strong levels of γ-tubulin remaining at the centrosome, similar to in untransfected cells (Fig. 5.8D). The triple L642Q/L649Q/L656Q mutant GFP-NEDD1 (572-660 aa) displayed a more consistent effect, with most cells retaining strong γ-tubulin staining in the centrosome (Fig. 5.8E). The numbers of cells with reduced levels of γ-tubulin at the centrosome were counted. Whilst 72% of cells transfected with wild type GFP-NEDD1 (572-660 aa) displayed reduced levels of γ-tubulin at the centrosome, only 31% of cells transfected with the single L642Q mutant, and 10% of cells transfected with the triple mutant had reduced γ-tubulin at the centrosome. This suggests that the L642Q mutation of NEDD1 compromises the binding of NEDD1 to γ-tubulin, and this is even more pronounced with the triple L642Q/L649Q/L656Q mutation of NEDD1. Hence, the binding of NEDD1 to γ-tubulin requires the correct helical conformation of NEDD1 in amino acids 599-660.

5.8. Identifying other NEDD1 binding proteins

In addition to assessing the interaction of NEDD1 with γ-tubulin, this study then aimed to identify other binding partners that may regulate the function of this protein. To identify both centrosomal and non-centrosomal interacting partners of NEDD1, a flag-tagged NEDD1 construct was immunoprecipitated from mammalian cells using flag-conjugated beads rather than a flag antibody, to minimise non-specific binding of proteins to the beads. The sample was separated on an acrylamide gel and silver stained to detect any interacting proteins. Multiple bands were identified that were not present in negative controls (Fig. 5.9A). Five sections were excised from the gel and subjected to proteomic analysis (Christopher Bagley and Megan Retallick, Adelaide Proteomics Facility). Thirteen proteins were identified from the analysis (Fig. 5.9B). Interestingly, NEDD1 was identified in two

Fig. 5.8 Mutations of NEDD1 within the helical structure affect γ-tubulin localisation

The localisation of wild type and mutant GFP-NEDD1 (572-660 aa) constructs and their effects on γ-tubulin were assessed in NIH-3T3 cells. Cells are stained with NEDD1 (green) and γ-tubulin (red). The box on the right is an enlargement of the γ-tubulin stained centrosomes in the transfected cells. Each image contains representative transfected and non-transfected cells.

(**A**) Wild type (WT) NEDD1 (572-660 aa) does not localise to the centrosomes, and causes a dramatic reduction in γ-tubulin levels at the centrosome.

(**B-D**) L642Q NEDD1 (572-660 aa) does not localise to the centrosome, and has varied effects on γ-tubulin localisation. In some cells, γ-tubulin levels are greatly reduced at the centrosome (**B**), whereas in others the levels of γ-tubulin appears similar to untransfected cells [small reduction in (**C**), normal levels in (**D**)].

(**E**) The L642Q/L649Q/L656Q triple mutant NEDD1 (572-660 aa) does not affect the localisation of γ-tubulin to the centrosome in the majority of cells.

(**F**) The number of cells with reduced levels of γ-tubulin at the centrosome was counted for each transfection. Error bars show SEM, where n = 4 independent experiments.

Scale bars represent 10 μm.

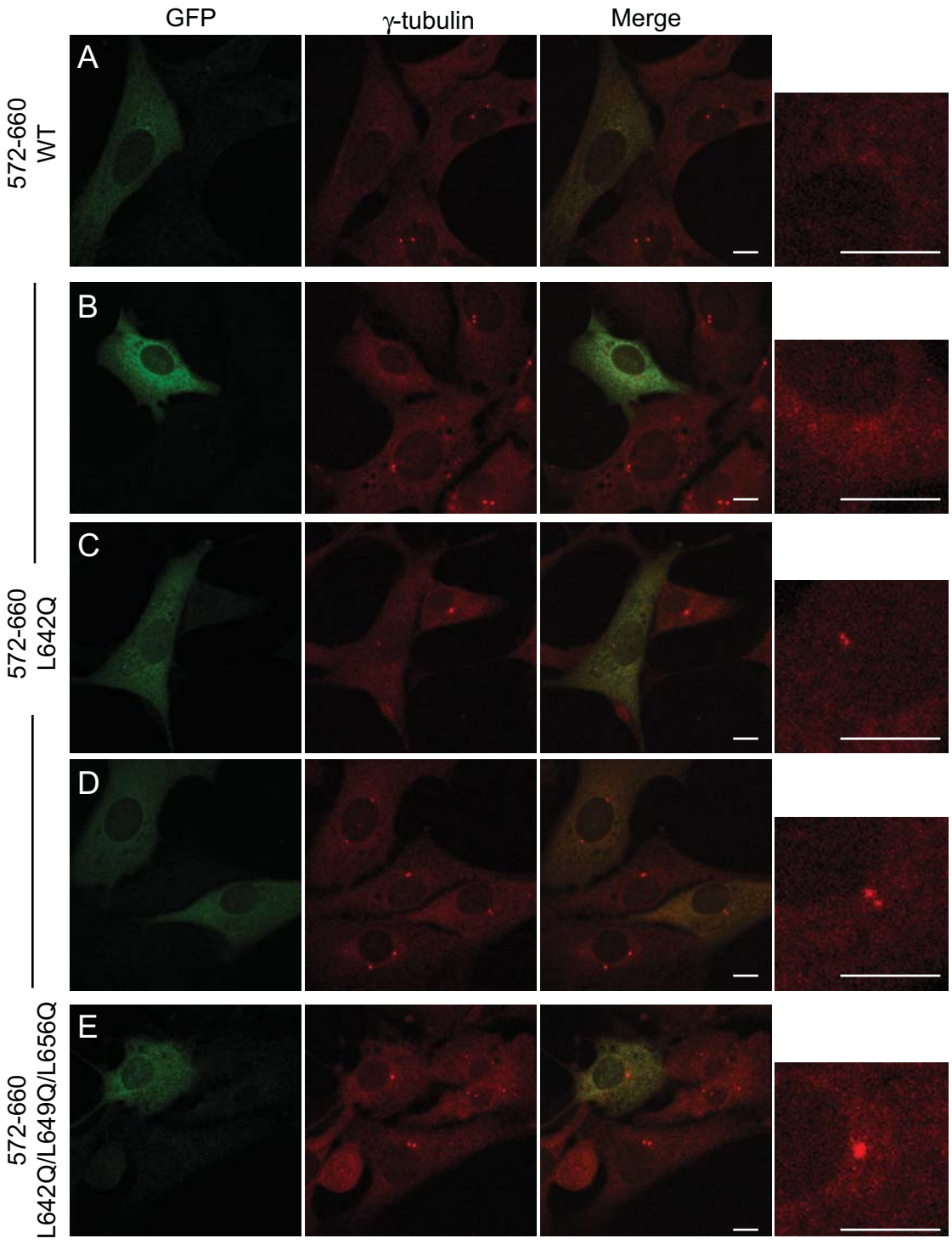
GFP
γ-tubulin
Merge
A
B
C
D
E
572-660 WT
572-660 L642Q
572-660 L642Q/L649Q/L656Q

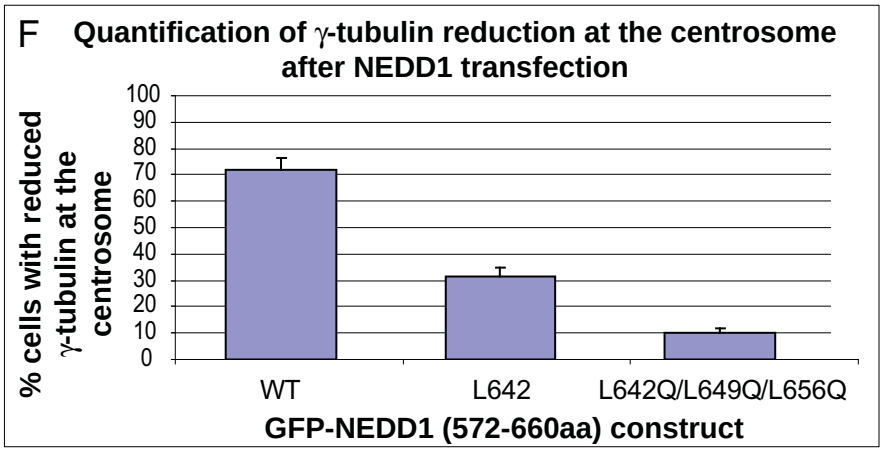
F
Quantification of γ-tubulin reduction at the centrosome after NEDD1 transfection
% cells with reduced γ-tubulin at the centrosome
100
90
80
70
60
50
40
30
20
10
0
WT
L642
L642Q/L649Q/L656Q
GFP-NEDD1 (572-660aa) construct

Fig. 5.9 Nedd1 interacts with multiple proteins

(**A**) Flag-tagged NEDD1 was expressed in HEK293T cells and assessed for interacting proteins by immunoprecipitation with flag-conjugated beads. Many proteins were present in the input on a silver stain gel, and immunoprecipitation resulted in a number of proteins apparently bound to NEDD1. Seven bands that were not present in negative control lanes (no antibody added, or untransfected cells immunoprecipitated with flag-conjugated beads) were excised from the gel, in five slices (Bands A-E) and subjected to proteomic analysis by Christopher Bagley and Megan Retallick (Adelaide Proteomics Facility).

(**B**) Thirteen proteins were identified by mass spectrometry, including NEDD1 at two different molecular weights. Accesssion no (NCBI protein accession number), No. match (number of peptides found in the analysis), % seq (percentage of protein sequence coverage), predicted MW (molecular weight as predicted from the sequence, daltons), observed MW (molecular weight as calculated from the position on the gel, daltons).

A

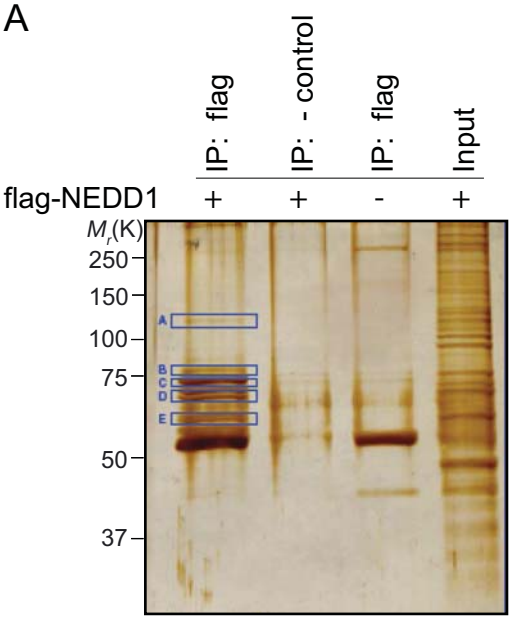

B

Sample	Protein Identification	Accesion no.	No. match	% seq	Predicted MW (Da)	Observed MW (Da)
Band A	Heat shock protein 105 kDa (HSP105)	Q92598	4	4	97,716	120,000
Band B	NEDD1	Q8NHV4	5	6	72,548	76,000
Band C	78 kDa glucose-related protein precursor (GRP 78)	P11021	8	11	72,402	73,000
	75 kDa glucose-related protein precursor (GRP 75)	P38646	6	12	73,920	
	NEDD1	Q8NHV4	5	6	72,548	
	RNA-binding protein FUS	P35637	1	2	53,622	
Band D	Heat shock protein 1 70 kDa (HSP70)	P08107	14	25	70,294	70,000
	Heat shock protein 71 kDa (HSP71)	P11142	16	27	71,082	
	Desmoglein-1 precursor (DG1)	Q02413	1	1	114,670	
	Junction Plakoglobin (JUP)	P14923	1	1	82,245	
Band E	T-complex protein 1 subunit gamma (TCP-1-gamma)	P49368	9	16	61,066	62,000
	T-complex protein 1 subunit zeta (TCP-1-zeta)	P40227	8	16	58,313	
	T-complex protein 1 subunit alpha (TCP-1-alpha)	P17987	6	11	60,819	
	T-complex protein 1 subunit epsilon (TCP-1-epsilon)	P48643	8	14	60,089	

separate bands, at molecular weights of approximately 76 kDa and 73 kDa. Presumably the higher molecular weight band represents the phosphorylated form of NEDD1 that has been previously described (see 1.8.5) (Luders *et al*., 2006). Among the other proteins identified, there were multiple heat shock proteins (HSP 105 kDa, 70 kDa, 71 kDa) and glucose-related proteins (GRP78, GRP75). The RNA-binding protein FUS was also identified, as well as two proteins involved in cell adhesion (desmoglein-1 and junction plakoglobin) and four isoforms of the TCP-1 chaperone family (gamma, zeta, alpha and epsilon). Of the proteins identified, of interest were the cell adhesion proteins and the TCP-1 family because of their previous links to the centrosome (Brown *et al*., 1996, Lechler and Fuchs, 2007).

5.9. NEDD1 does not interact with junction plakoglobin

The two cell adhesion proteins identified in the silver stain had only one matching peptide identified in the sample so required further validation to confirm their interaction with NEDD1. A construct of junction plakoglobin (JUP) fused to an N-terminal V5-tag was generated and expressed in mammalian cells with myc-tagged NEDD1 (Fig. 5.10, Inputs). Although each construct was immunoprecipitated with its corresponding antibody, junction plakoglobin was not detected when NEDD1 was immunoprecipitated, and vice-versa (Fig. 5.10, IP). In control samples not containing any V5-junction plakoglobin, a small amount of myc-NEDD1 was detected when immunoprecipitated with the V5 antibody, indicating that there was some non-specific NEDD1 binding. This was not increased when junction plakoglobin was present in the sample, suggesting that no interaction between NEDD1 and junction plakoglobin could be detected.

In order to test the interaction of desmoglein-1 with NEDD1 a GFP-tagged desmoglein-1 construct was co-transfected into cells with myc-tagged NEDD1. However, it was found that desmoglein-1 could not be sufficiently expressed and immunoprecipitated from the cells, for reasons unknown. Hence, an interaction of desmoglein-1 with NEDD1 could not be assessed, and requires further analysis.

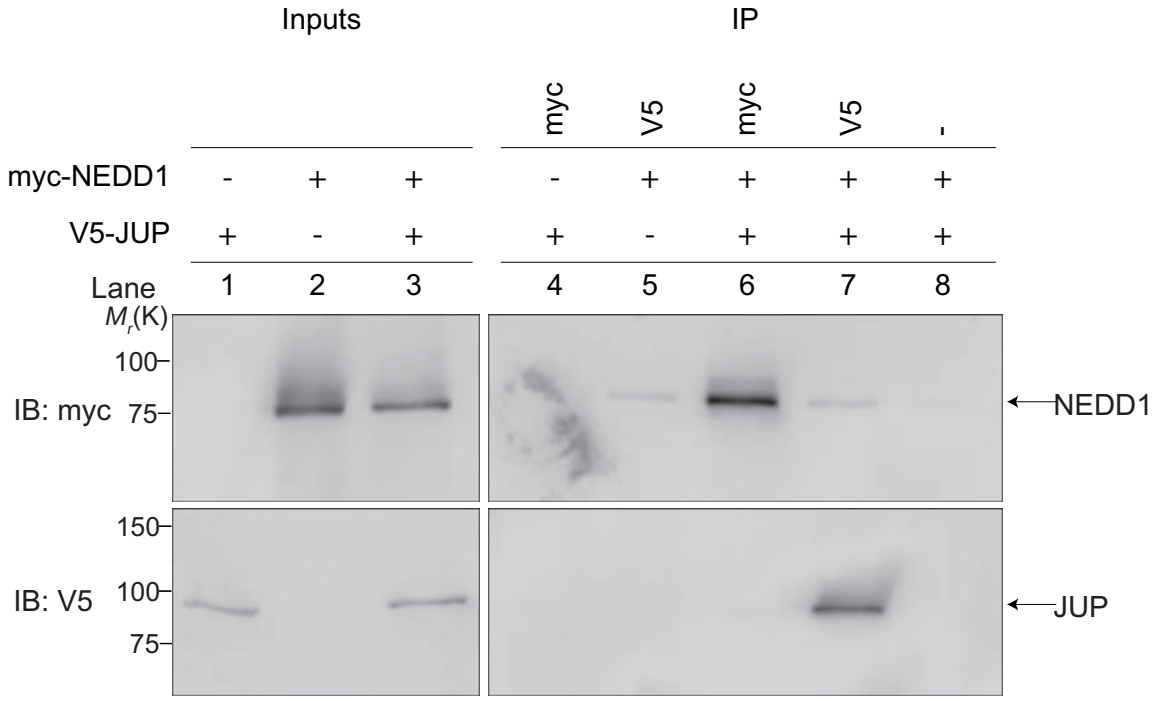

Fig. 5.10 NEDD1 does not interact with junction plakoglobin

HEK293T cells were transfected with myc-tagged NEDD1 and V5-tagged junction plakoglobin (JUP) to assess for an interaction. Both constructs express well separately (lanes 1 and 2), or in combination (lane 3) in the inputs (1:20 lysates loaded). As a negative control, when the myc antibody is used for immunoprecipitation in cells only over-expressing V5-JUP, no JUP is detected (lane 4). Similarly, when the V5 antibody is used for immunoprecipitation in cells only over-expressing myc-NEDD1, only a faint background band is detected for NEDD1 (lane 5). The myc antibody is able to immunoprecipitate myc-NEDD1, but no bound JUP is detectable (lane 6). Similarly, the V5 antibody is able to immunoprecipitate V5-JUP, but no bound NEDD1 is detectable above the levels seen in the negative control (lane 7). In another negative control, when no antibody was added, no proteins are detected (lane 8).

5.10. NEDD1 does interact with HSP-70 and TCP-1α

Aside from the cell adhesion proteins, a number of chaperones were also identified as potential NEDD1 interactors in the immunoprecipitation and silver stain gel. The heat shock protein (HSP) 70 is a ubiquitous chaperone protein that interacts with many other proteins and was not of particular interest to this study. However, to validate the silver stain results, an HSP70 antibody was obtained to test for an interaction with NEDD1. Due to the low levels of endogenous NEDD1, myc-tagged NEDD1 and endogenous HSP70 were expressed in cells, and the myc antibody was found to immunoprecipitate both myc-NEDD1 and HSP70 (Fig. 5.11A). In the reciprocal immunoprecipitations, the HSP70 antibody did not co-immunoprecipitate any NEDD1. However, the HSP70 antibody did not appear very efficient at immunoprecipitating HSP70 itself, as only a weak band was detected. Additionally, NEDD1 is not often able to be detected in reciprocal immunoprecipitations, presumably due to the hindered accessibility of the antibody to NEDD1 when other proteins are bound. Hence, from these results it was concluded that NEDD1 does appear to interact with HSP70.

The TCP-1 family of chaperones were of more interest to this study because of their previous link to the centrosome and γ-tubulin (Melki *et al*., 1993, Brown *et al*., 1996). Given that TCP-1α is the best studied member of this family and has well characterised antibodies available, this was the subunit chosen for analysis in this study. Myc-tagged NEDD1 and endogenous TCP-1α were expressed in cells, again due to the low levels of endogenous NEDD1, and the myc antibody immunoprecipitated both NEDD1 and TCP-1α (Fig. 5.11B). As mentioned for HSP70, the reciprocal immunoprecipitations did not reveal the interaction. Therefore, from these results it appears that NEDD1 does interact with TCP-1α.

Fig. 5.11 NEDD1 interacts with HSP70 and TCP-1α

HEK293T cells were transfected with myc-tagged NEDD1 and assessed for endogenous TCP1α or HSP70. Inputs are 1:20 of the lysates loaded. The lower band in each panel is IgG.

(**A**) Myc-NEDD1 and endogenous HSP70 express well in the inputs. A myc antibody is able to immunoprecipitate myc-NEDD1 and also HSP70. The HSP70 antibody is able to immunoprecipitate HSP70, although this is very weak. A faint band for myc-NEDD1 is also observed with HSP70 immunoprecipitation, however this is similar to the band observed when no antibody was added to the sample in the negative control. Hence, the interaction of NEDD1 and HSP70 can only be detected by NEDD1 immunoprecipitation.

(**B**) Myc-NEDD1 and endogenous TCP-1α express well in the inputs. A myc antibody is able to immunoprecipitate myc-NEDD1 and also TCP-1α. The TCP-1α antibody is able to immunoprecipitate TCP1α, as expected, but only a weak band for myc-NEDD1 is observed, which is similar to the band observed when no antibody is added to the sample in the negative control. Hence, as in previous examples, the interaction of NEDD1 and TCP-1α can only be detected by NEDD1 immunoprecipitation. The band marked by the asterisk is a smudge due to movement of the membrane whilst scanning.

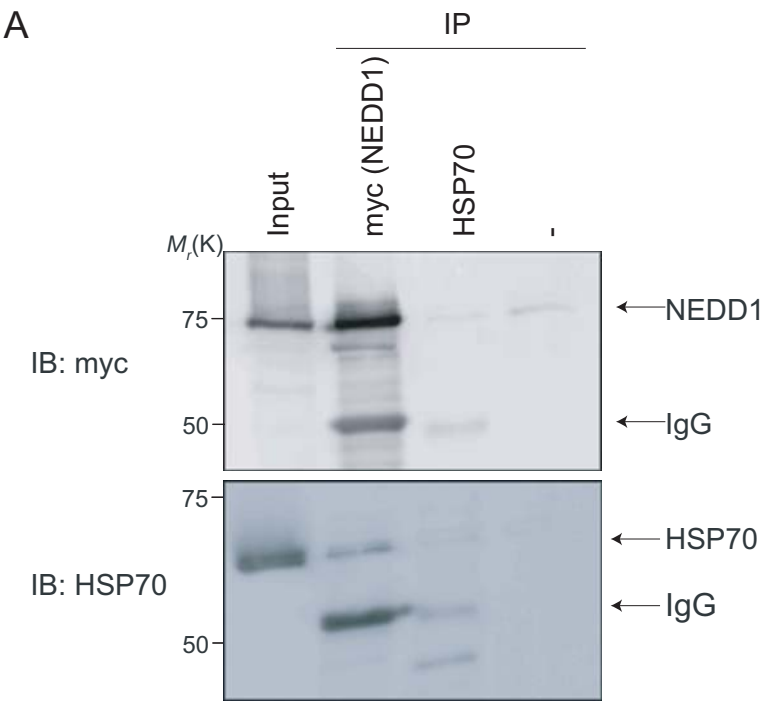
A
IP
Input
myc (NEDD1)
HSP70
-
M_r(K)
75
50
IB: myc
NEDD1
IgG
75
50
IB: HSP70
HSP70
IgG

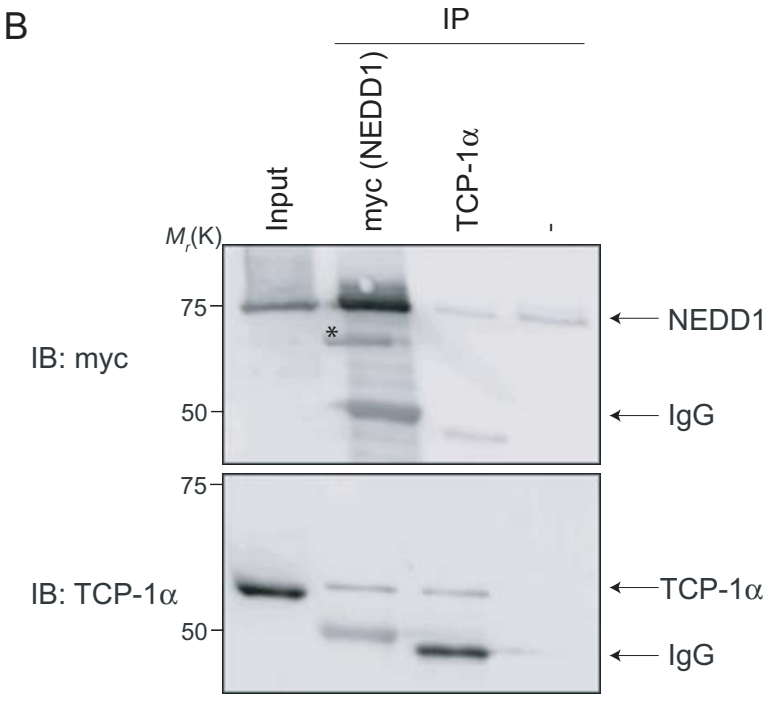
B
IP
Input
myc (NEDD1)
TCP-1α
-
M_r(K)
75
*
50
IB: myc
NEDD1
IgG
75
50
IB: TCP-1α
TCP-1α
IgG

5.11. NEDD1 depletion has minimal effect on TCP1α

Given that NEDD1 was shown to interact with TCP-1α, the function of this interaction was assessed using siRNA. An siRNA designed against human NEDD1 was able to efficiently deplete NEDD1 when compared to cells transfected with a control scrambled siRNA (Fig. 5.12). In these cells, there was minimal difference in the levels of TCP-1α protein. Hence, it appears that NEDD1 is not required for TCP-1α regulation.

5.12. TCP-1α depletion reduces NEDD1 phosphorylation

Conversely, to assess the importance of TCP-1α in NEDD1 function and regulation, an siRNA against TCP-1α was designed. This was able to efficiently deplete TCP-1α protein such that it was no longer detectable when compared to cells transfected with the control scrambled siRNA (Fig. 5.13). TCP-1α depletion also appeared to cause apoptosis (data not shown), although this was not investigated as has been shown previously (Liu *et al*., 2005). Importantly, after synchronisation in mitosis, NEDD1 in these lysates was detected as two bands by immunoblot, with the upper band presumably corresponding to the phosphorylated form of NEDD1 that has been previously described (Luders *et al*., 2006, Zhang *et al*., 2009). After depletion of TCP-1α, the levels of NEDD1 in the lower molecular mass band remained similar, but the upper band was greatly reduced. Hence, TCP-1α appears to be important in controlling the phosphorylation of NEDD1 and therefore its regulation and function.

5.13. Discussion

NEDD1 has previously been identified as a component of the γTuRC, along with the γTuRC proteins GCPs 2-6 The main function of the GCPs appears to be in microtubule nucleation, whereas NEDD1 is involved in the recruitment of the γTuRC to the centrosome. This has been shown to occur through the interaction of NEDD1 with γ-tubulin (Haren *et al*., 2006, Luders *et al*., 2006). Because of this, a loss of NEDD1 results in a failure of the γTuRC to

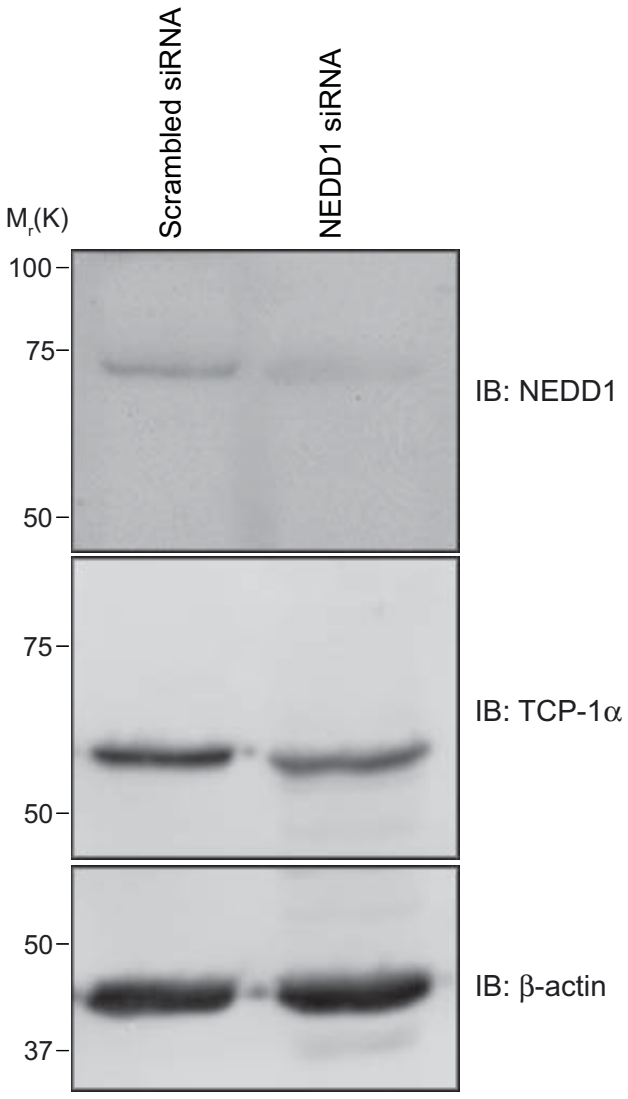

Fig. 5.12 Depletion of NEDD1 has minimal effect on TCP-1α

HeLa cells were transfected with a control scrambled siRNA or NEDD1 siRNA and immunoblotted for NEDD1 and TCP-1α expression. The NEDD1 siRNA is able to reduce NEDD1 protein levels, but does not significantly alter TCP-1α protein levels. β-actin serves as a loading control. This experiment was conducted with the help of Sonia Shalini in the laboratory.

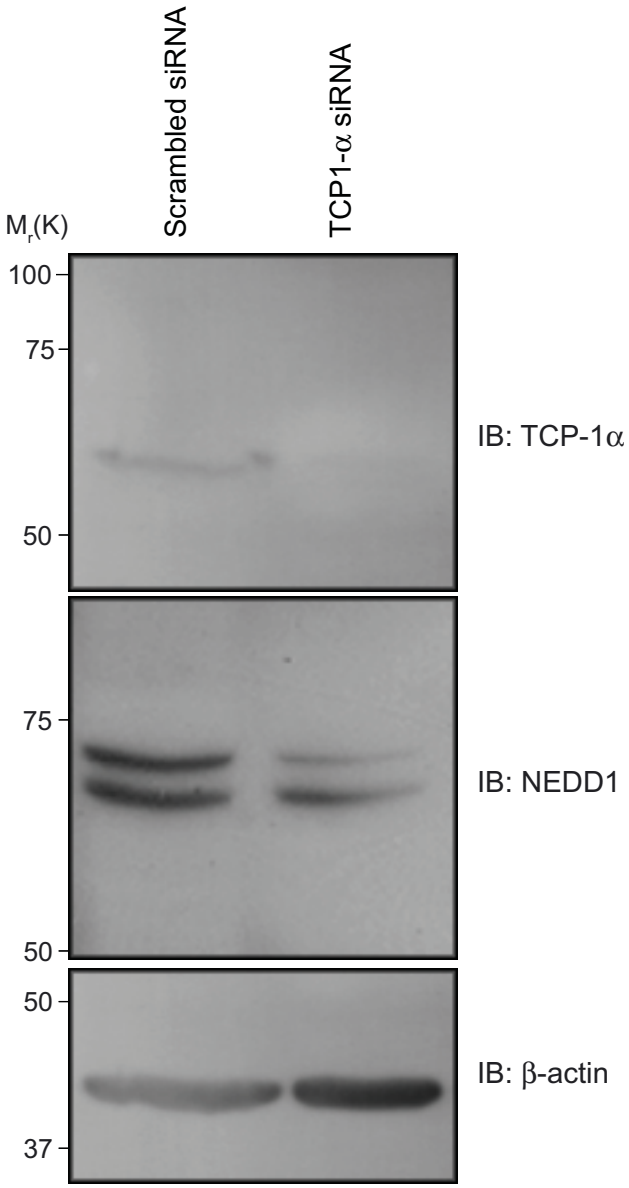

Fig. 5.13 Depletion of TCP-1α reduces the amount of phosphorylated NEDD1

HeLa cells were transfected with a control scrambled siRNA or TCP-1α siRNA, synchronised in mitosis (see 2.7.5) and assessed for TCP-1α and NEDD1 expression. The TCP-1α siRNA is able to reduce TCP-1α protein levels, such that it is no longer detectable. This also causes a substantial reduction in the amount of the higher molecular mass band of NEDD1, which correlates to the phosphorylated form of the protein. The levels of NEDD1 in the lower molecular mass band remain similar. β-actin serves as a loading control. This experiment was conducted with the help of Sonia Shalini in the laboratory.

localise to the centrosome and mitotic spindle which ultimately results in spindle defects and cell cycle arrest (Haren *et al*., 2006, Luders *et al*., 2006, Tillement *et al*., 2009). Importantly, the work described in this chapter confirms the interaction between NEDD1 and γ-tubulin, and demonstrates that it is direct, requiring no additional proteins such as the GCPs (Fig. 5.1 and 5.2). This suggests that other regulators of this complex that have been identified, such as the centrosomal proteins Cep192, Cdk5Rap2, Cep72 (Fong *et al*., 2008, Zhu *et al*., 2008a, Oshimori *et al*., 2009), the spindle protein FAM29A (Zhu *et al*., 2008b), and the mitotic kinases Plk1 and Cdk1 (Haren *et al*., 2009, Zhang *et al*., 2009), lie upstream of NEDD1 (schematic in Fig. 1.6).

This study also revealed that the region responsible for the NEDD1/γ-tubulin interaction contains a helical structure (Fig. 5.3) and is confined to amino acids 599-660 of NEDD1 (Fig. 5.4). Indeed, this region of NEDD1 does not localise to the centrosome, but since it binds to γ-tubulin, is able to sequester γ-tubulin away from the centrosome (Fig. 5.5). This is important, because this study has now identified a small portion of NEDD1 that interacts directly with γ-tubulin and can abrogate its function by mis-localising it away from the centrosome. In a recent study which identified that phosphorylation of NEDD1 by Cdk1 and Plk1 is important for its interaction with γ-tubulin, four Plk1 phosphorylation sites were identified (Zhang *et al*., 2009). These are S382, S397, S426 and S637, and mutation of all of these sites in combination reduced the binding of NEDD1 and γ-tubulin, although it was not abolished. Given that the present study has shown that 599-660 aa of NEDD1 is sufficient to bind γ-tubulin, this suggests that either S637 is the residue which is important for binding, or mutation of the other sites within full length NEDD1 causes a conformational change such that it is less efficient in its binding to γ-tubulin.

From the results of this study, it was predicted that the binding of γ-tubulin to amino acids 599-660 of NEDD1 was due to the helical conformation of this region of the protein. Hence, mutations were made in NEDD1 to try to disrupt this binding. The mutation of a single

leucine residue at 642 to glutamine (L642Q), which was predicted to disrupt the helical structure of the protein and prevent binding partners from interacting, was sufficient to cause a significant reduction in binding to γ-tubulin both *in vivo* and *in vitro* (Fig. 5.6 and 5.7). A triple L642Q/L649Q/L656Q mutant which disrupts additional residues predicted to be important for binding, caused an even greater reduction in the amount of γ-tubulin bound to NEDD1. In order to test the functional importance of these mutants, the localisation of γ-tubulin to the centrosome was assessed in transfected cells. Due to the presence of endogenous Nedd1 interfering with localisation studies, the 572-660 aa NEDD1 construct was used for these studies, because it displays a dominant-negative effect in sequestering γ-tubulin away from the centrosome (Fig. 5.5), overriding any endogenous Nedd1. In these experiments, expression of wild type GFP-NEDD1 (572-660 aa) resulted in a reduction of γ-tubulin at the centrosome in most cells, however this was only observed in 30% of cells transfected with the single L642Q mutant NEDD1 (572-660 aa) and 10% of triple mutant cells (Fig. 5.8). Hence, both the single and triple NEDD1 mutants are presumably important for the helical structure of NEDD1 and its binding to γ-tubulin. Whilst this study has identified the minimal region of NEDD1 required for its interaction with γ-tubulin, future analysis is needed to further confine the specific requirements for this interaction.

To gain further understanding about the function and regulation of NEDD1 and the γTuRC, the next aim of this study was to identify additional binding partners of NEDD1, other than γ-tubulin and FAM29A, which have already been linked to NEDD1 function (Zhu *et al*., 2008b). To try to uncover some of these partners, an immunoprecipitation of NEDD1 was conducted in mammalian cells. In this system, because of the low levels of endogenous NEDD1, over-expressed protein was used. Whilst this may have produced results that were superficial, all proteins identified were tested further to confirm or dispute the interactions. From the immunoprecipitation and mass spectrometry analysis of the interacting partners, 13 proteins were identified (Fig. 5.8). NEDD1 was identified in the sample at two different molecular weights, confirming that this protein can be detected as two bands on

immunoblot, presumably as a non-phosphorylated and phosphorylated form, as previously described (Luders *et al*., 2006, Zhang *et al*., 2009).

Of the interacting partners identified, the RNA binding protein FUS was not selected for further analysis. This protein had only one peptide match in the mass spectrometry analysis, and has previously been identified as a non-specific interacting partner that often appears in immunoprecipitations, and hence was likely to be a false-positive result (Trinkle-Mulcahy *et al*., 2008). Two additional proteins identified with a low number of matches in the sample were desmoglein-1 and junction plakoglobin, although the observed molecular weight of these proteins was substantially lower than the predicted molecular weight, perhaps due to protein cleavage, although this was not investigated. Both desmoglein-1 and junction plakoglobin are components of desmosomes. Desmosomes are intercellular junctions found in epithelial cells and are responsible for maintaining the structural integrity of tissues (Green and Jones, 1996, Cheng *et al*., 2005). It has recently become clear that desmosomes are linked to the centrosome and its role in microtubule organisation (Lechler and Fuchs, 2007). As cells differentiate, microtubules undergo a dramatic reorganisation. The change in microtubule organisation is in part due to the release of the microtubule anchoring centrosomal protein ninein from the centrosome and its recruitment to cell-cell junctions by the desmosomal protein junction plakoglobin (Mogensen *et al*., 2000, Lechler and Fuchs, 2007). Several other centrosome proteins such as Nudel (Guo *et al*., 2006), BBS4 (Kim *et al*., 2004), CAP350 and FOP (Yan *et al*., 2006) have been involved in microtubule anchoring and reorganisation. Given that NEDD1 has been shown to bind microtubules in *Xenopus* (Liu and Wiese, 2008), it is therefore possible that it also plays a role in microtubule anchorage at desmosomes. Hence the interaction of NEDD1 with junction plakoglobin and desmoglein-1 seemed plausible. However, in the immunoprecipitation reactions conducted in this chapter, an interaction between NEDD1 and junction plakoglobin could not be observed (Fig. 5.9). Therefore, either this protein identified from the silver stain gel was a false-positive or the conditions were not correct to detect an interaction. The interaction of NEDD1 with desmoglein-1 could not be assessed

for technical reasons. Therefore further work is required to conclusively determine if these proteins do interact.

In the proteomic analysis of interacting partners of NEDD1, there were also many chaperone proteins identified. Molecular chaperones have long been known to play important roles in the folding and maturation of newly synthesised proteins. More recently, they have also been identified as participating in regulating the assembly of the microtubule skeleton and the centrosome (Brown *et al*., 1996, Lange *et al*., 2000, Agueli *et al*., 2001). Whilst chaperones are often found in protein complexes when proteins are over-expressed (Gingras *et al*., 2007), their interaction with NEDD1 in this system was worth investigating given the link of the centrosome to multiple chaperone proteins (see below). This study identified multiple heat shock proteins (HSPs) and glucose-related proteins (GRPs) that co-immunoprecipitated with NEDD1. HSP70 family proteins are found in various cellular compartments and interact with proteins being synthesised or translocated into organelles (Tavaria *et al*., 1996). This interaction stabilises the protein and maintains it in an unfolded state until synthesis or translocation is completed (Goloubinoff and De Los Rios, 2007, Meimaridou *et al*., 2009). The GRP chaperones in the endoplasmic reticulum (ER) are related to HSPs but are induced by stresses that disrupt the function of the ER and cause unfolded proteins to accumulate in the lumen, such as glucose starvation or oxygen deprivation (Easton *et al*., 2000).

Due to the availability of antibodies and the fact that some chaperones have been localised to the centrosome, including HSP73, HSP70 (Agueli *et al*., 2001), and HSP90 (Lange *et al*., 2000), HSP70 was chosen for further analysis. Indeed, co-immunoprecipitations showed that NEDD1 does interact with HSP70 when over-expressed (Fig. 5.11). Additional support for this interaction is that HSP70, like NEDD1, can also be detected on the spindle fibres of the mitotic apparatus and has a role in the polymerisation of microtubules by assisting tubulin and other proteins involved in the organisation of the spindle (Agueli *et al*., 2001). In *Drosophila*, genetic studies have shown that another related chaperone, HSP90, and its co-

chaperone Sgt1 are required for the successful completion of mitosis (Lange *et al*., 2000, Martins *et al*., 2009). Loss of function of these chaperones induces dispersion of the pericentriolar material, failure of some mitotic markers to be recruited to MTOCs, defects in microtubule organisation and chromosome segregation, primarily as a result of defects in centrosome maturation and integrity (Lange *et al*., 2000, de Carcer *et al*., 2001, Donaldson *et al*., 2001). It is tempting to speculate that the interaction of the HSP70 chaperone with NEDD1 could be important in maintaining NEDD1 function, which is also important for centrosome integrity, however further work would be required to investigate this.

Another family of cytosolic chaperones, the eukaryotic HSP60 chaperonin family (GroEL in eubacteria) also bind newly synthesised and unfolded proteins and are thought to provide a shielded environment for protein folding and assembly to occur (Lewis *et al*., 1992, Yaffe *et al*., 1992). One of these chaperonins, the T-complex polypeptide-1 (TCP-1 or CCT), was also identified as an interacting partner of NEDD1 in the immunoprecipitation screen. In contrast to the HSPs, chaperonins are multimeric complexes, arranged in stacks of 2 rings each consisting of about 8 subunits in eukaryotes (Gebauer *et al*., 1998). Non-native proteins are individually encaged within barrel-like cavities where protein folding occurs (McLaughlin *et al*., 2002). These chaperonins are not up-regulated after heat shock or other metabolic stress. Whilst it was originally thought that TCP-1 chaperonins interacted with a limited number of substrates including actin and tubulins (Sternlicht *et al*., 1993, Brown *et al*., 1996), the list has now grown to about 15% of all newly synthesised proteins (Thulasiraman *et al*., 1999, Liu *et al*., 2005).

In co-immunoprecipitation reactions to verify the interaction of NEDD1 with the TCP-1 family, the alpha subunit (TCP-1α) was chosen for analysis because it is the best characterised of the subunits. Indeed, NEDD1 and TCP-1α were found to interact (Fig. 5.10). Support for this reflecting a functional interaction is provided by many connections between the TCP-1 family and microtubule organisation. Most importantly, mutations in the TCP-1 locus are associated with microtubule abnormalities (Silver and Remis, 1987).

Indeed, TCP-1 has been observed to localise partly to the major MTOC, the centrosome, although it is also found throughout the cytoplasm and a small amount in the nucleus (Brown *et al*., 1996). Functionally, the importance of TCP-1 at the centrosome has been demonstrated in mammalian cells, as cells depleted of TCP-1 by antibody injection are unable to support new centrosomal microtubule growth (Brown *et al*., 1996). These previously published observations suggest that the interaction between NEDD1 and TCP-1α is likely to be functionally important. Therefore, to examine the importance of the NEDD1/TCP-1α interaction, the effect of depletion of each of the proteins was investigated. The depletion of NEDD1 by siRNA had minimal effect on TCP-1α levels (Fig. 5.11) (Haren *et al*., 2006, Luders *et al*., 2006). This was as expected, as the regulation of TCP-1 itself involves its interaction with native proteins such as Hop/p60 and phosducin-like protein (PhLP) (Gebauer *et al*., 1998, McLaughlin *et al*., 2002). Given that NEDD1 is a centrosomal protein, it was not expected to be important in TCP-1α regulation.

Conversely, it has previously been shown that TCP-1α depletion leads to a G2/M arrest (Liu *et al*., 2005). Long term TCP-1α depletion (4 days) causes apoptosis (Liu *et al*., 2005). The mechanism for this TCP-1α induced apoptosis appears to involve its regulation of cell cycle proteins, particularly Cdc20 (Won *et al*., 1998, Camasses *et al*., 2003). Indeed, TCP-1α has been shown to promote the generation of functional Cdc20 which then activates the anaphase promoting complex (APC) to initiate anaphase and allow cellular progression through mitosis (Camasses *et al*., 2003). Cdc20 from TCP-1α mutant cells loses the ability to bind the APC, which then causes cell cycle arrest and eventually leads to apoptosis. Therefore the TCP-1α chaperonin appears to play a crucial role in cell cycle progression by regulating the folding of key cell cycle players.

Importantly, TCP-1α also appears to regulate NEDD1. As well as apoptosis, the depletion of TCP-1α from mammalian cells caused a reduction in the phosphorylated form of NEDD1 (Fig. 5.12), which is important for mitotic progression (Luders *et al*., 2006, Zhang *et al*.,

2009). A possible explanation for this can be drawn from the effect of TCP-1α on another centrosomal protein that is important in mitosis, Plk1 (Garcia-Alvarez *et al*., 2007). It has been shown that Plk1 interacts with TCP-1α, and its depletion produces a similar phenotype to TCP-1α depletion, inducing cell cycle arrest (Liu *et al*., 2005). Normally, at the onset of mitosis Plk1 phosphorylates Cdc25C which subsequently activates Cdc2 and stimulates entry into mitosis (Kumagai and Dunphy, 1996). In TCP-1α depleted cells, Plk1 is inactivated and so the cell cycle is arrested (Liu *et al*., 2005). The direct delivery of purified active Plk1 reverses the cell cycle arrest in TCP-1α depleted cells, suggesting that the mis-folding of Plk1 is at least partially responsible for the TCP-1α depletion phenotype. Therefore it appears that TCP-1α is required for the biogenesis of functional Plk1. Given the recent study demonstrating that the phosphorylation of NEDD1 by Plk1 is important for the recruitment of NEDD1 and γ-tubulin to the centrosome and spindle, and therefore correct mitotic spindle assembly (Zhang *et al*., 2009), it is no surprise that TCP-1α depletion results in a lack of phosphorylated NEDD1. It is probable that the reduction of TCP-1α which causes an inactivation of Plk1, results in a downstream loss of Plk1 phosphorylation of NEDD1. This correlates well with another study showing that a reduction of NEDD1 and Plk1 has a synergistic effect by potentiating the anti-mitotic activity of each treatment (Tillement *et al*., 2009). Whether TCP-1α also directly regulates NEDD1 by promoting correct protein folding is unknown. Hence, NEDD1 is regulated by a complex pathway, involving kinases (Haren *et al*., 2009, Zhang *et al*., 2009), other centrosome and spindle proteins (Zhu *et al*., 2008a, Zhu *et al*., 2008b) and chaperones, as shown in this study.

In summary, this chapter has provided a detailed characterisation of the interaction of NEDD1 with the core centrosomal protein γ-tubulin. This knowledge now provides a greater understanding of how γ-tubulin is targeted to the centrosome, and the minimal requirements for this recruitment. In addition, this chapter has revealed TCP-1α as a novel interacting partner of NEDD1 that contributes to its function and regulation. Further investigations into

the other identified novel interactors are required to determine their possible roles in NEDD1 function.

6. Identification and characterisation of zebrafish NEDD1

6.1. Introduction

Given the centrosomal localisation and function of NEDD1, and its dynamic expression during mouse embryogenesis (chapter 3), it was expected that this protein would play an important role during development. However, due to the early embryonic lethality of mouse knockouts of centrosomal proteins it has not been possible to study the function of these proteins in later stages of development (Hudson *et al*., 2001, Yuba-Kubo *et al*., 2005). Therefore, an alternative model was sought to investigate the role of NEDD1 during development.

Zebrafish posses many benefits for developmental studies including the conservation of genes involved in cell growth and proliferation (Shepard *et al*., 2004), and the rapid maturation of translucent embryos. Embryogenesis progresses from the 1 cell zygote stage (0 h post fertilisation; hpf), through a series of well defined stages (Fig. 6.1) (Kimmel *et al*., 1995). Not long after 24 hpf, embryos develop a heartbeat and circulation of blood cells. By 72 hpf, larvae hatch from their protective casing (chorion) and display food seeking behaviour. Sexual maturity is reached by 3-4 months post fertilisation. Zebrafish also provide a simple system to deplete specific genes in order to study their importance during development. This system uses morpholino anti-sense oligonucleotides (MOs) to knockdown gene expression, which function by redirecting splicing or blocking translation of mRNA transcripts in the cytosol (Summerton, 1999). As a result, protein translation is inhibited leading to a rapid and specific knockdown. Hence, this system was chosen as a model to study the role of NEDD1 during development.

Whilst there has been much work analysing the cell cycle in zebrafish (Kane, 1999), there has been limited analysis of the centrosome in this species. However, at least two studies have characterised the function of specific centrosomal proteins in zebrafish development. The primary function of the proteins analysed in these studies (Cep70, Cep131 and Cep290) was shown to be their contribution to ciliogenesis, as depletion led to shortened

Period	Stage	hpf	Description
Zygote	1 cell	0	Newly fertilised egg, cytoplasm streams towards the animal pole
Cleavage	2 cell to 64 cell	0.75	6 cleavages to form 64 blastomeres, rapid and synchronous
Blastula	128 cell to 30% epiboly	2.25	Metasynchronous divisions, embryo enters midblastula transition and epiboly begins
Gastrula	50% epiboly to bud	5.25	Epiboly continues, morphogenetic cell movements of involution, convergence and extension occur, producing the primary germ layers and embryonic axis
Segmentation	1 somite to 26 somite	10	Somites develop, primary organs become visible, tailbud becomes more prominent and embryo elongates
Pharyngula	Primordium 5 to high pec	24	Body axis straightens, completed set of somites, nervous system is hollow and expanded, circulation and pigmentation begin
Hatching	Long pec to protruding mouth	48	Rapid development of organs, fins, jaws and gills develop, hatching occurs
Early Larvae		72	Swim bladder inflates, food seeking and active avoidance behaviour

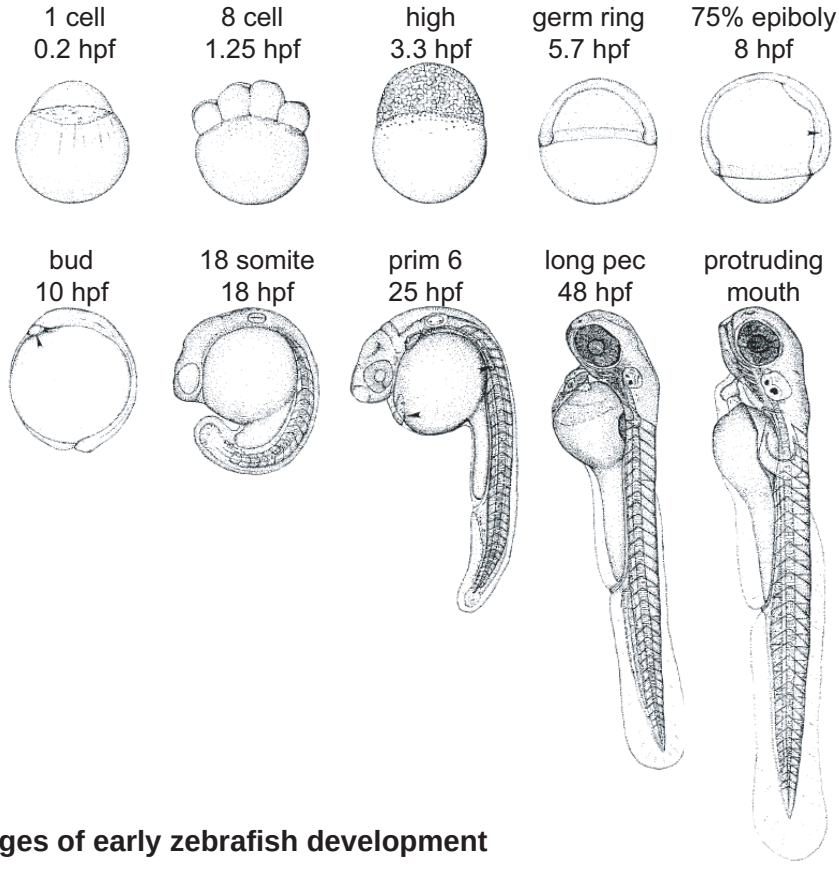

Fig. 6.1 Stages of early zebrafish development

Zebrafish undergo rapid development with easily distinguishable stages as described, due to the transparent nature of embryos. Diagrams of some representative stages are shown. By 72 hpf the embryos have hatched and display food seeking and avoidance behaviours. (hpf) hours post fertilisation. (Adapted from Kimmel *et al*., 1995).

cilia and phenotypes associated with this such as abnormal kidney, ear and eye development (Sayer *et al*., 2006, Wilkinson *et al*., 2009). Hence the centrosomal proteins analysed thus far do appear to be important in zebrafish development, although not necessarily in cell division.

Prior to this study, a zebrafish homologue of NEDD1 had not been described. However, due to its conserved sequence and function in other species, including *Xenopus* (Liu and Wiese, 2008), it was predicted that a NEDD1 homologue would exist in zebrafish. Therefore, the aim of this chapter was to identify a zebrafish homologue of NEDD1 and to compare its localisation and function to mammalian NEDD1. Additionally, it was endeavoured to determine whether this gene is important during development, using targeted depletion in zebrafish embryos.

6.2. Identification of zebrafish NEDD1

A *Danio rerio* (zebrafish) homologue of NEDD1 (zNEDD1) was identified by a BLAST search of the human NEDD1 protein sequence. This search revealed a previously uncharacterised zebrafish nucleotide sequence encoding a predicted protein of 676 amino acids (accession number: NM_213506), that upon alignment using Clustal W2 is 44% identical and 60% similar to human NEDD1 (Fig. 6.2A). The 79 residues at the C-terminus of these proteins are 68% identical and 99% similar, suggesting functional conservation and further indicating that this protein is the zebrafish homologue of NEDD1. As in human NEDD1, which has seven WD40 motifs in the N-terminal half of the protein, zNEDD1 also contains seven WD40 motifs lying within a similar region of the protein (Fig. 6.2B). A phylogenetic analysis of this protein with known NEDD1 homologues from other species shows that *Danio rerio* NEDD1 shares a common ancestor with multiple species, and is closest to *Xenopus laevis* in evolutionary distance (Fig. 6.2C).

Fig. 6.2 Identification of a zebrafish NEDD1 homologue

(**A**) A Clustal W2 alignment (see 2.2) of *Homo sapiens* NEDD1 (human, NP_001128647.1) and *Danio rerio* (zebrafish, NP_998671) reveals that these proteins are highly similar. Amino acid colour code: red (small), blue (acidic), magenta (basic), green (hydroxyl + amine + basic). "*" identical residues, ":" conserved substitutions, "." semi-conserved substitutions.

(**B**) A Scansite motif search (see 2.2) of human and zebrafish NEDD1 shows that they both contain seven WD40 domains, in similar locations in the N-terminal halves of the proteins.

(**C**) NEDD1 protein sequences from different species were aligned and sorted into a phylogram tree with Clustal W2. Branch lengths are proportional to the amount of inferred evolutionary change. *Homo sapiens* (human), *Mus musculus* (mouse), *Xenopus laevis* (frog), *Danio rerio* (fish), *Arabidopsis thaliana* (plant), *Drosophila melanogaster* (fly).

A

```
Human      MQENLRFASSGDDIKIWDASSMTLVDKFNPHTSPHGISSICWSSNNNFLVTASSSGDKIV 60
Zebrafish  MEDVTRLVSSGDCLKIWDSSSMTVVEQFNPHSATHPVAQVCWSSSNQYVVSASSIGDKLV 60

Human      VSSCKCKPVPLLELAEGQKQTCVNLNSTSMYLVSGGLNNTVNIWDLKSKRVHRSLKDHKD 120
Zebrafish  VSSLKSSPVPVMELGEGKKQTRVSLNSTSQFLVSGGLDNTVNIWDLKTKRLHRTLKDHKE 120

Human      QVTCVTYNWNDCYIASGSLSGEIILHSVTTNLSSTPFGHGSNQSVRHLKYSLFKKSLLGS 180
Zebrafish  EVTCVSFNGGDSYIASGSTSGDIILHSITTNLSSKPFGHGPNVPIHDLRYSLVKRSLLGT 180

Human      VSDNGIVTLWDVNSQSPYHNFDSVHKAPASGICFSPVNELLFVTIGLDKRIILYDTSSKK 240
Zebrafish  VSDSGSVALWDANTQKELHLFEGAHKAPCSGLAFSPANDLLFVTVGLDKKIVCYDTSSKI 240

Human      LVKTLVADTPLTAVDFMPDGATLAIGSSRGKIYQYDLRMLKSPVKTISAHKTSVQCIAFQ 300
Zebrafish  VFRNKQVESPLTAIDFTPDGAGLVVGSTQGRIYLYDLRNLSAPVKINTAHKTSVTCIRFQ 300

Human      YST---VLTKSSLNKGCSNKPTTVNKRSVNVNAAS----------------GGVQNSG 339
Zebrafish  NSTSKLKSTKSSSKSSQSNKRISVKLGSSQQTGPSTPTSTVTPIVSGSEFPGDGQAQVPG 360

Human      -----IVREAPATSIATVLP-QPMTSAMGKGTVAVQEKAGLPRSINTDTLSKETDSGKNQ 393
Zebrafish  PSAEVFSREAEGQLSQDQMPNVEKFSSIGRNSLNLDIFSPLNDGFKSHGFADTSRNGGSI 420

Human      DFSSFDDTGKSSLG---------DMFSPIRDDAVVNKGSDESIGKGDGFDFLPQLNSVFP 444
Zebrafish  DVFSREAEGQQTADRFRVGRNSLDIFSPVRDDYKGHRLSDVSSGKKD-FEYLPHFPGGSS 479

Human      PRKNPVTSSTSVLHSSPLNVFMGSPGKEENENRDLTAESKKIYMGKQESKDSFKQLAKLV 504
Zebrafish  QRKTPLGTPGSRCYSP--SVVQTPPIKEEESTTTPPQQTDVQNGTKVEKSNGVRQEYDAI 537

Human      TSGAESGNLNTSPSSNQTRNSEKFEKPENEIEAQLICEPPINGSSTPNPKIASSVTAGVA 564
Zebrafish  TTPPAAQSTRIQSVQPQFNTPEPSQR--RDLSTQLTYDSPISRAPAPAPPAAAAAPAAAV 595

Human      SSLSEKIADSIGNNRQNAPLTSIQIRFIQNMIQETLDDFREACHRDIVNLQVEMIKQFHM 624
Zebrafish  ES---------------APLTSVQMNFVRNMIHEALEDFRDTCHRDIINLQVEMVRQFYI 640

Human      QLNEMHSLLERYSVNEGLVAEIERLREENKRLRAHF 660
Zebrafish  QLNEIHGLIEKYSVNDSLVEEIERLKEENKRLRANY 676
```

B

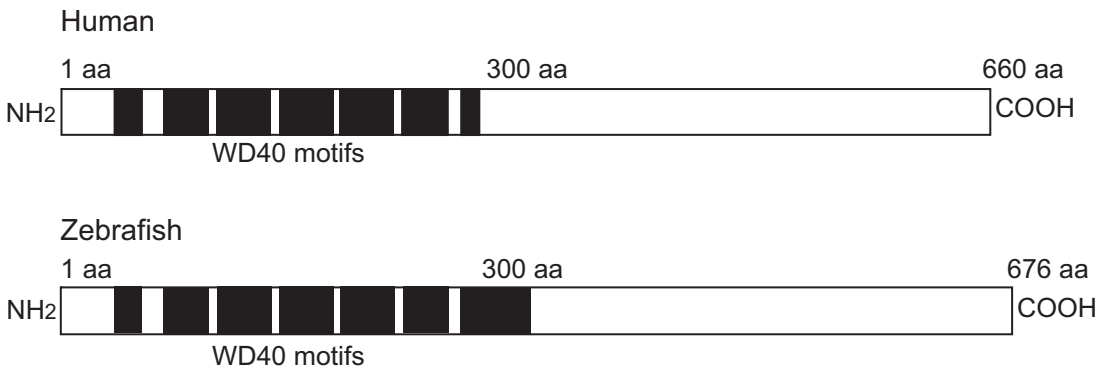

C

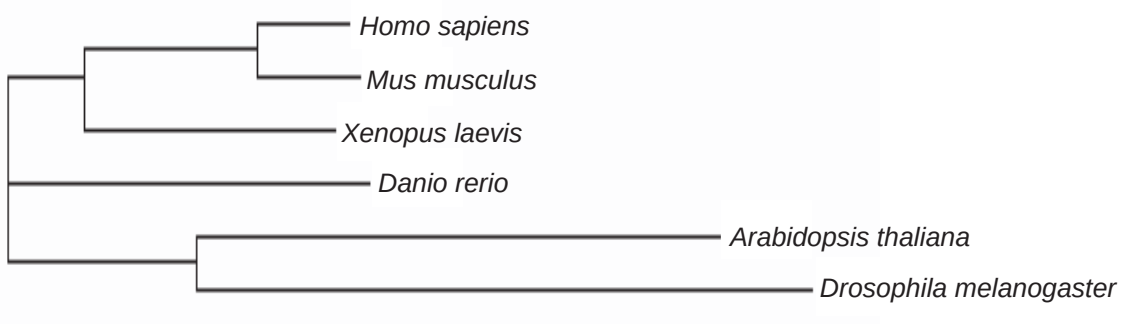

Upon analysis of the mRNA sequence of the predicted *zNEDD1* gene, it was apparent that the open reading frame was composed of 17 exons (Fig. 6.3A). The DNA was amplified from RNA extracted from 24 hpf zebrafish embryos using primers designed to the 5' start of the sequence and the end of the open reading frame to give a product of 2222 base pairs (Fig. 6.3B). Upon sequencing of this PCR product using internal primers, many variations from the published sequence (NM_213506) were identified. However, all encoded silent base changes, or missense changes in amino acids that were identified as polymorphisms as they could be found in other expressed sequence tags (ESTs) of the same gene (data not shown).

6.3. *zNEDD1* mRNA is high in neural regions and down-regulated in development

In order to begin the characterisation of *zNEDD1*, an *in situ* hybridisation analysis was conducted to map the expression of mRNA during zebrafish development (see Fig. 6.1 for stages of development). In early embryogenesis (1 cell to germ ring stage) *zNEDD1* was distributed uniformly throughout all developing tissues (Fig. 6.4A). This expression was increased during the 75% epiboly and bud stages of the embryo, before decreasing again as the embryo progressed through development. By 72 hpf there was a marked reduction in *zNEDD1* mRNA expression. This expression was specific to *zNEDD1*, as staining was absent in the sense controls (Fig. 6.4B, three representative stages shown). Upon analysis of higher magnification dorsal views of embryos at the 18 somite and 24 hpf stages, it was apparent that *zNEDD1* expression was highest in all neural regions (Fig. 6.4C). At the 18 somite stage, this was most evident in the neural tube. At 24 hfp, in addition to the neural tube, there was strongest *zNEDD1* expression in the retina and the lens of the eye. This widespread expression within the developing neural system correlates with the highest concentration of proliferating cells within the embryos at these developmental stages (Wullimann and Knipp, 2000). Again, staining was absent in the sense controls (Fig. 6.4D).

Fig. 6.3 Cloning of zNEDD1

(**A**) The *zNEDD1* mRNA sequence (NM_213506) was retrieved from PubMed, and the intron/exon boundaries retrieved from ensembl (see 2.2) (highlighted in yellow). Primers were designed against the 5' end of the promoter and the 3' stop codon (underlined). The start (atg) and stop (tag) codons are shown in red. Grey sequence represents non-coding regions.

(**B**) The zNEDD1 PCR product is shown from cDNA transcribed from RNA extracted from 24 hpf wild type zebrafish embryos, at the correct size of approximately 2.2 kBp. No band is present in the control lacking cDNA.

A

```
   1 gagcccagcg gcgtgccgta gtggcggttc cttaccggag ccacggatgt tcaaacttta
  61 tcgatatgac aaagttttag tttcaaataa aagggcacat ttatttaacc acagtggatg
 121 tattgacaac tatataccag catatcattt acattgtcta cacttgtaca atgtaaaaca
 181 aggctgctgg gatggaggac gtcacacggc tggtgtcgtc cggtgactgt ctgaagatct
 241 gggactcgag ctcgatgaca gtggtggagc agtttaatcc tcacagtgcc acacatccgg
 301 tggctcaagt gtgctggagc agcagcaatc agtatgtggt cagtgccagc agtataggag
 361 acaaactggt tgtgtccagt ctcaagtcct ctcctgttcc agtcatggag ctcggtgaag
 421 ggaaaaaaca aacccgtgtg agtctgaact ccacatcaca gtttctagtc agtggtggac
 481 tggataacac tgttaatatc tgggacctca agacaaaacg actgcaccga acccttaagg
 541 atcacaagga ggaggtgacg tgcgtgtctt ttaatggagg agacagctac atcgcatcag
 601 gctccactag cggagacatc atcctccaca gcatcacaac caacctgtcc agcaaacctt
 661 tcggccacgg gccaaatgtg cctattcatg atctgaggta ctctctggtg aagcgctctc
 721 tgctgggcac ggtgtctgac agtggatctg tggccctttg ggatgccaac actcagaagg
 781 agctgcactt atttgaaggg gcgcacaaag ccccctgttc aggactggct ttctccccag
 841 ccaacgattt actcttcgtt actgtaggcc tggacaagaa gatcgtctgc tatgacacct
 901 caagcaaaat agtgtttcgt aataaacagg tggagtctcc actcacagct attgatttta
 961 ctcctgatgg agctggactg gtcgtgggct caacgcaggg ccgaatctac ctgtatgacc
1021 tgagaaacct cagcgcaccg gtcaaaatta acacagctca caagacctca gtgacatgca
1081 ttcgcttcca gaactccacc tccaagttaa agtccaccaa atcatccagc aagtcttctc
1141 aatcaaataa aaggatctca gtcaagctgg gcagcagtca gcagacggga ccctccaccc
1201 caacatctac tgtcacaccc attgtttccg gatctgagtt tcctggagat ggtcaagccc
1261 aagtcccagg tccatctgct gaggtgtttt ctcgagaggc agagggtcag ctcagtcaag
1321 atcagatgcc caatgttgag aaattcagca gcatcggacg aaatagttta aacctggaca
1381 ttttctcccc tctaaatgat ggttttaaat cacatggctt tgctgatact tcaagaaatg
1441 gcggcagtat agatgttttc tcaagggaag cagaaggaca gcagaccgct gaccgcttca
1501 gagtcggcag aaacagcctg gacatctttt cacctgtacg agacgattac aaagggcaca
1561 gactgagtga tgtatcaagt ggaaagaaag actttgaata tctacctcat ttccctggag
1621 gctcatccca gaggaagact ccgttgggca ctcctggcag ccgctgctac agtccgtctg
1681 tggtgcagac tccaccaatc aaagaagagg agtccaccac taccctcca cagcagactg
1741 atgtccagaa cggcaccaag gtggagaaga gtaacggtgt acggcaggag tatgatgcca
1801 tcaccacacc ccctgcagct cagagcacgc gaattcagtc cgttcagcct cagttcaaca
1861 caccagagcc cagtcagagg agagatcttt ccacacagct cacatatgat tcccccatca
1921 gcagagctcc tgcacctgct cctcctgctg ctgctgctgc tccagccgca gcagtggagt
1981 ctggctccact cacttctgta cagatgaact ttgtccgtaa catgattcat gaggcactgg
2041 aggacttcag agacacgtgt catcgagaca tcatcaatct acaggtggag atggttcgcc
2101 agttctacat ccagttgaat gaaatccacg gtctgattga gaaatactcc gtgaacgact
2161 cgctcgtcga agagatcgaa agactgaaag aggaaaacaa aagactacga gccaactatt
2221 agagcaggct catgtgtctg ccagtgcctt cactctgttt gtcatatcgg cacactttta
2281 tatccgcttc agctcatgaa gagtgttttt gtaagatttc tatgccataa aaacagatgg
2341 aaatgaaaag aactcatttt gttttctctc caaggtgtgc tttgtacatc ctgactagtt
2401 tactgaaaaa ctacatgtat tggcacttag gatgagtaga gtgaatagac atctcagtgt
2461 ggattttgca acctattttt gccacatgat ttttgaaaac tgcatgccaa aaatgaagaa
2521 aggacactgg tgaacataga tatgtttgta ttttcgcttc agaagtgtgt gtaggtcaga
2581 ggtgctcaac cctgttccta cagatctacc ttcctgcaga gttcagctcc agccctgatc
2641 taccctgaac acacctgaac taatcaatta ggacctgaac agcactggat aattgcaagc
2701 aggtgtgttt gatgtgggtt gcagctgaaa tctgctggaa ggtagatctc caggaacagg
2761 gttgagcact gctgctgtag gttctatgaa tgcaagtgct ttaatacaca acaaatagtt
2821 gcaatcagtt ttatacaatt ttgaaatgac taactccaaa ctattgtcct gtacactgtg
2881 ctattaatcc acatttgtaa gacgtcttcc tatggactgg cctaaataaa ttatttctgc
2941 aaaaaaaaaa aaaaaaaa
```

B

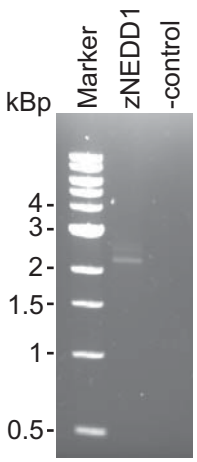

Fig. 6.4 *zNEDD1* mRNA is highest in neural regions and down-regulated during development

Expression of *zNEDD1* mRNA was detected by *in situ* hybridisation using an anti-sense or sense probe against amino acids 1-422 of *zNEDD1* (see 2.10.3). (**A**-**B**) lateral views, (**C**-**D**) dorsal views.

(**A**) In early developmental stages (1 cell to germ ring) *zNEDD1* displays a ubiquitous expression in all cells, revealed by the anti-sense probe. This expression increases in cells at the 75% epiboly and bud stages, and decreases as development proceeds.

(**B**) No staining is present in embryos probed with a sense control (8 cell, 75% epiboly and 24 hpf representative stages shown).

(**C**) After dissection of the yolk sac, dorsal views of embryos show that *zNEDD1* is concentrated along the neural tube at the 18 somite stage and also in the polarised cells of the lens and retina at the 24 hpf stage. This is more evident at higher magnification (right panels).

(**D**) No staining is present in the sense controls at the 18 somite and 24 hpf stages.

Scale bars represent 100 μm.

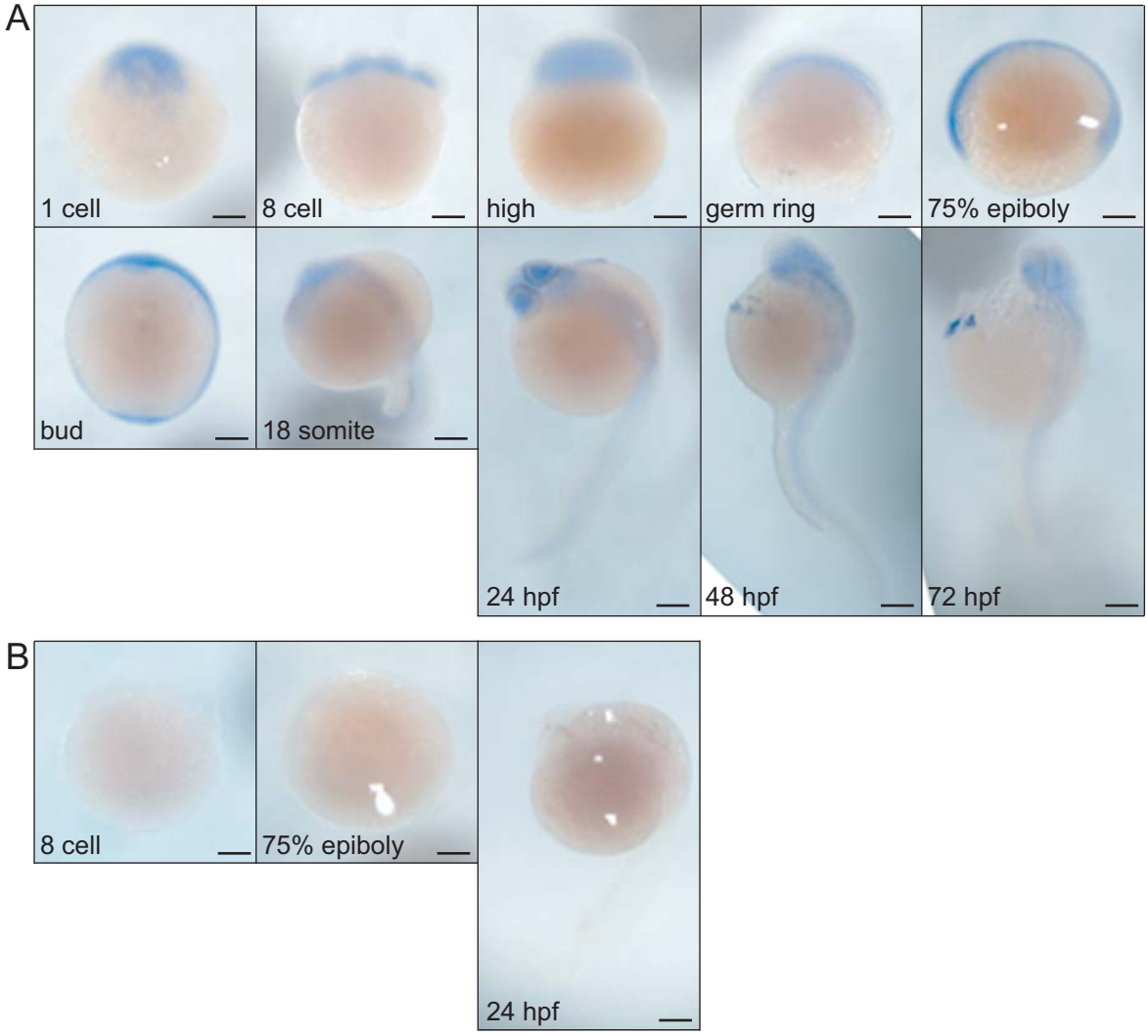
A
1 cell
8 cell
high
germ ring
75% epiboly
bud
18 somite
24 hpf
48 hpf
72 hpf
B
8 cell
75% epiboly
24 hpf
C
18 somite
neural tube
24 hpf
neural tube
retina
lens
D
18 somite
24 hpf

6.4. Generation of zNEDD1 antibodies

In order to next analyse zNEDD1 protein levels, antibodies to zNEDD1 were generated against the C-terminal 252 amino acids of zNEDD1 fused to GST (Fig. 6.5A). This region was chosen as it is similar to the region used to generate the mammalian NEDD1 antibody, which is effective at detecting NEDD1 (chapters 3-5). The antisera from two rabbits immunised with the recombinant GST-zNEDD1 (425-676 aa) protein detected this antigen in a dose-dependent manner (Fig. 6.5B), whereas the pre-immune sera gave a very faint band, probably because of the high amount of protein loaded. The antiserum was also able to detect a band of the expected size for zNEDD1 (approximately 75 kDa) when full length zNEDD1 was expressed in mammalian cells (Fig. 6.5C). Several non-specific bands or degradation products were also present. When affinity purified, the serum detected zNEDD1 with reduced non-specific background.

6.5. zNEDD1 protein levels are down-regulated after early development

The previously described antibody was not suitable for whole-mount staining, and hence the developmental expression of zNEDD1 protein was assessed by immunoblot. Total protein was extracted from embryos at different stages and assessed for zNEDD1. There was a high level of maternal zNEDD1 contribution, which was evident until the midblastula transition (Fig. 6.6A, first three lanes) (Kane and Kimmel, 1993, Pelegri, 2003). Consistent with the *in situ* data (Fig. 6.3), the zygotic level of zNEDD1 remained high early in development and was down-regulated from about the 75% epiboly stage. From the 18 somite stage it was barely detectable (Fig. 6.6A). γ-tubulin has been used previously as a loading control since it has been shown to be expressed at similar levels during all stages of development (Schenck *et al*., 2008). This was also observed in this study, as γ-tubulin levels remained constant during the time course (Fig. 6.6A). Given that zNEDD1, but not γ-tubulin, was greatly reduced from the 18 somite stage onwards, this suggests that these two proteins are not developmentally regulated in the same manner (Fig. 6.6B). To confirm equal protein loading in later stages of development, β-actin levels were also assessed,

Fig. 6.5 Generating zNEDD1 antibodies

(**A**) The C-terminal 252 aa of zNEDD1 was excised from pBlueScript KS-zNEDD1 ORF at *Xho*I and *Not*I and fused to an N-terminal GST-tag, creating a protein of 478 aa (approximately 53 kDa) (see 2.10.5).

(**B**) 10 and 5 μg of GST-zNEDD1 (425-676 aa) expressed in bacteria, was immunoblotted with the antisera from two rabbits immunised with this same antigen. The sera detects the antigen in a dose-dependent manner. Both rabbits display a similar affinity for zNEDD1. Only a faint band is detected with pre-immune sera.

(**C**) Serum from rabbit #1 was used for all further experiments. This serum also detects full length (FL) zNEDD1 when pcDNA3.1-zNEDD1 is transfected into HEK293T cells, but not pcDNA3.1 vector alone. When purified, the serum detects zNEDD1 with reduced non-specific bands or degradation products.

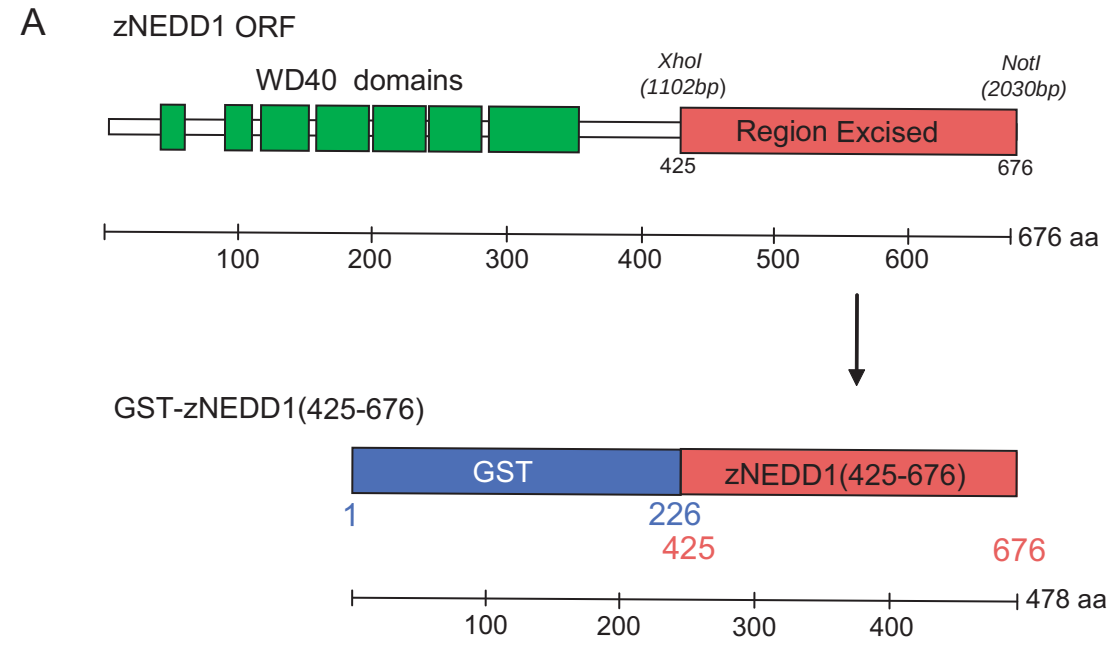
A
zNEDD1 ORF
WD40 domains
XhoI
(1102bp)
NotI
(2030bp)
Region Excised
425
676
100
200
300
400
500
600
676 aa
GST-zNEDD1(425-676)
GST
zNEDD1(425-676)
1
226
425
676
100
200
300
400
478 aa

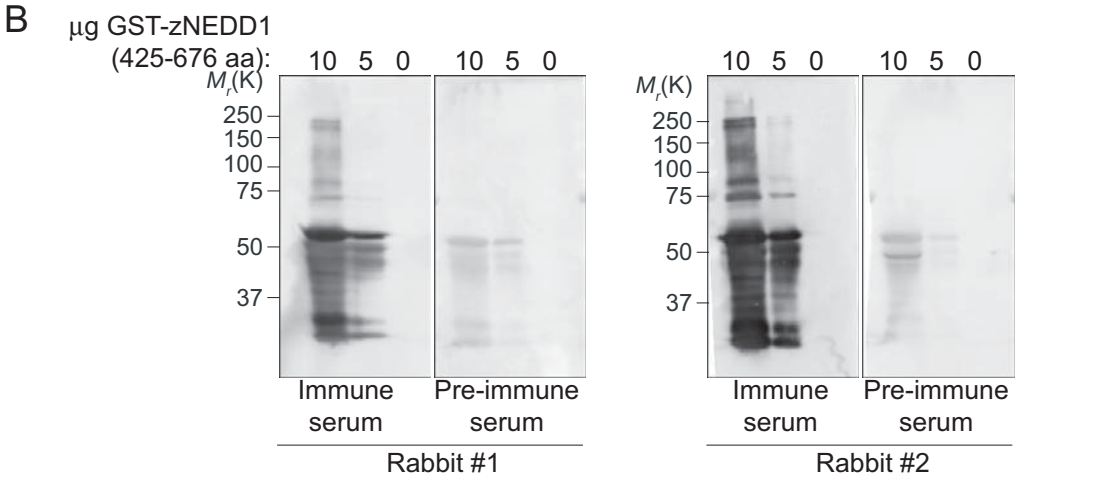
B
µg GST-zNEDD1
(425-676 aa):
10 5 0
10 5 0
Mr(K)
250
150
100
75
50
37
Immune serum
Pre-immune serum
Rabbit #1
Rabbit #2

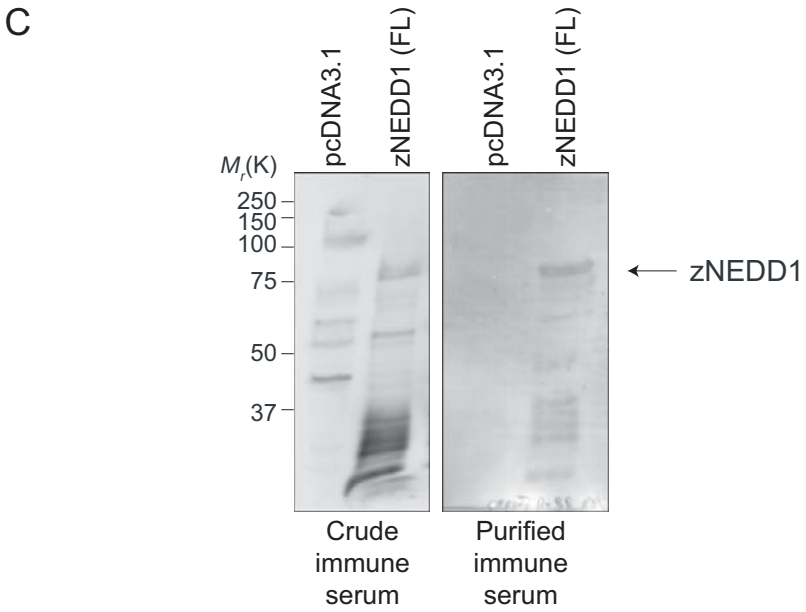
C
pcDNA3.1
zNEDD1 (FL)
Mr(K)
250
150
100
75
50
37
zNEDD1
Crude immune serum
Purified immune serum

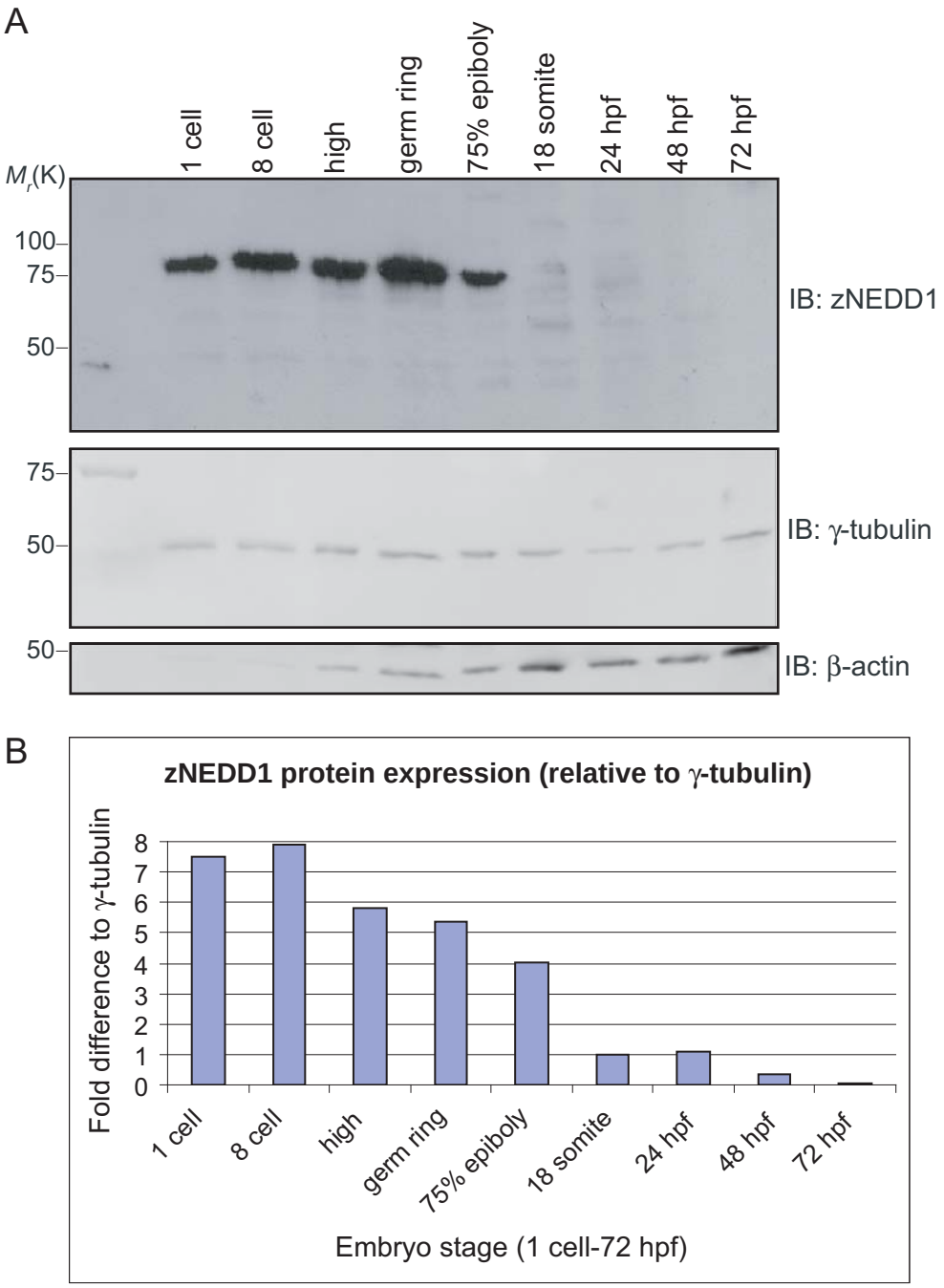

Fig. 6.6 zNEDD1 protein expression is down-regulated during development

Zebrafish embryos were collected at various hpf and protein extracted for immunoblot analysis after removal of the yolk.

(**A**) There is a high level of zNEDD1 maternal protein (first three stages), and also at the beginning of zygotic translation (germ ring). This is down-regulated from the 75% epiboly stage, and there is barely detectable expression from the 18 somite stage onwards. Levels of γ-tubulin remain constant. Levels of β-actin are somewhat constant after expression becomes detectable at the high stage.

(**B**) When normalised to γ-tubulin, zNEDD1 levels are gradually reduced from the 8 cell stage and greatly reduced from the 18 somite stage.

since this protein has also been used as a loading control (Duffy *et al*., 2005). In this study, β-actin maternal expression was low, but was up-regulated from the time of zygotic expression (high stage) and remained fairly constant during development (Fig. 6.6B).

6.6. zNEDD1 localises to the centrosome and interacts with γ-tubulin

Thus far, this study has shown that zNEDD1 displays a similar expression pattern to mammalian Nedd1 (chapter 3), with ubiquitous expression that is highest in neural regions early in development and down-regulated as embryogenesis proceeds. To assess zNEDD1 function, a full length zNEDD1 construct was transfected into mammalian cells and examined for its localisation. Similar to mammalian NEDD1 (chapter 4), zNEDD1 localised to the centrosomes of cells, with a small amount in the cytoplasm, and there was perfect co-localisation with γ-tubulin (Fig. 6.7A).

To examine if zNEDD1 could also interact with γ-tubulin as seen for mammalian NEDD1, zNEDD1 was expressed in mammalian cells and immunoprecipitated using the zNEDD1 antibody. Given that γ-tubulin is highly conserved, mammalian γ-tubulin was used for this study. Both zNEDD1 and γ-tubulin were detected in the inputs and γ-tubulin was also detected when zNEDD1 or γ-tubulin was immunoprecipitated (Fig. 6.7B). As seen for mammalian NEDD1, the reciprocal interaction could not be detected. However, it appears that zNEDD1 and γ-tubulin do interact.

An alignment of the mammalian and zebrafish proteins reveals that the region 572-660 aa of human NEDD1 initially found to interact with γ-tubulin (Luders *et al*., 2006), shows a high degree of homology with residues 598-676 of zNEDD1 (Fig. 6.7C). Additionally, the smaller region 599-660 aa of human NEDD1 found to interact with γ-tubulin in this study (Fig. 5.4) correlates with 615-676 aa of zNEDD1 and these regions are 70% identical and 98% similar (Fig. 6.7C). To test their interaction with γ-tubulin, myc-tagged zNEDD1 proteins were expressed in mammalian cells. Upon immunoprecipitation using the myc antibody, γ-tubulin

Fig. 6.7 zNEDD1 localises to the centrosome and interacts with γ-tubulin

(**A**) pcDNA3.1-zNEDD1 was transfected into NIH-3T3 cells and assessed for its localisation. zNEDD1 co-localises with γ-tubulin in the centrosome, and a small amount is also present in the cytoplasm. The scale bar represents 40 μm.

(**B**) pcDNA3.1-zNEDD1 or pcDNA3.1 alone were transfected into HEK293T cells and assessed for an interaction with endogenous γ-tubulin. Expression of zNEDD1 and γ-tubulin is confirmed in the input lysates (1:20 lysates loaded). The zNEDD1 antibody is able to efficiently immunoprecipitate zNEDD1. γ-tubulin is also immunoprecipitated with zNEDD1 and with the γ-tubulin antibody. In the absence of antibody or in cells transfected with pcDNA3.1 alone, no γ-tubulin is immunoprecipitated. The bands at approximately 50 kDa are IgGs.

(**C**) Human and zebrafish NEDD1 proteins were aligned using Clustal W2. For a description of the colour coding and alignment symbols see the legend for Fig. 6.2. The alignment shows the regions from 565 aa of human NEDD1 and 596 aa of zNEDD1. The region 572-660 aa of human NEDD1 correlates well to 598-676 aa of zNEDD1, although there are 10 aa missing at the C-terminal region of the zebrafish homologue. The region 599-660 aa of human NEDD1 correlates well to 615-676 aa of zNEDD1.

(**D**) The interaction of truncated forms of zNEDD1 and γ-tubulin was assessed using endogenous γ-tubulin and myc-tagged zNEDD1 constructs. The expression of all zNEDD1 constructs and γ-tubulin is confirmed in the inputs (1:20 lysates loaded). All myc-zNEDD1 constructs are able to be immunoprecipitated with a myc antibody. γ-tubulin is able to be immunoprecipitated with full length (1-676 aa), 598-676 aa and 615-676 aa zNEDD1 only. In the absence of a zNEDD1 construct or an antibody, γ-tubulin is not immunoprecipitated.

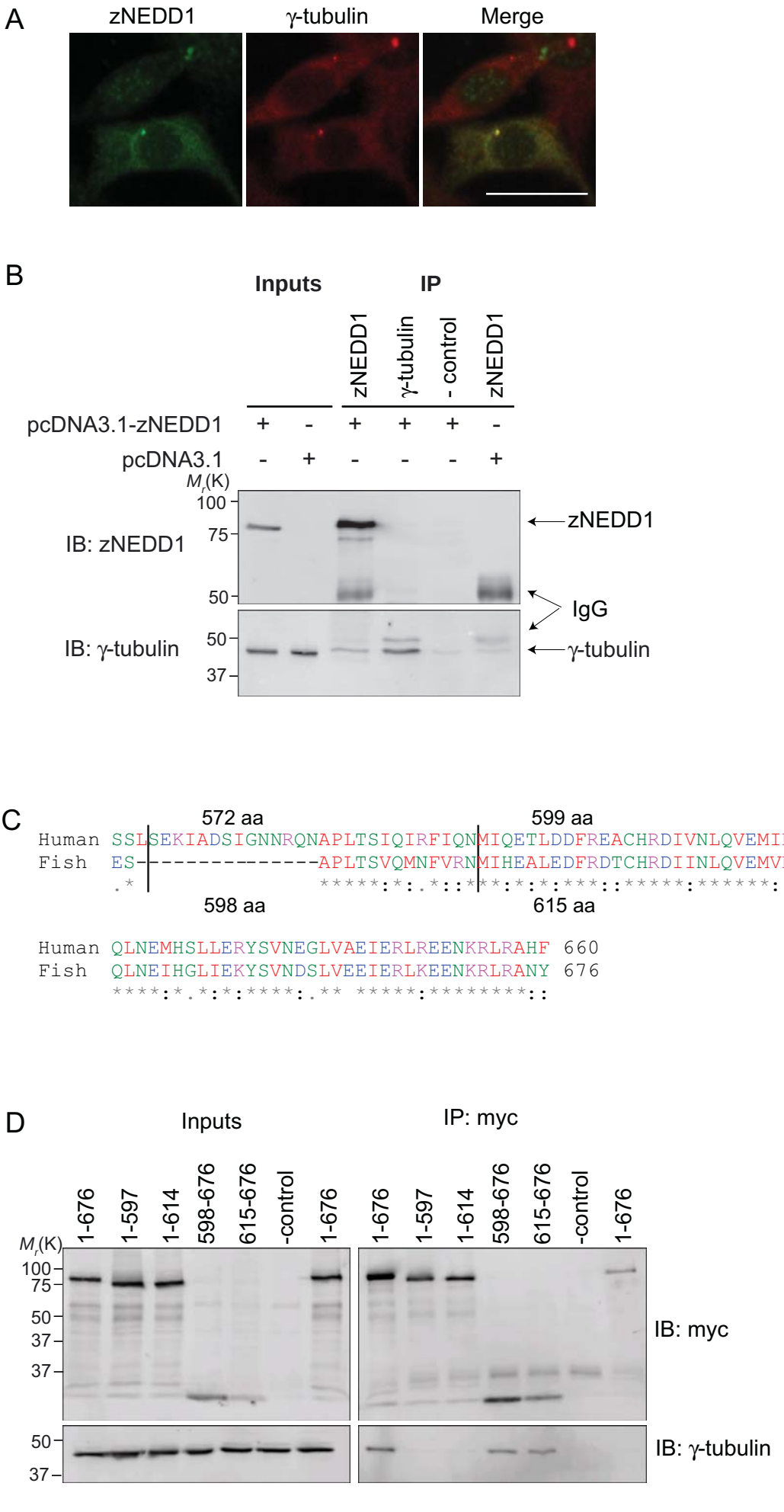
A
zNEDD1
γ-tubulin
Merge
B
Inputs
IP
zNEDD1
γ-tubulin
- control
zNEDD1
pcDNA3.1-zNEDD1 + - + + + -
pcDNA3.1 - + - - - +
Mr(K)
100
75
50
IB: zNEDD1
zNEDD1
IgG
50
37
IB: γ-tubulin
γ-tubulin
C
572 aa
599 aa
Human SSLSEKIADSIGNNRQNAPLTSIQIRFIQNMIQETLDDFREACHRDIVNLQVEMIKQFHM 624
Fish ES----------APLTSVQMNFVRNMIHEALEDFRDTCHRDIINLQVEMVRQFYI 640
598 aa
615 aa
Human QLNEMHSLLERYSVNEGLVAEIERLREENKRLRAHF 660
Fish QLNEIHGLIEKYSVNDSLVEEIERLKEENKRLRANY 676
D
Inputs
IP: myc
1-676
1-597
1-614
598-676
615-676
-control
1-676
Mr(K)
100
75
50
37
37
IB: myc
50
37
IB: γ-tubulin

was detected interacting with full length zNEDD1 (1-676 aa), and constructs containing amino acids 598-676 or 615-676 (Fig. 6.7D). No γ-tubulin was immunoprecipitated by other constructs lacking the C-terminal end of zNEDD1 (1-597 aa and 1-614 aa). Hence, similar to human NEDD1, residues 615-676 of zNEDD1 are sufficient for its interaction with γ-tubulin.

6.7. zNEDD1 protein can be reduced using morpholinos

To determine the importance of zNEDD1 during development, and to identify specific roles it may play, the effect of reducing zNEDD1 protein in early embryogenesis was examined. Morpholinos (MOs) have been widely used to silence or deplete the expression of proteins during zebrafish development, and their effects have been shown to last for up to 96 h (Kloosterman *et al*., 2007). Hence, two MOs were designed to block the translation of zNEDD1 when injected into fertilised zebrafish embryos. One MO was generated to bind upstream (5') of the ATG start codon (MO1), and the other MO targeted the region spanning the ATG codon (MO2) (Fig. 6.8A). A 5-base mismatch morpholino was also designed against MO1, however this morpholino proved to be toxic to the embryos for reasons unknown, and so a standard control morpholino was employed instead, which comprises a oligomer with no known target sequence in zebrafish (Control MO, GeneTools). To test the efficacy of the MOs, various concentrations were injected into zebrafish embryos at the 1 cell stage, and protein extracted from the embryos at 24 hpf. A final concentration of 0.25 mM was found to be the lowest concentration effective in depleting zNEDD1 expression, whilst not being toxic to the embryos (data not shown). When 0.25 mM of MO1 or MO2 alone was injected into embryos, there was an approximately 50% reduction in zNEDD1 protein levels, as assessed by immunoblot (Fig. 6.8B). When the two MOs were combined (0.125 mM each), there was an additive affect, achieving about 80% depletion of zNEDD1 protein. The protein levels of both γ-tubulin and β-actin were unchanged. The levels of zNEDD1 protein expression were normalised to γ-tubulin, and consistently showed similar levels of depletion (Fig. 6.8C).

Fig. 6.8 zNEDD1 protein can be reduced by morpholino injection

(**A**) Two morpholinos (MOs) were designed by GeneTools. MO1 targets the *zNEDD1* mRNA sequence upstream (5') of the ATG start codon (green). MO2 spans the ATG start codon (yellow). Both MOs block translation of zNEDD1. The open reading frame of zNEDD1 is in blue, and the atg start codon is underlined. Non-coding sequence is shown in grey.

(**B**) Protein was extracted from injected embryos at 24 hpf and 20 μg of each sample assessed by immunoblotting. Injection of 0.25 mM of either MO reduces zNEDD1 protein levels when compared to control, and this is further reduced when MO1+2 are co-injected at 0.125 mM each.

(**C**) Upon quantification of the intensity of bands from three independent experiments using ImageQuant software, 0.25 mM of each individual MO causes about 50% reduction of zNEDD1 when normalised to γ-tubulin and compared to control injected embryos, and about 80% when injected in combination (0.125 mM each). The errors bars represent SEM, n = 3 independent experiments using approximately 20 embryos each.

A

```
  1 gagcccagcg gcgtgccgta gtggcggttc cttaccggag ccacggatgt tcaaacttta
 61 tcgatatgac aaagttttag tttcaaataa aagggcacat ttatttaacc acagtggatg
121 tattgacaac tatataccag catatcattt acattgtcta cacttgtaca atgtaaaaca
181 aggctgctgg gatggaggac gtcacacggc tggtgtcgtc cggtgactgt ctgaagatct
```

B

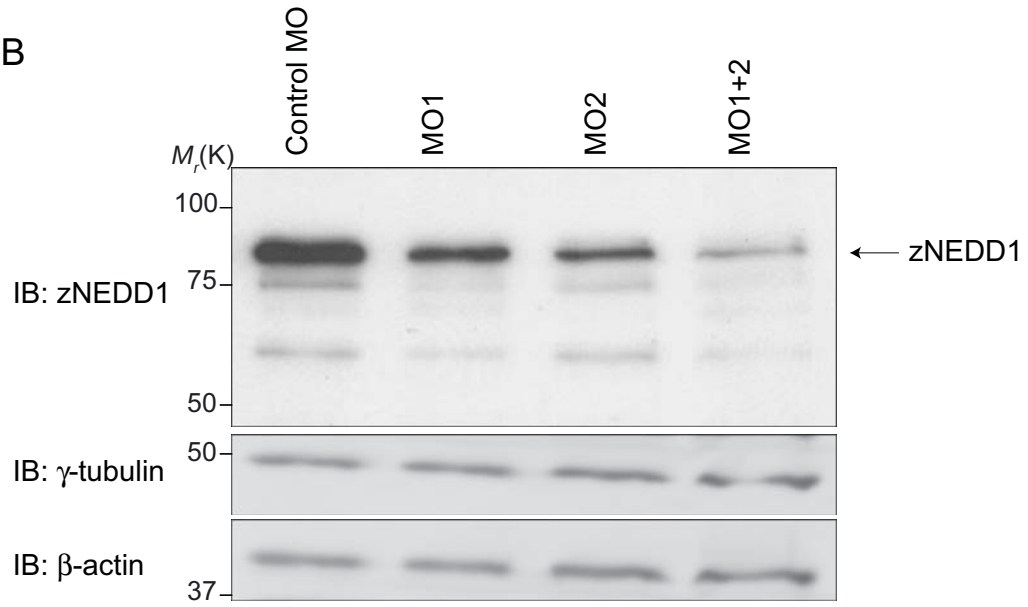

C

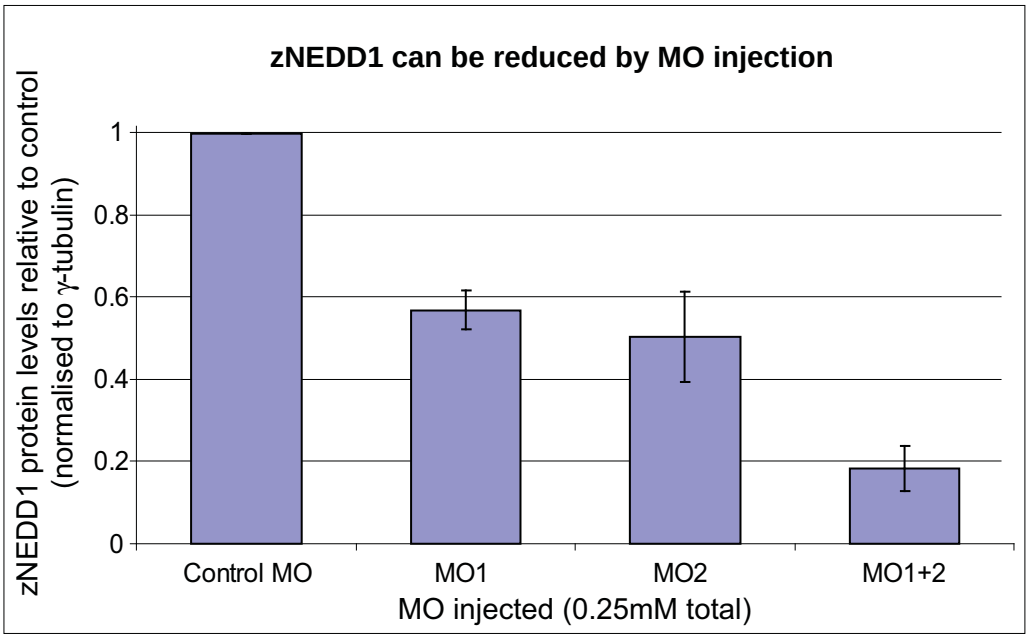

6.8. zNEDD1 depleted embryos are severely deformed with disorganised brains

To determine the physiological role of zNEDD1 during development, the phenotypes of embryos depleted of this protein by MO injection were analysed. Embryos injected with a high dose (1 mM) of combined zNEDD1 MOs (zNEDD1 MO1+2) did not survive to 24 hpf, and those injected with a low dose (0.1 mM) showed no phenotypic abnormalities (data not shown). When compared to control injected embryos, those injected with an intermediate dose of zNEDD1 MO1+2 (0.25 mM total) mostly survived to 24 hpf, but displayed a global deformed phenotype. However, there appeared to be more specific defects in the brain, with disorganisation of normal patterning and size such that the overall structure of the heads was smaller (Fig. 6.9). Hence this concentration of MO was chosen for further analysis. At 24 hpf, the uninjected and control injected embryos developed normally and many clearly defined structures of the brain such as the ventricles (tectal and fourth ventricle labelled) and the cerebellum could be observed (Fig. 6.9A-B). The forebrain, midbrain and hindbrain could also be identified and their boundaries easily distinguished. In addition, the eyes were easily delineated. All zNEDD1 depleted embryos displayed abnormalities, but there was some variability in the extent of these defects, which is common for MO injection (Schenck *et al*., 2008), presumably depending on the variability in the level of knockdown of zNEDD1 (Fig. 6.9C-E).

It was possible to arbitrarily categorise the zNEDD1 morphants into mild, moderate and severely abnormal phenotypes, with the majority of zNEDD1 depleted fish displaying moderate levels of abnormalities. When compared to uninjected and control injected, all zNEDD1 depleted embryos displayed abnormal shortened tails with a curved body axis, however defects in the nervous system were of more interest to this study and were pursued further (Fig. 6.9A-E). In cases of mild abnormalities, the eyes remained largely intact, and the midbrain and hindbrain were present and well defined (Fig. 6.9C). However, the forebrain was not properly developed. This phenotype was more obvious in cases of

Fig. 6.9 zNEDD1 depleted embryos are severely deformed with associated brain disorganisation

Embryos were viewed under light microscopy at 24 hpf to visualise phenotypes after zNEDD1 depletion. First two panels are lateral view, third panel is dorsal view. Eye (e), tectal ventricle (tv), cerebellum (ce), fourth ventricle (iv), hindbrain (hb), forbrain (fb), midbrain (mb).

(**A**-**B**) Uninjected and control injected embryos are identical in appearance with well defined structures in the brain.

(**C**-**E**) Most zNEDD1 depleted embryos (zNEDD1 MO1+2) display a global deformed phenotype which varies between embryos. (**C**) In cases of mild defects, the forebrain appears disorganised, but the midbrain, hindbrain and eyes appear to develop normally. (**D**) In moderate cases, the disorganisation of the forebrain is more severe, and areas of the ventricular system also appear disturbed with patches of black cell masses. (**E**) In severe cases, there are more black cell masses, no clear delineation of the forebrain, midbrain and hindbrain and the eyes are obliterated.

(**F**) In embryos co-injected with *zNEDD1* mRNA (zNEDD1 MO1+2+RNA), the phenotypes are rescued to a large extent and the brain structures are restored.

Scale bars represent 100 μm.

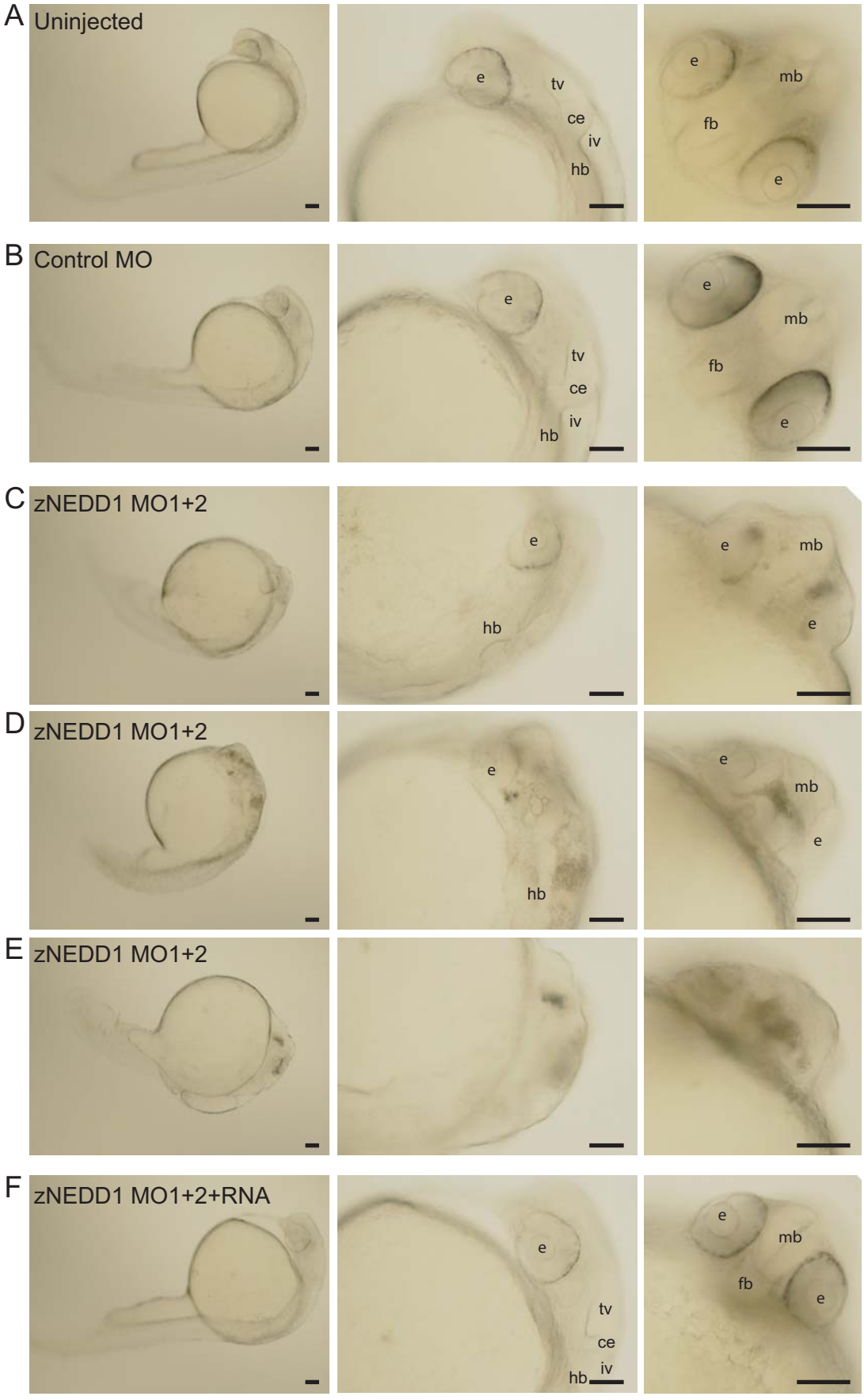
A
Uninjected
e
tv
ce
iv
hb
e
mb
fb
e
B
Control MO
e
tv
ce
iv
hb
e
mb
fb
e
C
zNEDD1 MO1+2
e
hb
e
mb
e
D
zNEDD1 MO1+2
e
hb
e
mb
e
E
zNEDD1 MO1+2
F
zNEDD1 MO1+2+RNA
e
tv
ce
iv
hb
e
mb
fb
e

moderate abnormalities, with the forebrain appearing severely disorganised and containing aggregates of black masses, presumably representing dead cells (Fig. 6.9D). The ventricular system was also abnormal in size and shape, although midbrain and hindbrain structures were still defined. The eyes were present. In zNEDD1 depleted embryos classed as being severely abnormal, the eyes were completely obliterated (Fig. 6.9E). There appeared to be more black masses, and the midbrain, hindbrain and forebrain structures could not be delineated. This indicates that there were significant abnormalities in patterning and organisation during brain development in the zNEDD1 morphants.

6.9. Phenotypes of zNEDD1 depleted embryos can be rescued by mRNA

In order to verify that the observed phenotypes were due to the specific MO effect of inhibition of zNEDD1 translation and not off-targets effects, the combined MOs were injected into embryos together with capped full length *zNEDD1* mRNA. Importantly, co-injection with *zNEDD1* mRNA largely rescued the phenotypes, such that these embryos appeared similar to uninjected embryos (Fig. 6.9F). To verify this further, greater numbers of embryos were analysed for abnormalities after MO injection (Fig. 6.10A). When compared to uninjected embryos, embryos injected with zNEDD1 MO1+2 displayed obvious phenotypic abnormalities (as in Fig. 6.9), and only 31% appeared normal and similar to uninjected embryos. However, upon co-injection of zNEDD1 MO1+2 with *zNEDD1* mRNA, approximately 80% of embryos appeared morphologically normal. This is similar to levels seen in control injected embryos, which experience a low percentage of defects due to the injection procedure. The rescue of morphology was shown to be due to the significant restoration of zNEDD1 protein levels by the co-injection (Fig. 6.10B). Interestingly, zNEDD1 appeared as a doublet on this immunoblot, possible representing a phosphorylated form of the protein, as seen for mammalian NEDD1, although this was not explored further. Together, these results indicate that the reduction in zNEDD1 caused by MO injection is specifically responsible for the observed phenotypic abnormalities.

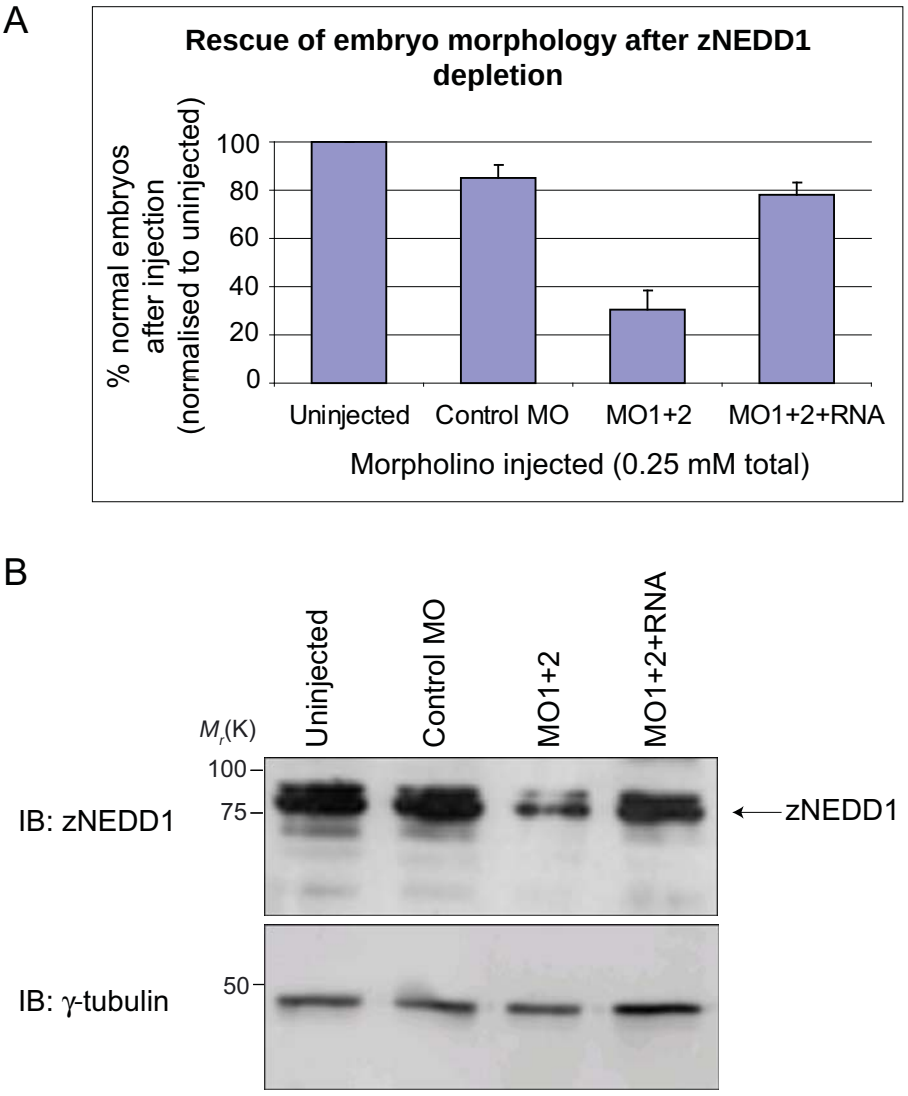

Fig. 6.10 zNEDD1 depletion can be rescued by co-injection with *zNEDD1* mRNA

Embryos were injected with control MO, the combined zNEDD1 MO1+2, or zNEDD1 MO1+2 together with 5 ng capped *zNEDD1* mRNA.

(**A**) Only 31% of embryos injected with zNEDD1 MO1+2 display normal morphology resembling uninjected embryos. This is rescued by the co-injection with *zNEDD1* mRNA which results in 78% of embryos now appearing morphologically indistinguishable from uninjected embryos (MO1+2+RNA). This is comparable to the 85% normal embryos seen with the control injection (see 6.9 for phenotype analysis). The errors bars represent SEM, n = 3 independent experiments using approximately 50 embryos each.

(**B**) 24 h after injection, protein was extracted and 20 μg of each sample immunoblotted for zNEDD1 and γ-tubulin. zNEDD1 MO injection greatly reduces zNEDD1 levels and this is restored by co-injection with *zNEDD1* mRNA. γ-tubulin serves as a loading control, since this is not affected by zNEDD1 depletion.

6.10. zNEDD1 depleted embryos display a high level of apoptosis

The black cell masses apparent in the phenotypic analysis of zNEDD1 depleted embryos suggested that these morphants display a high level of cell death. To investigate this further, embryos were assessed for apoptosis by TUNEL staining. Whilst uninjected and control injected embryos exhibited very few apoptotic cells (Fig. 6.11A-B), zNEDD1 depleted embryos consistently displayed a higher level of apoptosis present throughout the whole embryo, but concentrated in the brain and neural tube (6.11C). In particular, there were a high number of apoptotic cells in the forebrain, correlating with the gross morphological abnormalities and cell death seen in this region of the brain in Fig. 6.9. Co-injection with *zNEDD1* mRNA rescued this phenotype (Fig. 6.11D), indicating that the apoptosis is caused by the reduction in zNEDD1, and not by injury caused by MO injection or toxicity of the MO solution.

6.11. zNEDD1 depleted embryos still undergo apoptosis after co-depletion of p53

It is known that some MOs non-specifically induce p53 activity which results in increased levels of cell death (Robu *et al*., 2007). In order to discount this as the cause for the apoptosis seen when injecting with zNEDD1 MOs, co-injections were performed with a previously characterised p53 MO which reduces off-target effects (Nowak *et al*., 2005, Robu *et al*., 2007). TUNEL staining revealed that zNEDD1 depletion induced apoptosis as seen previously when compared to controls (Fig. 6.12A-C), and after co-injection with the p53 MO apoptosis was still occurring (Fig. 6.12D). However, the number of TUNEL positive cells appeared to be lower in the co-injected embryos. This suggests that either some of the apoptosis in embryos depleted of zNEDD1 by MO injection relies on p53 activity, or is an off-target effect. Given the rescue of this phenotype by co-injection by *zNEDD1* mRNA (Fig. 6.11), this indicates that the former option is more likely, and off-target effects are not responsible for the apoptosis.

Fig. 6.11 zNEDD1 depletion causes a high level of apoptosis

Uninjected and MO injected embryos were assessed for apoptosis by TUNEL staining at 24 hpf.

(**A**-**B**) Uninjected and control injected embryos display very few TUNEL positive apoptotic cells.

(**C**) zNEDD1 MO1+2 injected embryos show a high level of apoptosis, primarily concentrated in the forebrain and the neural tube. Representative examples of two embryos are shown.

(**D**) The apoptosis is rescued by co-injection with *zNEDD1* mRNA.

Scale bars represent 500 μm.

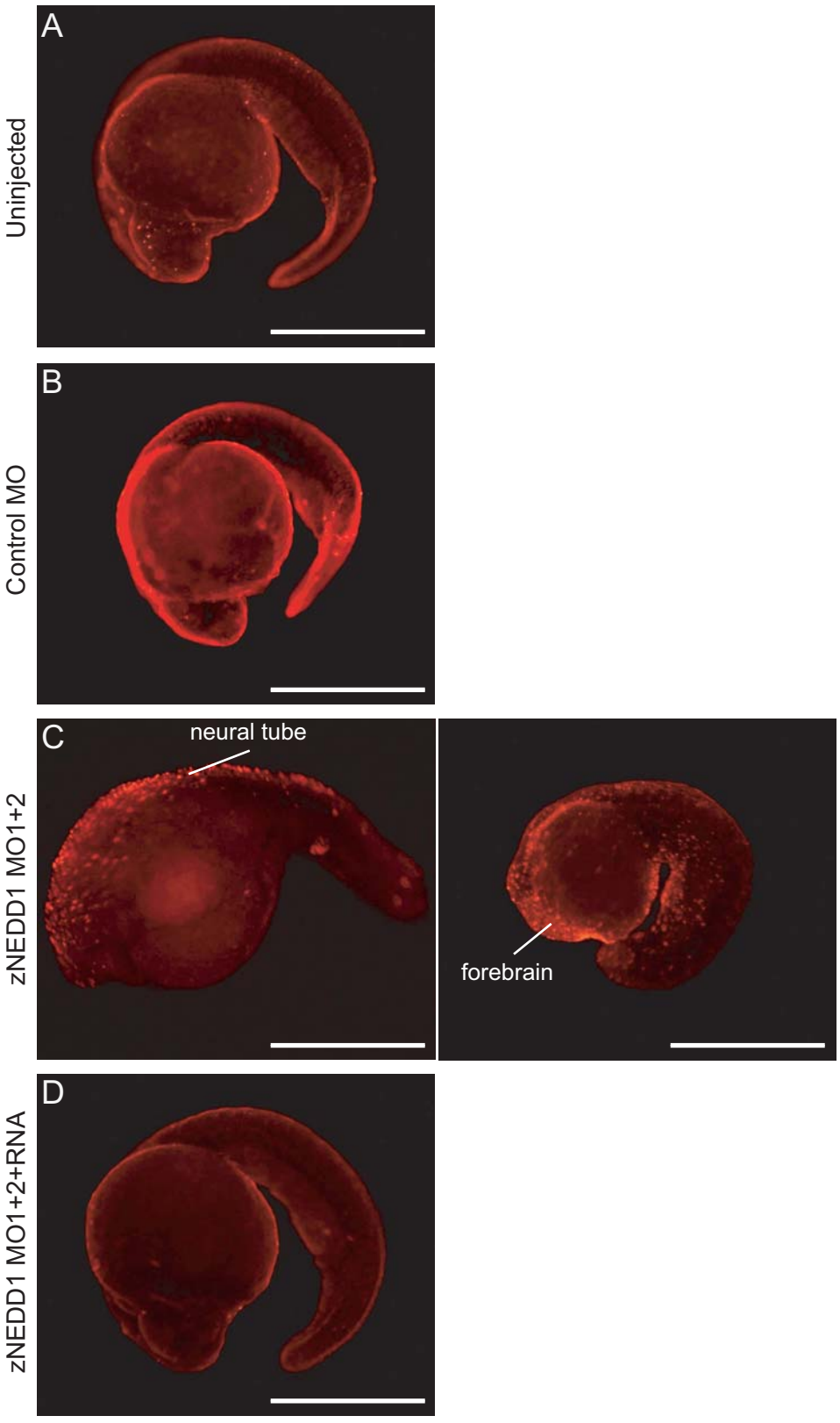
A
Uninjected
B
Control MO
C
neural tube
zNEDD1 MO1+2
forebrain
D
zNEDD1 MO1+2+RNA

Fig. 6.12 Apoptosis caused by zNEDD1 depletion still occurs with concurrent p53 depletion

Embryos were injected with zNEDD1 MO1+2 and/or p53 MO and assessed for apoptosis by TUNEL staining at 24 hpf.

(**A**-**B**) Uninjected and p53 MO injected embryos consistently display very few TUNEL positive apoptotic cells.

(**C**) Injection of zNEDD1 MO1+2 causes an increase in the amount of apoptotic cells. Two representative embryos are shown.

(**D**) Co-injection of zNEDD1 MO1+2 and p53 MOs still results in apoptosis, although there are not as many TUNEL positive cells as in zNEDD1 MO1+2 injection alone. Two representative embryos are shown.

Scale bars represent 500 μm.

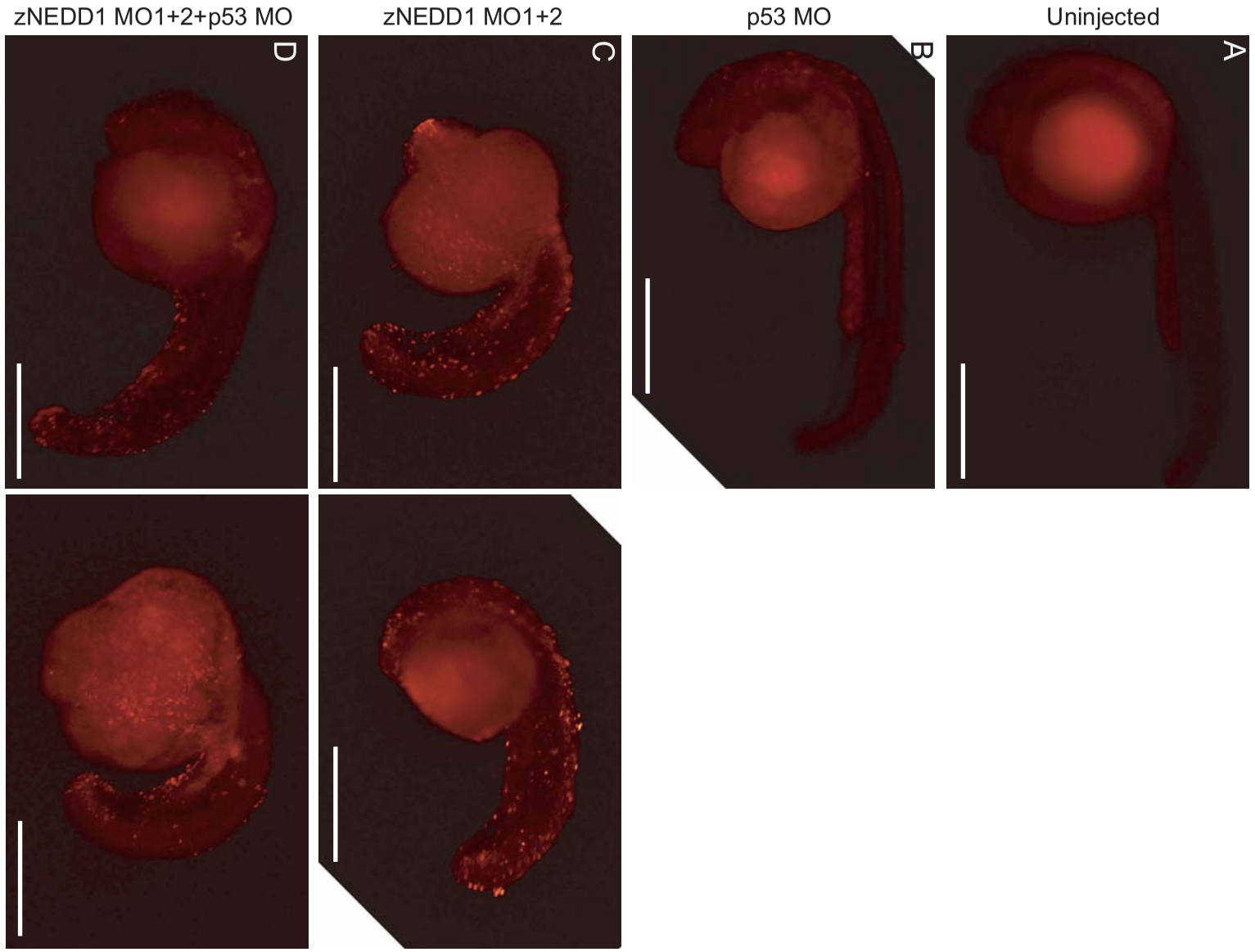
zNEDD1 MO1+2+p53 MO
zNEDD1 MO1+2
p53 MO
Uninjected
D
C
B
A

6.12. zNEDD1 depleted embryos display mitotic arrest

Depletion of mammalian NEDD1 has been shown to cause mitotic arrest (Haren *et al*., 2006, Luders *et al*., 2006). Hence, it was next aimed to assess whether there were any changes in the mitotic index of zNEDD1 depleted zebrafish embryos by staining for phosphorylated histone H3 (pH3), which is present during the G2 and M phases of the cell cycle (Hendzel *et al*., 1997). Uninjected and control injected embryos displayed a low number of pH3 positive cells as previously observed (Murphey *et al*., 2006), because mitosis comprises a very short part of the cell cycle (Fig. 6.13A-B). zNEDD1 depleted embryos displayed an increase in the amount of pH3 positive cells when compared to uninjected or control injected embryos (Fig. 6.13C). As there did not appear to be an increase in total cell numbers or size of the embryos (Fig. 6.9), this suggests that many cells may have been arrested in mitosis. The mitotic cells were present throughout the embryo, but again appeared concentrated in the brain and neural tube. Co-injection with *zNEDD1* mRNA partially rescued this phenotype, although unlike other in phenotypes this was not completely restored, for reasons unknown (Fig. 6.13D). However, it was speculated that the incomplete restoration of zNEDD1 proteins levels may have been sufficient to arrest some cells in mitosis.

6.13. zNEDD1 depleted embryos undergo neurogenesis, but present poorly patterned neuronal structures

Given the mitotic arrest and increased apoptosis in zNEDD1 depleted embryos, it was no surprise that these embryos displayed other morphological abnormalities. Specifically, the disorganised appearance of brains in the zNEDD1 morphants (Fig. 6.9) suggested that these embryos may exhibit neuronal defects. To characterise this further, embryos at 24 hpf were stained with an antibody to HuC, a protein that maintains high expression in post-mitotic cells in most regions of the nervous system (Kim *et al*., 1996). All embryos were developmentally age matched, as can be seen by the normal development of structures such as the eyes in most cases (Fig. 6.14A-D).

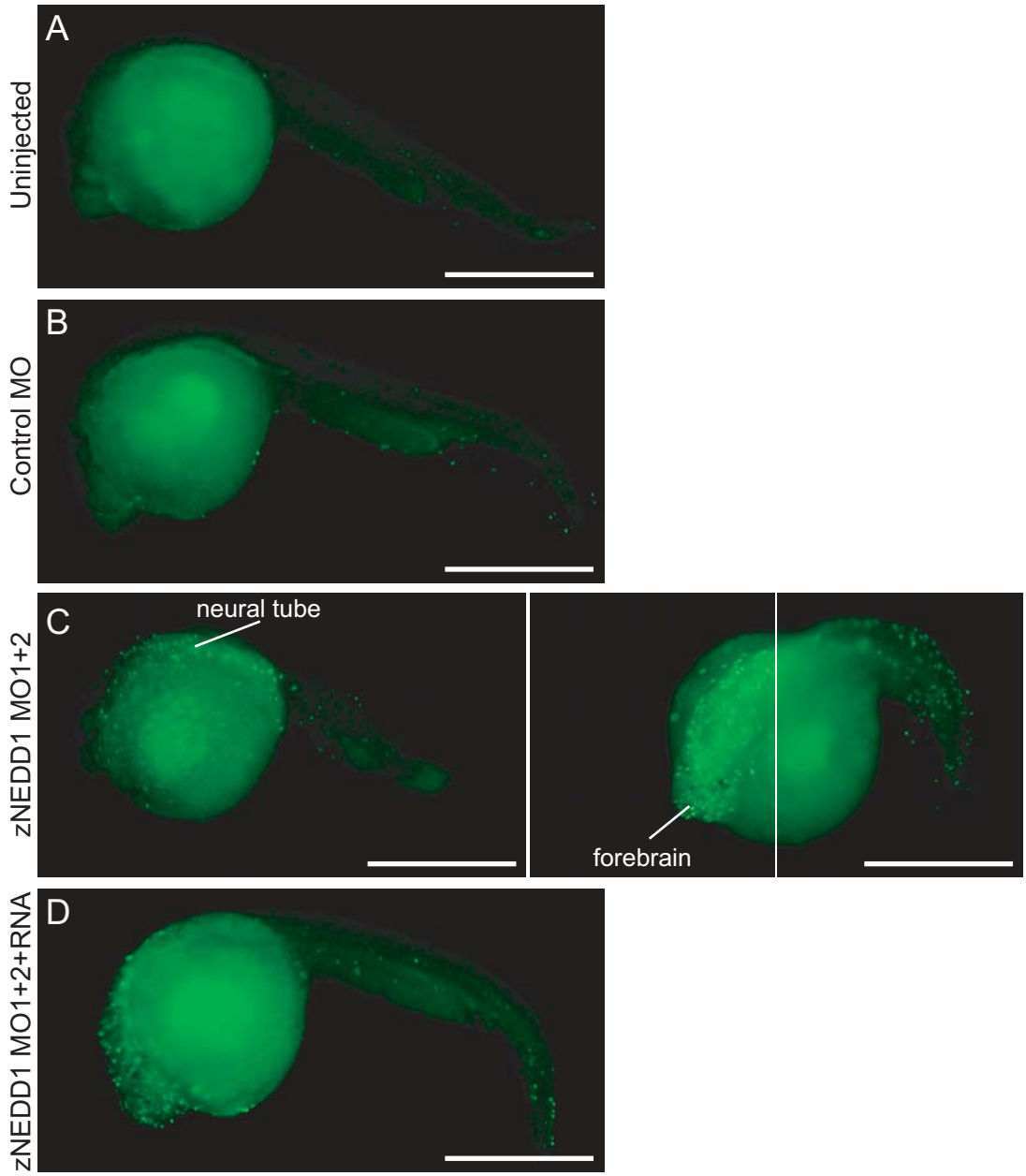

Fig. 6.13 zNEDD1 depletion causes an increase in mitotic cells

Uninjected or MO injected embryos were assessed for mitotic cells by pH3 staining at 24 hpf.

(**A**-**B**) Uninjected and control injected embryos display low levels of pH3 positive cells.

(**C**) zNEDD1 MO1+2 injected embryos have an increased amount of pH3 positive cells, primarily in the brain and neural tube. Two representative embryos are shown. The division in the right embryo shows two different focal planes.

(**D**) zNEDD1 MO1+2 injected embryos rescued with *zNEDD1* mRNA partially restores the level of pH3 staining.

Scale bars represent 500 µm.

Fig. 6.14 zNEDD1 depletion causes disorganised brains and defects in post-mitotic neuronal patterning

Uninjected or MO injected fish were assessed for post-mitotic neurons by HuC antibody staining at 24 hpf.

(**A**-**D**) Embryos are photographed at 4x magnification (lateral orientation). (**A**-**B**) Uninjected and control injected embryos show faint but normal HuC staining in different areas of the brain and in the neural tube. (**C**) zNEDD1 MO1+2 injected embryos are still positive for HuC staining, however they appear morphologically abnormal. (**D**) This is rescued by co-injection with *zNEDD1* mRNA.

(**E**-**H**) Enlarged lateral images of the neural tube in the trunk show that HuC post-mitotic neurons in this region are largely unaffected by zNEDD1 MO1+2 injection.

(**I**-**L**) Enlarged dorsal images of the brain region of embryos show HuC predominantly in the cranial ganglia and in the forebrain region. (**I**, **J**) HuC staining is well organised, and the forebrain, midbrain and hindbrain regions are clearly defined in uninjected and control injected embryos. (**K'** and **K''**) Two zNEDD1 depleted embryos are shown with varying degrees of abnormalities. (**K'**) In zNEDD1 depleted embryos with moderate abnormalities, the cranial ganglia are still present but show distorted patterning, and the overall size and definition of the brain structures are reduced. (**K''**) In zNEDD1 depleted embryos with severe abnormalities, the cranial ganglia are more distorted, and the brain structures disorganized and indistinguishable. (**L**) Normal HuC staining and brain structures are shown after co-injection with *zNEDD1* mRNA. Eye (e), forebrain (fb), midbrain (mb), hindbrain (hb). All scale bars represent 100 μm.

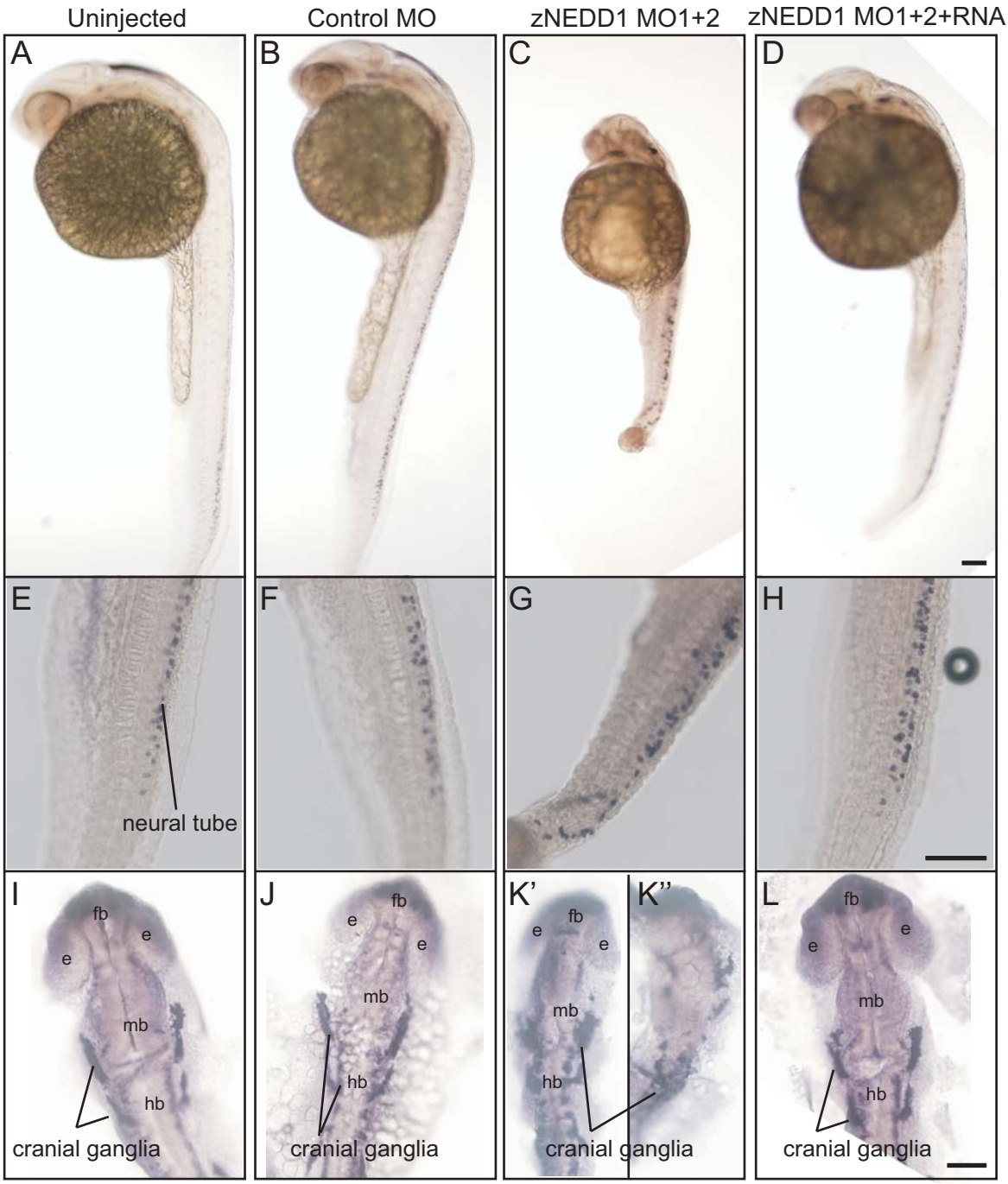
Uninjected
Control MO
zNEDD1 MO1+2
zNEDD1 MO1+2+RNA
A
B
C
D
E
F
G
H
neural tube
I
J
K'
K''
L
fb
e
mb
hb
cranial ganglia

In uninjected, control injected and zNEDD1 MO1+2+RNA co-injected rescued embryos, HuC staining was similar to published data, with faint expression in multiple regions of the brain and a continuous population of post-mitotic neurons throughout the rostrocaudal axis of the neural tube (Park *et al*., 2000, Mawdsley *et al*., 2004) (Fig. 6.14A, B, D). These neurons were still present in zNEDD1 depleted embryos, even though the embryos had growth defects and abnormalities at this stage (Fig. 6.14C). Upon closer analysis of the staining in the trunk of these embryos, the HuC-positive neurons consistently appeared similar in number and patterning to uninjected, control and rescued embryos (Fig. 6.14E-H). In regions of the brain however, there was a variable effect of zNEDD1 depletion on neuronal patterning, with the majority of embryos displaying a moderate phenotype. In a dorsal view of embryos at 24 hpf, HuC is normally present in regions of the forebrain and in cranial ganglia, as seen in uninjected, control and rescued embryos (Fig. 6.14I, J, L). After zNEDD1 depletion, embryos that displayed moderate abnormalities (forebrain, midbrain and hindbrain still visible, as well as remnants of eyes) still contained many HuC-positive neurons, although there was distorted patterning of the cranial ganglia (Fig. 6.14K'). Additionally, it was observed that the brain structures were reduced in size, which is consistent with the increase in cell death described previously in the brain (Fig. 6.11). In embryos that displayed severe morphological defects (no discernable forebrain, midbrain and hindbrain structures, or eyes), HuC-positive neurons were again present, but the cranial ganglia were even more severely distorted (Fig.6.14K''). Hence, zNEDD1 depletion from zebrafish embryos does not appear to affect the differentiation or number of post-mitotic neurons, but does cause severe defects in neuronal organisation in the brain.

To further characterise the effects of zNEDD1 depletion on neural development, embryos were also analysed for Rohon-Beard (RB) sensory neurons which reside along the neural tube (Cambray-Deakin and Burgoyne, 1987). In uninjected and control injected embryos, characteristic acetylated α-tubulin staining revealed RB cells and their axonal projections between the tracts of the dorsal longitudinal fasciculus (Fig. 6.15A-B) (Bernhardt *et al*.,

Fig. 6.15 zNEDD1 depletion causes defects in Rohon-Beard sensory neurons

Uninjected or MO injected fish were assessed for acetylated α-tubulin staining at 24 hpf. Embryos are shown from a lateral view. RB (Rohon-beard cells).

(**A**-**B**) Uninjected and control injected embryos display a normal neural tube, with characteristic staining of acetylated α-tubulin in RB sensory neurons and their axons within the dorsal longitudinal fasciculus.

(**C**) zNEDD1 MO1+2 injected embryos that show mild or moderate abnormalities have a reduced amount of RB cells and fasciculated axons, but the neural tube appears relatively normal.

(**D**) zNEDD1 MO1+2 injected embryos that show severe abnormalities have very few RB cells, a marked reduction in bundling of fasciculated axons, and incomplete neural tube formation.

(**E**) These phenotype is rescued by co-injected with *zNEDD1* mRNA.

Scale bars represent 40 μm.

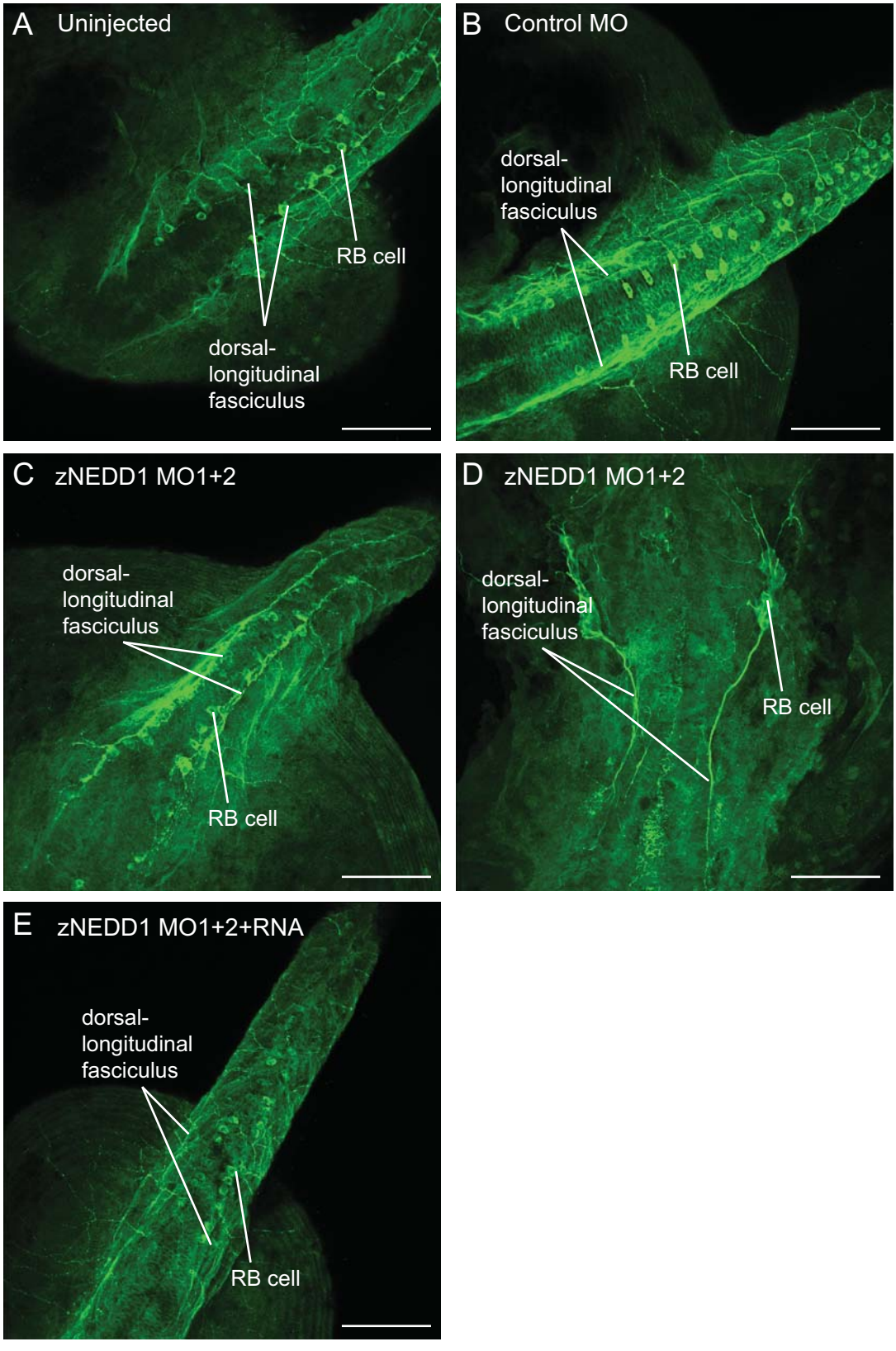
A Uninjected
RB cell
dorsal-
longitudinal
fasciculus
B Control MO
dorsal-
longitudinal
fasciculus
RB cell
C zNEDD1 MO1+2
dorsal-
longitudinal
fasciculus
RB cell
D zNEDD1 MO1+2
dorsal-
longitudinal
fasciculus
RB cell
E zNEDD1 MO1+2+RNA
dorsal-
longitudinal
fasciculus
RB cell

1990). In zNEDD1 depleted embryos, there was variability in the extent of abnormalities seen, again presumably due to the extent of zNEDD1 depletion. Embryos with mild and moderate phenotypes displayed a relatively normal morphology of the neural tube, but had greatly reduced acetylated α-tubulin staining, with a decrease in RB cells and a marked reduction in the fasciculation of their axons (Fig. 6.15C). Severely abnormal zNEDD1 morphants displayed scarce RB cells, residing in the proximal region only. No distal RB cells were observed. Axons were disorganised and displayed markedly reduced fasciculated bundling, probably due to the reduction in neurons present in these embryos (Fig.6.15D). It was also easily observed with these acetylated α-tubulin staining embryos that the neural tube was markedly abnormal, suggesting spina bifida (incomplete closure of the neural tube) was occurring. As seen for other phenotypes, co-injection with *zNEDD1* mRNA rescued the defects with no evidence of spina bifida. Thus, as well as disrupting post-mitotic HuC neurons, the depletion of zNEDD1 also causes abnormalities in the amount and patterning of RB sensory neurons, their axonal outgrowth and fasciculation, and neural tube formation.

6.14. Depletion of zNEDD1 causes a loss of γ-tubulin from the centrosome

Given that NEDD1 is a centrosomal protein, and centrosomes are important in many processes such as cell division and polarity, there could be many reasons for the abnormalities resulting from zNEDD1 depletion. In mammalian cells, the most important function of NEDD1 identified thus far has been its role in recruiting γ–tubulin to the centrosome (Haren *et al*., 2006, Luders *et al*., 2006), although this does not seem to be true in some other species (see 1.8.6). It was hypothesised that the inability of γ–tubulin to localise to the centrosome in zNEDD1 depleted embryos may contribute to the phenotypic abnormalities observed in this study. Therefore, it was next assessed whether zNEDD1 is important in the recruitment of γ–tubulin to the centrosome in zebrafish.

Due to the inability to observe centrosomes clearly in whole mount immunohistochemistry, embryos were sectioned and stained for zNEDD1 and γ–tubulin. At 24 hpf, in all cells of control injected embryos, zNEDD1 and γ–tubulin perfectly co-localised in centrosomes. This was most obvious in regions of high proliferation such as in the trunk neural tube, which is well formed at this stage and composed of polarised neurons (Kimmel, 1993). The centrosomes were intensely stained with zNEDD1 and γ–tubulin at the apical surface in these cells (Fig. 6.16A). In zNEDD1 depleted embryos, there was a dramatic reduction in the levels of expression of centrosomal zNEDD1 and γ–tubulin in the same region (shown in dotted lines, Fig. 6.16B). The organisation of the neural tube was also disturbed, as seen previously, with cells appearing to have lost some polarity, although this was not analysed further. In the brain, there are many regions of high proliferation, such as in the ventricles. Again, in control injected embryos zNEDD1 and γ–tubulin perfectly co-localised in centrosomes in polarised cells of the hindbrain (Fig. 6.16C, section through the fourth ventricle shown). This intense centrosomal expression of these proteins was again reduced in zNEDD1 depleted embryos (Fig. 6.16D), and the ventricles were less well formed. Similar observations were made in the forebrain, with zNEDD1 and γ–tubulin displaying strong centrosomal expression and perfectly co-localising in control injected embryos (Fig. 6.16E), and a marked reduction in the centrosomal expression of both proteins in zNEDD1 depleted embryos (Fig. 6.16F). Thus, similar to mammalian NEDD1, zNEDD1 appears to be required for the recruitment of γ–tubulin to centrosomes. Therefore, it was hypothesised that the centrosomal reduction of γ–tubulin in zNEDD1 depleted embryos may contribute to the observed morphological abnormalities.

6.15. Discussion

This study describes the identification and characterisation of a zebrafish homologue of NEDD1, which displays highly conserved regions of sequence and motif similarity to mammalian NEDD1 (Fig. 6.2 and 6.3). Analysis of mRNA and protein revealed that zNEDD1 is highly expressed early in embryonic stages, particularly in neural regions, and is

Fig. 6.16 zNEDD1 depletion causes a loss of γ-tubulin from centrosomes

Frozen cryosections of control or zNEDD1 MO1+2 injected embryos were stained for zNEDD1 and γ-tubulin at 24 hpf.

(**A**) In the neural tube of the trunk of control injected embryos, zNEDD1 and γ-tubulin display a high level of expression co-localising in centrosomes of polarised neural cells.

(**B**) In embryos injected with NEDD1 MO1+2, there is a reduction in both zNEDD1 and γ-tubulin centrosomal expression in cells in a similar region of the neural tube. There is also disruption of the organisation of the neural tube.

(**C**, **E**) In control injected embryos, in the fourth ventricle of the hindbrain (**C**) and in a slice through the forebrain (**E**), there is again high expression of zNEDD1 and γ-tubulin in the centrosomes of highly proliferating cells in the ventricular region.

(**D**, **F**). In zNEDD1 MO1+2 injected embryos, centrosomal zNEDD1 and γ-tubulin are both reduced in the hindbrain (**D**) and the forebrain (**F**). The structures of the ventricles are also disturbed in these embryos.

Scale bars represent 40 μm.

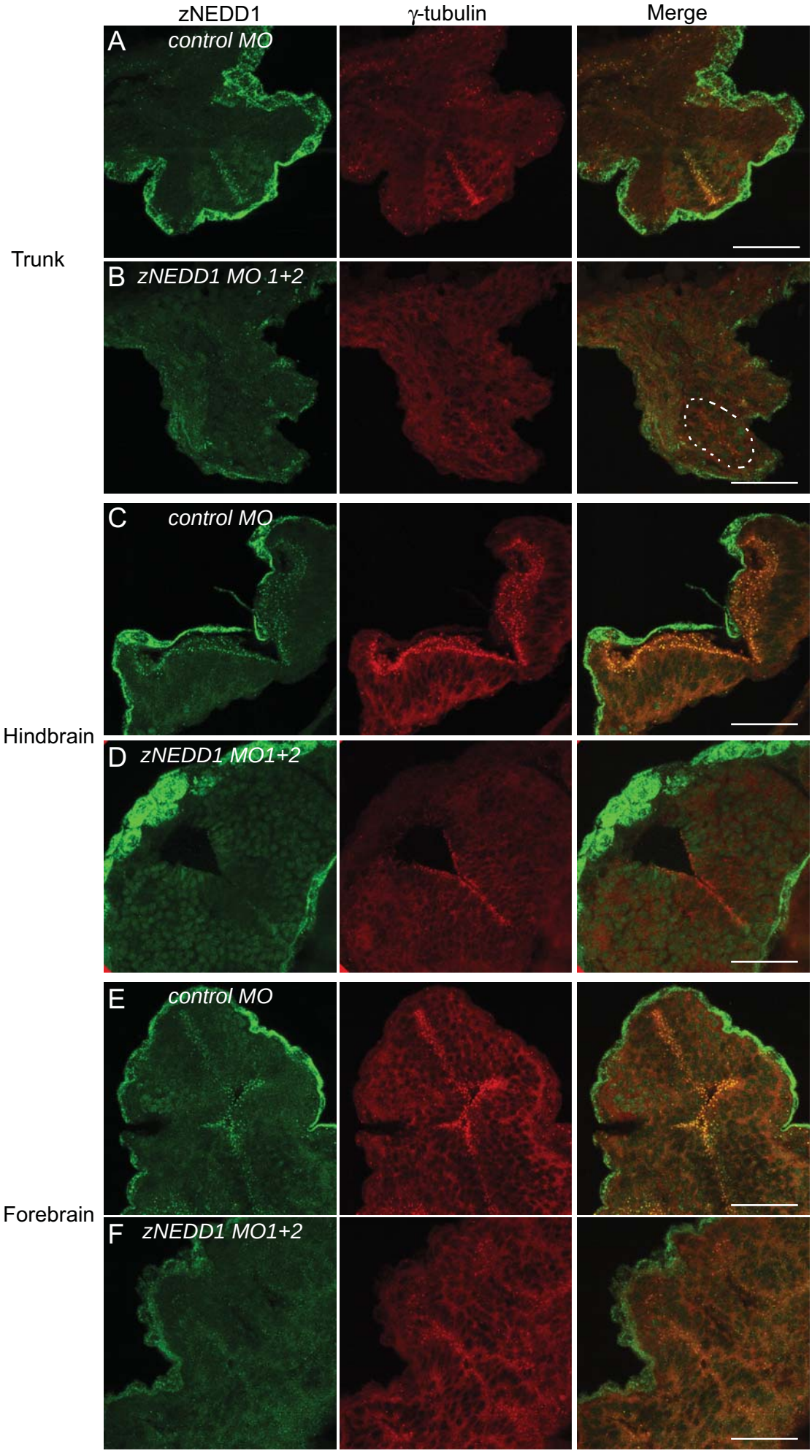
zNEDD1
γ-tubulin
Merge
A control MO
B zNEDD1 MO 1+2
C control MO
D zNEDD1 MO1+2
E control MO
F zNEDD1 MO1+2
Trunk
Hindbrain
Forebrain

then down-regulated as embryogenesis proceeds. The high expression of *zNEDD1* correlates with the time of the most rapid proliferation occurring in the embryo (Wullimann and Knipp, 2000). This aligns well with the expression of mammalian NEDD1 (chapter 3) and suggests that zNEDD1 may be important in early development, particularly in the nervous system at times of rapid proliferation (Fig. 6.4 and 6.6). Importantly, zNEDD1 appears to function in a similar manner to homologues identified in mammals (Haren *et al*., 2006, Luders *et al*., 2006), *Drosophila* (Gunawardane *et al*., 2003, Verollet *et al*., 2006) and *Xenopus* (Liu and Wiese, 2008) by localising to the centrosome and interacting with γ-tubulin (Fig. 6.7). However, unlike the dynamic expression of zNEDD1, the level of γ-tubulin remains constant during embryogenesis (Fig. 6.6), suggesting that there may be additional γ-tubulin-independent functions of zNEDD1. It is plausible that this protein is important in other cellular processes besides its established role in microtubule organisation, and further work is required to identify these possible functions of zNEDD1.

Given that a *bona fide* zebrafish homologue of NEDD1 had now been identified, the zebrafish model was utilised to analyse the role of zNEDD1 during development. As discussed in the introduction (see 1.7), this model provides many advantages for developmental studies. One of the advantages is the ability to deplete proteins of interest to varying levels using MOs. Using a zNEDD1 antibody raised in this study (Fig. 6.5), a combination of two MOs was found to reduce zNEDD1 protein expression by approximately 80% (Fig. 6.8). This dosage of MOs did not result in death of the embryos but provided morphological differences from control injected siblings. There was a small degree of variability between zNEDD1 depleted embryos, with most displaying a moderate phenotype. However, all zNEDD1 depleted embryos exhibited developmental abnormalities, in particular smaller heads and disorganised brains (Fig. 6.9). Mild and moderate phenotypes presented most prominent defects in the forebrain and the ventricular system. In severe phenotypes, all regions of the brain were affected, with no clear delineation of any of the brain structures. The eyes were also obliterated. The highest level of cell death and other abnormalities was seen in the forebrain, but the reasons for this are currently unknown and

requires further investigation. Importantly, the observed phenotypes were the result of specific zNEDD1 depletion, as co-injection of the MOs with *zNEDD1* mRNA, which restored zNEDD1 protein levels, was able to rescue the phenotypes (Fig. 6.9 and 6.10). Hence, zNEDD1 is critical for development, especially in the proper formation of the brain.

Correlating with the morphological abnormalities, it was revealed that zNEDD1 depleted embryos displayed a high level of apoptosis (Fig. 6.11). Importantly, this was occurring primarily in the brain and neural tube which are regions of high zNEDD1 expression (Fig. 6.4). Interestingly, although this apoptosis was still occurring after co-depletion of p53, which is often up-regulated after MO injection, there was a reduction in the amount of apoptotic cells in these embryos (Fig. 6.12). As many proteins induce apoptosis by stabilising or up-regulating p53, it is feasible that zNEDD1 depletion may exert some of its affects through the p53 pathway (Meulmeester and Jochemsen, 2008).

In addition to cell death, consistent with the depletion of NEDD1 in mammals resulting in an increased mitotic index (Haren *et al*., 2006, Luders *et al*., 2006), zebrafish embryos with reduced zNEDD1 had a higher incidence of pH3 mitotic staining, indicative of mitotic arrest (Fig 6.13). Given that the increase in mitotic cells and the observed apoptosis were occurring in similar regions of the embryo, it is likely that the apoptosis was a downstream consequence of the mitotic arrest. Interestingly, this phenotype resembles the zebrafish *cassiopeia* mutant, which displays an increased mitotic index and increased numbers of apoptotic cells (Pfaff *et al*., 2007). Whilst many zebrafish mutant strains and embryos with specific depletions result in these phenotypes, the *cassiopeia* mutant is of interest because it harbours a loss-of-function of the SCL-interrupting locus (SIL) gene (Aplan *et al*., 1990). This gene is normally expressed specifically in mitosis (Izraeli *et al*., 1997). Embryos depleted of SIL have extremely disorganised mitotic spindles and often lack one or both centrosomes (Pfaff *et al*., 2007). Hence, it has been hypothesised that SIL may be required for proper centrosome duplication or for microtubule organisation, as its disruption leads to centrosome dissociation from the mitotic spindle. Therefore, given that the phenotypes

observed in embryos depleted of zNEDD1 resemble those of SIL depletion, they are likely to be indeed due to its centrosomal function and importance in organising a correct mitotic spindle.

At later stages of development, the *cassiopeia* mutant zebrafish acquire additional morphological defects, including anterior neural cell death at 24 hpf, ventral or dorsal tail curvature and cardiac oedema at 36 hpf before dying 7-10 days post fertilisation (Pfaff *et al*., 2007). Although the scope of this study limited the analysis of zNEDD1 depleted embryos to 24 hpf, observations did indicate that tail curvature and oedema were occurring in some fish at later time points (data not shown). However, there were striking defects in neural organisation at 24 hpf (Fig. 6.9 and 6.14). Initially obvious was the disruption of defined ventricles and other structures in the brain, as well as disruption of the eyes in embryos with severe abnormalities, as discussed earlier. By inhibiting cell proliferation, it has been demonstrated that the amount of proliferation occurring in the midbrain and hindbrain neural tube surrounding the ventricles correlates with future ventricle size (Lowery and Sive, 2005). Hence, it is plausible that the zNEDD1 depleted cells in this study may be arresting in mitosis and then undergoing apoptosis, therefore not allowing cell proliferation and resulting in smaller brain ventricle structures.

Upon closer analysis, it was apparent that post-mitotic neurons were present in zNEDD1 depleted embryos, but they were not correctly patterned in the brain of these morphants (Fig. 6.14). In addition, a reduction of zNEDD1 caused defects in RB sensory neurons and their axonal projections (Fig. 6.15). These defects included a reduction in the amount of cells, and also in their fasciculated axonal organisation. The neural tube was also affected in severely deformed embryos, suggesting that spina bifida was occurring. Hence, zNEDD1 may also regulate the proliferation, organisation and migration of neurons, which are processes that are known to involve the centrosome (Higginbotham and Gleeson, 2007). Therefore this protein contributes to multiple aspects of CNS development, likely due to its critical role in the centrosome.

Aside from the results presented in this chapter, there have been limited studies assessing the role of the centrosome in zebrafish development. However it is apparent that depletion of the other zebrafish centrosomal proteins analysed thus far can also cause defects in the nervous system. Indeed, it has been demonstrated that depletion of the centrosomal protein CEP290 (nephrocystin-6) from zebrafish embryos results in developmental defects of the CNS such as smaller eyes, lower brain mass and defects of the cerebellum, retina and otic cavity (Sayer *et al*., 2006). Some of these regions of the nervous system were similarly affected by zNEDD1 depletion, highlighting the general importance of centrosomal proteins in CNS development. In addition, depletion of CEP290 causes retinal degeneration and kidney abnormalities such as pronephric cysts, due to its function in cilia (Chang *et al*., 2006, Sayer *et al*., 2006). Support for the importance of centrosomal proteins in ciliary function in zebrafish has come from a recent study showing that depletion of the zebrafish homologues of Cep70 and Cep131 results in embryos with a curved tail, shortened body axis and ectopic otoliths (a structure in the inner ear) also due to shortened cilia (Wilkinson *et al*., 2009). Hence Cep70 and Cep131 appear to function in zebrafish primarily as components of the cilia rather than the centrosome. The effect of zNEDD1 depletion on cilia formation and function was not investigated in the scope of this study. However, given the link of these other centrosomal proteins to ciliary function, and the localisation of zNEDD1 to the base of cilia in mouse embryos (chapter 3), it is feasible that zNEDD1 depletion also causes ciliary defects in zebrafish. Further studies are required to investigate this function for zNEDD1.

Mechanistically, it was hypothesised that the phenotypes resulting from the depletion of zNEDD1 in this study may result, at least in part, from the inhibition of its interaction with γ-tubulin. As discussed previously, mammalian NEDD1 is essential for the recruitment of γ-tubulin to the centrosome, where it nucleates microtubules and allows correct mitotic progression. Homologues in *Drosophila* and *Xenopus* are not required for this centrosomal γ-tubulin recruitment (see 1.8.6) (Gunawardane *et al*., 2003, Verollet *et al*., 2006, Liu and

Wiese, 2008). Interestingly, this study has revealed that a depletion of NEDD1 from zebrafish also causes a reduction in γ-tubulin at the centrosome (Fig. 6.16). This was consistently seen in different regions of the embryo, but was most obvious in the brain and neural tube where there is rapid proliferation at 24 hpf. Hence, zNEDD1 functions to recruit γ-tubulin to the centrosome in zebrafish, and this is presumably important for correct mitotic progression and embryonic development, especially in regions of the CNS, such as the brain.

It is surprising that zebrafish NEDD1 functions more similarly to mammalian NEDD1 than to the *Xenopus* homologue, XNEDD1. However, it is possible that this difference in recruitment of γ-tubulin is a result of varying conditions in experimental systems, such as the contribution of maternal deposits, and does not reflect a true functional difference. Support for this comes from the fact that XNEDD1 has been analysed in egg extracts, which is an *in vitro* model, and may produce results that are not replicated in *vivo* (Liu and Wiese, 2008). The recruitment of γ-tubulin to the centrosome was assessed in the ability of *Xenopus* extracts to complement salt-extracted centrosomes. The addition of wild type or XNEDD1-depleted extracts, which had 10-20% of XNEDD1 remaining, was able to restore the microtubule-nucleating activity of the centrosome, and γ-tubulin was recruited to the centrosomes normally (Liu and Wiese, 2008). However, perhaps the small amount of residual endogenous NEDD1 in the extract was sufficient for γ-tubulin recruitment. Additionally, over-expression of the C-terminal half of XNEDD1 in extracts reduced the amount of γ-tubulin at the centrosome by 50% (Liu and Wiese, 2008). Presumably, this was due to a similar effect to mammalian NEDD1, where this construct acts in a dominant-negative fashion by binding to γ-tubulin and sequestering it away from the centrosome. This suggests that XNEDD1 may also recruit γ-tubulin to the centrosome. However, it still remains possible that there are true functional differences of NEDD1 between species, and it would be interesting to characterise this further.

In summary, this chapter has identified a zebrafish homologue of NEDD1, which interacts with γ-tubulin and localises to the centrosome as in other species. The reduction of zNEDD1 in embryos was found to be embryonically lethal, or have dramatic consequences on development, depending on the extent of protein depletion. Most obvious was the disorganisation of structures in the brain, highlighted by the abnormal patterning of neurons. Importantly, zNEDD1 depletion also caused a loss of γ-tubulin from centrosomes *in vivo*, which indicates that this homologue functions similarly to mammalian NEDD1. This suggests that zNEDD1 may exert its effects through the inhibition of a functional centrosome and a lack of microtubule nucleation. Hence, NEDD1 is an essential protein required for correct embryonic development of zebrafish, particularly in the CNS.

7. General Discussion

Given its discovery in our laboratory, this research set out to characterise NEDD1, which was a protein of unknown function. Shortly after commencement of this study, a role for this protein was described in mammalian cells (Haren *et al*., 2006, Luders *et al*., 2006), and it was proposed to be the homologue of the *Drosophila melanogaster* protein Dgp71WD (Gunawardane *et al*., 2003). Consistent with initial observations in this study and analysis of the *Drosophila* homologue, NEDD1 was demonstrated to be a centrosomal protein (Gunawardane *et al*., 2003, Verollet *et al*., 2006, Manning and Kumar, 2007).

Centrosomes are important for development (Nigg, 2004), however their precise functions in embryogenesis have not been well investigated. Therefore, part of this study aimed to explore the expression and localisation of Nedd1 and the centrosome during mouse embryogenesis. Functionally, NEDD1 in mammalian cells has been shown to be required for the centrosomal and mitotic spindle recruitment of γ-tubulin, the resulting microtubule nucleation, and therefore the correct progression of a cell through mitosis (Haren *et al*., 2006, Luders *et al*., 2006). Consequently, this study also aimed to investigate the regulation of this protein, and how this contributes to cell cycle progression. Additionally, the interaction of NEDD1 with γ-tubulin was assessed in more detail, and other interacting partners of NEDD1 identified. Finally, to gain an understanding of the importance of this protein in an animal model, zebrafish were employed to investigate the effects of NEDD1 depletion on embryonic development. During the course of this study, NEDD1 homologues were also identified in other species (*Xenopus* and *Arabidopsis*), and were consistently shown to be critical for correct mitotic progression (Liu and Wiese, 2008, Zeng *et al*., 2009). However, the role of this protein in the centrosomal recruitment of γ-tubulin is inconsistent, as unlike mammalian NEDD1, *Drosophila* and *Xenopus* NEDD1 are mostly dispensable for targeting γ-tubulin to the centrosome (Verollet *et al*., 2006, Liu and Wiese, 2008). Hence, the zebrafish model of NEDD1 depletion was also utilised to asses the functional conservation of this protein, by determining whether NEDD1 is important for the centrosomal recruitment of γ-tubulin in this species.

Chapter 3 presents a characterisation of the expression and localisation of Nedd1, as a marker for the centrosome, during mouse embryonic development (Manning *et al*., 2008). Given that Nedd1 was initially discovered as being highly expressed in neural precursor cells of the mouse embryo (Kumar *et al*., 1992), the nervous system was chosen as the focus for this analysis. The results presented in this study demonstrate that in the brain and the eye, Nedd1 displays strong centrosomal expression in highly proliferating cells at E11.5. Interestingly, Nedd1 is also highly expressed in the cytoplasm of dorsal root ganglia neurons. This cytoplasmic expression is not seen for γ-tubulin, and hence a γ-tubulin-independent function for Nedd1 that it not based at the centrosome may exist in these cells. This is supported by the identification of NEDD1 in complexes lacking γ-tubulin in both mammalian cells and *Xenopus* extracts (Luders *et al*., 2006, Liu and Wiese, 2008). By E14.5, Nedd1 expression in the eye remains similar, but in the brain, where these cells decrease their proliferation rate (Kaufman, 1992), the expression of Nedd1 is reduced. Hence, Nedd1 has highest expression in the nervous system during early embryogenesis when there is the greatest need for rapid proliferation, and is down-regulated as development proceeds. Additionally, it was observed that Nedd1 displays a polarised expression in cells of the eye, as is known to be the case for centrosomes in many cell types (Tucker *et al*., 1992, Chenn *et al*., 1998, Srsen and Merdes, 2006). Indeed, Nedd1 has an apical distribution in all polarised tissues analysed thus far. The precise localisation of this protein, and therefore the centrosome, in polarised cells of the mouse embryo was mapped and provides a basis for further studies into the role of the centrosome in polarisation.

Given that Nedd1 is important in proliferation, and is essential for cell cycle progression, its regulation is of critical importance to the cell. Results presented in chapter 4 contribute to the knowledge of the regulation of NEDD1, by indicating that phosphorylation is the primary method of controlling NEDD1 protein levels during the cell cycle. A recent study into the phosphorylation of NEDD1 supports this observation, by revealing multiple phosphorylation sites that are important in the function of this protein (Zhang *et al*., 2009). However, the

interaction of NEDD1 with other proteins has also been implicated in its regulation, primarily by controlling the localisation of this protein (Zhu *et al*., 2008a, Zhu *et al*., 2008b). In addition, NEDD1 has been linked to proteasomal degradation (Didier *et al*., 2008). Hence the regulation of this protein is likely to be complex and it seems inevitable that further regulators of NEDD1 will be revealed in future studies.

This study has also demonstrated that Nedd1 is down-regulated in senescent MEFs, and this correlates with a loss of centrosomal integrity, although the mechanism for this remains unknown (chapter 4). In these senescent cells, centrosomes appear fragmented and often dispersed throughout the cell suggesting that they have lost their organisation and nuclear attachment. Centrosome disruption has been shown to cause senescence in other models (Srsen *et al*., 2006, Srsen and Merdes, 2006), but had not previously been investigated in MEFs that senesce as a consequence of oxidative stress after passaging in culture (Parrinello *et al*., 2003). Similarly, centrosome fragmentation has been observed in other studies, but not in MEFs (Date *et al*., 2006, Lawo *et al*., 2009). The implications of the findings in this chapter are broad, as MEFs are often used in many different types of studies. A detailed understanding of the events that occur during the culture of these cells is critical when making assumptions and interpreting results. Interestingly, the reduction of Nedd1 in senescent cells is not typical of all centrosomal proteins, as the levels of γ-tubulin remain unchanged. This explains why this observation may have escaped attention prior to this study, and suggests that Nedd1 may be specifically involved in the process of senescence. Indeed, the targeted reduction of Nedd1 in healthy MEFs was shown to cause the cells to enter premature senescence and display a similar loss of centrosomal integrity. Hence, this study has revealed an important function of Nedd1 in protecting cells from entering premature senescence, and provides further evidence for the important role that this protein plays in the cell cycle.

The function of NEDD1 in recruiting γ-tubulin to the centrosome and allowing correct mitotic progression (Haren *et al*., 2006, Luders *et al*., 2006), is thought to be the primary role of this

protein, and as such, it requires further characterisation. Therefore chapter 5 has described the interaction of NEDD1 and γ-tubulin in detail, showing that it is direct, and requires only the 62 amino acids at the C-terminus of NEDD1 (599-660 aa). It was predicted that the identification of this small region sufficient for binding may reveal additional γ-tubulin binding partners upon a BLAST search for proteins containing similar sequences. However, no significant matches of this region have been found in other proteins thus far.

Functionally, it was identified that the minimal region of NEDD1 found to bind γ-tubulin does not localise to the centrosome and can act as a dominant-negative form of NEDD1 by sequestering γ-tubulin away from the centrosome. This provides further support for the importance of the NEDD1/γ-tubulin interaction in controlling the localisation of γ-tubulin. Upon closer analysis of this sequence, it was found to reside in a region of helical structure of NEDD1. Indeed, it appears that the helical structure is important for this interaction, as mutating a single amino acid within this helix, from a hydrophobic leucine residue to a hydrophilic bulky glutamine residue (L642Q), abrogates the binding of this region of NEDD1 to γ-tubulin. As expected, this mutation also partially reverses the dominant-negative effect of expression of this region, by no longer sequestering γ-tubulin away from the centrosome. The mutation of two more residues within this region causes even more dramatic effects, with γ-tubulin levels virtually restored to normal at the centrosome. This indicates that this mutant can no longer bind to γ-tubulin and affect its localisation. Technically, it was not possible to determine the effect of these mutations in full length NEDD1, due to the complications of residual endogenous NEDD1 after siRNA depletion. However, future studies will be pursued to further characterise the precise requirements for the NEDD1/γ-tubulin interaction.

Thus far, two NEDD1 interactors FAM29A and Plk1, and several other centrosomal proteins, have been identified that contribute to the centrosomal or spindle localisation of NEDD1 and γ-tubulin (schematic in Fig. 1.6) (Fong *et al*., 2008, Zhu *et al*., 2008a, Zhu *et al*.,

2008b, Zhang *et al*., 2009). Given that a pool of NEDD1 exists independently of γ-tubulin (Luders *et al*., 2006), and displays a different cytoplasmic localisation in mouse embryonic development (chapter 3), identifying other binding partners of NEDD1 may provide more information about its function and regulation (Luders *et al*., 2006, Liu and Wiese, 2008). Hence, this study also attempted to identify additional NEDD1-interacting proteins. Two proteins were confirmed as interacting with NEDD1, the chaperones HSP70 and TCP-1α. Unfortunately, no proteins were identified that suggest an alternative function of NEDD1, and this may require a more sensitive screen and the use of different cell types. Since TCP-1α has previously been identified as a chaperone for γ-tubulin and has been associated with centrosomes and microtubule organisation (Melki *et al*., 1993, Brown *et al*., 1996), its interaction with NEDD1 was assessed further. Importantly, the depletion of TCP-1α leads to a loss of the phosphorylated form of NEDD1, but does not alter unphosphorylated protein levels. The mechanism for this remains unclear. However, TCP-1α is required for the mitotic function of other proteins, such as the kinase Plk1, which phosphorylates NEDD1 and is important for its centrosomal localisation (Zhang *et al*., 2009). Hence, the effect of TCP-1α depletion on NEDD1 may be indirect and mediated through a reduction of active Plk1. Alternatively, a loss of TCP-1α may directly inhibit the mitotically active phosphorylated form of NEDD1 due to the mis-folding of this protein. Given that the phosphorylated form of NEDD1 has been shown to be critical in the recruitment of γ-tubulin to the spindle and therefore for correct spindle formation (Luders *et al*., 2006, Zhang *et al*., 2009), the interaction and regulation of this protein by TCP-1α is of critical importance to the cell and merits further study.

Due to a lack of *in vivo* studies, the functional significance of NEDD1 during development was not well characterised prior to this study. It was expected that complete depletion of NEDD1 from embryos would result in early lethality, as observed for γ-tubulin knockout mice (Yuba-Kubo *et al*., 2005), whereas partial depletion may result in phenotypic abnormalities. In *Drosophila*, homozygous NEDD1 (Dgp71WD) mutants are viable but have a shorter life

span and the females are sterile (Verollet *et al*., 2006). It is interesting that these flies are viable, but perhaps maternal contribution allows for the development of embryos, as has been shown for mutants in other centrosomal genes such as *DSas-4* (Basto *et al*., 2006, Stevens *et al*., 2007). The development consequences of NEDD1 depletion were not analysed in detail in the *Drosophila* study. Aside from mammals and *Drosophila*, additional homologues of NEDD1 have now been characterised in *Xenopus* and *Arabidopsis*, and chapter 6 has extended this by presenting the characterisation of a zebrafish homologue of NEDD1 (zNEDD1) and assessing its role in development. Indeed, zNEDD1 behaves similarly to mammalian NEDD1 by localising to the centrosome and interacting with γ-tubulin through the equivalent region at the C-terminus of the protein. This is not surprising given the high degree of sequence similarity in this region.

Developmentally, zNEDD1 is expressed ubiquitously during early embryogenesis, although the levels appear highest in the nervous system. Unlike γ-tubulin expression, which remains constant during development (Liu and Lessman, 2008), zNEDD1 is down-regulated from the 18 somite stage of zebrafish embryogenesis. This suggests that zNEDD1 plays important functions in early embryogenesis, perhaps beyond its role in γ-tubulin-dependent processes. Indeed, the importance of zNEDD1 during early development is confirmed by the depletion of zNEDD1 with high doses of MOs, which is lethal to embryos. Importantly, lower doses of MOs, which are still able to significantly reduce zNEDD1 expression, cause cellular abnormalities including apoptosis and mitotic arrest, as has been shown for other proteins involved in cell proliferation (Pfaff *et al*., 2007). Morphologically, the most obvious defects are in the CNS, correlating with the regions of highest expression of zNEDD1. These defects manifest as poorly defined brain structures and ventricles, as well as the obliteration of eyes in some cases. The forebrain is the most severely affected structure, however the reason for this is unknown. In addition, neuronal patterning is disorganised, including in both post-mitotic neurons and RB sensory neurons and their axons. These results indicate that a reduction of zNEDD1 can cause defects other than cell cycle arrest, and suggest that as initially suspected NEDD1 might play a role in different aspects of

nervous system development (Manning and Kumar, 2007). This is consistent with reports of the function of the centrosome in other cellular processes, such as neural differentiation and migration (Badano *et al*., 2005, Higginbotham and Gleeson, 2007). It would be interesting to analyse the effect of zNEDD1 depletion on neural differentiation and migration more thoroughly. Additionally, further work would be required to determine the consequences of the reduction in zNEDD1 on other aspects of embryogenesis, such as the formation of cilia, which have previously been shown to require functional centrosomal proteins (Sayer *et al*., 2006, Wilkinson *et al*., 2009).

Given the interaction of zNEDD1 and γ-tubulin, it was predicted that the cellular and morphological abnormalities in embryos depleted of zNEDD1 may result from the inability of γ-tubulin to localise and function normally. Indeed, this study demonstrated that a reduction of zNEDD1 also causes a reduction in γ-tubulin at the centrosome. This observation is similar to the reported function of NEDD1 in mammalian cells, but contrasts to *Drosophila* and *Xenopus* homologues, where a reduction of NEDD1 does not result in a significant loss of γ-tubulin at the centrosome. There are multiple possibilities as to why these NEDD1 homologues function slightly differently (discussed in 6.15), but could be either due to variations in experimental design and interpretation, or due to *bona fide* functional differences in species. Either way, it is likely that the reduction in centrosomal γ-tubulin contributes to the phenotypes caused by zNEDD1 depletion in zebrafish development.

In conclusion, this study has contributed to the knowledge that NEDD1 is an important protein, in all species analysed thus far. This thesis has characterised NEDD1 in mouse embryonic development, MEF senescence, its interaction with γ-tubulin and other proteins, and its importance in zebrafish development. A number of interesting properties of this protein have been revealed, and many more questions have been raised. Perhaps one of the more significant is whether a γ-tubulin-independent function of NEDD1 exists, and if so, what this function might be? Since it was first identified as a centrosomal protein, the increasing numbers of publications that involve NEDD1 give credence to the intense appeal

of this protein by groups focused on cell and molecular biology. It will be of great interest to see what developments pertain to this protein in the future.

Bibliography

Aaku-Saraste, E., Hellwig, A. & Huttner, W. B. (1996). Loss of occludin and functional tight junctions, but not ZO-1, during neural tube closure--remodeling of the neuroepithelium prior to neurogenesis. *Dev Biol, 180*, 664-679.

Afonso, P. V., Zamborlini, A., Saib, A. & Mahieux, R. (2007). Centrosome and retroviruses: the dangerous liaisons. *Retrovirology, 4*, 27.

Agueli, C., Geraci, F., Giudice, G., Chimenti, L., Cascino, D. & Sconzo, G. (2001). A constitutive 70 kDa heat-shock protein is localized on the fibres of spindles and asters at metaphase in an ATP-dependent manner: a new chaperone role is proposed. *Biochem J, 360*, 413-419.

Akitaya, T. & Bronner-Fraser, M. (1992). Expression of cell adhesion molecules during initiation and cessation of neural crest cell migration. *Dev Dyn, 194*, 12-20.

Andersen, J. S., Wilkinson, C. J., Mayor, T., Mortensen, P., Nigg, E. A. & Mann, M. (2003). Proteomic characterization of the human centrosome by protein correlation profiling. *Nature, 426*, 570-574.

Ansley, S. J., Badano, J. L., Blacque, O. E., Hill, J., Hoskins, B. E., Leitch, C. C., Kim, J. C., Ross, A. J., Eichers, E. R., Teslovich, T. M., Mah, A. K., Johnsen, R. C., Cavender, J. C., Lewis, R. A., Leroux, M. R., Beales, P. L. & Katsanis, N. (2003). Basal body dysfunction is a likely cause of pleiotropic Bardet-Biedl syndrome. *Nature, 425*, 628-633.

Aplan, P. D., Lombardi, D. P., Ginsberg, A. M., Cossman, J., Bertness, V. L. & Kirsch, I. R. (1990). Disruption of the human SCL locus by "illegitimate" V-(D)-J recombinase activity. *Science, 250*, 1426-1429.

Atadja, P., Wong, H., Garkavtsev, I., Veillette, C. & Riabowol, K. (1995). Increased activity of p53 in senescing fibroblasts. *Proc Natl Acad Sci U S A, 92*, 8348-8352.

Badano, J. L. & Katsanis, N. (2006). Life without centrioles: cilia in the spotlight. *Cell, 125*, 1228-1230.

Badano, J. L., Teslovich, T. M. & Katsanis, N. (2005). The centrosome in human genetic disease. *Nat Rev Genet, 6*, 194-205.

Barr, F. A., Sillje, H. H. & Nigg, E. A. (2004). Polo-like kinases and the orchestration of cell division. *Nat Rev Mol Cell Biol, 5*, 429-440.

Basto, R., Brunk, K., Vinadogrova, T., Peel, N., Franz, A., Khodjakov, A. & Raff, J. W. (2008). Centrosome amplification can initiate tumorigenesis in flies. *Cell, 133*, 1032-1042.

Basto, R., Lau, J., Vinogradova, T., Gardiol, A., Woods, C. G., Khodjakov, A. & Raff, J. W. (2006). Flies without centrioles. *Cell, 125*, 1375-1386.

Bayer, S. A. & Altman, J. (1991). *Neocortical development,* (Editor ed.). New York, N.Y.: Raven Press.

Bellion, A., Baudoin, J. P., Alvarez, C., Bornens, M. & Metin, C. (2005). Nucleokinesis in tangentially migrating neurons comprises two alternating phases: forward migration of the Golgi/centrosome associated with centrosome splitting and myosin contraction at the rear. *J Neurosci, 25*, 5691-5699.

Ben-Porath, I. & Weinberg, R. A. (2005). The signals and pathways activating cellular senescence. *Int J Biochem Cell Biol, 37*, 961-976.

Bermingham-McDonogh, O., Oesterle, E. C., Stone, J. S., Hume, C. R., Huynh, H. M. & Hayashi, T. (2006). Expression of Prox1 during mouse cochlear development. *J Comp Neurol, 496*, 172-186.

Bernhardt, R. R., Chitnis, A. B., Lindamer, L. & Kuwada, J. Y. (1990). Identification of spinal neurons in the embryonic and larval zebrafish. *J Comp Neurol, 302*, 603-616.

Bertrand, P., Lambert, S., Joubert, C. & Lopez, B. S. (2003). Overexpression of mammalian Rad51 does not stimulate tumorigenesis while a dominant-negative Rad51 affects centrosome fragmentation, ploidy and stimulates tumorigenesis, in p53-defective CHO cells. *Oncogene, 22*, 7587-7592.

Bobinnec, Y., Moudjou, M., Fouquet, J. P., Desbruyeres, E., Edde, B. & Bornens, M. (1998). Glutamylation of centriole and cytoplasmic tubulin in proliferating non-neuronal cells. *Cell Motil Cytoskeleton, 39*, 223-232.

Boveri, T. (1901). Uber die Natur der Centrosomen. *Jena. Z. Med. Naturw, 28*, 1-220.

Brazel, C. Y., Romanko, M. J., Rothstein, R. P. & Levison, S. W. (2003). Roles of the mammalian subventricular zone in brain development. *Prog Neurobiol, 69*, 49-69.

Brown, C. R., Doxsey, S. J., Hong-Brown, L. Q., Martin, R. L. & Welch, W. J. (1996). Molecular chaperones and the centrosome. A role for TCP-1 in microtubule nucleation. *J Biol Chem, 271*, 824-832.

Bunz, F., Fauth, C., Speicher, M. R., Dutriaux, A., Sedivy, J. M., Kinzler, K. W., Vogelstein, B. & Lengauer, C. (2002). Targeted inactivation of p53 in human cells does not result in aneuploidy. *Cancer Res, 62*, 1129-1133.

Camasses, A., Bogdanova, A., Shevchenko, A. & Zachariae, W. (2003). The CCT chaperonin promotes activation of the anaphase-promoting complex through the generation of functional Cdc20. *Mol Cell, 12*, 87-100.

Cambray-Deakin, M. A. & Burgoyne, R. D. (1987). Posttranslational modifications of alpha-tubulin: acetylated and detyrosinated forms in axons of rat cerebellum. *J Cell Biol, 104*, 1569-1574.

Campisi, J. (2001). Cellular senescence as a tumor-suppressor mechanism. *Trends Cell Biol, 11*, S27-31.

Cepko, C. L., Austin, C. P., Yang, X., Alexiades, M. & Ezzeddine, D. (1996). Cell fate determination in the vertebrate retina. *Proc Natl Acad Sci U S A, 93*, 589-595.

Chae, S., Yun, C., Um, H., Lee, J. H. & Cho, H. (2005). Centrosome amplification and multinuclear phenotypes are Induced by hydrogen peroxide. *Exp Mol Med, 37*, 482-487.

Chan, J., Calder, G. M., Doonan, J. H. & Lloyd, C. W. (2003). EB1 reveals mobile microtubule nucleation sites in Arabidopsis. *Nat Cell Biol, 5*, 967-971.

Chang, B., Khanna, H., Hawes, N., Jimeno, D., He, S., Lillo, C., Parapuram, S. K., Cheng, H., Scott, A., Hurd, R. E., Sayer, J. A., Otto, E. A., Attanasio, M., O'Toole, J. F., Jin, G., Shou, C., Hildebrandt, F., Williams, D. S., Heckenlively, J. R. & Swaroop, A. (2006). In-frame deletion in a novel centrosomal/ciliary protein CEP290/NPHP6 perturbs its interaction with RPGR and results in early-onset retinal degeneration in the rd16 mouse. *Hum Mol Genet, 15*, 1847-1857.

Chawla, G., Lin, C. H., Han, A., Shiue, L., Ares, M., Jr. & Black, D. L. (2009). Sam68 regulates a set of alternatively spliced exons during neurogenesis. *Mol Cell Biol, 29*, 201-213.

Cheng, X., Den, Z. & Koch, P. J. (2005). Desmosomal cell adhesion in mammalian development. *Eur J Cell Biol, 84*, 215-223.

Chenn, A., Zhang, Y. A., Chang, B. T. & McConnell, S. K. (1998). Intrinsic polarity of mammalian neuroepithelial cells. *Mol Cell Neurosci, 11*, 183-193.

Chow, R. L. & Lang, R. A. (2001). Early eye development in vertebrates. *Annu Rev Cell Dev Biol, 17*, 255-296.

D'Assoro, A. B., Lingle, W. L. & Salisbury, J. L. (2002). Centrosome amplification and the development of cancer. *Oncogene, 21*, 6146-6153.

Dahm, R., Schonthaler, H. B., Soehn, A. S., van Marle, J. & Vrensen, G. F. (2007). Development and adult morphology of the eye lens in the zebrafish. *Exp Eye Res, 85*, 74-89.

Date, O., Katsura, M., Ishida, M., Yoshihara, T., Kinomura, A., Sueda, T. & Miyagawa, K. (2006). Haploinsufficiency of RAD51B causes centrosome fragmentation and aneuploidy in human cells. *Cancer Res, 66*, 6018-6024.

Dawe, H. R., Farr, H. & Gull, K. (2007). Centriole/basal body morphogenesis and migration during ciliogenesis in animal cells. *J Cell Sci, 120*, 7-15.

de Anda, F. C., Pollarolo, G., Da Silva, J. S., Camoletto, P. G., Feiguin, F. & Dotti, C. G. (2005). Centrosome localization determines neuronal polarity. *Nature, 436*, 704-708.

De Boer, L., Oakes, V., Beamish, H., Giles, N., Stevens, F., Somodevilla-Torres, M., Desouza, C. & Gabrielli, B. (2008). Cyclin A/cdk2 coordinates centrosomal and nuclear mitotic events. *Oncogene, 27*, 4261-4268.

de Carcer, G., do Carmo Avides, M., Lallena, M. J., Glover, D. M. & Gonzalez, C. (2001). Requirement of Hsp90 for centrosomal function reflects its regulation of Polo kinase stability. *EMBO J, 20*, 2878-2884.

Didier, C., Merdes, A., Gairin, J. E. & Jabrane-Ferrat, N. (2008). Inhibition of proteasome activity impairs centrosome-dependent microtubule nucleation and organization. *Mol Biol Cell, 19*, 1220-1229.

Dimri, G. P., Lee, X., Basile, G., Acosta, M., Scott, G., Roskelley, C., Medrano, E. E., Linskens, M., Rubelj, I., Pereira-Smith, O. & *et al*. (1995). A biomarker that identifies senescent human cells in culture and in aging skin in vivo. *Proc Natl Acad Sci U S A, 92*, 9363-9367.

Donaldson, M. M., Tavares, A. A., Hagan, I. M., Nigg, E. A. & Glover, D. M. (2001). The mitotic roles of Polo-like kinase. *J Cell Sci, 114*, 2357-2358.

Donovan, S. L. & Dyer, M. A. (2005). Regulation of proliferation during central nervous system development. *Semin Cell Dev Biol, 16*, 407-421.

Doxsey, S. (2001). Re-evaluating centrosome function. *Nat Rev Mol Cell Biol, 2*, 688-698.

Doxsey, S., Zimmerman, W. & Mikule, K. (2005). Centrosome control of the cell cycle. *Trends Cell Biol, 15*, 303-311.

Duffy, K. T., McAleer, M. F., Davidson, W. R., Kari, L., Kari, C., Liu, C. G., Farber, S. A., Cheng, K. C., Mest, J. R., Wickstrom, E., Dicker, A. P. & Rodeck, U. (2005). Coordinate control of cell cycle regulatory genes in zebrafish development tested by cyclin D1 knockdown with morpholino phosphorodiamidates and hydroxyprolyl-phosphono peptide nucleic acids. *Nucleic Acids Res, 33*, 4914-4921.

Easton, D. P., Kaneko, Y. & Subjeck, J. R. (2000). The hsp110 and Grp1 70 stress proteins: newly recognized relatives of the Hsp70s. *Cell Stress Chaperones, 5*, 276-290.

Fabbro, M., Zhou, B. B., Takahashi, M., Sarcevic, B., Lal, P., Graham, M. E., Gabrielli, B. G., Robinson, P. J., Nigg, E. A., Ono, Y. & Khanna, K. K. (2005). Cdk1/Erk2- and Plk1-dependent phosphorylation of a centrosome protein, Cep55, is required for its recruitment to midbody and cytokinesis. *Dev Cell, 9*, 477-488.

Faulkner, N. E., Dujardin, D. L., Tai, C. Y., Vaughan, K. T., O'Connell, C. B., Wang, Y. & Vallee, R. B. (2000). A role for the lissencephaly gene LIS1 in mitosis and cytoplasmic dynein function. *Nat Cell Biol, 2*, 784-791.

Feng, Y., Olson, E. C., Stukenberg, P. T., Flanagan, L. A., Kirschner, M. W. & Walsh, C. A. (2000). LIS1 regulates CNS lamination by interacting with mNudE, a central component of the centrosome. *Neuron, 28*, 665-679.

Fong, K. W., Choi, Y. K., Rattner, J. B. & Qi, R. Z. (2008). CDK5RAP2 is a pericentriolar protein that functions in centrosomal attachment of the gamma-tubulin ring complex. *Mol Biol Cell, 19*, 115-125.

Foster, F. S., Zhang, M., Duckett, A. S., Cucevic, V. & Pavlin, C. J. (2003). In vivo imaging of embryonic development in the mouse eye by ultrasound biomicroscopy. *Invest Ophthalmol Vis Sci, 44*, 2361-2366.

Fukasawa, K. (2005). Centrosome amplification, chromosome instability and cancer development. *Cancer Lett, 230*, 6-19.

Fukasawa, K. (2007). Oncogenes and tumour suppressors take on centrosomes. *Nat Rev Cancer, 7*, 911-924.

Fukasawa, K., Choi, T., Kuriyama, R., Rulong, S. & Vande Woude, G. F. (1996). Abnormal centrosome amplification in the absence of p53. *Science, 271*, 1744-1747.

Fuller, S. D., Gowen, B. E., Reinsch, S., Sawyer, A., Buendia, B., Wepf, R. & Karsenti, E. (1995). The core of the mammalian centriole contains gamma-tubulin. *Curr Biol, 5*, 1384-1393.

Garcia-Alvarez, B., de Carcer, G., Ibanez, S., Bragado-Nilsson, E. & Montoya, G. (2007). Molecular and structural basis of polo-like kinase 1 substrate recognition: Implications in centrosomal localization. *Proc Natl Acad Sci U S A, 104*, 3107-3112.

Gebauer, M., Melki, R. & Gehring, U. (1998). The chaperone cofactor Hop/p60 interacts with the cytosolic chaperonin-containing TCP-1 and affects its nucleotide exchange and protein folding activities. *J Biol Chem, 273*, 29475-29480.

Geldmacher-Voss, B., Reugels, A. M., Pauls, S. & Campos-Ortega, J. A. (2003). A 90-degree rotation of the mitotic spindle changes the orientation of mitoses of zebrafish neuroepithelial cells. *Development, 130*, 3767-3780.

Gergely, F. & Basto, R. (2008). Multiple centrosomes: together they stand, divided they fall. *Genes Dev, 22*, 2291-2296.

Gilbert, S. F. (2000). Paradigm shifts in neural induction. *Rev Hist Sci Paris, 53*, 555-579.

Gingras, A. C., Gstaiger, M., Raught, B. & Aebersold, R. (2007). Analysis of protein complexes using mass spectrometry. *Nat Rev Mol Cell Biol, 8*, 645-654.

Goldstein, S. (1990). Replicative senescence: the human fibroblast comes of age. *Science, 249*, 1129-1133.

Goloubinoff, P. & De Los Rios, P. (2007). The mechanism of Hsp70 chaperones: (entropic) pulling the models together. *Trends Biochem Sci, 32*, 372-380.

Gomez-Ferreria, M. A., Rath, U., Buster, D. W., Chanda, S. K., Caldwell, J. S., Rines, D. R. & Sharp, D. J. (2007). Human Cep192 is required for mitotic centrosome and spindle assembly. *Curr Biol, 17*, 1960-1966.

Gordon, C. (2002). The intracellular localization of the proteasome. *Curr Top Microbiol Immunol, 268*, 175-184.

Green, K. J. & Jones, J. C. (1996). Desmosomes and hemidesmosomes: structure and function of molecular components. *FASEB J, 10*, 871-881.

Gregory, W. A., Edmondson, J. C., Hatten, M. E. & Mason, C. A. (1988). Cytology and neuron-glial apposition of migrating cerebellar granule cells in vitro. *J Neurosci, 8*, 1728-1738.

Gromley, A., Jurczyk, A., Sillibourne, J., Halilovic, E., Mogensen, M., Groisman, I., Blomberg, M. & Doxsey, S. (2003). A novel human protein of the maternal centriole is required for the final stages of cytokinesis and entry into S phase. *J Cell Biol, 161*, 535-545.

Gunawardane, R. N., Martin, O. C. & Zheng, Y. (2003). Characterization of a new gammaTuRC subunit with WD repeats. *Mol Biol Cell, 14*, 1017-1026.

Guo, J., Yang, Z., Song, W., Chen, Q., Wang, F., Zhang, Q. & Zhu, X. (2006). Nudel contributes to microtubule anchoring at the mother centriole and is involved in both dynein-dependent and -independent centrosomal protein assembly. *Mol Biol Cell, 17*, 680-689.

Haren, L., Remy, M. H., Bazin, I., Callebaut, I., Wright, M. & Merdes, A. (2006). NEDD1-dependent recruitment of the gamma-tubulin ring complex to the centrosome is necessary for centriole duplication and spindle assembly. *J Cell Biol, 172*, 505-515.

Haren, L., Stearns, T. & Luders, J. (2009). Plk1-dependent recruitment of gamma-tubulin complexes to mitotic centrosomes involves multiple PCM components. *PLoS One, 4*, e5976.

Harley, C. B., Futcher, A. B. & Greider, C. W. (1990). Telomeres shorten during ageing of human fibroblasts. *Nature, 345*, 458-460.

Hartman, T. R., Liu, D., Zilfou, J. T., Robb, V., Morrison, T., Watnick, T. & Henske, E. P. (2009). The tuberous sclerosis proteins regulate formation of the primary cilium via a rapamycin-insensitive and polycystin 1-independent pathway. *Hum Mol Genet, 18*, 151-163.

Hatten, M. E. (2002). New directions in neuronal migration. *Science, 297*, 1660-1663.

Hayflick, L. & Moorhead, P. S. (1961). The serial cultivation of human diploid cell strains. *Exp Cell Res, 25*, 585-621.

Hendzel, M. J., Wei, Y., Mancini, M. A., Van Hooser, A., Ranalli, T., Brinkley, B. R., Bazett-Jones, D. P. & Allis, C. D. (1997). Mitosis-specific phosphorylation of histone H3 initiates primarily within pericentromeric heterochromatin during G2 and spreads in an ordered fashion coincident with mitotic chromosome condensation. *Chromosoma, 106*, 348-360.

Higginbotham, H. R. & Gleeson, J. G. (2007). The centrosome in neuronal development. *Trends Neurosci, 30*, 276-283.

Hinchcliffe, E. H., Miller, F. J., Cham, M., Khodjakov, A. & Sluder, G. (2001). Requirement of a centrosomal activity for cell cycle progression through G1 into S phase. *Science, 291*, 1547-1550.

Hirota, T., Kunitoku, N., Sasayama, T., Marumoto, T., Zhang, D., Nitta, M., Hatakeyama, K. & Saya, H. (2003). Aurora-A and an interacting activator, the LIM protein Ajuba, are required for mitotic commitment in human cells. *Cell, 114*, 585-598.

Hirotsune, S., Fleck, M. W., Gambello, M. J., Bix, G. J., Chen, A., Clark, G. D., Ledbetter, D. H., McBain, C. J. & Wynshaw-Boris, A. (1998). Graded reduction of Pafah1b1 (Lis1) activity results in neuronal migration defects and early embryonic lethality. *Nat Genet, 19*, 333-339.

Ho, L. H., Taylor, R., Dorstyn, L., Cakouros, D., Bouillet, P. & Kumar, S. (2009). A tumor suppressor function for caspase-2. *Proc Natl Acad Sci U S A, 106*, 5336-5341.

Hoffmann, I. (2004). Playing polo in G1: a novel function of polo-like kinase-2 in centriole duplication. *Cell Cycle, 3*, 1230-1231.

Horst, C. J., Johnson, L. V. & Besharse, J. C. (1990). Transmembrane assemblage of the photoreceptor connecting cilium and motile cilium transition zone contain a common immunologic epitope. *Cell Motil Cytoskeleton, 17*, 329-344.

Hudson, J. W., Kozarova, A., Cheung, P., Macmillan, J. C., Swallow, C. J., Cross, J. C. & Dennis, J. W. (2001). Late mitotic failure in mice lacking Sak, a polo-like kinase. *Curr Biol, 11*, 441-446.

Izraeli, S., Colaizzo-Anas, T., Bertness, V. L., Mani, K., Aplan, P. D. & Kirsch, I. R. (1997). Expression of the SIL gene is correlated with growth induction and cellular proliferation. *Cell Growth Differ, 8*, 1171-1179.

Jackman, M., Lindon, C., Nigg, E. A. & Pines, J. (2003). Active cyclin B1-Cdk1 first appears on centrosomes in prophase. *Nat Cell Biol, 5*, 143-148.

Jung, S. Y., Malovannaya, A., Wei, J., O'Malley, B. W. & Qin, J. (2005). Proteomic analysis of steady-state nuclear hormone receptor coactivator complexes. *Mol Endocrinol, 19*, 2451-2465.

Kane, D. A. (1999). Cell cycles and development in the embryonic zebrafish. *Methods Cell Biol, 59*, 11-26.

Kane, D. A. & Kimmel, C. B. (1993). The zebrafish midblastula transition. *Development, 119*, 447-456.

Kane, D. A., Maischein, H. M., Brand, M., van Eeden, F. J., Furutani-Seiki, M., Granato, M., Haffter, P., Hammerschmidt, M., Heisenberg, C. P., Jiang, Y. J., Kelsh, R. N., Mullins, M. C., Odenthal, J., Warga, R. M. & Nusslein-Volhard, C. (1996). The zebrafish early arrest mutants. *Development, 123*, 57-66.

Kasemeier-Kulesa, J. C., Kulesa, P. M. & Lefcort, F. (2005). Imaging neural crest cell dynamics during formation of dorsal root ganglia and sympathetic ganglia. *Development, 132*, 235-245.

Kaufman, M. H. (1992). *The atlas of mouse development,* (Editor ed.). London ; San Diego: Academic Press.

Keating, T. J., Peloquin, J. G., Rodionov, V. I., Momcilovic, D. & Borisy, G. G. (1997). Microtubule release from the centrosome. *Proc Natl Acad Sci U S A, 94*, 5078-5083.

Kellogg, D. R., Moritz, M. & Alberts, B. M. (1994). The centrosome and cellular organization. *Annu Rev Biochem, 63*, 639-674.

Keryer, G., Witczak, O., Delouvee, A., Kemmner, W. A., Rouillard, D., Tasken, K. & Bornens, M. (2003). Dissociating the centrosomal matrix protein AKAP450 from centrioles impairs centriole duplication and cell cycle progression. *Mol Biol Cell, 14*, 2436-2446.

Khodjakov, A. & Rieder, C. L. (2001). Centrosomes enhance the fidelity of cytokinesis in vertebrates and are required for cell cycle progression. *J Cell Biol, 153*, 237-242.

Khodjakov, A., Rieder, C. L., Sluder, G., Cassels, G., Sibon, O. & Wang, C. L. (2002). De novo formation of centrosomes in vertebrate cells arrested during S phase. *J Cell Biol, 158*, 1171-1181.

Kim, C. H., Ueshima, E., Muraoka, O., Tanaka, H., Yeo, S. Y., Huh, T. L. & Miki, N. (1996). Zebrafish elav/HuC homologue as a very early neuronal marker. *Neurosci Lett, 216*, 109-112.

Kim, J. C., Badano, J. L., Sibold, S., Esmail, M. A., Hill, J., Hoskins, B. E., Leitch, C. C., Venner, K., Ansley, S. J., Ross, A. J., Leroux, M. R., Katsanis, N. & Beales, P. L. (2004). The Bardet-Biedl protein BBS4 targets cargo to the pericentriolar region and is required for microtubule anchoring and cell cycle progression. *Nat Genet, 36*, 462-470.

Kimmel, C. B. (1993). Patterning the brain of the zebrafish embryo. *Annu Rev Neurosci, 16*, 707-732.

Kimmel, C. B., Ballard, W. W., Kimmel, S. R., Ullmann, B. & Schilling, T. F. (1995). Stages of embryonic development of the zebrafish. *Dev Dyn, 203*, 253-310.

Kloosterman, W. P., Lagendijk, A. K., Ketting, R. F., Moulton, J. D. & Plasterk, R. H. (2007). Targeted inhibition of miRNA maturation with morpholinos reveals a role for miR-375 in pancreatic islet development. *PLoS Biol, 5*, e203.

Knop, M., Pereira, G. & Schiebel, E. (1999). Microtubule organization by the budding yeast spindle pole body. *Biol Cell, 91*, 291-304.

Koblar, S. A., Krull, C. E., Pasquale, E. B., McLennan, R., Peale, F. D., Cerretti, D. P. & Bothwell, M. (2000). Spinal motor axons and neural crest cells use different molecular guides for segmental migration through the rostral half-somite. *J Neurobiol, 42*, 437-447.

Kramer, A., Mailand, N., Lukas, C., Syljuasen, R. G., Wilkinson, C. J., Nigg, E. A., Bartek, J. & Lukas, J. (2004). Centrosome-associated Chk1 prevents premature activation of cyclin-B-Cdk1 kinase. *Nat Cell Biol, 6*, 884-891.

Kulju, K. S. & Lehman, J. M. (1995). Increased p53 protein associated with aging in human diploid fibroblasts. *Exp Cell Res, 217*, 336-345.

Kumagai, A. & Dunphy, W. G. (1996). Purification and molecular cloning of Plx1, a Cdc25-regulatory kinase from Xenopus egg extracts. *Science, 273*, 1377-1380.

Kumar, S., Matsuzaki, T., Yoshida, Y. & Noda, M. (1994). Molecular cloning and biological activity of a novel developmentally regulated gene encoding a protein with beta-transducin-like structure. *J Biol Chem, 269*, 11318-11326.

Kumar, S., Tomooka, Y. & Noda, M. (1992). Identification of a set of genes with developmentally down-regulated expression in the mouse brain. *Biochem Biophys Res Commun, 185*, 1155-1161.

Lacey, K. R., Jackson, P. K. & Stearns, T. (1999). Cyclin-dependent kinase control of centrosome duplication. *Proc Natl Acad Sci U S A, 96*, 2817-2822.

Lange, B. M. (2002). Integration of the centrosome in cell cycle control, stress response and signal transduction pathways. *Curr Opin Cell Biol, 14*, 35-43.

Lange, B. M., Bachi, A., Wilm, M. & Gonzalez, C. (2000). Hsp90 is a core centrosomal component and is required at different stages of the centrosome cycle in Drosophila and vertebrates. *EMBO J, 19*, 1252-1262.

Larkin, M. A., Blackshields, G., Brown, N. P., Chenna, R., McGettigan, P. A., McWilliam, H., Valentin, F., Wallace, I. M., Wilm, A., Lopez, R., Thompson, J. D., Gibson, T. J. & Higgins, D. G. (2007). Clustal W and Clustal X version 2.0. *Bioinformatics, 23*, 2947-2948.

Lawo, S., Bashkurov, M., Mullin, M., Ferreria, M. G., Kittler, R., Habermann, B., Tagliaferro, A., Poser, I., Hutchins, J. R., Hegemann, B., Pinchev, D., Buchholz, F., Peters, J. M., Hyman, A. A., Gingras, A. C. & Pelletier, L. (2009). HAUS, the 8-subunit human Augmin complex, regulates centrosome and spindle integrity. *Curr Biol, 19*, 816-826.

Lechler, T. & Fuchs, E. (2007). Desmoplakin: an unexpected regulator of microtubule organization in the epidermis. *J Cell Biol, 176*, 147-154.

Lee, Y. R., Li, Y. & Liu, B. (2007). Two Arabidopsis phragmoplast-associated kinesins play a critical role in cytokinesis during male gametogenesis. *Plant Cell, 19*, 2595-2605.

Levy, M. Z., Allsopp, R. C., Futcher, A. B., Greider, C. W. & Harley, C. B. (1992). Telomere end-replication problem and cell aging. *J Mol Biol, 225*, 951-960.

Lewis, V. A., Hynes, G. M., Zheng, D., Saibil, H. & Willison, K. (1992). T-complex polypeptide-1 is a subunit of a heteromeric particle in the eukaryotic cytosol. *Nature, 358*, 249-252.

Li, J., Liu, Y., Kim, B. O. & He, J. J. (2002). Direct participation of Sam68, the 68-kilodalton Src-associated protein in mitosis, in the CRM1-mediated Rev nuclear export pathway. *J Virol, 76*, 8374-8382.

Ligon, L. A., Karki, S., Tokito, M. & Holzbaur, E. L. (2001). Dynein binds to beta-catenin and may tether microtubules at adherens junctions. *Nat Cell Biol, 3*, 913-917.

Lin, A. W., Barradas, M., Stone, J. C., van Aelst, L., Serrano, M. & Lowe, S. W. (1998). Premature senescence involving p53 and p16 is activated in response to constitutive MEK/MAPK mitogenic signaling. *Genes Dev, 12*, 3008-3019.

Liu, J. & Lessman, C. A. (2008). Changes of gamma-tubulin expression and distribution in the zebrafish (Danio rerio) ovary, oocyte and embryo. *Gene Expr Patterns, 8*, 237-247.

Liu, L. & Wiese, C. (2008). Xenopus NEDD1 is required for microtubule organization in Xenopus egg extracts. *J Cell Sci, 121*, 578-589.

Liu, X., Lin, C. Y., Lei, M., Yan, S., Zhou, T. & Erikson, R. L. (2005). CCT chaperonin complex is required for the biogenesis of functional Plk1. *Mol Cell Biol, 25*, 4993-5010.

Lowe, S. W. & Sherr, C. J. (2003). Tumor suppression by Ink4a-Arf: progress and puzzles. *Curr Opin Genet Dev, 13*, 77-83.

Lowery, L. A. & Sive, H. (2005). Initial formation of zebrafish brain ventricles occurs independently of circulation and requires the nagie oko and snakehead/atp1a1a.1 gene products. *Development, 132*, 2057-2067.

Luders, J., Patel, U. K. & Stearns, T. (2006). GCP-WD is a gamma-tubulin targeting factor required for centrosomal and chromatin-mediated microtubule nucleation. *Nat Cell Biol, 8*, 137-147.

Malicki, J. (1999). Development of the retina. *Methods Cell Biol, 59*, 273-299.

Manning, J. & Kumar, S. (2007). NEDD1: function in microtubule nucleation, spindle assembly and beyond. *Int J Biochem Cell Biol, 39*, 7-11.

Manning, J. A., Colussi, P. A., Koblar, S. A. & Kumar, S. (2008). Nedd1 expression as a marker of dynamic centrosomal localization during mouse embryonic development. *Histochem Cell Biol, 129*, 751-764.

Martins, T., Maia, A. F., Steffensen, S. & Sunkel, C. E. (2009). Sgt1, a co-chaperone of Hsp90 stabilizes Polo and is required for centrosome organization. *EMBO J, 28*, 234-247.

Mawdsley, D. J., Cooper, H. M., Hogan, B. M., Cody, S. H., Lieschke, G. J. & Heath, J. K. (2004). The Netrin receptor Neogenin is required for neural tube formation and somitogenesis in zebrafish. *Dev Biol, 269*, 302-315.

McDermott, K. M., Zhang, J., Holst, C. R., Kozakiewicz, B. K., Singla, V. & Tlsty, T. D. (2006). p16(INK4a) prevents centrosome dysfunction and genomic instability in primary cells. *PLoS Biol, 4*, e51.

McKenzie, E., Krupin, A. & Kelley, M. W. (2004). Cellular growth and rearrangement during the development of the mammalian organ of Corti. *Dev Dyn, 229*, 802-812.

McLaughlin, J. N., Thulin, C. D., Hart, S. J., Resing, K. A., Ahn, N. G. & Willardson, B. M. (2002). Regulatory interaction of phosducin-like protein with the cytosolic chaperonin complex. *Proc Natl Acad Sci U S A, 99*, 7962-7967.

Meads, T. & Schroer, T. A. (1995). Polarity and nucleation of microtubules in polarized epithelial cells. *Cell Motil Cytoskeleton, 32*, 273-288.

Megraw, T. L., Kao, L. R. & Kaufman, T. C. (2001). Zygotic development without functional mitotic centrosomes. *Curr Biol, 11*, 116-120.

Meimaridou, E., Gooljar, S. B. & Chapple, J. P. (2009). From hatching to dispatching: the multiple cellular roles of the Hsp70 molecular chaperone machinery. *J Mol Endocrinol, 42*, 1-9.

Melki, R., Vainberg, I. E., Chow, R. L. & Cowan, N. J. (1993). Chaperonin-mediated folding of vertebrate actin-related protein and gamma-tubulin. *J Cell Biol, 122*, 1301-1310.

Meulmeester, E. & Jochemsen, A. G. (2008). p53: a guide to apoptosis. *Curr Cancer Drug Targets, 8*, 87-97.

Mikule, K., Delaval, B., Kaldis, P., Jurcyzk, A., Hergert, P. & Doxsey, S. (2007). Loss of centrosome integrity induces p38-p53-p21-dependent G1-S arrest. *Nat Cell Biol, 9*, 160-170.

Miyazaki, T. & Arai, S. (2007). Two distinct controls of mitotic cdk1/cyclin B1 activity requisite for cell growth prior to cell division. *Cell Cycle, 6*, 1419-1425.

Mogensen, M. M., Malik, A., Piel, M., Bouckson-Castaing, V. & Bornens, M. (2000). Microtubule minus-end anchorage at centrosomal and non-centrosomal sites: the role of ninein. *J Cell Sci, 113 (Pt 17)*, 3013-3023.

Muresan, V., Joshi, H. C. & Besharse, J. C. (1993). Gamma-tubulin in differentiated cell types: localization in the vicinity of basal bodies in retinal photoreceptors and ciliated epithelia. *J Cell Sci, 104 (Pt 4)*, 1229-1237.

Murphey, R. D., Stern, H. M., Straub, C. T. & Zon, L. I. (2006). A chemical genetic screen for cell cycle inhibitors in zebrafish embryos. *Chem Biol Drug Des, 68*, 213-219.

Murphy, S. M., Preble, A. M., Patel, U. K., O'Connell, K. L., Dias, D. P., Moritz, M., Agard, D., Stults, J. T. & Stearns, T. (2001). GCP5 and GCP6: two new members of the human gamma-tubulin complex. *Mol Biol Cell, 12*, 3340-3352.

Nakagawa, S. & Takeichi, M. (1998). Neural crest emigration from the neural tube depends on regulated cadherin expression. *Development, 125*, 2963-2971.

Narita, M., Nunez, S., Heard, E., Lin, A. W., Hearn, S. A., Spector, D. L., Hannon, G. J. & Lowe, S. W. (2003). Rb-mediated heterochromatin formation and silencing of E2F target genes during cellular senescence. *Cell, 113*, 703-716.

Nigg, E. A. (2001). Mitotic kinases as regulators of cell division and its checkpoints. *Nat Rev Mol Cell Biol, 2*, 21-32.

Nigg, E. A. (2002). Centrosome aberrations: cause or consequence of cancer progression? *Nat Rev Cancer, 2*, 815-825.

Nigg, E. A. (2004). *Centrosomes in development and disease,* (Editor ed.). Weinheim: Wiley-VCH.

Nowak, M., Koster, C. & Hammerschmidt, M. (2005). Perp is required for tissue-specific cell survival during zebrafish development. *Cell Death Differ, 12*, 52-64.

Obenauer, J. C., Cantley, L. C. & Yaffe, M. B. (2003). Scansite 2.0: Proteome-wide prediction of cell signaling interactions using short sequence motifs. *Nucleic Acids Res, 31*, 3635-3641.

Oshimori, N., Li, X., Ohsugi, M. & Yamamoto, T. (2009). Cep72 regulates the localization of key centrosomal proteins and proper bipolar spindle formation. *EMBO J*.

Otegui, M. S., Verbrugghe, K. J. & Skop, A. R. (2005). Midbodies and phragmoplasts: analogous structures involved in cytokinesis. *Trends Cell Biol, 15*, 404-413.

Pan, J. & Snell, W. (2007). The primary cilium: keeper of the key to cell division. *Cell, 129*, 1255-1257.

Papan, C. & Campos-Ortega, J. A. (1999). Region-specific cell clones in the developing spinal cord of the zebrafish. *Dev Genes Evol, 209*, 135-144.

Park, H. C., Hong, S. K., Kim, H. S., Kim, S. H., Yoon, E. J., Kim, C. H., Miki, N. & Huh, T. L. (2000). Structural comparison of zebrafish Elav/Hu and their differential expressions during neurogenesis. *Neurosci Lett, 279*, 81-84.

Paronetto, M. P., Messina, V., Bianchi, E., Barchi, M., Vogel, G., Moretti, C., Palombi, F., Stefanini, M., Geremia, R., Richard, S. & Sette, C. (2009). Sam68 regulates translation of target mRNAs in male germ cells, necessary for mouse spermatogenesis. *J Cell Biol, 185*, 235-249.

Parrinello, S., Samper, E., Krtolica, A., Goldstein, J., Melov, S. & Campisi, J. (2003). Oxygen sensitivity severely limits the replicative lifespan of murine fibroblasts. *Nat Cell Biol, 5*, 741-747.

Pastuglia, M., Azimzadeh, J., Goussot, M., Camilleri, C., Belcram, K., Evrard, J. L., Schmit, A. C., Guerche, P. & Bouchez, D. (2006). Gamma-tubulin is essential for microtubule organization and development in Arabidopsis. *Plant Cell, 18*, 1412-1425.

Pei, Y. F. & Rhodin, J. A. (1970). The prenatal development of the mouse eye. *Anat Rec, 168*, 105-125.

Pelegri, F. (2003). Maternal factors in zebrafish development. *Dev Dyn, 228*, 535-554.

Pfaff, K. L., Straub, C. T., Chiang, K., Bear, D. M., Zhou, Y. & Zon, L. I. (2007). The zebra fish cassiopeia mutant reveals that SIL is required for mitotic spindle organization. *Mol Cell Biol, 27*, 5887-5897.

Pines, J. (1995). Cyclins and cyclin-dependent kinases: a biochemical view. *Biochem J, 308 (Pt 3)*, 697-711.

Pines, J. & Rieder, C. L. (2001). Re-staging mitosis: a contemporary view of mitotic progression. *Nat Cell Biol, 3*, E3-6.

Piperno, G., LeDizet, M. & Chang, X. J. (1987). Microtubules containing acetylated alpha-tubulin in mammalian cells in culture. *J Cell Biol, 104*, 289-302.

Ponten, J. (1976). The relationship between in vitro transformation and tumor formation in vivo. *Biochim Biophys Acta, 458*, 397-422.

Raynaud-Messina, B. & Merdes, A. (2007). Gamma-tubulin complexes and microtubule organization. *Curr Opin Cell Biol, 19*, 24-30.

Rice, P., Longden, I. & Bleasby, A. (2000). EMBOSS: the European Molecular Biology Open Software Suite. *Trends Genet, 16*, 276-277.

Rizzolo, L. J. & Joshi, H. C. (1993). Apical orientation of the microtubule organizing center and associated gamma-tubulin during the polarization of the retinal pigment epithelium in vivo. *Dev Biol, 157*, 147-156.

Robu, M. E., Larson, J. D., Nasevicius, A., Beiraghi, S., Brenner, C., Farber, S. A. & Ekker, S. C. (2007). p53 activation by knockdown technologies. *PLoS Genet, 3*, e78.

Rost, B., Yachdav, G. & Liu, J. (2004). The PredictProtein server. *Nucleic Acids Res, 32*, W321-326.

Roychowdhury, S. & Rasenick, M. M. (2008). Submembraneous microtubule cytoskeleton: regulation of microtubule assembly by heterotrimeric Gproteins. *FEBS J, 275*, 4654-4663.

Salas, P. J., Rodriguez, M. L., Viciana, A. L., Vega-Salas, D. E. & Hauri, H. P. (1997). The apical submembrane cytoskeleton participates in the organization of the apical pole in epithelial cells. *J Cell Biol, 137*, 359-375.

Salisbury, J. L., Suino, K. M., Busby, R. & Springett, M. (2002). Centrin-2 is required for centriole duplication in mammalian cells. *Curr Biol, 12*, 1287-1292.

Sanada, K. & Tsai, L. H. (2005). G protein betagamma subunits and AGS3 control spindle orientation and asymmetric cell fate of cerebral cortical progenitors. *Cell, 122*, 119-131.

Sayer, J. A., Otto, E. A., O'Toole, J. F., Nurnberg, G., Kennedy, M. A., Becker, C., Hennies, H. C., Helou, J., Attanasio, M., Fausett, B. V., Utsch, B., Khanna, H., Liu, Y., Drummond, I., Kawakami, I., Kusakabe, T., Tsuda, M., Ma, L., Lee, H., Larson, R. G., Allen, S. J., Wilkinson, C. J., Nigg, E. A., Shou, C., Lillo, C., Williams, D. S., Hoppe, B., Kemper, M. J., Neuhaus, T., Parisi, M. A., Glass, I. A., Petry, M., Kispert, A., Gloy, J., Ganner, A., Walz, G., Zhu, X., Goldman, D., Nurnberg, P., Swaroop, A., Leroux, M. R. & Hildebrandt, F. (2006). The centrosomal protein nephrocystin-6 is mutated in Joubert syndrome and activates transcription factor ATF4. *Nat Genet, 38*, 674-681.

Schatten, H. (2008). The mammalian centrosome and its functional significance. *Histochem Cell Biol, 129*, 667-686.

Schenck, A., Goto-Silva, L., Collinet, C., Rhinn, M., Giner, A., Habermann, B., Brand, M. & Zerial, M. (2008). The endosomal protein Appl1 mediates Akt substrate specificity and cell survival in vertebrate development. *Cell, 133*, 486-497.

Schoenwolf, G. C. & Desmond, M. E. (1984). Neural tube occlusion precedes rapid brain enlargement. *J Exp Zool, 230*, 405-407.

Serrano, M., Lin, A. W., McCurrach, M. E., Beach, D. & Lowe, S. W. (1997). Oncogenic ras provokes premature cell senescence associated with accumulation of p53 and p16INK4a. *Cell, 88*, 593-602.

Shay, J. W., Pereira-Smith, O. M. & Wright, W. E. (1991). A role for both RB and p53 in the regulation of human cellular senescence. *Exp Cell Res, 196*, 33-39.

Shepard, J. L., Stern, H. M., Pfaff, K. L. & Amatruda, J. F. (2004). Analysis of the cell cycle in zebrafish embryos. *Methods Cell Biol, 76*, 109-125.

Sherr, C. J. & DePinho, R. A. (2000). Cellular senescence: mitotic clock or culture shock? *Cell, 102*, 407-410.

Sherwood, S. W., Rush, D., Ellsworth, J. L. & Schimke, R. T. (1988). Defining cellular senescence in IMR-90 cells: a flow cytometric analysis. *Proc Natl Acad Sci U S A, 85*, 9086-9090.

Shiloh, Y. (2001). ATM and ATR: networking cellular responses to DNA damage. *Curr Opin Genet Dev, 11*, 71-77.

Sibon, O. C. (2003). Centrosomes as DNA damage regulators. *Nat Genet, 34*, 6-7.

Silver, L. M. & Remis, D. (1987). Five of the nine genetically defined regions of mouse t haplotypes are involved in transmission ratio distortion. *Genet Res, 49*, 51-56.

Sloboda, R. D. & Rosenbaum, J. L. (2007). Making sense of cilia and flagella. *J Cell Biol, 179*, 575-582.

Sluder, G. (2005). Two-way traffic: centrosomes and the cell cycle. *Nat Rev Mol Cell Biol, 6*, 743-748.

Sluder, G. & Nordberg, J. J. (2004). The good, the bad and the ugly: the practical consequences of centrosome amplification. *Curr Opin Cell Biol, 16*, 49-54.

Smith, T. F., Gaitatzes, C., Saxena, K. & Neer, E. J. (1999). The WD repeat: a common architecture for diverse functions. *Trends Biochem Sci, 24*, 181-185.

Srsen, V., Gnadt, N., Dammermann, A. & Merdes, A. (2006). Inhibition of centrosome protein assembly leads to p53-dependent exit from the cell cycle. *J Cell Biol, 174*, 625-630.

Srsen, V. & Merdes, A. (2006). The centrosome and cell proliferation. *Cell Div, 1*, 26.

Stein, G. H., Drullinger, L. F., Soulard, A. & Dulic, V. (1999). Differential roles for cyclin-dependent kinase inhibitors p21 and p16 in the mechanisms of senescence and differentiation in human fibroblasts. *Mol Cell Biol, 19*, 2109-2117.

Sternlicht, H., Farr, G. W., Sternlicht, M. L., Driscoll, J. K., Willison, K. & Yaffe, M. B. (1993). The t-complex polypeptide 1 complex is a chaperonin for tubulin and actin in vivo. *Proc Natl Acad Sci U S A, 90*, 9422-9426.

Stevens, N. R., Raposo, A. A., Basto, R., St Johnston, D. & Raff, J. W. (2007). From stem cell to embryo without centrioles. *Curr Biol, 17*, 1498-1503.

Sumara, I., Gimenez-Abian, J. F., Gerlich, D., Hirota, T., Kraft, C., de la Torre, C., Ellenberg, J. & Peters, J. M. (2004). Roles of polo-like kinase 1 in the assembly of functional mitotic spindles. *Curr Biol, 14*, 1712-1722.

Summerton, J. (1999). Morpholino antisense oligomers: the case for an RNase H-independent structural type. *Biochim Biophys Acta, 1489*, 141-158.

Takai, S., Yoshida, Y., Noda, M., Yamada, K. & Kumar, S. (1995). Assignment of the developmentally regulated gene NEDD1 to human chromosome 12q22 by fluorescence in situ hybridization. *Hum Genet, 95*, 96-98.

Tavaria, M., Gabriele, T., Kola, I. & Anderson, R. L. (1996). A hitchhiker's guide to the human Hsp70 family. *Cell Stress Chaperones, 1*, 23-28.

Thulasiraman, V., Yang, C. F. & Frydman, J. (1999). In vivo newly translated polypeptides are sequestered in a protected folding environment. *EMBO J, 18*, 85-95.

Tillement, V., Haren, L., Roullet, N., Etievant, C. & Merdes, A. (2009). The centrosome protein NEDD1 as a potential pharmacological target to induce cell cycle arrest. *Mol Cancer, 8*, 10.

Todaro, G. J. & Green, H. (1963). Quantitative studies of the growth of mouse embryo cells in culture and their development into established lines. *J Cell Biol, 17*, 299-313.

Trainor, P. A. (2005). Specification of neural crest cell formation and migration in mouse embryos. *Semin Cell Dev Biol, 16*, 683-693.

Trinkle-Mulcahy, L., Boulon, S., Lam, Y. W., Urcia, R., Boisvert, F. M., Vandermoere, F., Morrice, N. A., Swift, S., Rothbauer, U., Leonhardt, H. & Lamond, A. (2008). Identifying specific protein interaction partners using quantitative mass spectrometry and bead proteomes. *J Cell Biol, 183*, 223-239.

Tucker, J. B., Paton, C. C., Richardson, G. P., Mogensen, M. M. & Russell, I. J. (1992). A cell surface-associated centrosomal layer of microtubule-organizing material in the inner pillar cell of the mouse cochlea. *J Cell Sci, 102 (Pt 2)*, 215-226.

Uehara, R., Nozawa, R. S., Tomioka, A., Petry, S., Vale, R. D., Obuse, C. & Goshima, G. (2009). The augmin complex plays a critical role in spindle microtubule generation for mitotic progression and cytokinesis in human cells. *Proc Natl Acad Sci U S A, 106*, 6998-7003.

Uetake, Y. & Sluder, G. (2004). Cell cycle progression after cleavage failure: mammalian somatic cells do not possess a "tetraploidy checkpoint". *J Cell Biol, 165*, 609-615.

Verollet, C., Colombie, N., Daubon, T., Bourbon, H. M., Wright, M. & Raynaud-Messina, B. (2006). Drosophila melanogaster gamma-TuRC is dispensable for targeting gamma-tubulin to the centrosome and microtubule nucleation. *J Cell Biol, 172*, 517-528.

Wang, Y., Ji, P., Liu, J., Broaddus, R. R., Xue, F. & Zhang, W. (2009). Centrosome-associated regulators of the G(2)/M checkpoint as targets for cancer therapy. *Mol Cancer, 8*, 8.

Westerfield, M. (1995). *The Zebrafish Book: A guide to the laboratory use of Zebrafish (Danio rerio).* (Editor ed.). Eugene: University of Oregon Press.

Wiese, C. & Zheng, Y. (1999). Gamma-tubulin complexes and their interaction with microtubule-organizing centers. *Curr Opin Struct Biol, 9*, 250-259.

Wilkinson, C. J., Carl, M. & Harris, W. A. (2009). Cep70 and Cep131 contribute to ciliogenesis in zebrafish embryos. *BMC Cell Biol, 10*, 17.

Won, K. A., Schumacher, R. J., Farr, G. W., Horwich, A. L. & Reed, S. I. (1998). Maturation of human cyclin E requires the function of eukaryotic chaperonin CCT. *Mol Cell Biol, 18*, 7584-7589.

Wong, C. & Stearns, T. (2003). Centrosome number is controlled by a centrosome-intrinsic block to reduplication. *Nat Cell Biol, 5*, 539-544.

Woo, K. & Fraser, S. E. (1995). Order and coherence in the fate map of the zebrafish nervous system. *Development, 121*, 2595-2609.

Wright, W. E. & Shay, J. W. (2000). Telomere dynamics in cancer progression and prevention: fundamental differences in human and mouse telomere biology. *Nat Med, 6*, 849-851.

Wullimann, M. F. & Knipp, S. (2000). Proliferation pattern changes in the zebrafish brain from embryonic through early postembryonic stages. *Anat Embryol (Berl), 202*, 385-400.

Wynshaw-Boris, A. & Gambello, M. J. (2001). LIS1 and dynein motor function in neuronal migration and development. *Genes Dev, 15*, 639-651.

Yaffe, M. B., Farr, G. W., Miklos, D., Horwich, A. L., Sternlicht, M. L. & Sternlicht, H. (1992). TCP1 complex is a molecular chaperone in tubulin biogenesis. *Nature, 358*, 245-248.

Yan, X., Habedanck, R. & Nigg, E. A. (2006). A complex of two centrosomal proteins, CAP350 and FOP, cooperates with EB1 in microtubule anchoring. *Mol Biol Cell, 17*, 634-644.

Yuba-Kubo, A., Kubo, A., Hata, M. & Tsukita, S. (2005). Gene knockout analysis of two gamma-tubulin isoforms in mice. *Dev Biol, 282*, 361-373.

Zeng, C. J., Lee, Y. R. & Liu, B. (2009). The WD40 Repeat Protein NEDD1 Functions in Microtubule Organization during Cell Division in Arabidopsis thaliana. *Plant Cell, 21*, 1129-1140.

Zhang, X., Chen, Q., Feng, J., Hou, J., Yang, F., Liu, J., Jiang, Q. & Zhang, C. (2009). Sequential phosphorylation of Nedd1 by Cdk1 and Plk1 is required for targeting of the {gamma}TuRC to the centrosome. *J Cell Sci*.

Zhao, J., Ren, Y., Jiang, Q. & Feng, J. (2003). Parkin is recruited to the centrosome in response to inhibition of proteasomes. *J Cell Sci, 116*, 4011-4019.

Zhu, F., Lawo, S., Bird, A., Pinchev, D., Ralph, A., Richter, C., Muller-Reichert, T., Kittler, R., Hyman, A. A. & Pelletier, L. (2008a). The mammalian SPD-2 ortholog Cep192 regulates centrosome biogenesis. *Curr Biol, 18*, 136-141.

Zhu, H., Coppinger, J. A., Jang, C. Y., Yates, J. R., 3rd & Fang, G. (2008b). FAM29A promotes microtubule amplification via recruitment of the NEDD1-gamma-tubulin complex to the mitotic spindle. *J Cell Biol, 183*, 835-848.

Zhu, J., Woods, D., McMahon, M. & Bishop, J. M. (1998). Senescence of human fibroblasts induced by oncogenic Raf. *Genes Dev, 12*, 2997-3007.

Zimmerman, W. C., Sillibourne, J., Rosa, J. & Doxsey, S. J. (2004). Mitosis-specific anchoring of gamma tubulin complexes by pericentrin controls spindle organization and mitotic entry. *Mol Biol Cell, 15*, 3642-3657.

Zolessi, F. R., Poggi, L., Wilkinson, C. J., Chien, C. B. & Harris, W. A. (2006). Polarization and orientation of retinal ganglion cells in vivo. *Neural Dev, 1*, 2.